

**MOUNTAIN PRECIPITATION ANALYSIS FOR THE ESTIMATION OF FLOOD
RUNOFF IN COASTAL BRITISH COLUMBIA**

By

ATHANASIOS LOUKAS

Dipl. Eng., Aristotle University of Thessaloniki, 1988

M.A.Sc., University of British Columbia, 1991

A THESIS SUBMITTED IN PARTIAL FULFILLMENT OF
THE REQUIREMENTS FOR THE DEGREE OF
DOCTOR OF PHILOSOPHY

in

THE FACULTY OF GRADUATE STUDIES
DEPARTMENT OF CIVIL ENGINEERING

We accept this thesis as conforming
to the required standard

THE UNIVERSITY OF BRITISH COLUMBIA

August 1994

© ATHANASIOS LOUKAS, 1994

In presenting this thesis in partial fulfillment of the requirements for an advanced degree at the University of British Columbia, I agree that the Library shall make it freely available for reference and study. I further agree that permission for extensive copying of this thesis for scholarly purposes may be granted by the head of my department or by his or her representatives. It is understood that copying or publication of this thesis for financial gain shall not be allowed without my written permission.

(Signature)

Department of Civil Engineering

The University of British Columbia
Vancouver, Canada

Date 1 - 9 - 1994

ABSTRACT

A study of the precipitation distribution in coastal British Columbia is described and a technique is proposed for the reliable estimation of the frequency of rainfall generated floods from ungauged watersheds in the region. A multi-disciplinary investigation was undertaken encompassing the areas of hydrometeorology, meteorological modelling and hydrological modelling. Study components included analysis of long- and short-term precipitation in two medium sized watersheds located in southwestern coastal British Columbia; development of a 24-hour design storm for coastal British Columbia; generalization of the results over the coastal region of British Columbia; examination of the precipitation distribution during flood producing storms; identification of the applicability of a meteorological model for the estimation of short-term precipitation; and development of a physically-based stochastic-deterministic procedure for the estimation of flood runoff from ungauged watersheds of the region.

Based on an assessment of the atmospheric processes which affect climate, it was found that the strong frontal storms which form over the North Pacific Ocean and travel eastward generate the majority of the precipitation during the winter and fall months, whereas convective rainshowers and weak frontal storms produce the dry summer period precipitation.

Examination of the annual, seasonal, and monthly precipitation in the two study watersheds, the Seymour River and the Capilano River watersheds, showed that the variation of annual and winter and fall precipitation with elevation follows a curvilinear pattern, increasing up to middle position of the watersheds at an elevation of about 400 m and then decreasing or levelling off at the upper elevations. The summer precipitation is more uniformly distributed over the watersheds than the winter precipitation and accounts for about

25% of the total annual precipitation. The Bergeron two-cloud mechanism has been identified as the dominant rainfall producing mechanism during the winter and fall months.

Analysis of regional data and results of other regional studies indicate that the curvilinear pattern found in this study is more general and is similar for the whole of coastal British Columbia and the coastal Pacific Northwest.

Study of the 175 storms in the Seymour River watershed showed that the individual storm precipitation is distributed in a pattern similar to that of the annual precipitation and this distribution pattern is not affected by the type of the event. Furthermore, the analysis showed that the storm time distribution is not affected by the elevation, type of the storm, its duration, and its depth. Also, analysis of the data from three sparsely located stations of coastal British Columbia indicated that the time distribution of the storms does not change significantly over the region.

With regard to the development of techniques for the better estimation of flood runoff, a 24-hour design storm has been developed by using the data from the Seymour River watershed. Analysis of its spatial distribution revealed that this 24-hour design storm is distributed in a similar pattern to that of the annual precipitation. Also, it was found that the 24-hour extreme rainfall of various return periods is a certain percentage of the mean annual precipitation. Comparison with regional data and results of other regional studies showed that the developed design storm can be transposed over the whole coastal region of British Columbia. A comparative study and rainfall-runoff simulation for a real watershed showed that from the widely used synthetic hyetographs, only the Soil Conservation Service Type IA storm or the 10% time probability distribution curve of this study can accurately generate the flood runoff from watersheds of the region.

The above results of the short-term precipitation distribution with elevation and in time were tested for extreme storms. Five periods of historical large flood producing storms were

analyzed and it was shown that the findings of the short-term precipitation analyses are valid for these extreme storms.

The BOUND_P meteorological model was used for the estimation of storm precipitation in the mountainous area which covers the two study watersheds, but the results showed that this particular model is not capable of simulating the precipitation observed in the area. As a result, the initial intention of coupling the model with a hydrological model for the estimation of the runoff was abandoned.

The above results of the analysis of precipitation in coastal British Columbia and the findings of previous research on the watershed response of coastal mountainous watersheds have been combined and used for the development of a physically-based stochastic-deterministic procedure. The procedure uses the method of derived distributions and Monte Carlo simulation to estimate the flood frequency for ungauged watersheds of the region. The procedure has been tested with data from eight coastal British Columbia watersheds and compared with the results of other widely used regional techniques. This comparison showed that the method is reliable and efficient, and requires very limited data, which can be found from a topographical map and the Rainfall Frequency Atlas for Canada.

TABLE OF CONTENTS

ABSTRACT	ii
LIST OF TABLES	xi
LIST OF FIGURES	xiii
ACKNOWLEDGMENT	xxii
1. INTRODUCTION.....	1
2. STUDY AREA AND DATA SETS.....	6
2.1 Regional Climate.....	6
2.2 The Study Watersheds.....	10
2.2.1 Topography.....	10
2.2.2 Interaction of weather systems with the local topography.....	12
2.3 Data Sets.....	13
3. ANNUAL AND SEASONAL PRECIPITATION DISTRIBUTION.....	24
3.1 Introduction.....	24
3.2 Spatial Distribution of Precipitation.....	25
3.2.1 Annual and seasonal precipitation distribution in the Seymour River valley.....	25
3.2.2 Annual and seasonal precipitation distribution in the Capilano River valley.....	27
3.2.3 Monthly precipitation distribution in the two study watershed valleys.....	29

3.2.4	Comparison of mountain and valley precipitation.....	32
3.3	Temporal Variation of Precipitation.....	35
3.3.1	Seymour river watershed.....	35
3.3.2	Capilano river watershed.....	36
3.4	Spatial Variation of Precipitation.....	36
3.4.1	Seymour river watershed.....	37
3.4.2	Capilano river watershed.....	39
3.5	Comparison with Other Studies and Regional Data.....	40
3.6	Meteorological Mechanisms Affecting the Precipitation Distribution.....	45
3.7	Summary.....	47
4.	STORM PRECIPITATION DISTRIBUTION.....	63
4.1	Introduction.....	63
4.2	Data Sets.....	64
4.3	Spatial Distribution of Storms.....	66
4.3.1	Storm precipitation.....	66
4.3.1.1	Spatial variation.....	67
4.3.2	Duration and average storm intensity.....	69
4.3.3	Maximum hourly intensity.....	70
4.3.4	Relative start time.....	70
4.4	Time Distribution of Storms.....	71
4.4.1	Research Procedure.....	72
4.4.2	Results.....	74
4.5	Antecedent Precipitation.....	78
4.6	Summary.....	80

5.	24-HOUR DESIGN STORM FOR COASTAL BRITISH COLUMBIA.....	98
5.1	Introduction.....	98
5.2	Data Sets and Method of Analysis.....	100
5.3	Time Distribution.....	102
5.4	Spatial Distribution.....	106
5.5	Antecedent Rainfall.....	111
5.6	Simulation of Peak Storm Flow at Jamieson Creek Watershed.....	113
5.7	Summary.....	117
6.	STUDY OF HISTORICAL LARGE STORMS.....	133
6.1	Introduction.....	133
6.2	The July 11-12, 1972 Rainstorm.....	134
6.2.1	Synoptic conditions.....	134
6.2.2	Spatial distribution.....	135
6.2.3	Time distribution.....	136
6.3	The December 13-18, 1979 Rainstorms.....	137
6.3.1	Synoptic conditions.....	137
6.3.2	The December 13-14, 1979 storm.....	138
6.3.2.1	Spatial distribution.....	138
6.3.2.2	Time distribution.....	140
6.3.3	The December 16-18, 1979 storm.....	140
6.3.3.1	Spatial distribution.....	140
6.3.3.2	Time distribution.....	141
6.4	The October 25-31, 1981 Rainstorms.....	142
6.4.1	Synoptic conditions.....	142

6.4.2	The October 25-28, 1981 storm.....	143
6.4.2.1	Spatial distribution.....	143
6.4.2.2	Time distribution.....	144
6.4.3	The October 28-31, 1981 storm.....	145
6.4.3.1	Spatial distribution.....	145
6.4.3.2	Time distribution.....	146
6.5	The November 8-11, 1990 Rainstorm.....	146
6.5.1	Synoptic conditions.....	146
6.5.2	Spatial distribution.....	147
6.5.3	Time distribution.....	149
6.6	The November 21-24, 1990 Rainstorm.....	149
6.6.1	Synoptic conditions.....	149
6.6.2	Spatial distribution.....	149
6.6.3	Time distribution.....	151
6.7	Summary.....	151
7.	APPLICATION OF A METEOROLOGICAL MODEL.....	160
7.1	Introduction.....	160
7.2	General Description of the BOUND _P Model.....	163
7.2.1	Overview.....	163
7.2.1.1	The wind model.....	164
7.2.1.2	The water flux model.....	166
7.2.1.3	Estimation of precipitation.....	168
7.3	Data Sets.....	169
7.4	Application.....	171

7.4.1	Complications.....	171
7.4.2	Results.....	173
7.4.2.1	Calibration of the model.....	174
7.4.2.2	Analysis of the regression coefficients.....	177
7.4.2.3	Verification of the model.....	179
7.5	Summary.....	181
8.	A PHYSICALLY BASED STOCHASTIC-DETERMINISTIC PROCEDURE FOR THE ESTIMATION OF FLOOD RUNOFF.....	202
8.1	Introduction.....	202
8.2	Procedure.....	207
8.2.1	Rainfall model.....	208
8.2.2	Watershed response model.....	212
8.3	Application and Results.....	216
8.4	Sensitivity Analysis.....	220
8.5	Comparison with Regional Techniques.....	225
8.5.1	Methods.....	226
8.5.1.1	Index flood method.....	226
8.5.1.2	Method of direct regression of quantiles (DRQ).....	227
8.5.1.3	Method of regression for distribution parameters (RDP)....	227
8.5.1.4	B.C. Environment method.....	228
8.5.1.5	Russell's Bayesian methodology.....	229
8.5.2	Application.....	230
8.5.3	Results.....	238
8.6	Summary.....	242

9.	CONCLUSIONS AND RECOMMENDATIONS.....	272
9.1	Conclusions.....	272
9.2	Recommendations.....	276
REFERENCES.....		279
APPENDICES.....		299
A	PRECIPITATION AND STREAMFLOW STATIONS USED IN THE STUDY OF LONG-TERM PRECIPITATION.....	299
B	RELATIONSHIP BETWEEN EXTREME 24-HOUR RAINFALL AND MEAN ANNUAL PRECIPITATION.....	309
C	CHARACTERISTICS OF THE 44 BASINS USED FOR THE TESTING OF THE MODIFIED SNYDER FORMULA.....	318

LIST OF TABLES

2.1	Mean monthly precipitation for representative coastal British Columbia stations...	8
2.2	Precipitation stations in the Seymour River watershed.....	14
2.3	Precipitation stations in the Capilano River watershed.....	15
3.1	Regression coefficients for the monthly precipitation-Seymour River watershed...	30
3.2	Regression coefficients for the monthly precipitation-Capilano River watershed...	31
3.3	Comparison of the annual precipitation gradient for the valley and mountain slope	33
3.4	Regression coefficients for the monthly precipitation-Lower Capilano valley, Hollyburn and Grouse mountains.....	34
4.1	Characteristics of the coastal British Columbia stations whose data analyzed.....	77
5.1	Characteristics of the coastal British Columbia stations used in the analysis of the 24-hour extreme rainfall time distribution.....	104
5.2	Ratio of the 24-hour rainfall and mean annual precipitation for various coastal subregions of British Columbia.....	110
5.3	Probability distribution of antecedent rainfall for the maximum 24-hour storms for various number of days.....	112
5.4	Comparison of the simulated peak flows (m^3/sec) using various hyetographs with the observed flows of Jamieson Creek watershed.....	116
7.1	Precipitation stations used in the application of the BOUND _P model.....	175
8.1	The characteristics of the eight watersheds used in the study.....	219
8.2	Sensitivity Index Values (SI, %) for the mean annual 24-hour rainfall (R_m).....	222
8.3	Sensitivity Index Values (SI, %) for the standard deviation of the 24-hour rainfall (σ_R).....	222
8.4	Sensitivity Index Values (SI, %) for the mean of storage factor (KF_m).....	223

8.5	Sensitivity Index Values (SI, %) for the coefficient of variation of KF (CV_{KF})...	223
8.6	Sensitivity Index Values (SI, %) for the mean of infiltration abstractions parameter (I_f).....	224
8.7	Sensitivity Index Values (SI, %) for the coefficient of variation of I_f (CV_{If}).....	224
8.8	Sensitivity Index Values (SI, %) for the form of the parameters.....	225
8.9	Characteristics of coastal British Columbia watersheds used in the study.....	232
8.10	Regional equations of instantaneous peak flow for the method of Direct Regression of Quantiles.....	234
8.11	Regional equations of daily peak flow for the method of Direct Regression of Quantiles.....	235
8.12	Comparison of estimated instantaneous peak flow (m^3/sec) for various return periods using various methods.....	240
8.13	Comparison of estimated daily peak flow (m^3/sec) for various return periods using various methods with the fitted Extreme Value type I distribution and the observed flows.....	241
A1	Precipitation stations in coastal British Columbia.....	300
A2	Streamflow gauging stations in coastal British Columbia.....	307
B1	Characteristics of the sixty-one stations used in the analysis of the 24-hour extreme rainfall.....	310
C1	Characteristics of the basins used in the independent test of the modified Snyder formula.....	319

LIST OF FIGURES

2.1	Map showing coastal British Columbia.....	19
2.2	Mean monthly temperatures for coastal British Columbia stations.....	20
2.3	The location and instrumentation of the study watersheds.....	21
2.4	Area-elevation curves for the two study watersheds.....	22
2.5	Comparison of the precipitation accumulations with the snow course data.....	23
3.1	The distribution of the annual and seasonal precipitation along the topographic profile of the Seymour River watershed.....	49
3.2	The distribution of the annual and seasonal precipitation along the topographic profile of the Capilano River watershed.....	50
3.3	The coefficients of variation of the annual and seasonal precipitation at the Seymour River watershed.....	51
3.4	(a) The distribution of the monthly precipitation at selected stations at the Seymour River watershed and (b) its coefficients of variation.....	52
3.5	The coefficients of variation of the annual and seasonal precipitation at the Capilano River watershed.....	53
3.6	(a) The distribution of the monthly precipitation at selected stations at the Capilano River watershed and (b) its coefficients of variation.....	54
3.7	Monthly distribution of the correlation coefficient between several stations in the Seymour River watershed.....	55
3.8	Spatial correlation functions of annual, seasonal, and November and August precipitation in the Seymour River watershed.....	56

3.9	Monthly distribution of the correlation coefficient between several stations in the Capilano River watershed.....	57
3.10	Spatial correlation functions of annual, seasonal, and November and August precipitation in the Capilano River watershed.....	58
3.11	(a) Distribution of the annual and seasonal precipitation with elevation and (b) coefficients of variation for the annual and seasonal precipitation at different elevations in the North Cascades, Washington State (after data of Rasmussen and Tangborn, 1976).....	59
3.12	Distribution of the mean annual runoff with mean basin elevation for northern Cascades region (after data of Rasmussen and Tangborn, 1976).....	60
3.13	Distribution of annual precipitation (a) and its coefficients of variation (b) with elevation for the coastal British Columbia stations (269 stations).....	61
3.14	Distribution of the mean annual runoff with mean basin elevation for coastal British Columbia stations.....	62
4.1	a) Monthly distribution of the average annual precipitation at station S-1 and b) Monthly distribution of the 175 storms analyzed.....	82
4.2	a) Precipitation ratio to base station (Vancouver Harbour) for various stations and types of events and b) its coefficient of variation.....	83
4.3	Spatial correlation functions for the various types of storms.....	84
4.4	(a) Storm continuity at various elevations and types of storms and (b) Coefficient of variation of storm continuity.....	85
4.5	(a) Storm duration ratio to base station for various elevations and types of storms and (b) Coefficient of variation of storm duration ratio.....	86

4.6	(a) Ratio of the average storm intensity to base station for various elevations and types of storms and (b) its coefficient of variation.....	87
4.7	Ratio of the maximum hourly intensity to base station for various elevations and types of storms and (b) its coefficients of variation.....	88
4.8	Storm relative start time to the base station at different elevations and types of storms.....	89
4.9	Time distribution probability curves at station 25B.....	90
4.10	Comparison of the time distribution probability curves for different stations and elevations in the Seymour River watershed.....	91
4.11	Comparison of the time distribution probability curves for different type of events at the station 25B in the Seymour River watershed.....	92
4.12	The effect of the storm duration on the time probability distribution curves (Station S-1).....	93
4.13	The effect of the storm precipitation on the time probability distribution curves (Station S-1).....	94
4.14	Comparison of the time probability distribution curves for the Seymour River watershed and three coastal British Columbia stations.....	95
4.15	Probability of equality or exceedance of antecedent precipitation at station S-1 for (a) October to March storms and (b) April to September storms.....	96
4.16	Comparison of the probability of equality or exceedance of the antecedent precipitation for different elevations for (a) winter and (b) summer.....	97
5.1	Distribution of the coastal British Columbia stations with (a) years of record and (b) station elevation.....	120
5.2	Monthly distribution of the occurrence of the annual maximum 24-hour storms at Vancouver Harbour (53 years).....	121

5.3	Time probability distributions of 24-hour storms for station S-1.....	122
5.4	Comparison of the time probability distributions for various storms a) ten percent curves, b) fifty percent curves, and c) ninety percent curves.....	123
5.5	Average time probability distributions for the Seymour River watershed.....	124
5.6	Comparison of the average storm time distribution in the Seymour River watershed with the results of the Melone (1986) analysis for coastal British Columbia.....	126
5.7	Comparison of the average storm time distribution in the Seymour River watershed with the results of the Hogg (1980) analysis for coastal British Columbia.....	127
5.8	Comparison of the time probability distributions of the Seymour River watershed with three coastal British Columbia stations, a) ten percent curves, b) fifty percent curves, and c) ninety percent curves.....	128
5.9	Comparison of synthetic storms with the average time probability distributions of the Seymour River watershed.....	129
5.10	Distribution of rainfall with elevation for various return periods in the Seymour River watershed.....	130
5.11	Relationship of the 10-year 24-hour rainfall and mean annual precipitation for the sixty-one recording stations in the coastal British Columbia.....	131
5.12	The watershed model flow chart.....	132
5.13	Estimation of the 10-year flood for the Jamieson Creek watershed using synthetic and derived hyetographs.....	133
6.1	Comparison of the time distribution of the July 11-12, 1972 storm with time probability distribution curves at (a) station 10A and (b) station 14A.....	153
6.2	Comparison of the time distribution of the December 12-14, 1979 storm with time probability distribution curves at (a) station Vancouver Harbour, (b) station 10A and (c) station 14A.....	154

6.3	Comparison of the time distribution of the December 16-19, 1979 storm with time probability distribution curves at (a) station Vancouver Harbour, (b) station 10A and (c) station 14A.....	155
6.4	Comparison of the time distribution of the October 25-28, 1981 storm with time probability distribution curves at (a) station Vancouver Harbour, (b) station 10A, (c) station 14A and (d) station 25B.....	156
6.5	Comparison of the time distribution of the October 28-31, 1981 storm with time probability distribution curves at (a) station Vancouver Harbour, (b) station 10A, (c) station 14A and (d) station 25B.....	157
6.6	Comparison of the time distribution of the November 8-11, 1990 storm with time probability distribution curves at (a) station Vancouver Harbour, (b) station 14A and (c) station 25B.....	158
6.7	Comparison of the time distribution of the November 21-24, 1990 storm with time probability distribution curves at (a) station Vancouver Harbour, (b) station 10A and (c) station 14A.....	159
7.1	Three dimensional map of the calculation domain (latitude and longitude in degrees and elevation in meters with vertical scale 1: 17,500).....	182
7.2	Three dimensional map of the model domain (latitude and longitude in degrees and elevation in meters with vertical scale 1:32,500).....	183
7.3	Topographical contour map of the calculation domain (latitude and longitude in degrees).....	184
7.4	Topographical contour map of the model domain (latitude and longitude in degrees).....	185
7.5	Undisplaced water flux (mm) for November 10, 1990 (12:00 UTC).....	186
7.6	Undisplaced water flux (mm) for November 11, 1990 (00:00 UTC).....	187

7.7	Displaced water flux (mm) for November 10, 1990 (12:00 UTC).....	188
7.8	Displaced water flux (mm) for November 11, 1990 (00:00 UTC).....	189
7.9	Predicted precipitation (mm) for November 10, 1990.....	190
7.10	Objectively analyzed precipitation (mm) for November 10, 1990.....	191
7.11	Scattergraphs of observed and predicted precipitation for calibration for a) November 10, 1990 and b) total storm period between November 8-13, 1990.....	192
7.12	Regression coefficients versus the average domain precipitation a) A1 and b) A2..	193
7.13	Regression coefficients versus the average domain precipitation a) A3 and A4.....	194
7.14	Regression between the average domain precipitation and the coefficient A1.....	195
7.15	Regression between the precipitation difference between U.B.C. and Grouse mountain resort and the coefficient A4.....	196
7.16	Undisplaced water flux (mm) for August 29, 1991(12:00 UTC).....	197
7.17	Undisplaced water flux (mm) for August 30, 1991 (00:00 UTC).....	198
7.18	Displaced water flux (mm) for August 29, 1991 (12:00 UTC).....	199
7.19	Displaced water flux (mm) for August 30, 1991 (00:00 UTC).....	200
7.20	Scattergraphs of observed and predicted precipitation for verification for a) August 28, 1991 and b) total storm between August 26-30, 1991.....	201
8.1	Isopleths of the mean annual 24-hour rainfall in coastal British Columbia (After Rainfall Frequency Atlas for Canada, Hogg and Carr, 1985).....	244
8.2	Isopleths of the standard deviation of the mean annual 24-hour rainfall in coastal British Columbia (After Rainfall Frequency Atlas for Canada, Hogg and Carr, 1985).....	245
8.3	Comparison of the frequency of the observed and simulated hourly peak flow using the 24-hour, the 12-hour and the 6-hour storms for the Carnation Creek watershed	246

8.4	Comparison of the observed and simulated cumulative time probability distributions for the coastal British Columbia.....	247
8.5	Scattergraph between computed and observed time lag for 43 North America basins (Data after Watt and Chow, 1985).....	248
8.6	Flow chart of the Monte Carlo simulation.....	249
8.7	Map showing the location of the eight coastal British Columbia watersheds where the proposed procedure has been applied.....	250
8.8	Flood frequency curves for the Capilano River watershed a) hourly flows, b) daily flows and c) flood volume.....	251
8.9	Flood frequency curves for the Carnation Creek watershed a) hourly flows, b) daily flows and c) flood volume.....	252
8.10	Flood frequency curves for the Chapman Creek watershed a) hourly flows, b) daily flows and c) flood volume.....	253
8.11	Flood frequency curves for the Zeballos River watershed a) hourly flows, b) daily flows and c) flood volume.....	254
8.12	Flood frequency curves for the North Alouette River watershed a) hourly flows, b) daily flows and c) flood volume.....	255
8.13	Flood frequency curves for the Oyster River watershed a) hourly flows, b) daily flows and c) flood volume.....	256
8.14	Flood frequency curves for the Hirsch Creek watershed a) hourly flows, b) daily flows and c) flood volume.....	257
8.15	Flood frequency curves for the San Juan River watershed a) hourly flows, b) daily flows and c) flood volume.....	258
8.16	Sensitivity of the procedure to the change of mean 24-hour rainfall depth (R_m) for a) hourly flow, b) daily flow and c) flood volume for Carnation	

Creek watershed.....	259
8.17 Sensitivity of the procedure to the change of standard deviation of the 24-hour annual rainfall (σ_R) for a) hourly flow, b) daily flow and c) flood volume for Carnation Creek watershed.....	260
8.18 Sensitivity of the procedure to the change of mean storage factor of fast runoff (KF_m) for a) hourly flow, b) daily flow and c) flood volume for Carnation Creek watershed.....	261
8.19 Sensitivity of the procedure to the change of coefficient of variation of storage factor (CV_{KF}) for a) hourly flow, b) daily flow and c) flood volume for Carnation Creek watershed.....	262
8.20 Sensitivity of the procedure to the change of mean final infiltration abstractions (I_{fm}) for a) hourly flow, b) daily flow and c) flood volume for Carnation Creek watershed.....	263
8.21 Sensitivity of the procedure to the change of coefficient of variation of infiltration abstractions (CV_{If}) for a) hourly flow, b) daily flow and c) flood volume for Carnation Creek watershed.....	264
8.22 Sensitivity of the procedure to the form of procedure parameters for a) hourly flow, b) daily flow and c) flood volume for Carnation Creek watershed.....	265
8.23 Homogeneity test for peak instantaneous flow for coastal British Columbia stations.....	266
8.24 Homogeneity test for peak daily flow for coastal British Columbia stations.....	267
8.25 Dimensionless frequency curve of instantaneous peak flow for coastal British Columbia (Index Flood Method).....	268

8.26	Dimensionless frequency curve of daily peak flow for coastal British Columbia (Index Flood Method).....	269
8.27	Comparison of the frequency of the observed instantaneous peak flow with the frequency of the simulated instantaneous peak flow using various methods for the Sarita River watershed.....	270
8.28	Comparison of the frequency of the observed daily peak flow with the frequency of simulated daily peak flow using various methods for the Sarita River watershed.....	271
B1	Relationship of the 2-year 24-hour rainfall and mean annual precipitation for the sixty-one recording stations in coastal British Columbia.....	312
B2	Relationship of the 5-year 24-hour rainfall and mean annual precipitation for the sixty-one recording stations in coastal British Columbia.....	313
B3	Relationship of the 10-year 24-hour rainfall and mean annual precipitation for the sixty-one recording stations in coastal British Columbia.....	314
B4	Relationship of the 25-year 24-hour rainfall and mean annual precipitation for the sixty-one recording stations in coastal British Columbia.....	315
B5	Relationship of the 50-year 24-hour rainfall and mean annual precipitation for the sixty-one recording stations in coastal British Columbia.....	316
B6	Relationship of the 100-year 24-hour rainfall and mean annual precipitation for the sixty-one recording stations in coastal British Columbia.....	317

ACKNOWLEDGMENT

I would like to thank my thesis supervisor Dr. M.C. Quick who, throughout my study, encouraged and advised me, giving me guidance, but also leaving me the freedom of thinking and deciding. I am also thankful to the supervisory committee members, Dr. W.F Caselton, Dr. S.T. Chieng, Dr. D.L. Golding and Dr. S.O. Russell for their long discussions and valuable comments on my thesis.

I appreciate the assistance received from the Forest Hydrology Group of the University of British Columbia, Dr. D.L. Golding and, especially, Mr. Kuochi Rae, who has been responsible for collecting and processing the data from the Seymour River and Capilano River watersheds.

This thesis was made possible by the financial assistance given to me by the University of British Columbia and the Greek Ministry of National Economy which supported me throughout my doctorate studies with a University Graduate Fellowship and a N.A.T.O. Science and Engineering Scholarship, respectively. This research was also funded by a graduate scholarship awarded by the Earl R. Peterson Memorial Fund.

Finally I would like to dedicate my thesis to my wife, Kyriaki Maniati-Loukas, who contributed in many aspects of this study which could not have been conducted without her moral support, assistance and inspiration, my newly born daughter, Irene-Evdokia, and my parents, George and Irene Loukas, in appreciation for their love, caring and undying support throughout these long years at school.

CHAPTER 1

INTRODUCTION

Reliable prediction of runoff requires knowledge of the distribution of precipitation in both space and time. The analysis of precipitation can be done for different time-scales ranging from annual, seasonal, monthly time-scales down to daily, hourly and even shorter time-scales. For long-term reservoir operation, water supply and irrigation, the longer time-scales are adequate. On the other hand, the study of precipitation in short-term scales (daily, hourly, and storm precipitation) is necessary for the simulation of the runoff and especially of flood flow from the watersheds. For the long time-scales, the spatial variability within a single climate region is most likely to be associated with those physiographic factors that influence the meteorological mechanisms that generate precipitation. Over the long term, relationships between individual gauge totals should be stable as long as the prevailing precipitation generating mechanisms remain the same. This should also be true for the seasonal and monthly scales, although seasonal differences in meteorological patterns could produce seasonally variable spatial relationships.

While the effects of spatial variability in precipitation may be stable over the long time-scales, this may not be generally true over short time periods. The interaction of the meteorological elements with the topography of the area can be greatly different from storm to storm resulting in different spatial distribution patterns. This is evident in areas where precipitation is generated by convective rainstorms which usually cover small areas less than 30 km^2 and are quite variable in their spatial distribution. However, in areas where precipitation is generated by frontal storms, it is expected that the spatial variability of the short-term precipitation may be as stable as the longer-term precipitation. In this case the precipitation data should be examined for similarities between the spatial distribution patterns

Chapter 1. INTRODUCTION

of the long-term and the short-term precipitation, because if such similarities exist, then long-term data can be used for the estimation of the short-term precipitation patterns in other areas of the same climatic region. This is significant mainly because most of the precipitation stations are storage gauges, capable of measuring long- and medium-term precipitation but not the short-term precipitation.

Another important aspect of the precipitation is the temporal variability of the storm. This is particularly critical for the assessment of the short time-scale precipitation since it is used in the development of the storm hydrographs. Many recent studies have shown the importance of the accurate assessment of the storm precipitation on the resulting hydrograph (Beven and Hornberger, 1982; Bras et al., 1985; Watts and Calver, 1991). It is therefore important to analyze both the spatial and temporal variability of the short-term precipitation in order to improve the estimation of the storm-producing precipitation.

All the above aspects of precipitation become more difficult to study in mountainous regions where it is often unfeasible to install precipitation gauges at upper elevations because hillslopes are steep, weather is harsh, and lack of roads and transportation make the collection of precipitation data difficult. Also, the physiographic features and the complex atmospheric processes significantly modify the distribution of precipitation and make the reliable estimation of precipitation difficult (Sevruk, 1989). Hence, in the mountainous areas where large variability in the precipitation exists, the gauge network is never adequate to define the detailed precipitation distribution. As an example, in coastal British Columbia there are 269 precipitation stations, both recording and storage gauges, for an area of about 210,000 km². The sparse data network makes the application of hydrology very difficult. On the other hand, the mountainous regions are valuable water resource areas because the streamflows are used for the industrialized and populated areas which exist downstream in the regions. The water

Chapter 1. INTRODUCTION

may be used in various ways, such as for industry, water supply, irrigation, power generation, and recreation.

In the last two decades many models have been developed for the estimation and study of the precipitation. These models have concentrated on modeling the meteorological causes of spatial and temporal variation. This can be done implicitly using stochastic or mathematical representations of dynamic cells of rainfall during storms (Amoroch and Wu, 1977; Georgakakos, 1986; Rodriguez-Iturbe and Eagleson, 1987) or explicitly by modeling the physics of storm development and progression (Browning et al., 1973; Harrold, 1973; Hill and Browning, 1979; Hoskins, 1983). However, in order to make these models applicable in practice, they need to be tested against real precipitation data. Thus, there is a need for empirical studies on the spatial and temporal characteristics of precipitation on different time scales (Berndtsson and Niemczynowicz, 1988), and only a few such studies currently exist. This lack of understanding of the precipitation mechanisms on a regional basis, limits the accuracy of water resources plans and water management.

Even if all the above aspects of precipitation are carefully studied and reliable hydrological models are developed and used, the main problem in hydrology is to match recent scientific achievements with practical engineering applications. It is necessary to develop methods that incorporate all the acquired knowledge in such a way that is easy to apply and significantly improves the solution of the problems or satisfy newly raised objectives. The aim of this Thesis is to address the above concerns, to study the precipitation distribution in the mountainous coastal British Columbia and to use the results for the development of techniques for the reliable estimation of flood frequency for ungauged watersheds.

An investigation was undertaken encompassing the areas of hydrometeorology, meteorological modeling and hydrologic modeling. This research program examines the

Chapter 1. INTRODUCTION

precipitation distribution in long-, medium- and short-term time-scales in time and space for the coastal British Columbia and proposes a new procedure for the estimation of flood frequency from ungauged watersheds of the region. Specifically, the location and the topography of the two study watersheds and the coastal British Columbia are presented in Chapter 2. The weather systems and the climate of the region are discussed in detail, and the precipitation data sets used in the study are presented and their accuracy is tested.

Examination of the precipitation starts with an analysis of the annual, seasonal, and monthly accumulations on the two study watersheds in Chapter 3. This analysis examines the spatial distribution of the long- and medium-term precipitation and associates this distribution with the physiographical features of the area. In addition the temporal and spatial variability of the precipitation in these time-scales are studied. The results are compared with regional precipitation and runoff data and the transferability of the results to other areas of coastal British Columbia and the Pacific Northwest is investigated as well.

In Chapter 4, the storm precipitation distribution both in space and time is analyzed in one of the two study watersheds where hourly data are available. The storms are categorized into various types of precipitation events according to temperature and then the effects of elevation, type of events, storm precipitation and duration on the storm spatial and temporal distribution are investigated. The transferability of the findings to other areas of coastal British Columbia is examined. Similarities between the storm spatial distribution and the longer-term precipitation spatial distribution are identified.

In engineering practice the concept of the design storm is frequently used for the estimation of the flood runoff and for mountainous and rural watersheds it is common practice to use the 24-hour design storm. For this reason the development of the 24-hour storm for the coastal British Columbia is investigated in Chapter 5. The spatial distribution of the design storm is studied in one of the two study watersheds and the relationships between the annual

Chapter 1. INTRODUCTION

precipitation and the 24-hour storm precipitation are identified. The effect of elevation and the severity of the storm on the time distribution is examined. The results are compared with regional data and the transferability of the results over the coastal British Columbia is investigated.

The spatial and temporal distribution of seven severe storms in the study area are compared with the results of the analysis of the storm precipitation, and the similarities and differences are discussed in Chapter 6. The study of the synoptic conditions of these severe storms helps in understanding the atmospheric processes of the flood producing storms in the area.

In addition to the statistical analysis of the precipitation data, the precipitation distribution is studied with the help of a meteorological model in Chapter 7. The main parts of the model are described and discussed. The model is applied to the study area and the results are compared with the observed data. The model's ability to generate the observed precipitation distribution is discussed.

The results of the analysis of the short-term precipitation analysis are combined with a hydrologic model in a physically based stochastic-deterministic procedure to generate estimates of the frequency of peak flow runoff in Chapter 8. The procedure is applied to coastal British Columbia watersheds and the results are compared with the observed flow data. Furthermore, a sensitivity analysis of the method is performed and the results of the method are compared with the results from other techniques used for the estimation of the frequency of peak flow from ungauged watersheds.

CHAPTER 2

STUDY AREA AND DATA SETS

The objective of this chapter is to provide background information for the study. Firstly, the characteristics of the regional climate of coastal British Columbia are discussed, then the topography of the two study watersheds and the interaction of the local topography with the weather systems are outlined and finally, the data sets used in the analysis are presented.

2.1 Regional Climate

Coastal British Columbia (Fig. 2.1) is part of a larger geographical and climatic region, the coastal Pacific Northwest which extends southward into Washington and Oregon bounded by the Cascade Mountain Range, and includes southeast Alaska immediately adjacent to northern British Columbia. The coastal Pacific Northwest receives most of its precipitation from the prevailing temperate cyclonic systems originating over the north Pacific Ocean, similar to climatic conditions which are repeated in several temperate regions, for example, in southern Chile, in New Zealand, and over the mountainous coastal northwestern Europe, especially in Norway (Kendrew and Kerr, 1955).

The main climatic features of the coastal region include relatively high annual precipitation with the wettest months occurring in fall and winter, and a relatively small annual range of temperature. The Coastal Mountain Range in British Columbia and southeast Alaska, as well as the Cascade Mountains in Washington and Oregon, modify the air flow which moves eastward from the Pacific Ocean. As a result, along the west facing slopes of the mountain ranges much higher cloud cover and precipitation are observed than the eastern slopes of the mountains. Within the coastal region local variations in precipitation and

Chapter 2. STUDY AREA AND DATA SETS

temperature exist because of the interaction of the weather systems with the local topography. For example, the southeastern lowlands of Vancouver Island, the islands of the Georgia Strait and the Fraser River estuary are located in the rain shadow area of Vancouver Island and the Olympic peninsula mountains. This zone is the driest area of the coastal region and also the warmest with more hours of bright sunshine during the summer months (Phillips, 1990).

Mean monthly precipitation data are included in Table 2.1 for representative stations extending from Vancouver in the south to Prince George in the north. The location of the stations is shown in Figure 2.1. These data illustrate the variability along the coast, and yet also show that the monthly precipitation distribution as a percentage of the total annual precipitation is similar for the whole region. Also, it is evident that the summer precipitation is only a small percentage of the total annual precipitation, whereas the largest volume of precipitation falls during the fall and winter months. Furthermore, comparison of these data shows that the period of high precipitation starts earlier in the northern than in the southern sub-regions of coastal British Columbia. Williams (1948) noted a southward progression in the occurrence of the maximum annual daily precipitation of about one degree of latitude for each 4.5 days.

Chapter 2. STUDY AREA AND DATA SETS

Table 2.1 Mean monthly precipitation for representative coastal British Columbia stations

Month	Vancouver Harbour		Carnation CDF		Courtenay		Kitimat		Prince Rupert Airport	
	mm	%	mm	%	mm	%	mm	%	mm	%
Jan	218	14	377	14	225	15	351	12	228	9
Feb	156	10	348	13	167	11	335	11	222	9
Mar	153	10	302	11	142	10	211	7	201	8
Apr	91	6	155	6	75	5	185	6	190	8
May	68	4	91	3	47	3	106	4	140	6
Jun	63	4	72	3	48	3	80	3	130	5
Jul	43	3	58	2	34	2	70	2	103	4
Aug	55	4	76	3	46	3	123	4	158	6
Sept	79	5	135	5	64	4	220	7	233	9
Oct	159	10	287	10	156	10	473	16	367	15
Nov	214	14	412	15	139	16	402	14	268	11
Dec	243	16	458	17	260	17	401	14	284	11
Annual	1540		2770		1503		2957		2523	

Temperature data plotted on Figure 2.2 for three representative stations along coastal British Columbia show the relatively small annual range at a given station. The mean winter temperatures along the coast remain at 2 to 4°C above freezing, which is the highest temperature of any part of Canada (Phillips, 1990) whereas the average summer temperature rarely increases above 18°C. Also, from Figure 2.2, a similar trend in mean monthly temperature distribution between stations is evident. Chapman (1952) noted an average reduction in mean annual temperature along the coast from 24°20' to 60° north latitude of about 0.6°C per degree of latitude.

The climate of the coastal British Columbia is caused by the weather systems that are developed over the North Pacific Ocean. Four pressure systems are dominant in Western

Chapter 2. STUDY AREA AND DATA SETS

Canada: the sub-tropical high pressures of the North Pacific, the low pressures of middle latitudes located south and east of the Aleutian Islands (Aleutian low), the high pressures over the Arctic, and the continental high pressures which are located over the Mackenzie valley in winter.

During the winter months the sub-tropical high pressures and the Aleutian low pressures dominate. The pressure systems induce westerly winds of variable direction and speed. The air mass, transported by the westerly winds, acquires large amounts of moisture during its passage over the Pacific Ocean so that when on encountering the rugged terrain of coastal British Columbia much precipitation is released. On a smaller scale, during the winter and fall months the Aleutian low pressures and the high inland pressures of the Pacific Northwest combine to produce strong pressure gradients over western Oregon, Washington, and British Columbia, and these pressure gradients induce strong east and southeast winds (Schaefer, 1978). These winds at Vancouver account for 52% of all winds in winter and 44% of the winds year around (Phillips, 1990) and displace the incoming weather systems to the north.

Although these rain producing low pressure systems are dominant in the whole of the coastal Pacific Northwest and especially in coastal British Columbia, there are also times when the continental Arctic high pressure systems dominate and cause cold dry air to be transported over the Rocky mountains and, occasionally, over the Coastal Mountains producing prolonged spells of very cold, dry weather.

In the summer months the weather systems weaken and move to the north, and the pressure gradient in the region is reversed. The warming of the land creates low pressures while the lower temperatures over the ocean create a high pressure system. A pressure gradient with a southeasterly direction develops in the area, but it is much weaker than the winter pressure gradient described above (Schaefer, 1978). Under the influence of this

Chapter 2. STUDY AREA AND DATA SETS

pressure gradient dry northwesterly winds prevail over the coastal British Columbia at this time of the year. During these summer months, occasional precipitation is generated by weak frontal systems, which are derived from the main low pressure systems which are now much further north. Occasionally strong summer rainstorms develop when local heating causes additional convective cloud development which can produce more intense bursts of rainfall.

2.2 The Study Watersheds

The two study watersheds, the Seymour River and the Capilano River watersheds are medium-sized mountainous watersheds located in the southwestern side of the Coastal Mountains just north of the City of Vancouver (Fig. 2.3). A reservoir is located in the Seymour River watershed and another in the Capilano River watershed, and both, along with the Coquitlam Lake reservoir, supply water to the greater Vancouver area. All three watersheds are under the protection and supervision of a municipal organization, the Greater Vancouver Regional District (GVRD).

In the next paragraphs, the topography of the study watersheds along with the interaction of the weather systems with the local physiographic features will be discussed.

2.2.1 Topography

The areas of the Seymour River and Capilano River watersheds are 180 km^2 and 195 km^2 , respectively. The two watersheds lie between three mountains, Hollyburn, Grouse, and Seymour, all located in the North Shore mountains. The elevations of the mountain peaks are: Hollyburn 1324 m, Grouse 1211 m, and Seymour 1450 m. The mountains lie on the northern

Chapter 2. STUDY AREA AND DATA SETS

side of Burrard inlet and their slopes are very steep, so that there is a rapid change in elevation in a short distance of about 10-14 km.

The elevation of the watersheds ranges from about 100 m at the downstream boundary to about 1800 m at the highest point of the divide with about 50 percent of the watersheds' area lying above 800 m (Fig. 2.4). Watershed land slopes are generally steep with a considerable area of shallow soils and occasional rock outcrops. The basic topographic features of the watersheds have resulted from the valleys being U-shaped by valley glaciation, which also rounded the lower peaks but sharpened the higher ones. The resulting profiles of the main valleys are gentle to moderately steep slopes in the valleys and abrupt steep slopes at the valley sides. At the higher elevations, the slopes become more mild, rounded at the lower peaks.

In the headwaters of both Seymour and Capilano Rivers the profile tends to change to V-shaped with hillsides having uniform slope. Most of the small, high elevation tributaries of both rivers have slopes greater than 40%.

The above topographic characteristics are dominant for both Seymour River and Capilano River watersheds. However, there are some differences. The Capilano river at the lower reaches, below the Capilano Lake reservoir, flows through a narrow canyon, while the Seymour river flows through an open U-shaped valley to its mouth at Burrard Inlet. Also, the Seymour River watershed is elongated while the Capilano River watershed is more rounded (Fig. 2.3).

The two study watersheds have a general north-south orientation. However, the Seymour River watershed turns to a northwest-southeast orientation after the middle distance between its mouth and its headwaters (Fig. 2.3). These variations of the local topography of the study watersheds may affect the local climate and will be examined in the analysis of precipitation in the two watersheds.

Chapter 2. STUDY AREA AND DATA SETS

2.2.2 Interaction of weather systems with the local topography

The humid Pacific Ocean air masses, discussed in the previous section, meet massive barriers in their path to the East. First the westerly systems meet the Vancouver Island ranges which rise to average heights of 2000 m. These mountain ranges protect the Vancouver area from the direct onslaught of storms moving off the North Pacific ocean. To a lesser extent such protection is also offered by the Olympic Mountains of northwest Washington (Harry and Wright, 1967).

As the storms continue eastward, they impinge upon the mainland Coastal Mountains. The air mass, which has been modified by its passage over the Vancouver Island mountains, still has high humidity and releases large volumes of precipitation when it is forced to rise over the North Shore Mountains or funnel into the deep dissected valleys. For example, the largest observed annual precipitation in the coastal British Columbia has been measured in the middle of the Seymour River watershed where the funneling of the incoming air mass and the orographic lifting produces heavy precipitation.

In the wintertime, the North Shore mountains protect the area from outbreaks of cold Arctic air. Only the major surges are able to overcome the mountain barrier, and at these times the cold north wind sweeps the area and brings spells of clear cold weather. However, the cold air retreats as a Pacific storm advances, resulting in snowfall which often turns to rainfall as the warmer air moves into the area.

Much of the precipitation in the two study watersheds falls as rain, although snow occurs at the high elevations often as a mixture of rain and snow, or wet snow. The study watersheds are so well protected by the mountains both to the east and west that surface winds are, in general, light, and their direction depends on the local topography.

Chapter 2. STUDY AREA AND DATA SETS

2.3 Data Sets

Various precipitation data sets will be used for the analysis of precipitation in coastal British Columbia in this study. The main analysis will be based on data from the two study watersheds, Seymour River and Capilano River watersheds and will be presented in this section. Other data sets that will be used later in the analysis are presented whenever they are used.

The data used in the analysis has been taken from 9 stations in Seymour River watershed and 7 stations in Capilano River watershed for the period 1971-1990 (Fig. 2.3). The data set from the Vancouver Harbour station is used to assess the zero elevation precipitation. The precipitation stations are of two types, manual storage gauges and recording gauges. Some of the stations are maintained by the Atmospheric Environment Service (A.E.S.) and others by the Faculty of Forestry at the University of British Columbia (U.B.C.). The upper elevation stations in the two study watersheds have been installed as part of an ongoing research program between the Faculty of Forestry of the University of British Columbia and the Greater Vancouver Regional District (GVRD).

Tables 2.2 and 2.3 show the characteristics of the stations. The A.E.S. storage gauges are A.E.S. type B Standard rain gauges whereas the U.B.C. storage gauges are Sacramento type. The A.E.S. recording gauges are M.S.C. tipping bucket rain gauges and the U.B.C. gauges are Belfort weighing type. There are six recording stations in the Seymour River watershed that record hourly precipitation whereas all the stations in the Capilano River watershed are storage gauges. The stations cover an elevation range of about 850 m in the Seymour River watershed and 610 m in the Capilano River watershed. Such elevation coverage is difficult to find elsewhere in coastal British Columbia where the precipitation network is very sparse.

Chapter 2. STUDY AREA AND DATA SETS

Table 2.2. Precipitation stations in the Seymour River watershed

Name	Elevation (m)	Type	Organization
North Vancouver			
Second Narrows	10	Storage	A.E.S.
Bridge (NV2B)			
Seymour Falls Dam (SFD)	247	Storage	A.E.S.
S-1*	260	Recording	U.B.C.
S-2	275	Storage	U.B.C.
10A	293	Recording	U.B.C.
14A	488	Recording	U.B.C.
21A	640	Recording	U.B.C.
25B**	762	Recording	U.B.C.
28A	853	Recording	U.B.C.

*Storage gauge before December 1983

**Installed in summer of 1980

Chapter 2. STUDY AREA AND DATA SETS

Table 2.3. Precipitation stations in the Capilano River watershed

Name	Elevation (m)	Type	Organization
Capilano (CAP)	93	Storage	A.E.S.
Cleveland Dam (CD)	157	Storage	A.E.S.
C-1	610	Storage	U.B.C.
C-2	320	Storage	U.B.C.
C-3	518	Storage	U.B.C.
C-4	427	Storage	U.B.C.
C-5	610	Storage	U.B.C.

All stations are located in the valleys of the watersheds but, as mentioned above, the stations cover an elevation range of about 610 m in Capilano River watershed and 850 m in the Seymour River watershed. Also the upper elevation stations are located in the headwaters of the Capilano River and Seymour River where the slopes are very steep ranging around 60-80%. For this reason, it is believed that these upper stations, 10A, 14A, 21A, 25B, 28A and C3, C4, C5, can accurately record the mountain precipitation of the headwaters area of the watershed.

The gauges are charged with antifreeze during the winter time so that both rain and snow accumulations are measured. The stations, installed in the forest, are located in the center of a clear-cut circle of a diameter of about twice the height of the adjacent trees which has been found to protect the precipitation catch from both wind and rain shadowing effects.

Chapter 2. STUDY AREA AND DATA SETS

However, to ensure accuracy, the precipitation measurements have been tested. Firstly, the precipitation records of two gauges, one with windshield and the other without windshield, 12 m apart at 762 m elevation, were compared and no significant difference was found (Kuochi Rae, personal communication). Secondly, the precipitation accumulations at various stations were compared with data from an adjacent snow course to test the accuracy of the snow measurement. The snow course is located at 1190 m elevation in the Orchid Lake sub-watershed of the Seymour River watershed and is operated by the GVRD.

Comparison with data from other snow courses in the area indicates that the accumulations at the Orchid Lake are higher than any other snow course in the southwestern coastal region (B.C. Environment, 1992). According to observations the first snow in the area usually falls during the first two weeks of November and the accumulation of snow continues to April.

In this comparison, the mean snow water equivalent accumulations at the Orchid Lake snow course from January 1 to April 1 for the period 1972 to 1990 are compared with the precipitation accumulations from the upper elevation stations of Seymour River watershed valley (Fig. 2.5). This comparison shows that the mean snow accumulation at the snow course is always lower than the precipitation accumulations at the valley stations. However, for the snowcourse, some precipitation may fall as rain and some snow will melt as the season progresses. Therefore to make a more meaningful comparison the snowmelt from the snowcourse has been modeled. The simplified energy equations for the estimation of the snowmelt proposed by Quick and Pipes (1989) are used. These equations have been successfully used in the UBC Watershed Model (Quick, 1993) and they require minimal data like the minimum and maximum daily air temperature. Air temperature data are not available at the Orchid Lake snow course so that the temperature data from the Grouse Mountain Resort station is used. The Grouse Mountain Resort station is located a few kilometers south of the

Chapter 2. STUDY AREA AND DATA SETS

Orchid Lake snow course and has similar elevation to the snow course (1105 m). The simulated snowmelt is added to the snow water accumulation and shows that the total accumulation or precipitation at the Orchid Lake snow course is lower than precipitation accumulations at the upper elevation stations 25B and 28A in the Seymour River watershed valley (Fig. 2.5). An underlying assumption in the above modeling procedure is that all the precipitation during the period from November to April is falling as snow. A study by Schaefer and Nikleva (1973) at the North Shore mountains has shown that the number of the snow days during the December to March period increases linearly with elevation at about 27 days per 300 m. For the elevation of the Orchid Lake snow course site (1190 m) the number of snow days is estimated as 96. This number is close to the precipitation days for the same period and so, indicates that the above assumption is valid.

Except for the above tests, the corrections that should have been applied to the measurements are calculated by the equations given by Sevruk (1982). The inaccuracies of the precipitation measurement can be classified into three categories, inaccurate precipitation catch because of the wind, evaporation losses and wetting losses. The corrections for inefficient precipitation catch because of the wind have been calculated using the equations for the U.S. standard recording gauge. Beaudry and Golding (1985) measured the wind speed in forest openings in Seymour River watershed with a R.M. Young No. 6001 anemometer as part of a snowmelt study. Beaudry and Golding found that the wind speed was minimum and in only few occasions was above the threshold velocity of 0.7 m/sec. It is shown that the correction of the precipitation for the wind is between 0 and 4% using the above wind speed and temperature data from the Seymour River watershed stations. The evaporation and wetting losses are considerably smaller because of the wet climate of the area year around. Furthermore, the effect of blowing and drifting snow is minimum because of the small wind speed.

Chapter 2. STUDY AREA AND DATA SETS

The above tests and comparison have shown that the precipitation measurements used in this study are reliable and they can be used without applying corrections.

Chapter 2. STUDY AREA AND DATA SETS

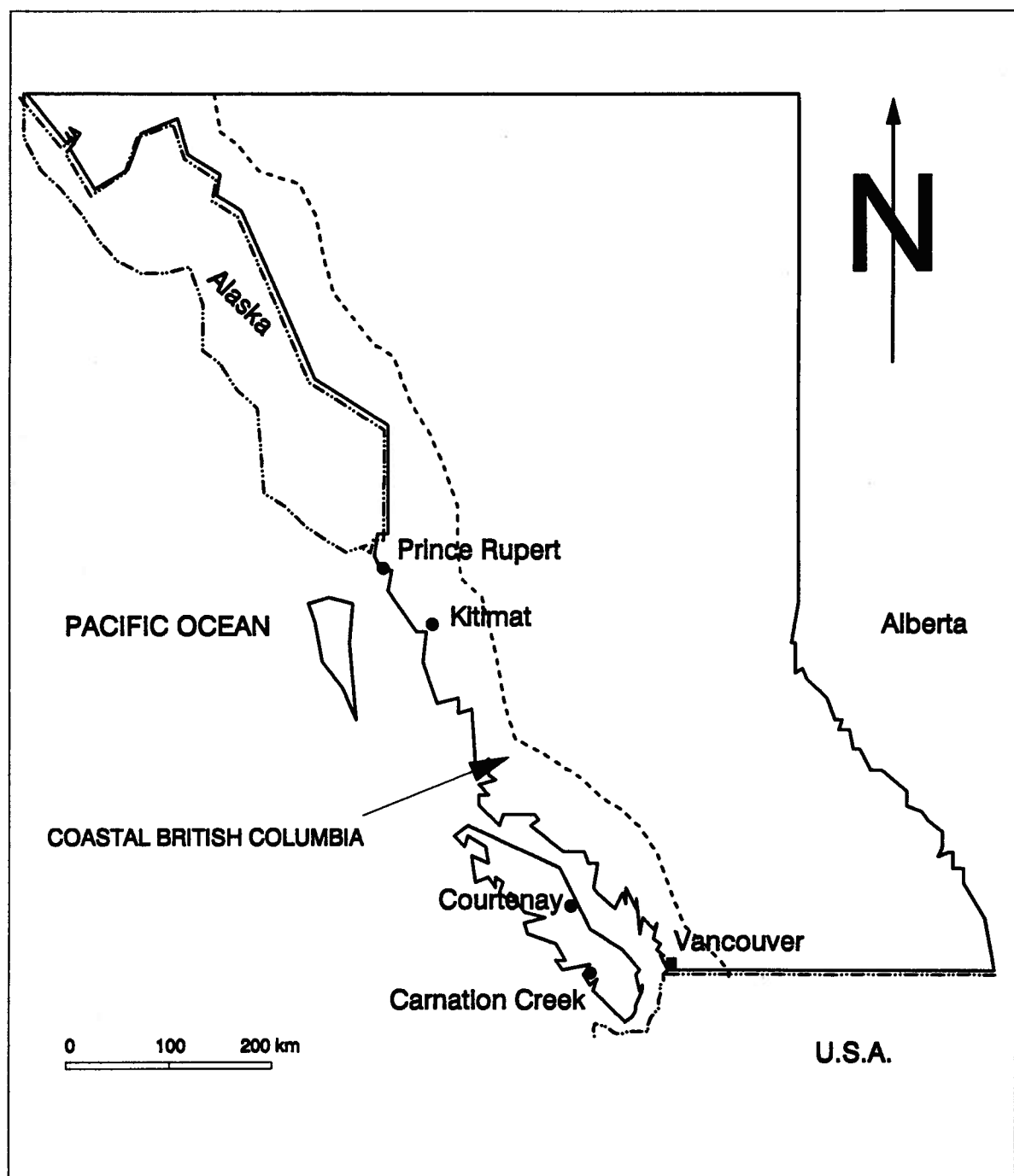


Fig. 2.1. Map showing coastal British Columbia

Chapter 2. STUDY AREA AND DATA SETS

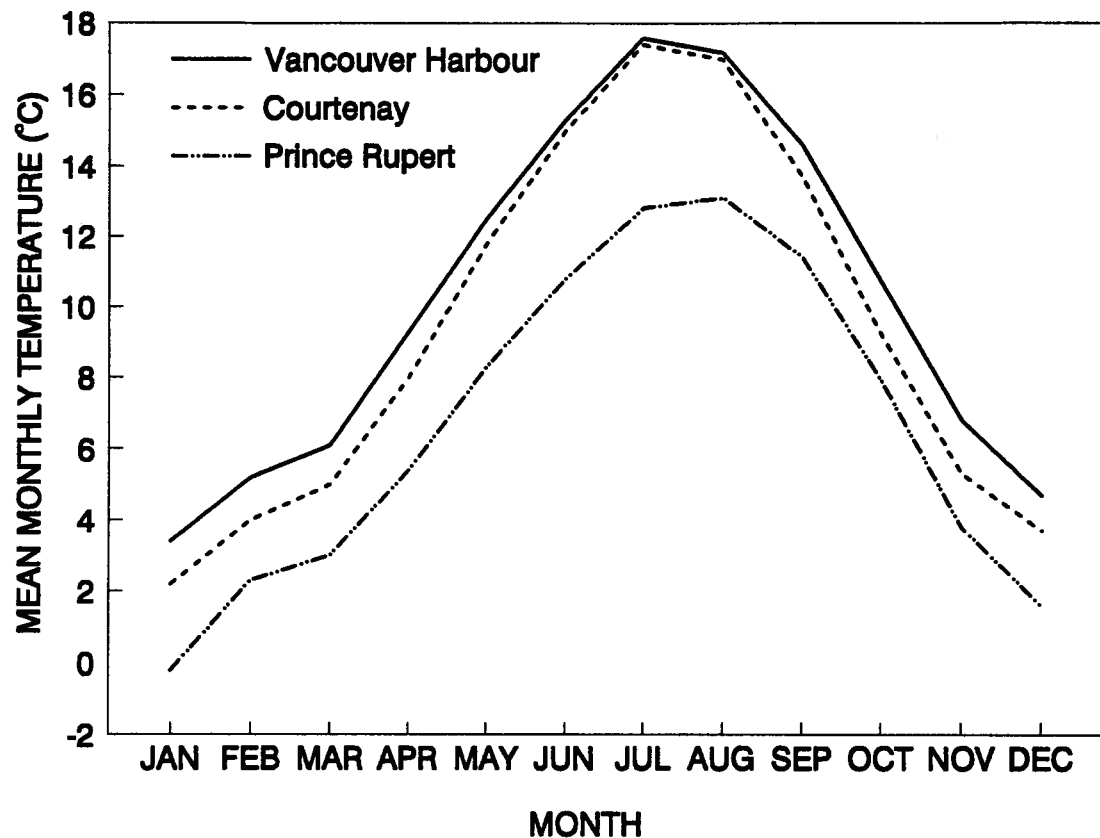


Fig. 2.2. Mean monthly temperatures for coastal British Columbia stations

Chapter 2. STUDY AREA AND DATA SETS

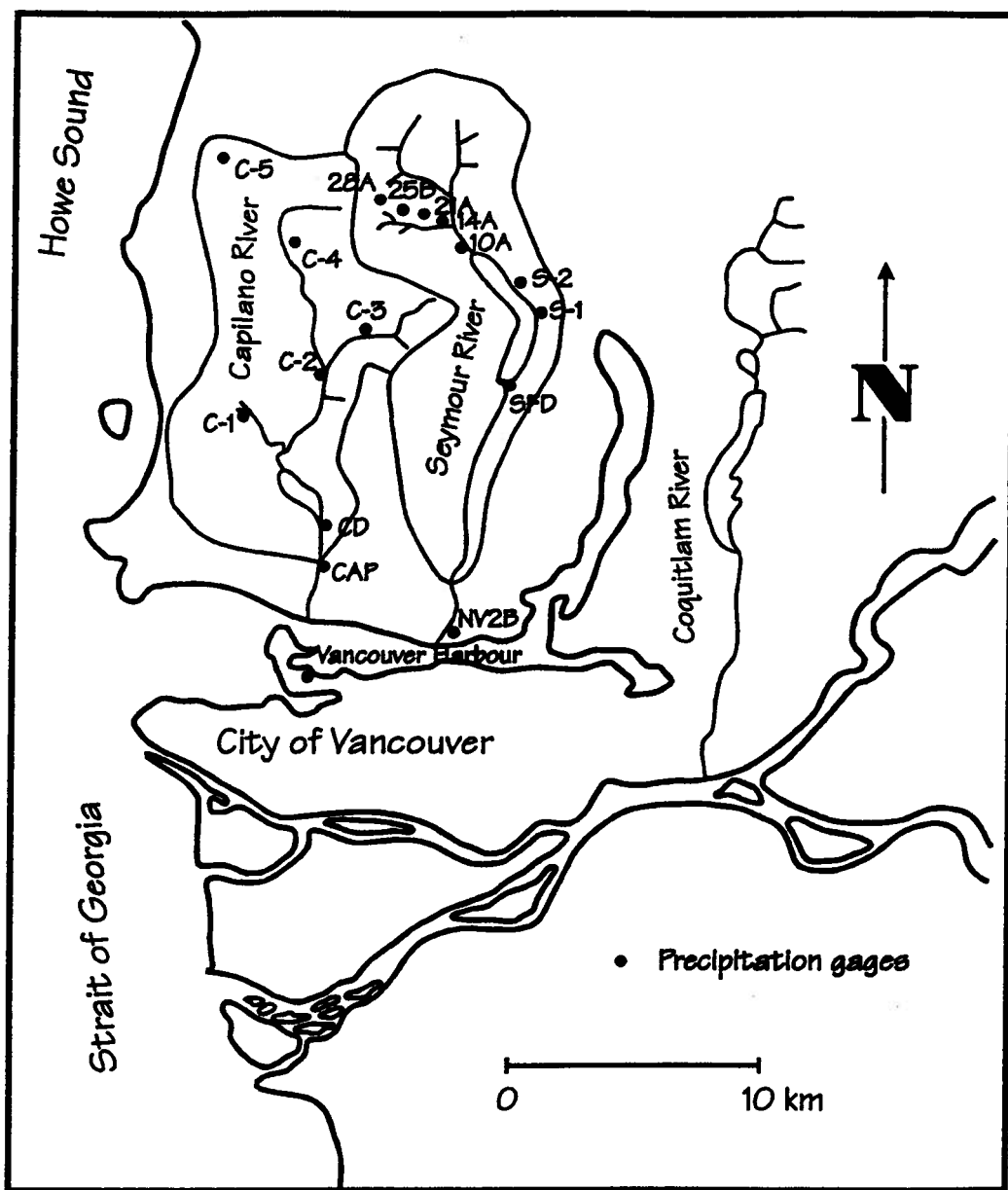


Fig. 2.3. The location and instrumentation of the study watersheds

Chapter 2. STUDY AREA AND DATA SETS

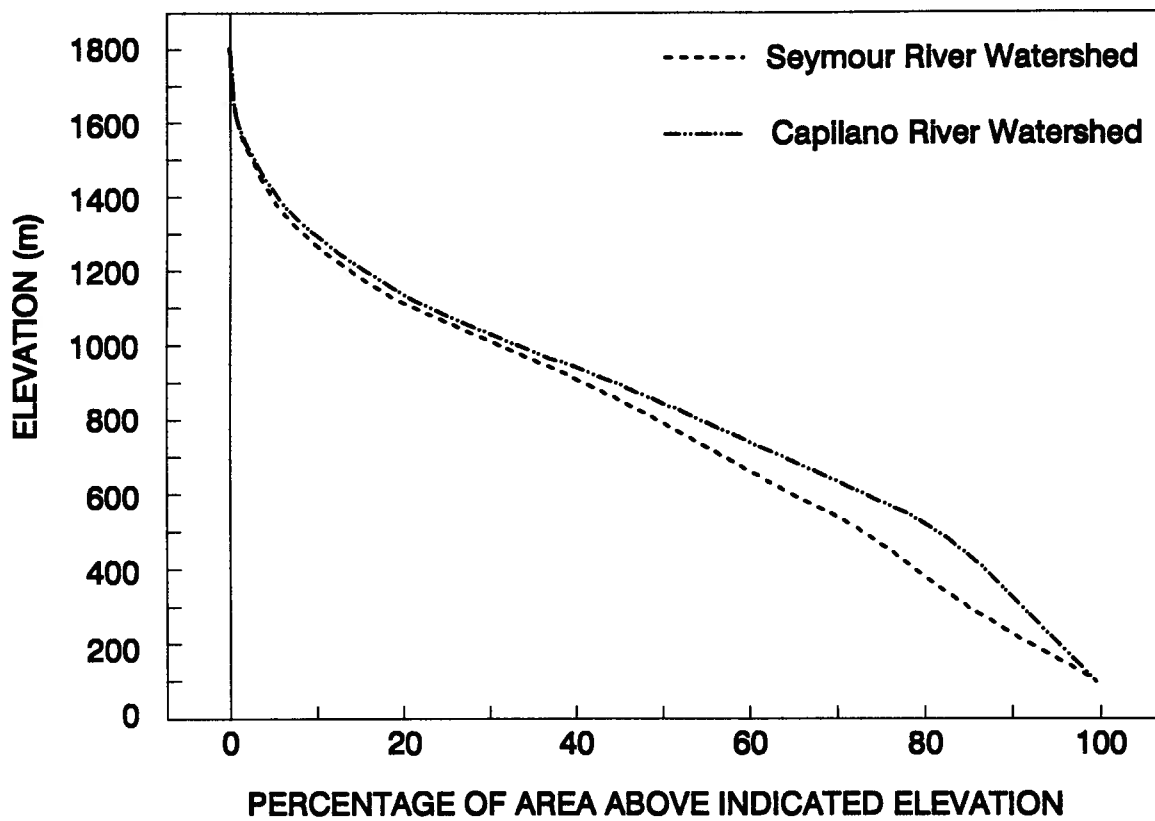


Fig. 2.4. Area-elevation curves for the two study watersheds

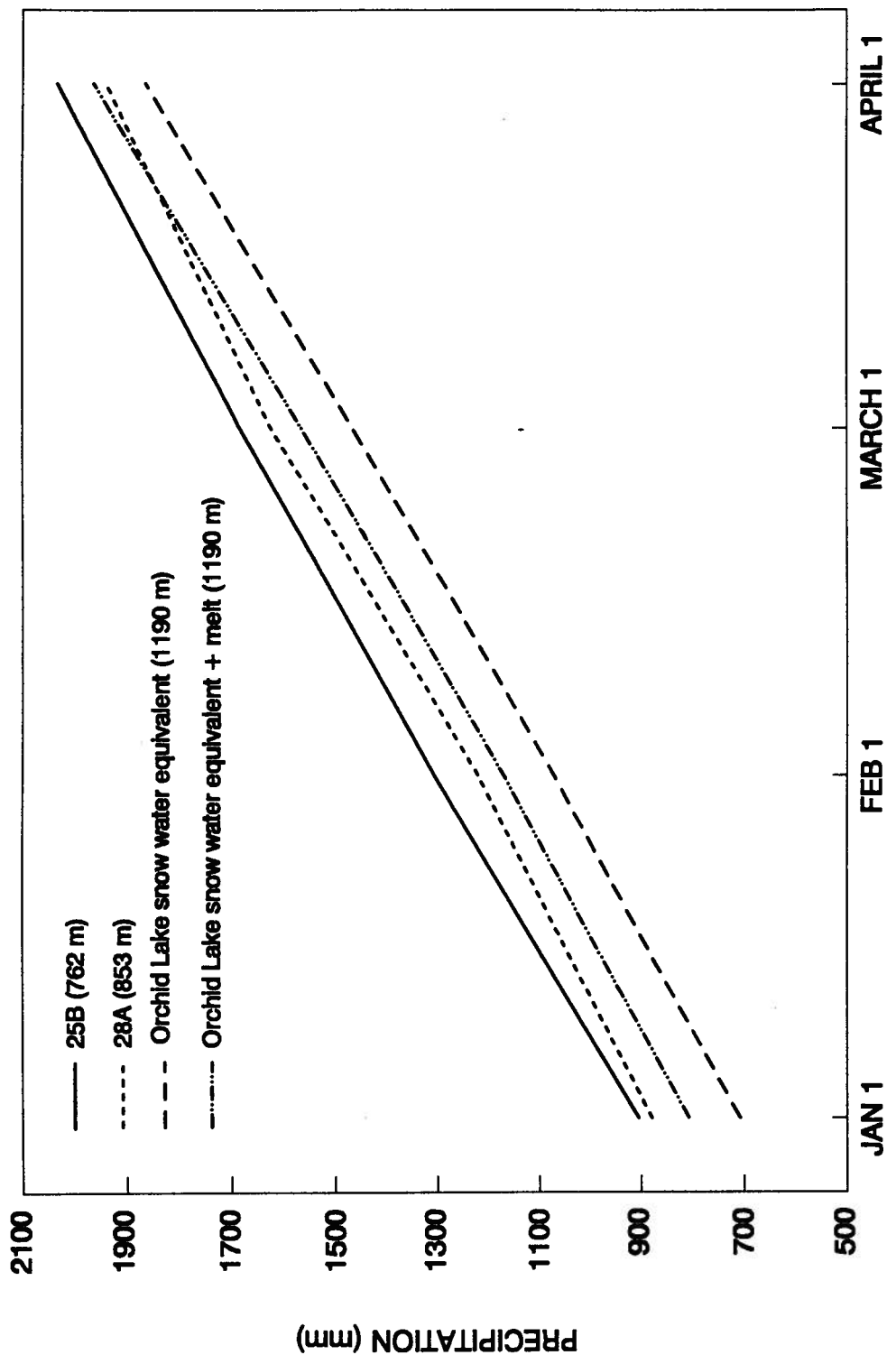


Fig. 2.5. Comparison of the precipitation accumulations with the snow course data

CHAPTER 3

ANNUAL AND SEASONAL PRECIPITATION DISTRIBUTION

3.1 Introduction

Several studies of the mountain precipitation have previously been carried out (e.g. Storr and Ferguson, 1972; Schaefer and Nikleva, 1973; Hanson, 1982; Chacon and Fernandez, 1985). These studies examined the distribution and the variation of precipitation in different climatic regions. The results of this type of study can help our understanding of the physical processes of precipitation generation, and can assist in the reliable prediction of precipitation distribution and runoff.

It is often assumed (Melone, 1986; Barry, 1992) that the precipitation distribution in the mid-latitude mountainous areas increases almost linearly with elevation. It is important for the assessment of hydrology of these regions to test this assumption for individual watersheds and for a whole region. Furthermore, it is important to investigate whether the distribution of precipitation can be adequately defined in terms of physiographic factors because in these mountainous regions the database is sparse. Comparison will be made between valley and mountain precipitation data. This comparison is necessary for the overall assessment of precipitation in the mountainous areas because most of the precipitation stations in these areas are located in the valleys. The elevation is usually used as the physiographic parameter to describe the precipitation distribution in space whereas other elements of topography like aspect and slope affect the precipitation distribution. However, in most studies the elevation is the most important topographic parameter that affects the precipitation distribution in space.

Chapter 3. ANNUAL AND SEASONAL PRECIPITATION DISTRIBUTION

In this Chapter, the study of long-term precipitation distribution on Coastal Mountains of British Columbia will be presented. The main part of the study will concentrate on the two study watersheds, the Seymour River and the Capilano River watersheds. First, the valley data will be analyzed and then they will be compared with the limited mountain slope data. The relationships of the precipitation with the topographic parameters will be identified. Also, comparison will be made with other data sources, including precipitation and runoff data from other watersheds of coastal British Columbia and the Pacific Northwest.

3.2 Spatial Distribution of Precipitation

3.2.1 Annual and seasonal precipitation distribution in the Seymour River valley

The precipitation stations in the Seymour River watershed used in the analysis are all located in the valley, but their elevation increases from 0 m to 853 m, as shown in Figure 2.3 and Table 2.2. The analysis showed that the mean annual precipitation increases quite steadily from the zero elevation station of Vancouver Harbour to the Seymour Falls Dam station at 247 m and shows an increase from 1600 mm/year to 4100 mm/year (Fig. 3.1). The increase in precipitation becomes smaller beyond this point, and finally, after station S-1, where the maximum of precipitation occurs (4200 mm/year), there is a steep decrease of precipitation to 3200 mm/year at 28A station, the highest station (Fig. 3.1).

The mean seasonal precipitation from October to March follows a pattern similar to the mean annual precipitation (Fig. 3.1). In contrast, during the April-September period the precipitation gradient becomes smaller below S-1 and larger above S-1 so that the precipitation is leveling off over the whole watershed. This six-month dry season from April

Chapter 3. ANNUAL AND SEASONAL PRECIPITATION DISTRIBUTION

to September accounts for only 25% of the annual total. The wet period from October to March accounts for about 75% of the annual precipitation and the precipitation gradients in the watershed during this wet period are about the same as the annual gradients.

The mean annual precipitation over the whole Seymour River watershed has been correlated with the physiographic features. The physiographic features used are: the station elevation, the horizontal distance from the beginning of the topographical slope, an azimuth parameter, and the average slope between stations. The azimuth was taken as the angle between the station S-1 and the other stations. The azimuth parameter is the $\cos(\text{azimuth} - 180^\circ)$. The station S-1 was selected because it is located at the position where the watershed orientation changes (Fig. 2.3). Application of stepwise linear regression shows that the distance and the elevation are the only significant independent parameters but these two parameters explain only 74% of the variation of the average annual precipitation, but better results are achieved if the analysis is split into two parts, for the upper and lower watershed, as will now be discussed. This subdivision is also suggested by the graphical plot in Figure 3.1.

By separating, the Seymour River watershed into lower and upper parts, below and above the station S-1 (Fig. 2.3), the curvilinear distribution of the annual precipitation can be replaced by two linear relationships. The annual precipitation at both the lower and the upper watershed have been correlated to the elevation and distance from the beginning of the topographical slope. Precipitation data from four stations in the lower watershed and seven stations in the upper watershed have been used. The following equations describe the precipitation-elevation and precipitation-distance relationships in the watershed:

Lower	$P=1658+9.38EL$	$R^2=0.998$	$See=69 \text{ mm}$	$n=4$	(3.1)
Upper	$P=4011-1.04EL$	$R^2=0.651$	$See=208 \text{ mm}$	$n=7$	(3.2)
Lower	$P=1559+116.06DS$	$R^2=0.982$	$See=224 \text{ mm}$	$n=4$	(3.3)
Upper	$P=6663-113.18DS$	$R^2=0.948$	$See=80 \text{ mm}$	$n=7$	(3.4)

Chapter 3. ANNUAL AND SEASONAL PRECIPITATION DISTRIBUTION

where, P is the mean annual precipitation (mm), EL is the elevation of the station (m), DS is the distance from the beginning of the topographic slope (km), and See is the standard error of estimate (mm). The above equations are significant at 5% significance level ($\alpha=0.05$)

For the lower watershed, the coefficients of determination and the standard error of estimate of the two regression equations (Eqs. 3.1 and 3.3) show that the mean annual precipitation is strongly related to both elevation and distance from the beginning of the topographical slope. However, for the upper watershed the relationship between the mean annual precipitation and distance is better than the relationship with the station elevation.

The analysis of the precipitation in the Seymour River watershed showed that the annual and seasonal precipitation increases up to the middle position of the watershed and then decreases at the upper elevations. The large increase of precipitation at the lower part of the watershed and the steep decrease at the upper watershed may be associated with the topography of the watershed. The Seymour River watershed which has a general north-south orientation, turns to a northwest-southeast orientation after its middle (Fig. 2.3). The increased convergence of the incoming air at this position may account for the steep positive and negative gradients at the lower and upper watershed, respectively. However, it is important to examine whether similar precipitation distribution is evident in an adjacent watershed which has a general north-south orientation. For this reason the precipitation distribution in Capilano River watershed will be examined in the next paragraphs.

3.2.2 Annual and seasonal precipitation distribution in the Capilano River valley

The eight precipitation stations used in the analysis represent an elevation range of 610 m (Table 2.3). The average annual precipitation, both the annual and seasonal, increases from an

Chapter 3. ANNUAL AND SEASONAL PRECIPITATION DISTRIBUTION

average of 1600 mm at Vancouver Harbour to about 4500 mm at the middle position of the watershed (station C-1), and then decreases and levels off at a value of 4000 mm (Fig. 3.2), which is similar to the precipitation distribution at the Seymour River watershed. It should be mentioned that the station C-1 is located in a small tributary of the Capilano River, the Sisters Creek. The orientation of the Sisters Creek is southeast, such that it can receive the incoming air mass directly and its large topographic gradient can trigger heavy precipitation. Unfortunately, the data set of this station, C-1, has many missing data and therefore, station C-1 has been excluded from the analysis.

The remaining precipitation stations indicate that the precipitation increases up to about the position of station C-2 and then levels off. This leveling off of the precipitation is occurring at about the middle distance from the start of the topographic slope.

The seasonal October to March precipitation follows the same pattern as the annual precipitation (Fig. 3.2). On the other hand, the summer seasonal precipitation from April to September is quite uniformly distributed over the watershed, and it is almost unaffected by the topography (Fig. 3.2).

It is therefore seen that the spatial distribution of the mean annual precipitation in the Capilano River watershed is similar to that of the Seymour River watershed. The only difference is that the precipitation at the upper watershed levels off while in the Seymour River watershed precipitation shows a decrease at the higher elevations. The change of the orientation of the Seymour River watershed after its middle position may account for this difference in the spatial distribution of precipitation between the two watersheds.

Because of the observed curvilinear distribution of precipitation the distribution of the annual precipitation at the Capilano River watershed is studied by dividing the watershed arbitrarily at station C-2 into an upper and lower section. The mean annual precipitation was again correlated to the topographical parameters. Precipitation data from four stations at the

Chapter 3. ANNUAL AND SEASONAL PRECIPITATION DISTRIBUTION

lower watershed and five stations in the upper watershed have been used and the following relationships have been developed:

Lower	$P=1483+6.76EL$	$R^2=0.983$	$See=148 \text{ mm}$	$n=4$	(3.5)
-------	-----------------	-------------	----------------------	-------	-------

Upper	$P=3597+0.41EL$	$R^2=0.329$	$See=90 \text{ mm}$	$n=4$	(3.6)
-------	-----------------	-------------	---------------------	-------	-------

Lower	$P=1430+106.18DS$	$R^2=0.964$	$See=69 \text{ mm}$	$n=4$	(3.7)
-------	-------------------	-------------	---------------------	-------	-------

Upper	$P=3832-1.55DS$	$R^2=0.009$	$See=109 \text{ mm}$	$n=4$	(3.8)
-------	-----------------	-------------	----------------------	-------	-------

where P, EL, DS and See are as previously stated. Equations 3.5 and 3.7 are significant at $\alpha=0.05$ whereas equation 3.6 is significant at $\alpha=0.01$ and equation 3.8 is not significant at $\alpha=0.01$.

The statistical parameters, R^2 and See, indicate that both relationships for the lower watershed are good. On the other hand, the relationships for the upper watershed between the annual precipitation and either the elevation or the distance from the beginning of the topographical slope indicate that there is almost no functional relationship between precipitation and either topographical parameters, because the mean annual precipitation at the upper Capilano River watershed is approximately constant, as can be seen from Figure 3.2.

3.2.3 Monthly precipitation distribution in the two study watershed valleys

Regression analyses were used to develop relationships between mean monthly precipitation and either elevation or distance from the beginning of the topographical slope (Tables 3.1 and 3.2). These relationships were developed based on the same lower and upper watershed gauge site stratification used in the mean annual analyses. Again the relationships for the lower watersheds are more consistent than those for the upper watersheds. The analyses show that during the wet season from October to April, there are steeper gradients for both the lower and upper watersheds. During the summer dry period from April to September, there is only small variation in the precipitation accumulations over the two study watersheds.

Chapter 3. ANNUAL AND SEASONAL PRECIPITATION DISTRIBUTION

Table 3.1

Regression coefficients for the monthly precipitation ($Y = a + bX$; Y=monthly precipitation; X=elevation (m) or distance from the beginning of the slope (km); a and b = coefficients)

SEYMOUR RIVER WATERSHED

	with elevation							
	Lower watershed (n=4)			See	Upper watershed (n=7)			See
	a	b	R2		a	b	R2	
January	189	1.124	0.988	22	446	-0.103	0.373	35
February	194	1.137	0.995	14	487	-0.128	0.521	32
March	164	0.976	0.997	9	443	-0.151	0.836	17
April	119	0.583	0.999	2	283	-0.114	0.758	17
May	93	0.509	0.985	11	204	-0.007	0.036*	10
June	73	0.335	0.995	4	145	-0.028	0.247	13
July	56	0.171	0.965	5	92	-0.002	0.024*	4
August	53	0.158	0.807	14	78	-0.007	0.038*	9
September	81	0.406	0.992	6	179	-0.035	0.291	14
October	154	1.102	0.996	13	400	-0.581	0.214	29
November	253	1.571	0.996	18	632	-0.171	0.531	42
December	242	1.232	0.995	16	607	-0.278	0.785	38

	with distance							
	Lower watershed (n=4)			See	Upper watershed (n=7)			See
	a	b	R2		a	b	R2	
January	177	13.933	0.974	32	757	-12.885	0.774	21
February	180	14.198	0.995	13	838	-14.692	0.923	13
March	153	12.143	0.992	16	748	-13.449	0.894	14
April	113	7.213	0.983	13	503	-9.807	0.754	17
May	88	6.259	0.956	19	255	-1.942	0.367	8
June	70	4.148	0.979	9	243	-3.961	0.671	8
July	55	2.083	0.921	9	113	-0.783	0.381	3
August	52	1.851	0.711	17	97	-0.795	0.069*	9
September	77	4.973	0.955	15	270	-3.843	0.476	12
October	143	13.571	0.969	14	613	-8.573	0.615	21
November	236	19.467	0.981	38	1091	-19.286	0.908	19
December	228	15.379	0.995	15	1162	-24.598	0.818	35

N.B. All equations are significant at $\alpha=0.05$ except for the ones noted

* Not significant at $\alpha=0.01$

Chapter 3. ANNUAL AND SEASONAL PRECIPITATION DISTRIBUTION

Table 3.2

Regression coefficients for the monthly precipitation ($Y=a+bX$; $Y=\text{monthly precipitation (mm)}$;
 $X=\text{elevation (m) or distance from the beginning of the slope (km)}$; a and $b = \text{coefficients}$)

CAPILANO RIVER WATERSHED

	with elevation								See	
	Lower watershed (n=4)			Upper watershed (n=4)			a	b	R2	
	a	b	R2	See	a	b				
January	169	0.705	0.999	4	364	0.099	0.699		10	
February	163	0.912	0.964	29	461	0.019	0.237		5	
March	131	0.808	0.942	33	392	0.069	0.232		19	
April	113	0.365	0.988	7	218	0.051	0.744		5	
May	85	0.349	0.992	5	178	0.068	0.416		12	
June	77	0.127	0.791	11	98	0.041	0.988		1	
July	58	0.118	0.958	4	87	0.031	0.483		5	
August	53	0.096	0.938	4	78	0.018	0.509		3	
September	77	0.271	0.991	4	144	0.056	0.896		3	
October	143	0.705	0.997	6	353	0.062	0.642		7	
November	212	1.038	0.961	35	575	-0.023	0.046*		16	
December	215	0.998	0.965	31	549	0.009	0.031*		8	
with distance										
	Lower watershed (n=4)			Upper watershed (n=4)			a	b	R2	See
	a	b	R2	See	a	b				
January	162	11.134	0.991	11	391	0.736	0.078*		17	
February	156	14.333	0.947	35	466	0.179	0.041*		6	
March	125	12.639	0.917	40	431	-0.246	0.006*		22	
April	110	5.723	0.967	11	227	0.561	0.177		8	
May	83	5.431	0.958	12	209	0.261	0.012*		16	
June	76	1.984	0.768	11	98	0.708	0.606		4	
July	57	1.884	0.967	4	94	0.253	0.071*		6	
August	53	1.502	0.911	5	75	0.431	0.562		3	
September	75	4.199	0.953	10	147	0.851	0.408		7	
October	137	11.096	0.981	16	371	0.412	0.058*		11	
November	203	16.325	0.945	41	605	-1.514	0.411		12	
December	207	15.711	0.951	37	569	-0.594	0.281		6	

N.B. All equations are significant at $\alpha=0.05$ except for the ones noted

*Not significant at $\alpha=0.01$

3.2.4 Comparison of mountain and valley precipitation

The distribution of precipitation over both the mountain slopes and the valleys is important for the assessment of the total hydrology of the mountainous regions. Mountain precipitation measurements are very limited and in this study the assessment of the mountain precipitation has been made using the data from Hollyburn Ridge at 930 m and Grouse Mountain Resort at 1128 m elevation for the period 1971-1990. These measurements will be compared with the data from the Capilano River watershed which has been used to assess the valley precipitation gradients.

The precipitation gradient for the mountain slopes and the valley region will be compared in two different ways, firstly, as a function of elevation, and secondly, as a function of distance from the start of the mountain region. The valley only reaches a high elevation at a considerable distance from the start of the mountains, and the precipitation gradients for similar elevations for the valley and mountain regions are quite different, as indicated in Table 3.3. However, the valley precipitation gradients at the same distance from the start of the mountain region are similar to the gradient at the immediately adjacent, but much higher mountain slope. Therefore, it appears that the valley convergence produces the same increase in precipitation as the orographic lifting caused by the mountain slopes.

Chapter 3. ANNUAL AND SEASONAL PRECIPITATION DISTRIBUTION

Table 3.3. Comparison of the annual precipitation gradient for the valley and mountain slope

	Gradient with elevation (mm/100 m)	Gradient with distance (mm/km)
Hollyburn Mountain	140	124
Grouse Mountain	129	134
Lower Seymour Valley	910	117
Lower Capilano Valley	680	125

The mean annual precipitation for stations in the lower Capilano watershed and at the two mountain stations has been correlated with the distance from the start of the slope and the percentage of barrier height, respectively, where the percentage of the barrier height for the mountain stations is the ratio of the station elevation to the mountain top elevation. For the valley stations, the elevation is assumed to be the elevation of the immediately adjacent mountain slope. The following equations describe these relationships:

$$P=1537 + 109.20DS \quad R^2=0.890 \quad \text{See}=283 \text{ mm} \quad n=7 \quad (3.9)$$

$$P=1692 + 1595.77BH \quad R^2=0.974 \quad \text{See}=112 \text{ mm} \quad n=7 \quad (3.10)$$

where P, DS, See are as previously stated and BH is the percentage of barrier height. The above equations are significant at $\alpha=0.05$.

The above relationships should not be extrapolated for the area beyond the Hollyburn and Grouse mountains because there are no data for the mountain slopes at this region. It would be very interesting and important to study the precipitation distribution at the mountain

Chapter 3. ANNUAL AND SEASONAL PRECIPITATION DISTRIBUTION

slopes beyond the first mountain peaks and to compare it with the known valley precipitation distribution.

Similar relationships have been developed for the monthly precipitation of the lower Capilano valley and the adjacent mountain slopes (Table 3.4). The results showed that the percentage of barrier height is a better overall predictor of the monthly precipitation for both valleys and the adjacent mountain slopes.

Table 3.4

Regression coefficients for the monthly precipitation ($Y=a+bX$; $Y=\text{monthly precipitation (mm)}$;
 $X=\text{distance from the beginning of the slope (km) or percentage of barrier height}$;
 a and $b = \text{coefficients}$)

Lower Capilano valley-Hollyburn and Grouse mountains

	with distance				with % of barrier height			
	a	b	R2	See	a	b	R2	See
January	161	11.048	0.953	18	204	92.872	0.521	38
February	149	14.069	0.837	46	218	79.374	0.299*	52
March	124	12.576	0.911	29	170	104.571	0.844	19
April	108	5.689	0.961	8	129	50.386	0.776	12
May	95	5.781	0.682	29	90	121.672	0.971	9
June	90	2.387	0.222*	33	70	100.073	0.996	3
July	68	2.161	0.306*	24	57	70.196	0.828	14
August	64	1.807	0.225*	25	49	73.299	0.943	8
September	87	4.528	0.606	27	79	104.552	0.987	5
October	150	11.433	0.884	31	165	172.108	0.902	24
November	206	16.367	0.939	31	258	159.486	0.856	28
December	200	15.501	0.931	31	266	108.91	0.742	28

N.B. All equations are significant at $\alpha=0.05$ except for the ones noted

* Significant at $\alpha=0.01$

3.3 Temporal Variation of Precipitation

The temporal variation of the annual, seasonal and monthly precipitation at the two study watersheds has been studied using the coefficient of variation CV where $CV = SD/X$, SD being the standard deviation, and X the average annual or monthly precipitation.

3.3.1 Seymour river watershed

The analysis showed that the variation of annual precipitation is least where the amount of precipitation is greatest and this occurs at the mid-position of the Seymour watershed. Conversely, the variability of the annual precipitation was greatest at both the lower and higher parts of the watershed where precipitation amounts are less (Fig. 3.3).

A similar pattern has been observed for the seasonal October to March precipitation, but no definable pattern is distinguishable for the summer precipitation (Fig. 3.3). However, the overall variation of precipitation for both seasons is small, having coefficient of variation of 15-20%. This is characteristic of a humid climate.

Examination of the average monthly precipitation showed that the precipitation decreases from January to July and August and then increases, having its maximum in November (Fig. 3.4a). On the other hand, the precipitation variation follows an opposite pattern being largest when the precipitation is least and vice versa (Fig. 3.4b). The variation for all stations is smallest in March and largest in August or July.

Chapter 3. ANNUAL AND SEASONAL PRECIPITATION DISTRIBUTION

3.3.2 Capilano river watershed

The analysis of the precipitation variation in the Capilano watershed showed an annual and seasonal pattern similar to the precipitation variation in the Seymour watershed. The smallest variation of the annual and wet period precipitation is observed at the mid-position of the watershed where the largest precipitation occurs, which is consistent with the more persistent cloud cover at this position resulting in more uniform precipitation. During the dry period, the smallest variation is observed at a higher elevation (Fig. 3.5). In general, the values of coefficient of variation range between 13-27 % with the largest values being observed at the lower and higher elevations.

The average monthly precipitation in the Capilano watershed shows almost exactly the same distribution pattern as in the Seymour watershed, decreasing from January to June, leveling off in July and August and increasing after September having the maximum in November (Fig. 3.6a). The coefficient of variation of the monthly precipitation follows an opposite pattern to that of the monthly precipitation. The smallest variation is observed in March or April and the largest in July or August. The general trend of variation is to decrease from January to April or March, to increase then till August and to decrease after September (Fig. 3.6b).

3.4 Spatial Variation of Precipitation

To study the spatial variability of precipitation the Pearson's correlation coefficient (r) is used:

$$r = \frac{\sum x_i x_j - \frac{\sum x_i \sum x_j}{N}}{\frac{1}{N} \left\{ \left[\sum x_i^2 - (\sum x_i)^2 \right] \left[\sum x_j^2 - (\sum x_j)^2 \right] \right\}^{0.5}} \quad (3.11)$$

where N is the number of pairs of values of stations i and j, and x is the annual, seasonal or monthly precipitation. The correlation coefficient gives the statistical association between the precipitation series at two stations. It will be assumed that the correlation coefficient is only a function of distance (Bras and Rodriguez-Iturbe, 1985). The correlation may be expressed as:

$$r(d) = r(0) \exp(-d/d_0) \quad (3.12)$$

where d is the distance between stations i and j, d_0 is the correlation radius (it is the distance at which the correlation reduces by a factor of e) and $r(0)$ is the value of the correlation function at a short distance (theoretically equal to 1, but because of random errors in the measurements it is less than 1). For the two study watersheds all the stations in the watershed are used to obtain the correlation functions.

3.4.1 Seymour River watershed

The monthly distributions of the correlation coefficients for seven stations in the Seymour River watershed are shown in Figure 3.7. The mean values of the correlation coefficient are large for the monthly, annual and seasonal totals during the period October-March, so that the precipitation at different stations is, in general, well correlated. The only exception is the correlation coefficients between the records of station 28A, the highest station, and Vancouver Harbour, the lowest station, for March and April (Fig. 3.7). The localized rain showers during that period of the year may account for this weak correlation.

The correlation functions for the annual, seasonal, and the wettest and driest months are shown in Figure 3.8. The highest correlation has been observed for the November precipitation (the wettest month) with r values larger than 0.88 for distances smaller than 32 km. The annual totals and the precipitation during the wet period October-March follow about the same pattern. On the other hand, the correlation coefficient decreases for the August precipitation (the driest month) and for the seasonal totals during the April-September period, having values smaller than 0.65 for distances smaller than 32 km.

The reason for these high values of r is that during the wet period October-March, the strong frontal systems cover the whole watershed with precipitation. During the dry period, from April to September, the source of precipitation is convective rain showers and weak frontal systems, which are a little more variable across the watershed, so that the coefficient of correlation is smaller than the values of r during the wet period.

The expressions of the correlation functions for the Seymour watershed and correspond to the curves of Figure 3.8 are:

$$\text{Annual total: } r(d)=0.964\exp(-0.005d) \quad (3.13)$$

$$\text{Seasonal total (Oct.-Mar.): } r(d)=0.974\exp(-0.005d) \quad (3.14)$$

$$\text{November total: } r(d)=0.950\exp(-0.003d) \quad (3.15)$$

$$\text{Seasonal total (Apr.-Sep.): } r(d)=0.931\exp(-0.013d) \quad (3.16)$$

$$\text{August total: } r(d)=0.960\exp(-0.013d) \quad (3.17)$$

It is therefore seen that the precipitation is highly correlated for distances shorter than 32 km.

3.4.2 Capilano River watershed

Figure 3.9 shows the monthly distributions of the correlation coefficients for the seven stations of Capilano River watershed. The values of the correlation coefficient are high and in most cases larger than 0.70. The highest correlation is observed during the wettest month, November.

The correlation functions for the annual, seasonal totals, and for the wettest and driest months are presented in Figure 3.10. The highest correlation is again observed during the wettest month, November. In November r takes values larger than 0.88 for distances smaller than 32 km. The correlation coefficient takes values larger than 0.83 and 0.79 for distances smaller than 32 km for the seasonal precipitation October-March and the annual totals, respectively. During the summer the correlation coefficients are larger than 0.74 for distances less than 32 km. For the driest month, August, the correlation coefficient is larger than any other month for distances smaller than 15 km. This can be explained because the precipitation is generated by convective rain showers, which result in higher correlation of precipitation for smaller distances.

The expressions for the correlation functions developed for the Capilano watershed and correspond to the curves of Figure 3.10 are:

$$\text{Annual total: } r(d)=0.940\exp(-0.006d) \quad (3.18)$$

$$\text{Seasonal total (Oct.-Mar.): } r(d)=0.931\exp(-0.004d) \quad (3.19)$$

$$\text{November total: } r(d)=0.918\exp(-0.002d) \quad (3.20)$$

$$\text{Seasonal total (Apr.-Mar.): } r(d)=0.973\exp(-0.009d) \quad (3.21)$$

$$\text{August total: } r(d)=0.950\exp(-0.006d) \quad (3.22)$$

The correlation analysis for both study watersheds showed that the correlation coefficient is usually large ranging from 0.80 for the wet period of October to March to 0.6 for the dry period of April to September, for distances less than 32 km.

3.5 Comparison with Other Studies and Regional Data

The transferability of the results of this study has been examined by comparing the results with other studies in the greater region of the coastal Pacific Northwest. It is very important to examine whether the leveling off of the precipitation at high elevations is a general result for the coastal Pacific Northwest, especially because some of the literature assumes that the precipitation in the mid-latitude areas increases almost linearly with elevation up to the top elevation (Barry, 1992). At least two studies have investigated the distribution of precipitation in the mountains of the Pacific Northwest region. In the first of these studies, Schermerhorn (1967) related the annual precipitation in the Northern Washington State to large scale topographic and latitude factors. When Schermerhorn plotted the mean annual precipitation against the station elevation, he found that the annual precipitation follows a curvilinear pattern increasing up to about 400-500 m elevation, and then decreasing at the upper elevations.

The second study, by Rasmussen and Tangborn (1976), analyzed the annual and seasonal precipitation of 38 stations on the west slopes of the North Cascades region of Washington, an area of about 20,000 km². They found that the annual precipitation increases with station elevation up to an elevation of 400-500 m, and then levels off at the upper elevations (Fig. 3.11a) but they concluded that this leveling was due to inaccurate data. A similar distribution was also observed for the winter precipitation, whereas, during summer, the precipitation was more uniformly distributed with elevation (Fig. 3.11a).

Chapter 3. ANNUAL AND SEASONAL PRECIPITATION DISTRIBUTION

In the same study, Rasmussen and Tangborn (1976) examined the coefficient of variation and showed that the summer precipitation is more variable than the annual and the winter precipitation, which have values of about 10-20 % (Fig. 3.11b), but no discernible change in coefficient of variation with elevation was observed.

In both these earlier studies, Rasmussen and Tangborn as well as Schermerhorn concluded that precipitation increases with elevation even though their data can be shown to be more consistent with the leveling off of precipitation, as found in the present study. They stated that the precipitation pattern observed was the result of inefficient precipitation gauges and inadequate location.

An indirect way for the examination of the precipitation distribution is by studying the runoff distribution with elevation over the whole region. The runoff is the result of precipitation, evapotranspiration, and change of basin storage. Studies in San Joaquin River basin in California (Longacre and Blaney, 1962), northeastern U.S.A. (Dingman, 1981) and the Alps (Barry, 1992) have shown that the evapotranspiration decreases rapidly with elevation. Longacre and Blaney (1962) measured the mean annual evaporation from reservoir water surfaces at various elevations in San Joaquin River basin. They found that the mean annual evaporation decreases linearly for the first 1200 m of elevation from 1800 mm to 1150 mm. Above the 1200 m there is a decrease to about 914 mm at 2400 m and above this elevation there is only a slight change with elevation. This change of evaporation with elevation is indicative of the pattern of evaporation decrease with elevation although the evapotranspiration values can be significantly lower because of soil water limitations. In another study, Dingman (1981) found that the mean annual evapotranspiration in New Hampshire and Vermont decreases linearly with elevation from 580 mm at sea level to 500 mm at 600 m. Similar results have been reported by Barry (1992) for the Alps but for higher

Chapter 3. ANNUAL AND SEASONAL PRECIPITATION DISTRIBUTION

elevations. It has been found that the mean annual evapotranspiration in the Alps decreases at a rate of 20 mm/100 m elevation from the sea level to 4000 m.

There are no available studies of evapotranspiration change with elevation in coastal British Columbia. The various measurements in this region have shown that the mean annual evapotranspiration in forested mountainous watersheds varies between 450 mm to 710 mm (Schaefer and Nikleva, 1973). It is reasonable to assume a linear decrease of evapotranspiration with elevation, as the previous studies have shown. In addition, runoff is much larger than evapotranspiration so that the final estimates of precipitation are not overly sensitive to the change of evapotranspiration with elevation.

The basin storage change is small when glaciers are not present, the accumulation of snow at high elevations melts during spring and summer, and there are no man-made reservoirs in the basin. Hence, if the runoff from a number of basins from the hydrologically homogeneous region of the coastal Pacific Northwest shows a definite distribution pattern with mean basin elevation, then its distribution can be used as a qualitative indication of the precipitation distribution with elevation over the region.

In the study of Rasmussen and Tangborn (1976), the mean annual runoff from 36 basins located in the western and eastern side of North Cascades was analyzed. From these data, eight basins located in the eastern rain shadow side of the Cascade Mountains were excluded. Figure 3.12 shows the distribution of the mean annual runoff of the remaining 28 basins as a function of their mean basin elevation. The mean annual runoff shows a similar pattern to that of the annual precipitation, except for one station. The mean annual runoff increases with the mean elevation of the basin up to about 800 m, and then decreases at the upper elevations.

The one basin that exhibited a high runoff value at a high elevation was found to have 53.3% of its area covered by glaciers (South Fork Cascade River in Fig. 3.12). The effects of

Chapter 3. ANNUAL AND SEASONAL PRECIPITATION DISTRIBUTION

glaciers on the basin runoff are well documented for the coastal Pacific Northwest (Fountain and Tangborn, 1985; Moore, 1992). Recent studies in the greater area of the Pacific Northwest have shown that the glaciers in the area are shrinking. For example, Pelto (1989) noted that the area of South Cascade Glacier in Washington State, decreased from 3.1 km² in 1955 to 2.8 km² in 1989, and Moore (1992) reported that the area of the Sentinel Glacier in British Columbia decreased from 1.85 km² in 1966 to 1.75 km² in 1989. Hence, the highly glacierized basins will show large runoff from this extra glacier melt.

Although these streamflow runoff studies generally confirm the precipitation analyses of this study, further confirmation can be obtained by examining precipitation data from other stations in coastal British Columbia. To carry out this examination, data from 269 precipitation stations located on the west slopes of the Coastal Mountains were analyzed. Precipitation data published by Environment Canada (1981) were used. The precipitation stations used in the analysis are shown in Table A1 in Appendix A. Figure 3.13a shows the distribution of the mean annual precipitation and its variation with the station elevation. The area of the coastal British Columbia is about 211,000 km², and the interaction of the weather systems with the topographical features causes this large variation. Although it is not possible to distinguish a definable pattern of precipitation distribution because of the large variation of precipitation for the same elevation, it is possible to observe certain trends. For example, it is evident that the mean annual precipitation does not continue to increase with elevation, and may even decrease at the higher elevations.

The above study on basin mean annual runoff in the north Cascade region has been extended by using data within coastal British Columbia. The purpose is to check the precipitation distribution with elevation observed at the coastal region of British Columbia, by analyzing the mean annual runoff from basins within the region. Streamflow data

Chapter 3. ANNUAL AND SEASONAL PRECIPITATION DISTRIBUTION

published by Environment Canada (1989) were used. Basins meeting the following criteria were considered for the analysis:

- the drainage area must lie in the west side of the Coastal Mountains,
- there must not be any storage impoundment,
- there must be more than nine years of record, and
- the glacierized percentage of the basin should be smaller than 1% of the total basin area.

Forty-seven basins meeting these criteria were selected for analysis. The streamflow stations used in the analysis are shown in Table A2 in Appendix A.

The mean annual runoff of each of the forty-seven basins was plotted against the mean basin elevation in Figure 3.14. The mean elevation of the basins was determined from 1:50,000 topographical maps. Although the variability is high, it is evident that the runoff increases with the mean basin elevation up to 400 m and then decreases at higher elevations, except for one basin (Fig. 3.14). This basin is the Zeballos River basin located in the west of Vancouver Island, and it exhibits one of the largest runoff responses in coastal British Columbia. Unfortunately, there are no precipitation data in the intermediate area to test the reliability of these runoff measurements.

The results of the Rasmussen and Tangborn (1976), and Schermerhorn (1967) studies, and the analyses presented above for coastal British Columbia precipitation and runoff were based on stations that are far apart and are not located in the same watershed. However, they cover large areas and give a good indication of the regional distribution of precipitation with elevation. All their results are comparable with the more detailed results found in this study for the Seymour River and Capilano River watersheds. The valley elevation where the maximum precipitation occurs, is about 400 m in the Capilano watershed, whereas in the

Chapter 3. ANNUAL AND SEASONAL PRECIPITATION DISTRIBUTION

Seymour watershed it is less because of the topography of the area, and these valley elevations correspond to neighboring mountain slope elevations of 1200 to 1300 m. Beyond these points of maximum precipitation, the precipitation either levels off or decreases. Furthermore, the uniformity of the summer precipitation distribution and the low values of the temporal variation of the winter and the annual precipitation observed in this study also have been revealed in the regional data.

Analysis of the coefficient of variation of the precipitation data from the 269 stations in coastal British Columbia showed that the variation of precipitation decreases at an elevation range of about 400-700 m and that the maximum variation is observed at the low or high-level station (Fig. 3.13b). These results support the findings of the analysis of the temporal variation of precipitation in the two study watersheds.

3.6. Meteorological Mechanisms Affecting the Precipitation Distribution

Examination of the precipitation distribution in the Seymour River and Capilano River watersheds revealed a distinct pattern of precipitation distribution which seems to repeat in the coastal region of the Pacific Northwest. The precipitation does not continue to increase with elevation but increases up to an elevation and then either decreases or levels off. The processes involved in the rapid production of hydrometeors in low-level orographically lifted air have been addressed by Bergeron's suggestion of a two-cloud system (Bergeron, 1960; Browning et al, 1974, 1975). According to the Bergeron's mechanism an upper "seeder" cloud is assumed to precipitate with no influence from the terrain. This cloud is associated with the ascent in the regional synoptic-scale disturbance. Its mid-troposphere position and its temperature cause the formation of ice crystals. The precipitation from the regional "seeder" cloud is partly evaporated on its way to the earth's surface. This decreases the precipitation

rate at the surface but moistens the low-level air. When this low-level air is orographically lifted or funneled in valleys, it reaches saturation quickly and a dense low-level cloud or fog is formed. This low-level cloud is called the "feeder" cloud, and is positioned at the low and middle elevations of the mountainous area and it is controlled by the orography. The falling hydrometeors collect cloud droplets, from this "feeder" cloud, and grow in size. Furthermore, the number of the falling droplets or ice crystals increases at the position of the low-level "feeder" cloud so that its position defines the position of the maximum precipitation.

The "seeder-feeder" mechanism is an idealization. In reality, the two clouds may be combined into one and the upper "seeder" cloud may be affected by the terrain (Smith, 1989).

It is believed that the Bergeron's two-cloud mechanism is responsible for the steep precipitation gradients at the lower study watersheds. Furthermore, Barry and Chorley (1987) noted that the elevation of the maximum precipitation is close to the mean cloud base. For the nearby Mount Seymour, Fitzharris (1975) estimated the layer of the mean cloud base at about 500 m or even lower. However, the elevation of this layer changes from storm to storm, and depends on the topography and the air mass characteristics. This mid-elevation position of the lower "feeder" cloud generates the steep precipitation gradients observed in the two study watersheds and indicated in the regional precipitation and runoff data.

Above the mid-position of the watersheds, the precipitation is generated mainly by the upper "seeder" cloud, which is either not influenced or influenced only to a small degree by the topography. As a result, the precipitation over the upper watershed becomes more uniform and levels off. This is the distribution that is observed in the Capilano River watershed. However, the precipitation in the valley of the Seymour River watershed decreases after its middle position. The change of Seymour valley orientation at this middle position may be responsible for the abrupt decrease of the precipitation at the upper elevations

Chapter 3. ANNUAL AND SEASONAL PRECIPITATION DISTRIBUTION

and the steeper gradients at the lower Seymour River watershed than the lower Capilano valley.

The "seeder-feeder" mechanism is likely to produce the precipitation in the study area during frontal storms. This type of precipitation occurs in winter and fall and accounts for about 75% of the annual precipitation.

In the summer, the precipitation becomes more uniform over the two watersheds. During this period, the strength of the weather systems decline and the precipitation in the area is produced either by convective rain showers or weak frontal systems. Under these conditions the air is able to intrude further in the watershed resulting in more uniform precipitation over the watersheds.

3.7 Summary

This study has shown that long-term precipitation distribution in the two study watersheds does increase linearly with elevation up to a certain position or elevation and then beyond this position the precipitation levels off or even decreases. This position seems to be around the middle of the watersheds where the valley elevation is about 400 m and the neighboring mountain elevation is about 1000 m. The Bergeron two cloud "seeder-feeder" system is assumed to be the mechanism that generates most of the precipitation in the area during the winter and fall months. During the summer the precipitation gradients in the study watersheds become smaller and more uniform precipitation is observed over the area.

Another important finding of this study is that the precipitation for both the lower valleys and the adjacent mountain slopes is similar. Correlation of the annual precipitation with the topographical features showed that the barrier height controls the precipitation

Chapter 3. ANNUAL AND SEASONAL PRECIPITATION DISTRIBUTION

generation for both the valley and the mountain slopes, and so can better explain the variation of the precipitation.

The temporal variation of the annual and seasonal October to March precipitation is, usually, small with the smallest variation being observed at the mid-watershed. The variability of the precipitation increases at the upper and lower elevations. The orographic lifting and the valley convergence are most efficient at the middle position of the watersheds, resulting in high cloud cover and precipitation. The lower part of the watersheds is slightly away from the effects of the orography and so it receives more variable precipitation.

The monthly precipitation decreases in summer and takes its maximum value in November. The temporal variation of monthly precipitation follows the opposite pattern. The largest variation is observed during the summer months for all elevations.

Application of the spatial correlation to the study watersheds showed that the spatial variation is generally small, even for the dry summer period and in all cases the correlation coefficient was larger than 0.65 for distances smaller than 32 km.

The results of this study, and especially the spatial distribution of the precipitation with elevation, have been compared with the results of two previous studies of precipitation in the coastal Pacific Northwest as well as with the findings of the precipitation and runoff analyses for coastal British Columbia. This comparison suggests that the precipitation distribution observed in the two study watersheds is more general and can possibly be used for the greater coastal area of the Pacific Northwest when data are not available. However, the findings of this study might not be applicable to other areas and should be compared with observed data to detect any similarities or differences.

Chapter 3. ANNUAL AND SEASONAL PRECIPITATION DISTRIBUTION

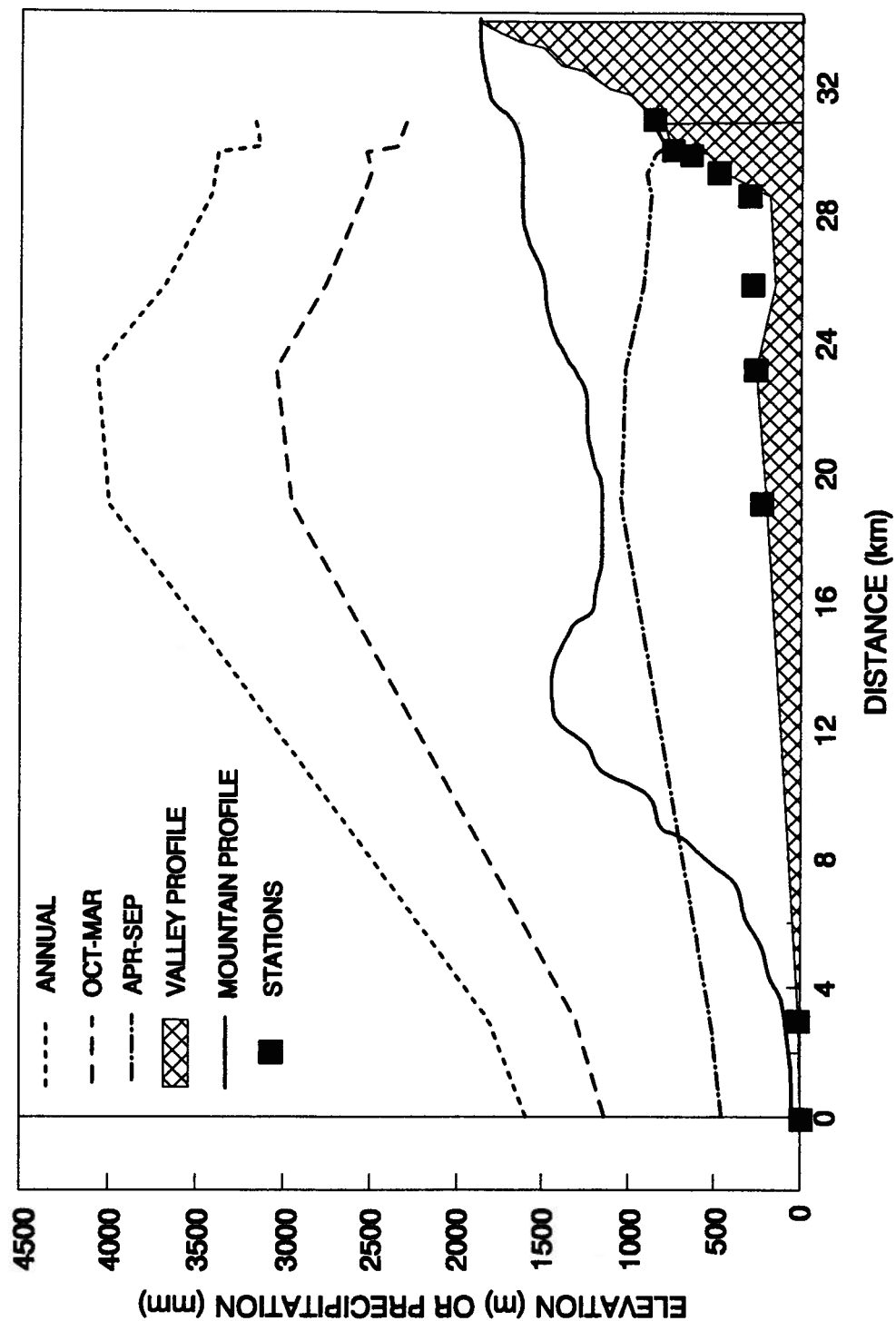


Fig. 3.1. The distribution of the annual and seasonal precipitation along the topographic profile of the Seymour River watershed.

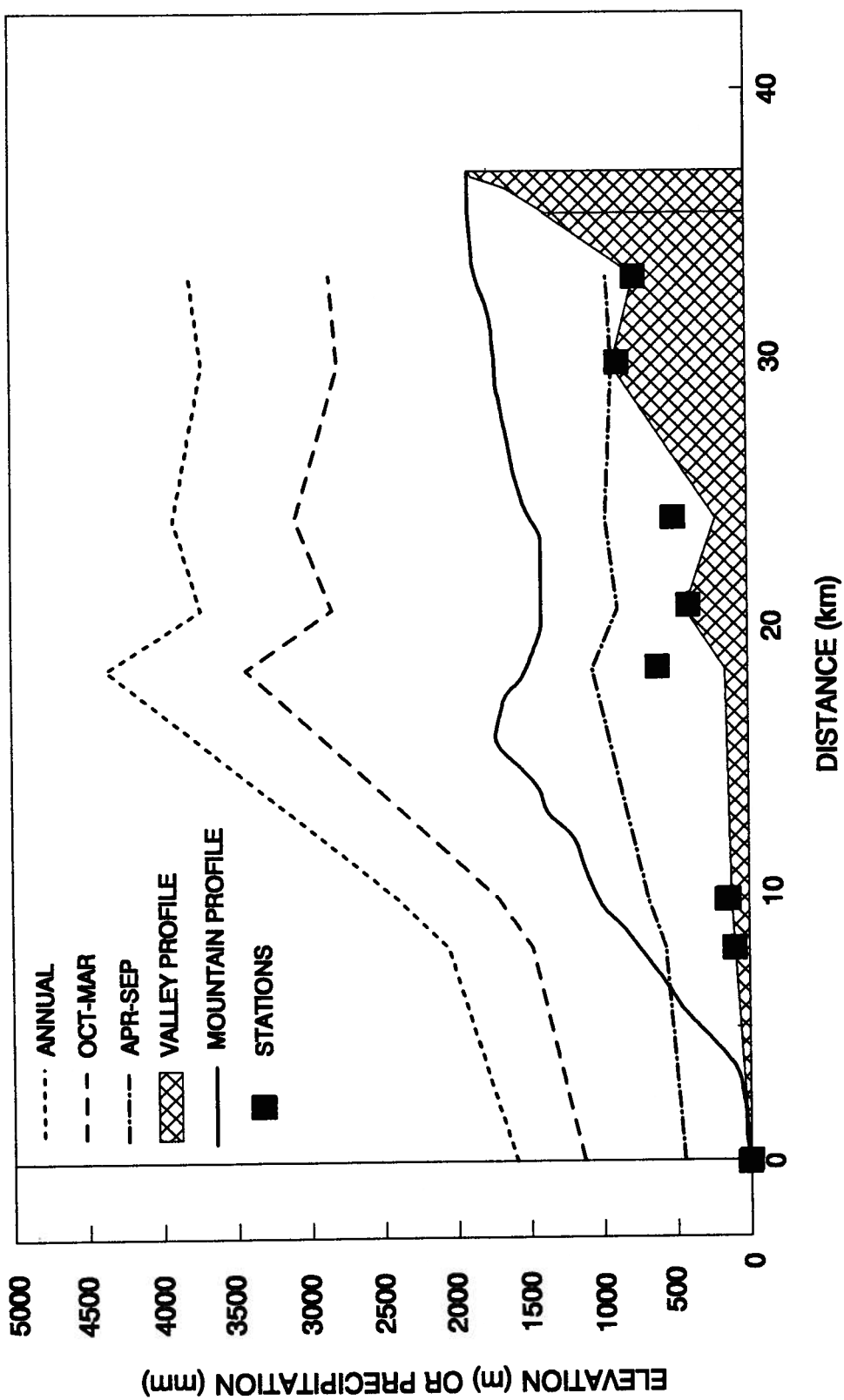


Fig. 3.2. The distribution of the annual and seasonal precipitation along the topographic profile of the Capilano River watershed.

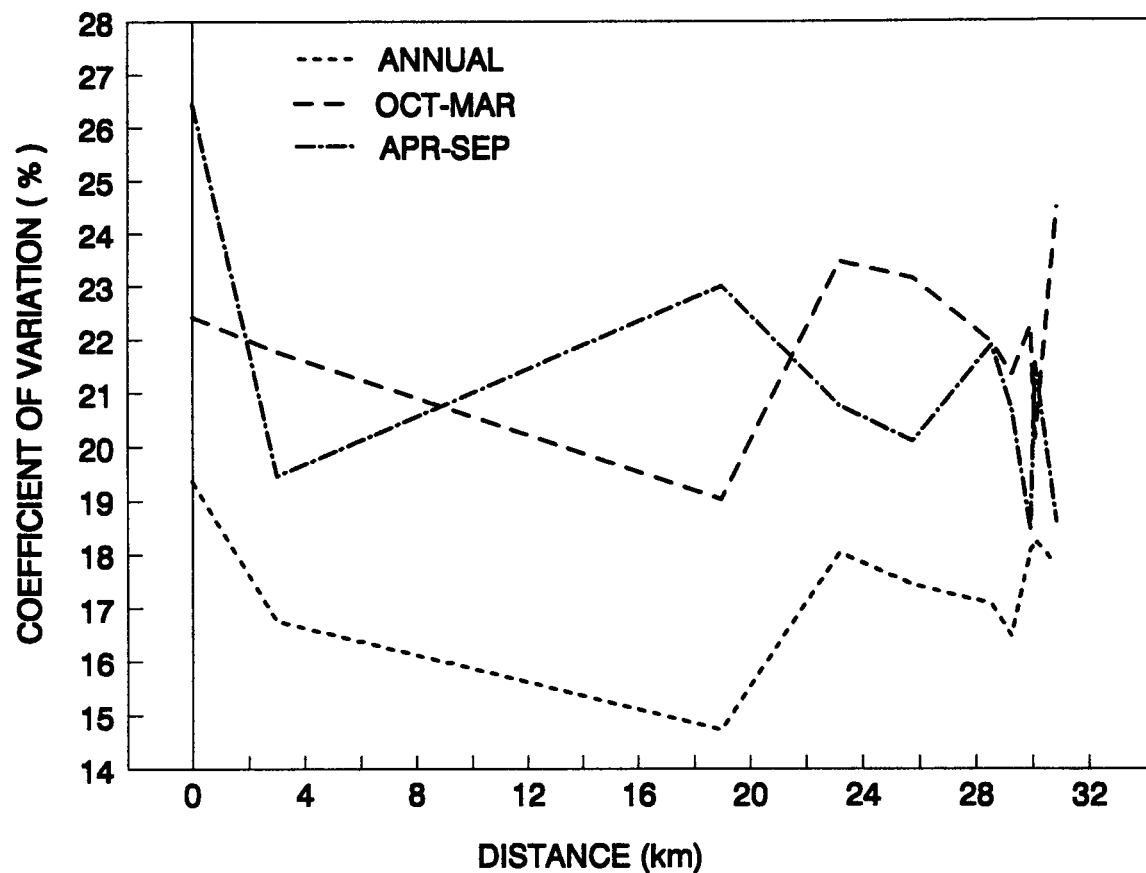


Fig. 3.3. The coefficients of variation of the annual and seasonal precipitation at the Seymour River watershed.

Chapter 3. ANNUAL AND SEASONAL PRECIPITATION DISTRIBUTION

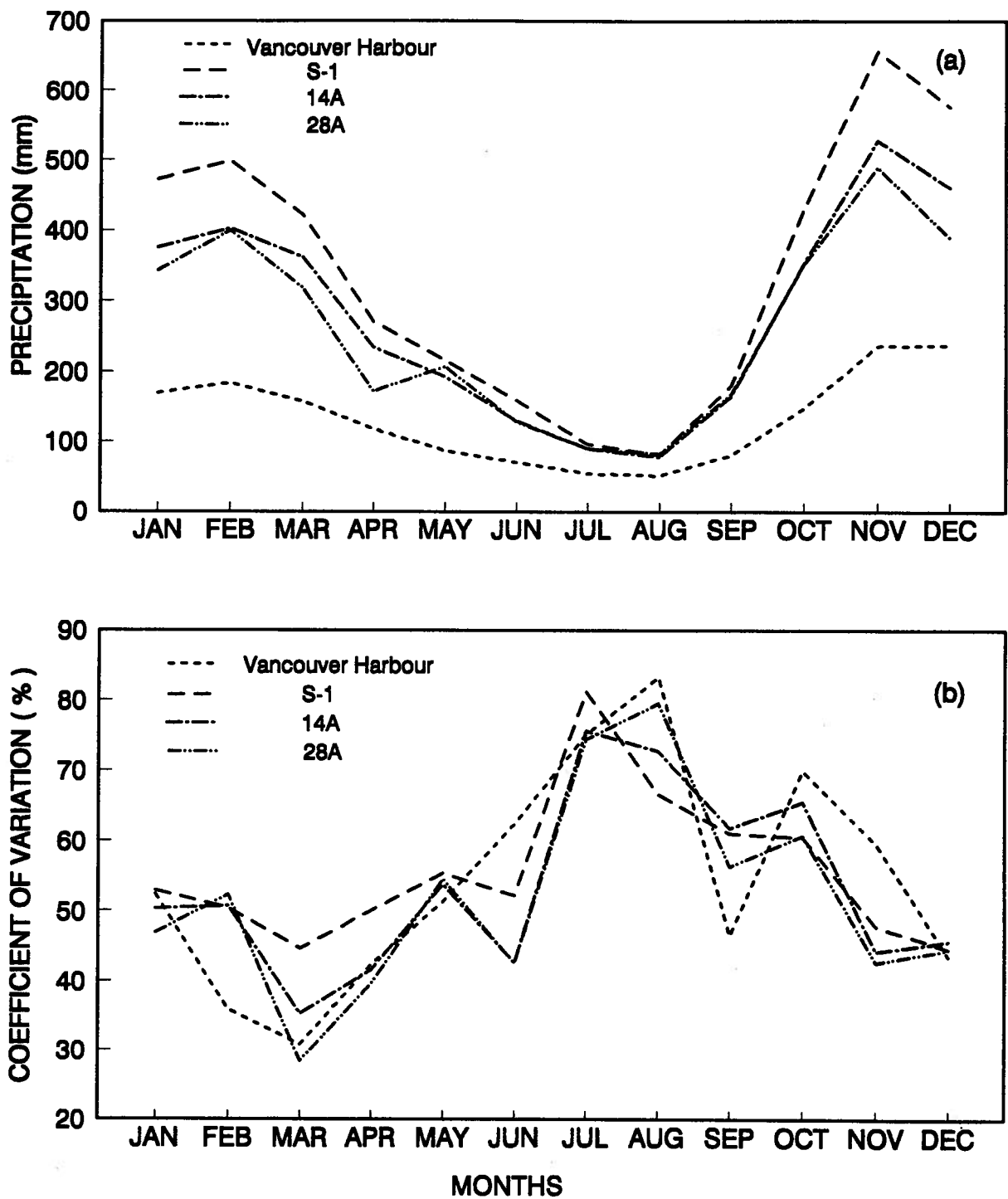


Fig. 3.4. (a) The distribution of the monthly precipitation at selected stations at the Seymour River watershed and (b) its coefficients of variation.

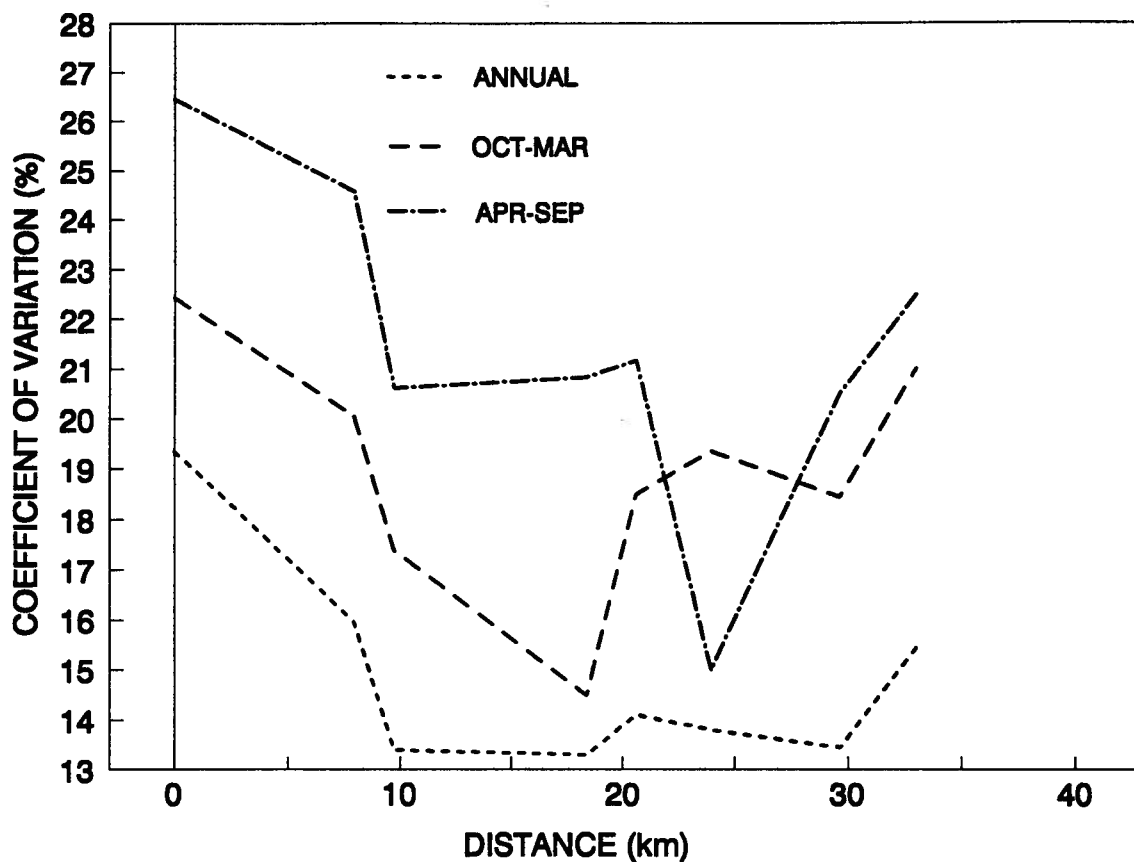


Fig. 3.5. The coefficients of variation of the annual and seasonal precipitation at the Capilano River watershed.

Chapter 3. ANNUAL AND SEASONAL PRECIPITATION DISTRIBUTION

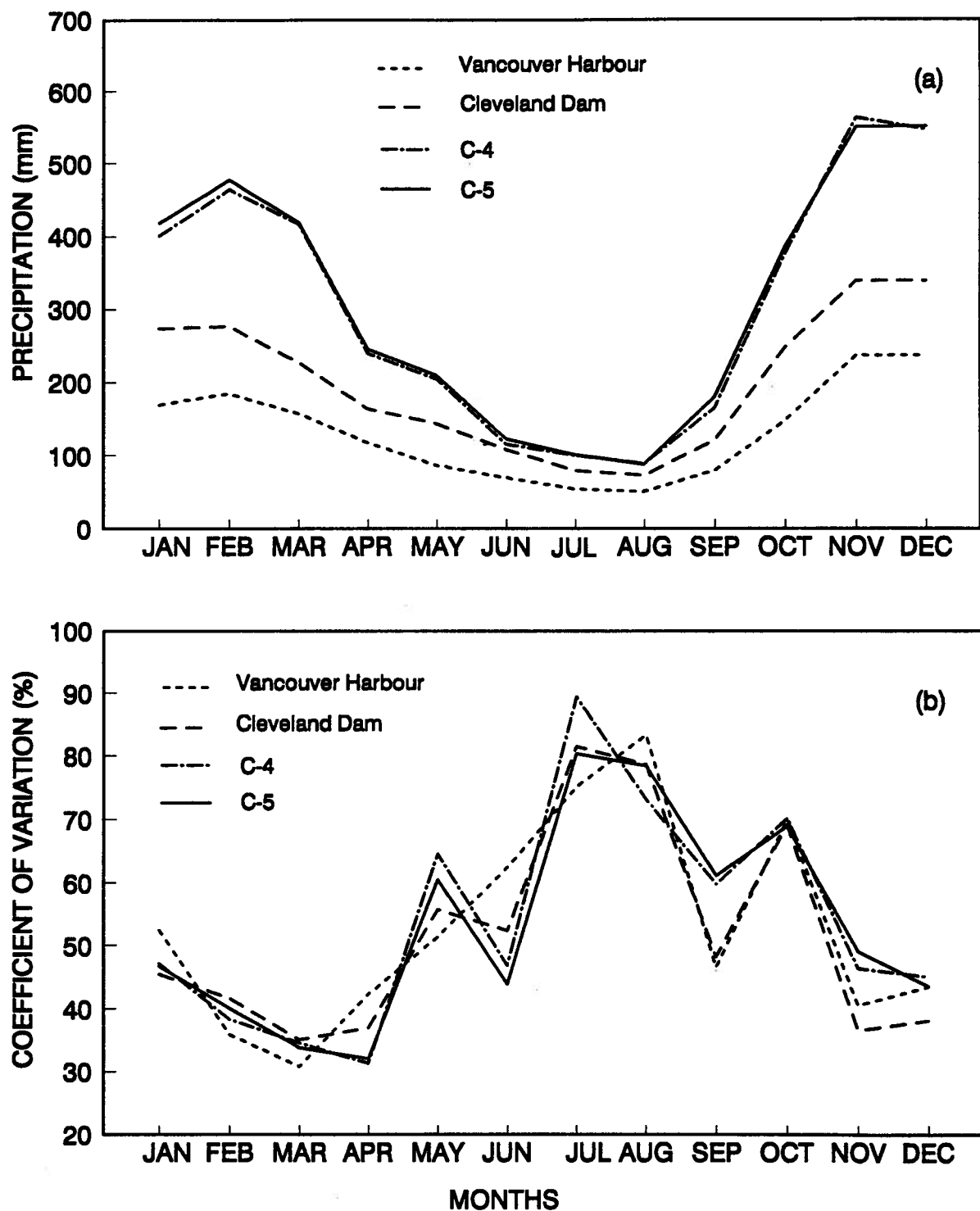


Fig. 3.6. (a) The distribution of the monthly precipitation at selected stations at the Capilano River watershed and (b) its coefficients of variation.

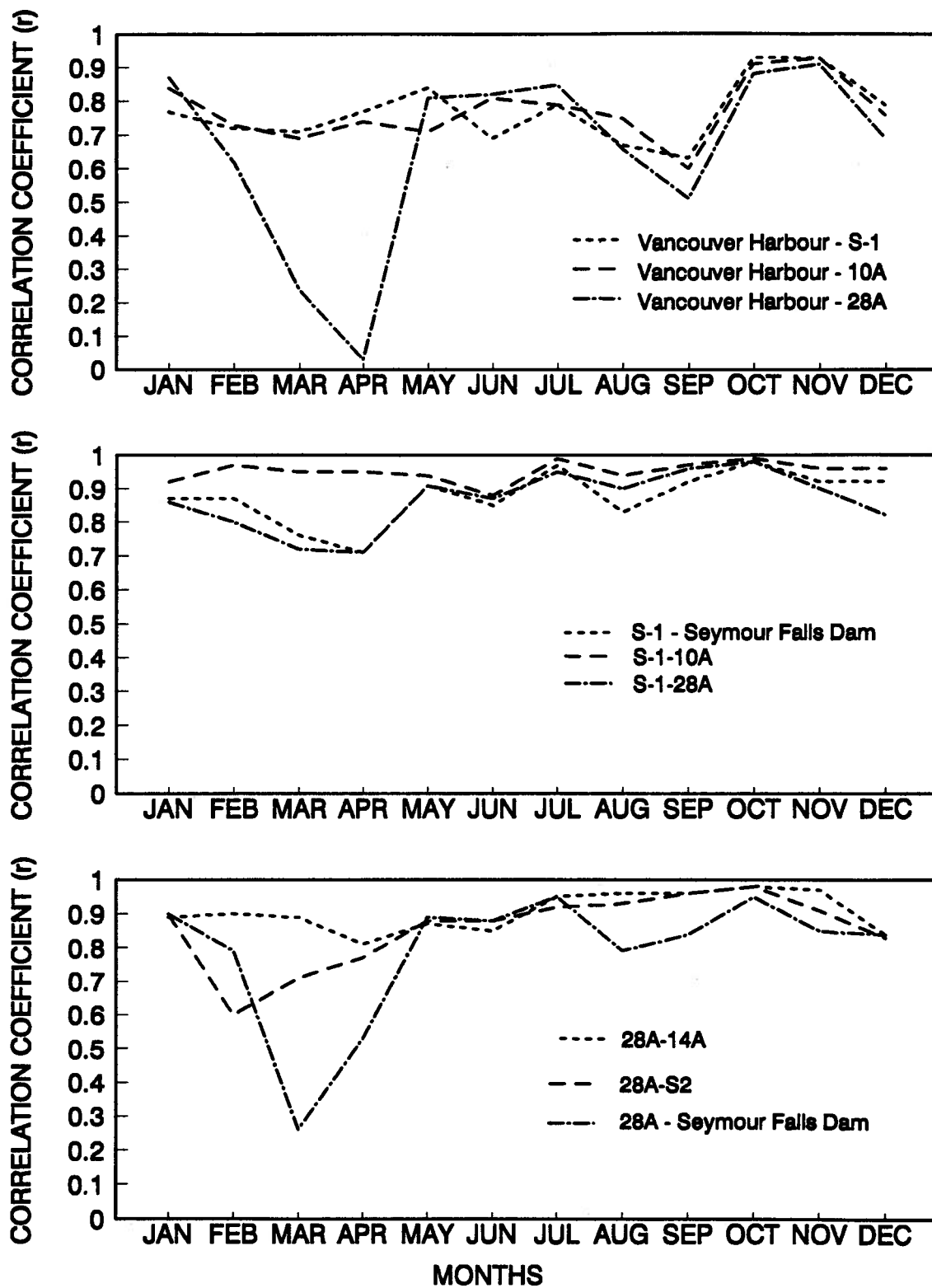


Fig. 3.7. Monthly distribution of the correlation coefficient between several stations in the Seymour River watershed.

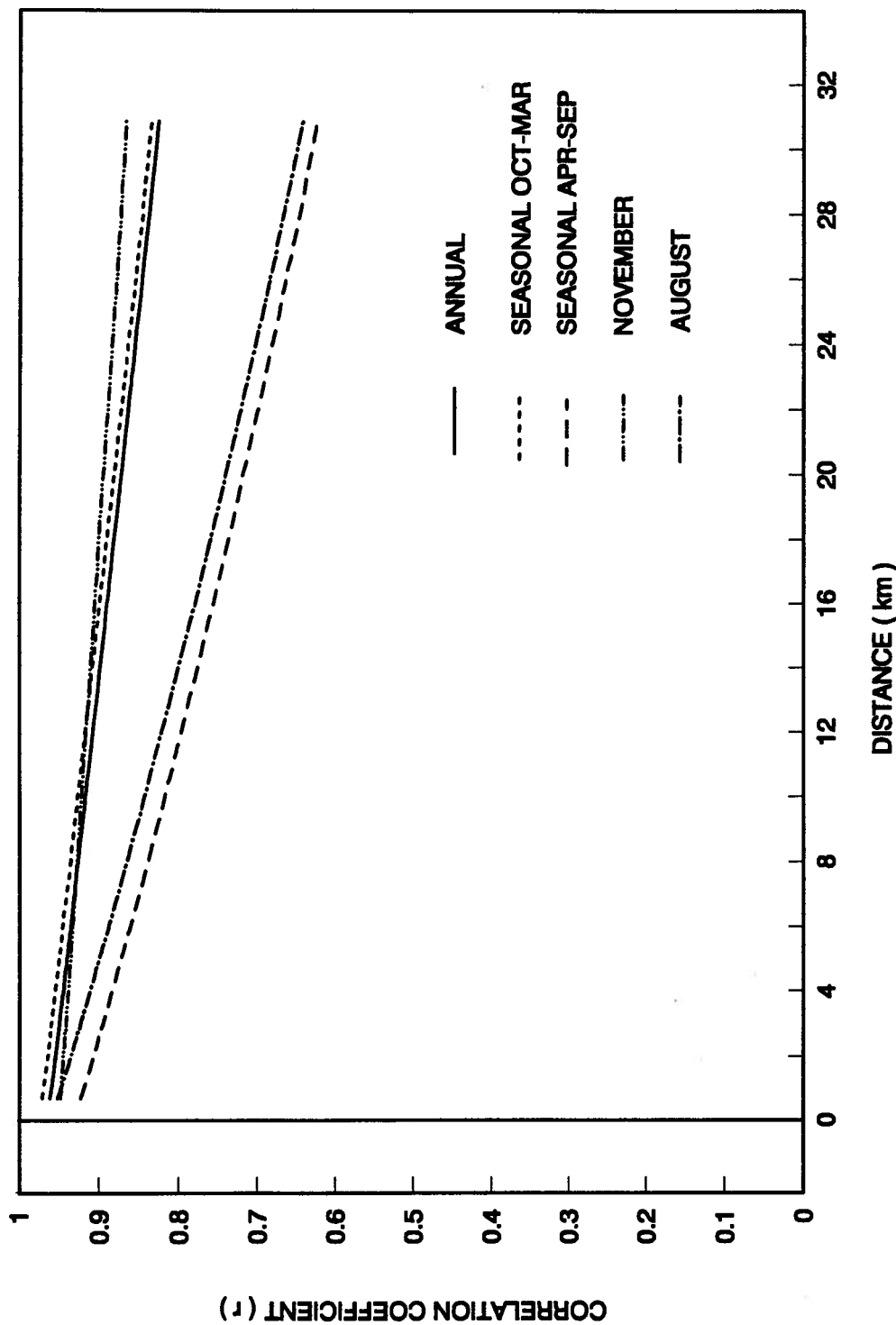


Fig. 3.8. Spatial correlation functions of annual, seasonal, and November and August precipitation in the Seymour River watershed.

Chapter 3. ANNUAL AND SEASONAL PRECIPITATION DISTRIBUTION

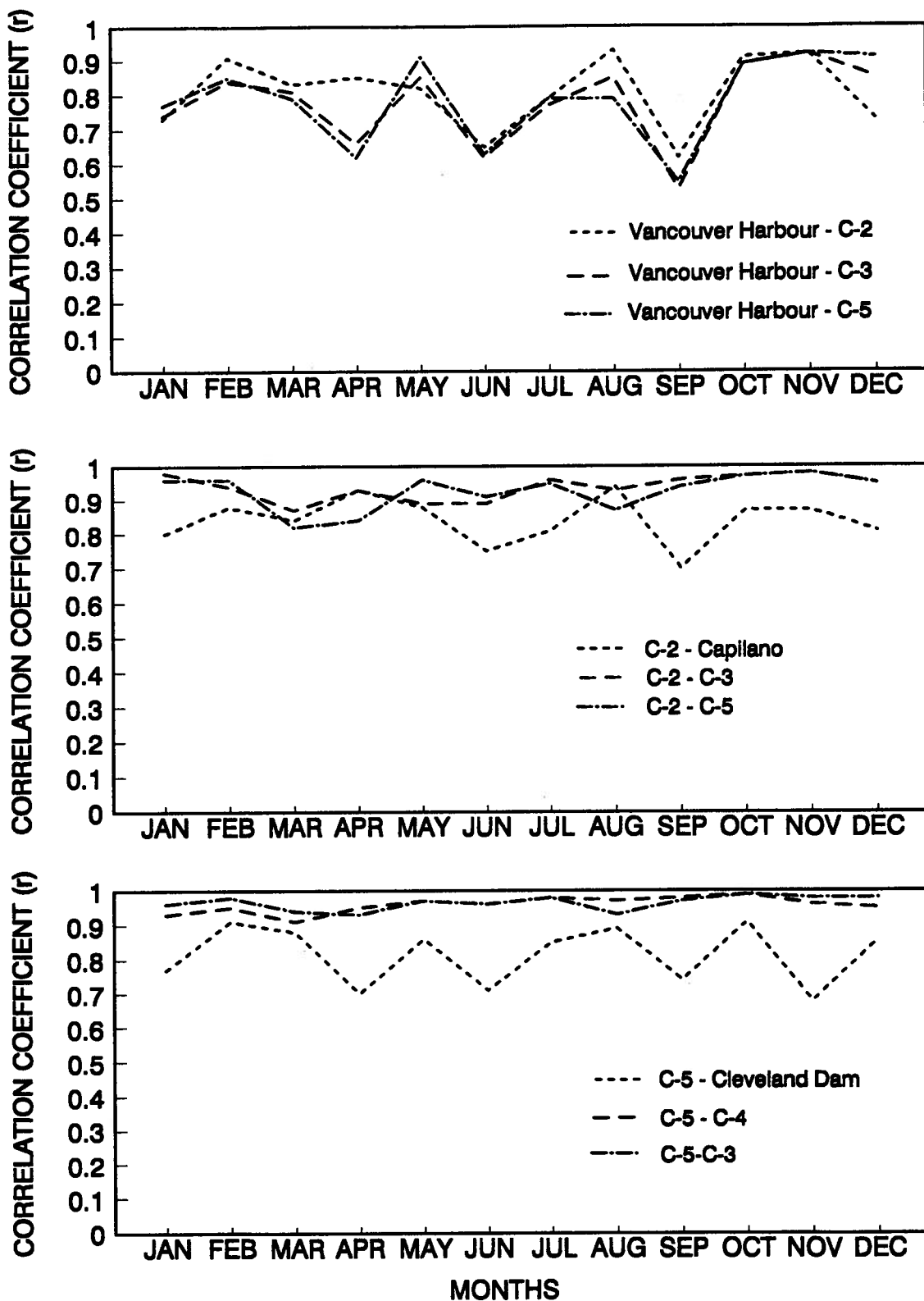


Fig. 3.9. Monthly distribution of the correlation coefficient between several stations in the Capilano River watershed.

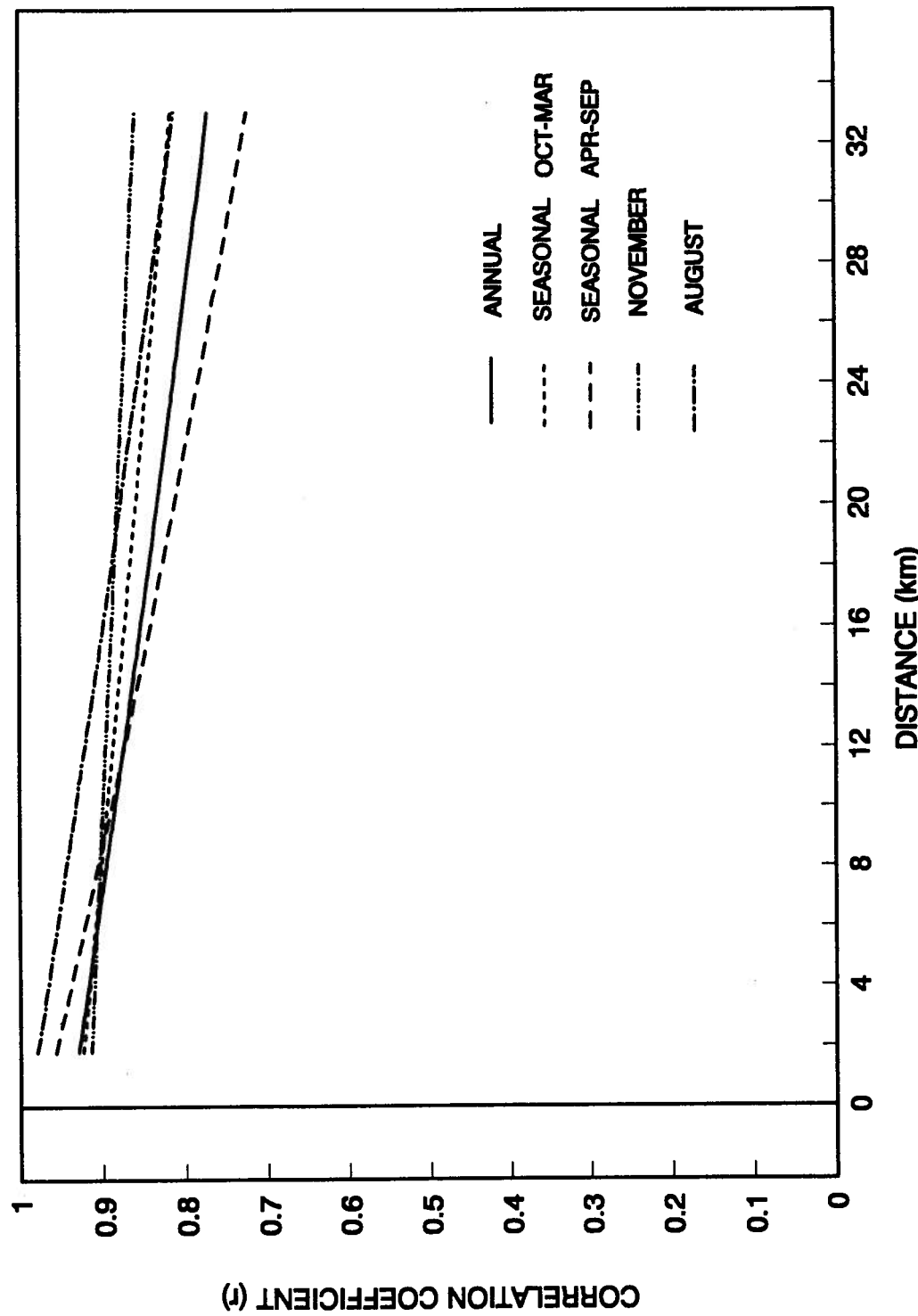


Fig. 3.10. Spatial correlation functions of annual, seasonal, and November and August precipitation in the Capilano River watershed.

Chapter 3. ANNUAL AND SEASONAL PRECIPITATION DISTRIBUTION

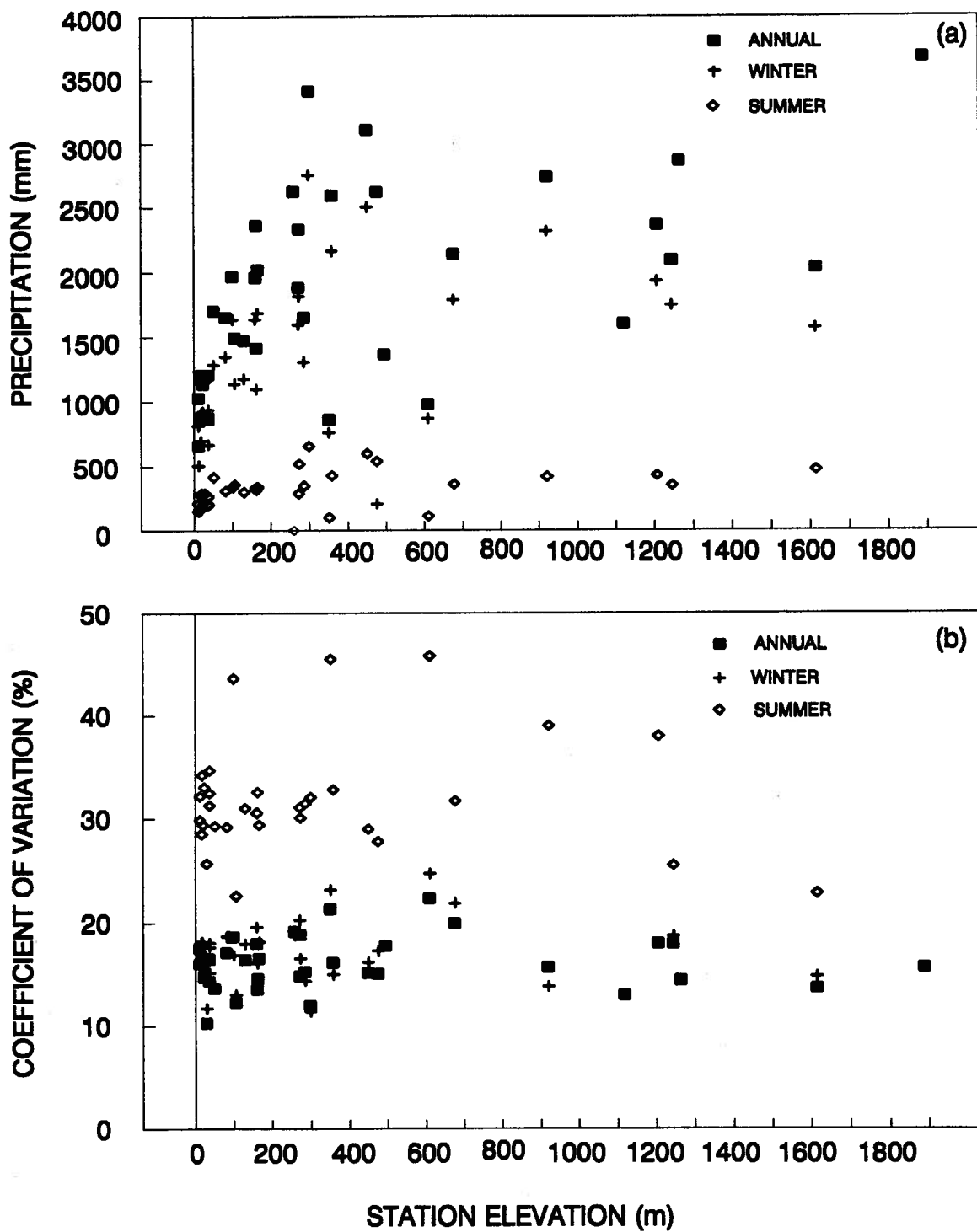
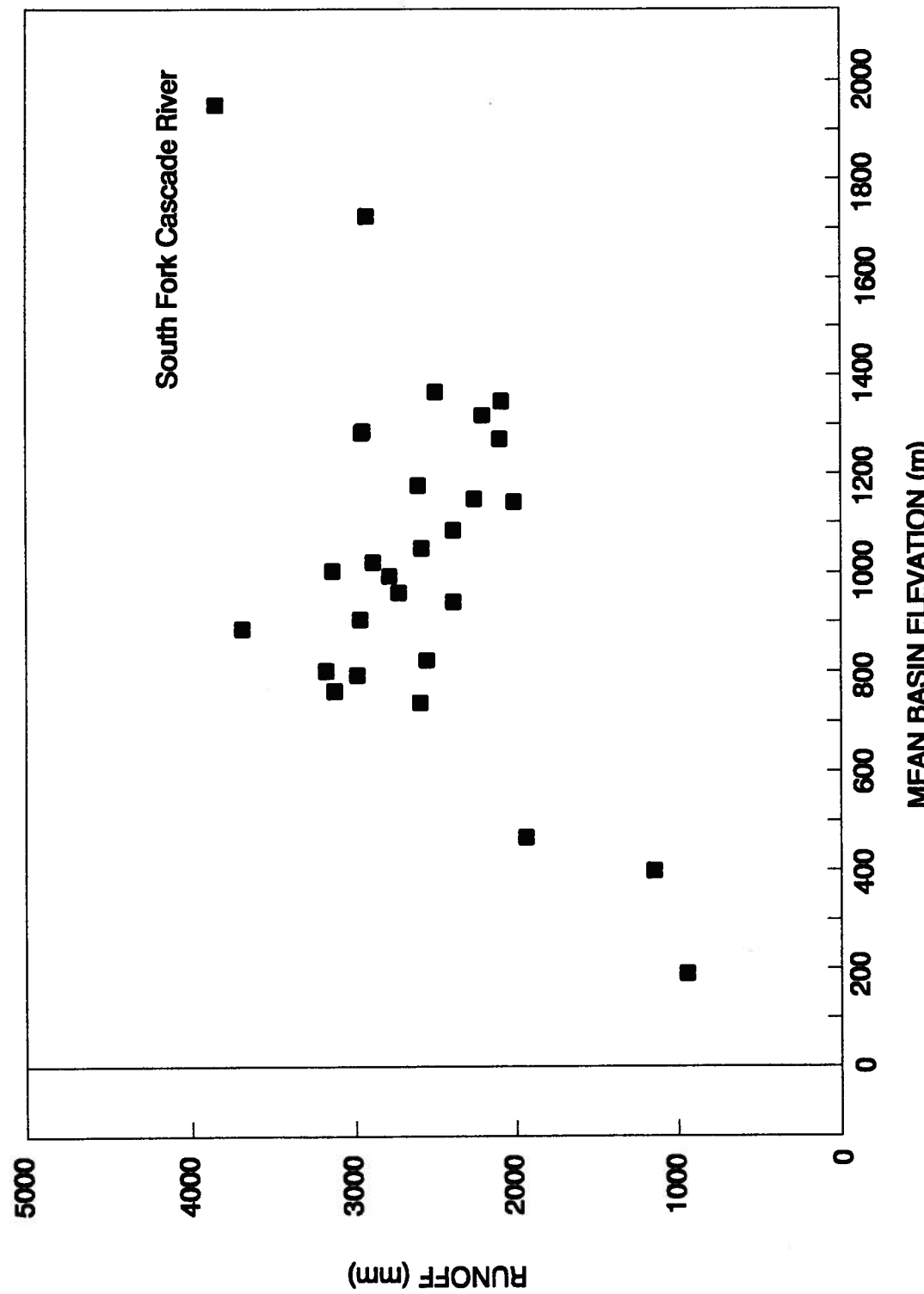


Fig.3.11 a) Distribution of the annual and seasonal precipitation with elevation and (b) coefficients of variation for the annual and seasonal precipitation at different elevations in the North Cascades, Washington State.
 (after data of Rasmussen and Tangborn, 1976)



**Fig. 3.12. Distribution of the mean annual runoff with mean basin elevation for northern Cascades region
(after data of Rasmussen and Tangborn, 1976)**

Chapter 3. ANNUAL AND SEASONAL PRECIPITATION DISTRIBUTION

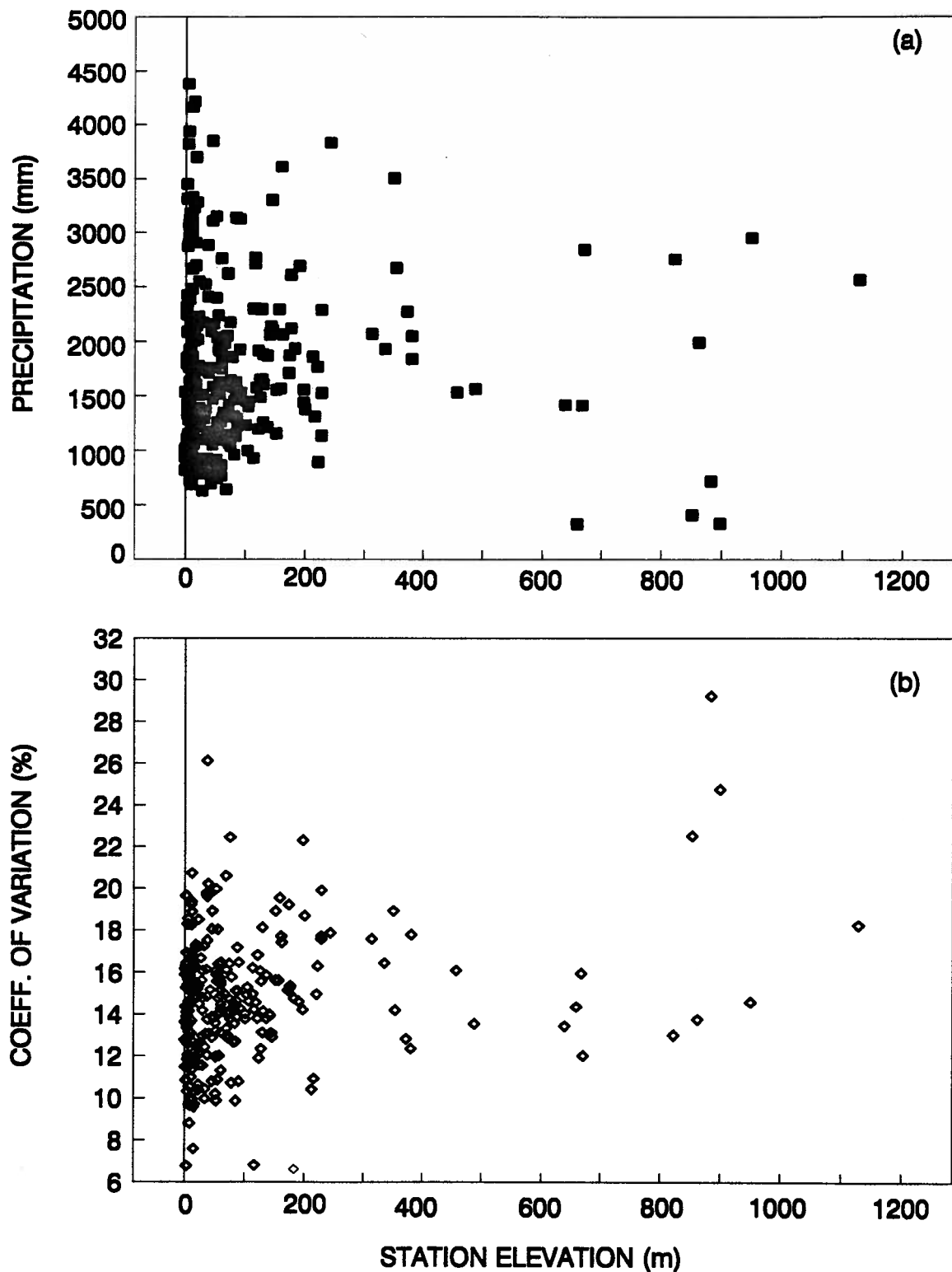


Fig. 3.13. Distribution of annual precipitation (a) and its coefficient of variation (b) with elevation for coastal British Columbia stations (269 stations).

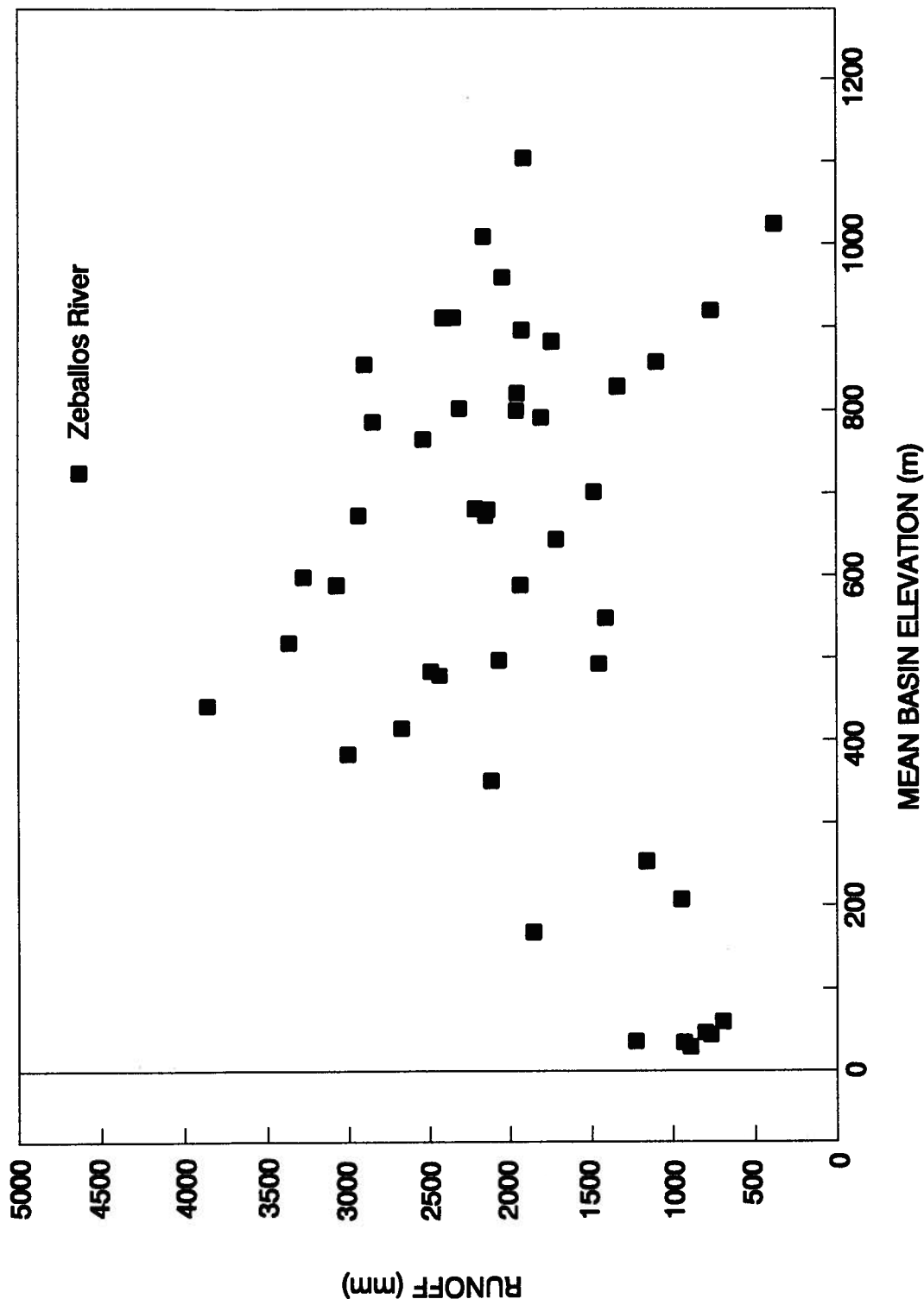


Fig. 3.14. Distribution of the mean annual runoff with mean basin elevation for coastal British Columbia stations.

CHAPTER 4

STORM PRECIPITATION DISTRIBUTION

4.1 Introduction

The precipitation distribution and variability in longer time-scales namely, annual, seasonal and monthly scales is adequate for long-term reservoir operation, water supply and irrigation. On the other hand, the knowledge of precipitation in short time-scales like daily, hourly and during a storm is necessary for the simulation of runoff and especially for flood flows. The importance of adequately defining the spatial and temporal distribution of storm precipitation for modeling streamflow and evaluating the runoff response of a watershed has been well recognized among hydrologists (Beven and Hornberger, 1982; Bras *et al*, 1985; Watts and Calver, 1991). The need for better estimation, description and modeling of precipitation has led hydrologists to identify the spatial and time variation of precipitation and quantify this variation in many different climates (Sharon, 1980; Berndtsson and Niemcynowicz, 1986; Hughes and Wright, 1988; Corradini and Melone, 1989; Wheater *et al*, 1991). The importance of the precipitation distribution becomes critical for the mountainous watersheds where the weather systems interact with the topography resulting in highly non-uniform precipitation over the area. Hence, it is necessary to study the precipitation in detail, in order to understand its distribution and, consequently, be able to predict the river flows with improved accuracy.

The objective of this chapter is to present the results of the study of spatial and time distribution of storm precipitation in the Seymour River watershed, to compare the results

Chapter 4. STORM PRECIPITATION DISTRIBUTION

with data from other coastal British Columbia stations and finally, to identify similarities between the distribution of the storm precipitation and the annual and seasonal precipitation.

4.2 Data Sets

The data for the analysis have been taken from six recording stations in the Seymour watershed for the period December 1983 to December 1990. The data from the stations S-1, 10A, 14A, 21A, 25B and 28A have been used (Table 2.2 and Fig. 2.3). The data set from the Vancouver Harbour station is used to assess the zero elevation precipitation. The stations are under the jurisdiction of two organizations, the Atmospheric Environment Service (A.E.S.) and the Faculty of Forestry of the University British Columbia (U.B.C.).

Data in hourly time increments have been used. The stations 21A and 28A (Table 2.2) are equipped with charts that can be read with an accuracy of three hours. The other four stations the precipitation can be read in hourly increments. Therefore, the stations 21A and 28A will not be used in the analysis of intensity and duration but they will be used in the study of the storm precipitation distribution.

A storm is defined as the precipitation period separated from the preceding and succeeding rainfall by 6 or more hours at all stations. All storms used had mean watershed precipitation exceeding 20 mm, and the average storm intensity was larger than 1 mm/h. Within the data period 175 network storms having total duration from 10 hours to 7 days qualified for the study.

Attention is paid so that the seasonal distribution of the storms analyzed follows the monthly precipitation distribution. Figure 4.1 compares the monthly distribution of the average annual precipitation distribution at station S-1 with the monthly distribution of the 175 storms analyzed.

Chapter 4. STORM PRECIPITATION DISTRIBUTION

The storms have been classified as rainfall events, mixed rain and snow events and snowfall events according to whether the temperature at 762 m elevation (station 25B) was above 2°C, between 0° and 2°C or below 0°C, respectively. The transitional air temperature from snow to rain has been examined by Rohrer (1989). Rohrer determined that this temperature is around 2°C. This same transitional temperature is used in the U.B.C. watershed model (Quick, 1993) for the classification of the precipitation into snow and rain.

The rainfall events have also been separated into summer and winter storms to examine if the distribution is different for the winter frontal and the summer convective rains. Forty-three events (25% of the 175 events) were classified as rainfall storms of the October-March period, fifty-three events (30% of the 175 events) as April to September rain storms, forty-four (25% of the 175 events) as snowfalls, and thirty five events (20% of the 175 events) as mixed snow and rain events.

The division of the events on the above categories has been made using air temperature data from the Vancouver Harbour and the 25B stations. The majority of the events had a duration larger than 24 hours so that the mean daily temperature was assumed to give the average temperature during the storms. For the periods of missing temperature data at station 25B, the Vancouver Harbour data and an average temperature lapse rate of -0.9°C per 100 m elevation was used to estimate the mean daily temperature at the higher elevation stations in the Seymour River watershed. This lapse rate was found from the temperature data at the stations Vancouver Harbour and 25B. It should be noted that during a particular storm it may snow at the upper elevations, while raining at the middle and lower elevations. Hence, the same storm can produce three types of precipitation, rainfall, snowfall, and mixed rain and snow, over the elevation range of the study watershed.

Chapter 4. STORM PRECIPITATION DISTRIBUTION

4.3 Spatial Distribution of Storms

The spatial distribution of the storms in the Seymour River watershed is investigated by examining the ratio of the value of certain storm features at each of the stations compared with the base station, Vancouver Harbour. The storm features analyzed are: the storm depth, the storm duration, the average storm intensity, the maximum hourly intensity and the relative start time of the storm. The spatial distribution of each of these storm features will be examined.

4.3.1 Storm precipitation

Based on the precipitation measured at the base station, the ratio of precipitation for all types of events increases to about 3.5 at 260 m (station S-1), and then decreases abruptly to about 2.8 at 293 m (station 10A). This large decrease coincides with the turn of the Seymour River valley to the northwest. For rainfall events during the winter period (October to March) the ratio seems to stabilize at a value of about 2.7 at the upper watershed (Fig. 4.2a). The April to September rain events show a leveling of the ratio up to an elevation of about 600 m and then the ratio increases to a maximum of 3.2 at 853 m (station 28A) (Fig. 4.2a). For the mixed events there is a constant decrease of the ratio to about 2.55 at 853 m (Fig. 4.2a). The snowfall events show a decrease in the ratio to about 2.3 at 600 m elevation, and then the ratio increases to 2.8 at 853 m (Fig. 4.2a).

The variation of the precipitation ratio increases up to the station S-1 (293 m), and then either levels off or increases. For the winter rainfall events the variation decreases after station S-1, but then levels off before increasing at the upper station. For the summer rainfalls the variation increases slowly for all elevations. The snow events and the mixed events show

Chapter 4. STORM PRECIPITATION DISTRIBUTION

similar variation, except for the snow events in which the variation increases at the top station at 853 m. Most of the variation at the upper watershed is high, between 30-60 % (Fig. 4.2b).

The above results indicate that the precipitation always increases with elevation up to the middle watershed, and then decreases and levels off at the upper elevations. This is evident for the winter rainfall storms and the mixed rain-snow events. However, the precipitation during the snow events and the summer rainfalls increases, on average, at the top station 28A at 853 m. A possible explanation is that at low temperatures the air is becoming more stable and after the subsidence that occurs immediately after the middle watershed, the snowfall increases again as the air is forced to lift over the steep headwater slopes of the watershed. Somewhat unexpectedly, there is a similar increase for summer rain events in the upper watershed, when convective instability may occur as the warm air is forced to rise over the steep slopes, generating larger precipitation and larger intensities at the upper watershed during the summer months (Barry, 1992). Data from more stations are required to substantiate this precipitation increase at the upper elevations during the snow and summer rain events, so that no definite conclusions can be made at present.

The above results also show that the storm precipitation has a similar distribution pattern to the distribution of the long-term precipitation, although the increase of storm precipitation with elevation is larger than the annual and seasonal precipitation increase. The storms analyzed in this study are the larger storms, which must therefore have a steeper precipitation gradient than the smaller storms.

4.3.1.1 Spatial variation

To study the spatial variability of the storm precipitation the correlation coefficient (r) is used as it has been used in Chapter 3 for the annual precipitation. It is again assumed that the

Chapter 4. STORM PRECIPITATION DISTRIBUTION

correlation coefficient is only function of distance. The underlying assumption of the spatial correlation is that the precipitation field is homogeneous and isotropic.

The spatial correlation functions developed in this way using the data sets for the 175 storms from the seven stations are:

$$\text{Rainfall October-March} \quad r(d) = 0.942\exp(-0.005d) \quad (4.1)$$

$$\text{Rainfall April-September} \quad r(d) = 0.924\exp(-0.008d) \quad (4.2)$$

$$\text{Snow} \quad r(d) = 0.925\exp(-0.003d) \quad (4.3)$$

$$\text{Mixed Rain and Snow} \quad r(d) = 0.999\exp(-0.010d) \quad (4.4)$$

Figure 4.3 shows the above correlation functions. All the types of storms have correlation coefficients larger than 0.75 for distances smaller than 32 km. Furthermore, the snow and the winter rainfall events have similar correlation functions and their values are always larger than the correlations for the April-September events.

These results show that during the snow and winter rainfall events the precipitation is the least variable in space and more consistent relationships exist between the storm accumulations of the various stations. The precipitation during the winter months is generated by strong frontal systems, and these systems cover large areas, producing more uniform precipitation over the medium-sized watershed.

On the other hand, the largest spatial variability is observed during the summer storms. The precipitation during this period of the year is produced by weak frontal systems and convective rains. Even though these types of precipitation systems cover the whole watershed, they produce more variable precipitation than the winter storms, but even so the overall spatial variability of precipitation can still be considered small.

Chapter 4. STORM PRECIPITATION DISTRIBUTION

4.3.2 Duration and average storm intensity

The total duration of the storm is assessed as the time when precipitation is first recorded at any station and the time that it ceases at all stations. At each individual station, the duration is the time period in which non-zero precipitation was recorded.

The ratio of storm duration at each station divided by the total duration gives an indication of the continuity of precipitation. The average duration of storm at zero elevation (Vancouver Harbour) is only 45 % of the total duration, whereas it is about 75 % at the mid and upper watershed. No significant differences have been observed for the different type of events (Fig. 4.4a). The variation of the storm continuity is larger (30 %-50 %) at the zero elevation and smaller (20 %) at the mid-position. The summer rainfalls and the snow events show the largest variation in storm continuity at the low elevations whereas for the mixed events the variation in storm continuity is larger at the upper watershed than at mid-elevation (Fig. 4.4b).

The relative storm duration at each station to that of the base station Vancouver Harbour has also been studied. The analysis shows that the duration is about twice at the mid-position and at the upper watershed (Fig. 4.5a). Small differences are observed among the different type of events. The variation of these results is larger at the upper watershed for snow events and summer rainfalls, and at the mid-position for the winter storms and the mixed events (Fig. 4.4b).

Comparing these results with the previous results of the storm precipitation, one can see that large precipitation at the upper watershed is mainly due to larger duration. A second reason for the large precipitation at the mid-position of the watershed is the larger average storm intensities. Examination of the average storm intensity (storm depth over duration) indicates that the average storm intensity at the mid-position is, on average, about 90 % larger

Chapter 4. STORM PRECIPITATION DISTRIBUTION

than the average storm intensity at zero elevation (Fig. 4.6a). At the upper watershed the average storm rate decreases except for the summer events for which the intensity increases. The convective nature of the precipitation during this period may account for this increase.

The variation of the average storm intensity is larger at the mid-position for the winter rainfalls and mixed events, and at the upper watershed for the summer rains and the snow events (Fig. 4.6b).

The above results show that the larger precipitation at the mid-position is due to the larger storm duration and the larger average storm intensities. However, the average intensity decreases at the upper watershed, and then levels off.

4.3.3 Maximum hourly intensity

The maximum hourly intensity increases from the base station to the mid-position of the watershed by about 100%, and then either decreases for higher elevation (mixed events), decreases and levels off (winter rainfalls) or decreases and then increases at the upper elevation (snow events and summer rainfall) (Fig. 4.7a). The largest variation of the maximum hourly intensity is observed at the upper elevation for all type of events except for the mixed events for which the largest variation is observed at the mid-position. The snow events and the summer rainfalls show the largest variation of the maximum hourly intensity (Fig. 4.7b).

4.3.4 Relative start time

Examination of the start time of the storms showed that the storms started most of the time at the mid-position of the watershed and later at the upper and lower watershed (Fig. 4.8). The

Chapter 4. STORM PRECIPITATION DISTRIBUTION

large convergence of the incoming air mass, due to the valley funneling and the orographic lifting increases the condensation so that the storms start first in the middle and upper watershed.

4.4 Time Distribution of Storms

The time distribution of rainfall within a storm is an important characteristic of the precipitation. There are very few studies that have dealt with the determination of the time distribution of storms. One classical study is that of Huff (1967) who analyzed 261 storms from a rain gage network covering a 1,037 km² area in Illinois. From these data, Huff developed a method of characterizing temporal distributions of storm precipitation. Recognizing the variability of hyetographs, Huff expressed temporal distributions of precipitation as isopleths of probabilities of dimensionless accumulated storm depths and durations. He also categorized the storms by the quartile of the storm having the maximum precipitation. These curves are known as "Huff curves" and have been used for design hyetographs inputs to hydrologic models (Terstriep and Stall, 1974; U.S.D.A., 1980; Bonta and Rao, 1992; Muzik, 1993). Bonta and Rao (1989) regionalized the Huff curves and developed dimensionless hyetographs for Ohio, Illinois and Texas, and studied the similarities and differences between these curves. They found that the Huff curves may be used throughout the Midwestern U.S.A. In an earlier paper, Bonta and Rao (1987) concluded that the sampling interval of precipitation data and the method identifying storms have only minor effects on the development of the Huff curves. On the other hand they found that the season of year exerts a significant effect on the Huff curves.

Coastal British Columbia and the greater region of the coastal Pacific Northwest have a totally different climate from that of the Midwestern U.S.A and therefore probably have

Chapter 4. STORM PRECIPITATION DISTRIBUTION

different precipitation time distribution curves. In this part of the thesis the 175 storms collected for seven years (1983-1990) in the Seymour River watershed will be used for the analysis and development of the time distribution of storms and the examination of the factors affecting the storm hyetographs.

4.4.1 Research Procedure

The procedure used by Huff (1967) is adopted for this study. The hyetographs of the 175 storms of variable duration will be used to determine the dimensionless hyetographs. These dimensionless hyetographs will then be used to express the temporal distribution of storms as probability distributions (Fig. 4.9). The 10% distribution means that 10% of the storms have a time distribution above this curve. In many cases a median time distribution will be most useful, but in others an extreme type of storm distribution (10% or 90%), may be used because such a distribution might maximize the runoff.

The only difference between the present study and Huff's work is that the empirical probability curves will not be classified by the quartile of the storm having the heaviest precipitation. Huff's data from Illinois consisted of about 67% thunderstorm rainfall, so that it was crucial for Huff to categorize the storms by quartile of maximum precipitation, because the large intensities during the periods of heavy precipitation have a major effect on the generation of the flood runoff. In coastal British Columbia most of the precipitation, as has been discussed in Chapter 2, is produced, even during the summer, by frontal systems. This frontal precipitation is characterized by the small to medium intensities and the long duration resulting in more uniform precipitation pattern, and therefore the classification of the storms by quartile of heaviest precipitation is rendered unnecessary.

Chapter 4. STORM PRECIPITATION DISTRIBUTION

The developed curves were compared both visually and statistically. The statistical test is by applying the Kolmogorov-Smyrnov (KS) two-sample test (Haan, 1978). This procedure tests for significant differences between two independent cumulative frequency distributions.

The analysis of the storm precipitation has been performed for the five stations used and for the four types of events. The objective is to evaluate, first, the effect of the elevation and then to identify any changes in the time distribution of the storms with elevation. The 50%, 10% and 90% time probability curves for all the stations in the study watershed will be compared.

Secondly, the effect of the event type on the time distribution of the storms will be examined comparing curves at the station 25B at 762 m elevation. These curves have been developed for each type of event, according to their earlier classification into October-March rainfall, April-September rainfall, snowfall, and mixed events of rain and snow. Again the time probability distribution curves 50%, 10% and 90% will be compared.

The third test will be to examine the effect of storm duration and storm precipitation depth on the storm time distribution. This test is critical for the identification of any significant changes of the hyetographs with storm duration and precipitation depth and it will be performed at station S-1.

Finally, data collected at three other coastal British Columbia stations have been analyzed and their time probability distribution curves have been developed. These results will be compared with the data from the Seymour River watershed. Large differences between the various sets of curves would indicate that the developed curves for the Seymour River watershed cannot be regionalized over large areas, but on the other hand, similarity between the curves developed for the Seymour River watershed and the curves for the other

Chapter 4. STORM PRECIPITATION DISTRIBUTION

three coastal British Columbia stations would indicate that they could be used for hydrologic design in the whole region of the coastal British Columbia.

4.4.2 Results

The time distribution of the analyzed 175 storms was determined for all stations in the study watershed. Figure 4.10 shows the comparison of the 10%, 50%, and 90% curves for all the five stations. Visual examination of these curves shows that there is no large difference between the developed curves except for the 90% curve for the Vancouver Harbour (Fig. 4.10). This curve deviates from the rest of the curves. However, the KS test showed no significant differences between any of the curves from any station at the 5% level. Hence, the elevation and the topography exert a large effect on the storm precipitation and duration but only affect the storm time distribution to a very small degree.

After classifying the storms into the different type of events, the time distribution probability curves were determined for each station. Very few storms at the lower elevations were either snowfalls or mixed events. For example, all the events in Vancouver Harbour were categorized as rainfall events whereas only seven events were snow storms and four were mixed snow and rain events at station S-1 at 260 m elevation. On the other hand, at station 25B at 762 m elevation forty-four storms were classified as snow storms, 35 events as mixed rain and snow events and the remaining events were rain storms. For this reason the effect of the different type of events on the storm time distribution is examined by using the developed curves at station 25B (Fig. 4.11). Visual comparison of the 10%, 50%, and 90% curves for the various types of events indicates very small differences among the curves for the various types of the events. Furthermore, the KS test showed no significant differences between any of the curves of the four types of the events at the 5% level, so that the effect of

Chapter 4. STORM PRECIPITATION DISTRIBUTION

the type of the events is minimal on the time distribution of the storms. This probably happens because similar storms during the winter produce the various types of the events. Moreover, it should be mentioned that it is the largest storms and the storms that cover the whole watershed that have been analyzed and this criterion might have excluded the rare convective storms that occur only at the upper watershed. Hence, the larger summer rainstorms have a similar time distribution to that of the winter storms. This is also evident from the comparison of the time distribution of the winter and summer rainstorms at all stations.

It is important to examine whether the time distribution of storms is affected by the storm depth and duration. For this reason, the storms at station S-1 are categorized into groups of storms having duration smaller than 24 hours (65 storms), between 24 hours and 48 hours (65 storms), and larger than 48 hours (45 storms). Examination of the 10%, 50%, and 90% curves shows that the storm duration affects the time distribution of the storms only to a very small degree (Fig. 4.12). Application of the KS test, also, shows that this variation is not statistically significant at the 5% level.

In a similar way the storms are classified according to the total storm precipitation into groups of storms having storm precipitation smaller than 50.8 mm (78 storms), between 50.8 mm and 101.6 mm (52 storms), and larger than 101.6 mm (45 storms). Visual examination of the median and the more extreme time distribution probability curves indicates that the storm time distribution is not affected by the total storm precipitation (Fig. 4.13). Furthermore, the KS test showed no significant differences between the various time probability distribution curves of any duration and storm precipitation group at the 5% level.

The above results suggest that one set of time probability distribution curves, derived from all 175 storms at all seven stations, can be used. In the next paragraphs this average time distribution probability curves will be used.

Chapter 4. STORM PRECIPITATION DISTRIBUTION

It is important that the storm time probability curves developed in this study should be compared with the time distribution of storms from other areas in the same climatic region. For this reason data from three stations located in different areas of coastal British Columbia were used to develop time distribution probability curves. Similarities between the developed curves for the Seymour River watershed and the curves for the other three stations would then indicate that the Seymour River watershed curves could be used for hydrologic design in areas of the greater climatic region. The stations used for this analysis are the Carnation Creek CDF station, the Courtenay Puntledge BCHP station, and the Kitimat station. These stations are A.E.S. stations and are located at different areas of the coastal British Columbia (Fig. 2.1). Because of the different microclimates of the areas of the three stations, different criteria were used for the selection of the storms analyzed (Table 4.1). The number of years of record is different for these stations and so is the number of the events used for the analysis. However, it is believed that these data depict the storm distribution pattern over coastal British Columbia.

Chapter 4. STORM PRECIPITATION DISTRIBUTION

Table 4.1. Characteristics of the coastal British Columbia stations whose data analyzed

Station Name	Minimum Depth (mm)	Sampling Interval (hrs)	Interstorm Interval (hrs)	Maximum Duration (hrs)	Usual Duration Range (hrs)	Period of Record	Number of Storms
Carnation Creek CDF	35	1	6	119	20-40	1975-1986	170
Courttenay Puntledge BCHP	20	1	6	80	12-30	1964-1991	334
Kitimat	30	1	6	86	20-40	1979-1991	128

Chapter 4. STORM PRECIPITATION DISTRIBUTION

The time distribution probability curves developed from the data from the three stations and the average curves developed for the Seymour River watershed are compared in Figure 4.14. The comparison shows that the time probability distribution curves of the three British Columbia stations are similar. Furthermore, these curves are similar to the average Seymour curves shape. Especially, the 90% curves have a similar shape and show very small deviation. There is larger deviation between the 10% and the 90% curves but the KS test showed that this variation is not significant at the 5% level.

The above results indicate that the average curves for the Seymour River watershed could probably be used for the distribution of design storm throughout the coastal British Columbia. However, the differences that do exist from one area to another need to be evaluated by using these curves in watershed models. If these differences in the time distribution probability curves do not significantly affect the simulation of the watershed response, then it is reasonable to use the time probability distribution curves developed in this study for the hydrologic design in the whole region.

4.5. Antecedent Precipitation

The antecedent precipitation is a traditional hydrologic index of the soil moisture conditions in a watershed. The soil moisture storage is of particular interest to the hydrologist especially when dealing with mountainous and rural watersheds. The impervious area in both of these watersheds is small and the response of the watershed to the precipitation input is controlled by the soil moisture storage. For this reason, the data from the Seymour River watershed have been analyzed to obtain the probability estimates of the magnitude of rainfall for periods of 1, 2, 3, and 5 days before the occurrence of the storm. The analysis has been done separately for the October-to-March (winter) storms and the April-to-September (summer) storms.

Chapter 4. STORM PRECIPITATION DISTRIBUTION

Figure 4.15 shows the probability curves of the antecedent precipitation of several days at station S-1. According to the analysis the antecedent precipitation is high at station S-1 especially during the winter months. During the summer period the antecedent precipitation probability curves of several days become more uniform and the antecedent precipitation significantly decreases compared to the winter period. For example, there is 50% probability that the 1-day antecedent precipitation will be larger than 10 mm during the months from October to March, whereas there is only 15% probability that the one-day antecedent precipitation will be larger than 10 mm during the months from April to September.

The antecedent precipitation probability curves at three sites in the study watershed is also compared (Fig. 4.16). It has been assumed that the station Vancouver Harbour, S-1, and 25B represent the lower, middle, and the upper watershed, respectively. This analysis showed that the antecedent precipitation during the October-to-March period follows a spatial pattern similar to that of the storm precipitation presented earlier in this Chapter. The antecedent precipitation increases up to middle watershed (station S-1), and then decreases at the upper watershed (station 25B). However, the antecedent probability curves converge for the low probability levels and similar conditions exist over the middle and upper watershed (Fig. 4.16a).

The examination of the antecedent precipitation probability curves during the April to September period showed that the soil moisture conditions are more uniform for the whole watershed and for all the probability levels (Fig. 4.16b).

Even though the antecedent conditions could vary over the whole region of coastal British Columbia, the results of this section could be used as a first approximation in absence of measured data.

Chapter 4. STORM PRECIPITATION DISTRIBUTION

4.6 Summary

The above results show that the topography of the Seymour River watershed plays a very significant role in the distribution of precipitation. The largest precipitation is observed at the mid-position of the watershed. At this position the valley orientation changes to a northwest-southeast direction. The increased convergence of the incoming air mass produces large precipitation, about 200% larger than the zero elevation precipitation. This increase, on average, is due to the larger average storm intensities combined with the larger duration. After this middle position the precipitation becomes more uniform at the upper watershed and the significance of the average storm intensities diminishes so that the larger duration is responsible for the large precipitation amounts.

The precipitation in the coastal British Columbia is generated mainly by strong frontal systems coming from a southwest direction. This frontal precipitation is characterized by the small to moderate intensities and long duration. As a result, the median time distribution of all types of storms is found to be linear. The time distribution of storms is not affected by the elevation, the type of the event, the storm depth and duration. Analysis of the precipitation records of three stations in coastal British Columbia showed that the time probability distribution curves found for the Seymour River watershed may be used in other areas of the region.

The antecedent precipitation of several days has been examined. The results showed that the antecedent precipitation is relatively high for the whole watershed. However, it increases with elevation especially in the winter period and for low probability levels. In summer the antecedent precipitation is affected less by the elevation and drier conditions prevail.

Chapter 4. STORM PRECIPITATION DISTRIBUTION

The results of this study should be tested over the same climatic region in order to generalize them and test the transferability of the findings. Such work has already been done for the time distribution but not for the spatial distribution of the precipitation. In coastal British Columbia there are 96 recording gauges across an area of about 210,000 km². The sparcity of the data precludes the examination of the distribution of precipitation in space within a hydrologic unit such as a watershed, and for a short-time scale, such as a storm period. This study indicates that the storm precipitation has a similar distribution pattern to that of the annual and seasonal precipitation. In Chapter 3 it has been shown that the annual and seasonal precipitation distribution across the coastal British Columbia is similar to that found in the Seymour River watershed, increasing with elevation up to 400-800 m and then either leveling off or decreasing at the upper elevations. In light of the findings presented in this Chapter, it can be assumed that the storm precipitation follows a similar pattern to that of the annual precipitation. This distribution can be used as a first approximation in the absence of measurements in the greater climatic region of coastal British Columbia.

Chapter 4. STORM PRECIPITATION DISTRIBUTION

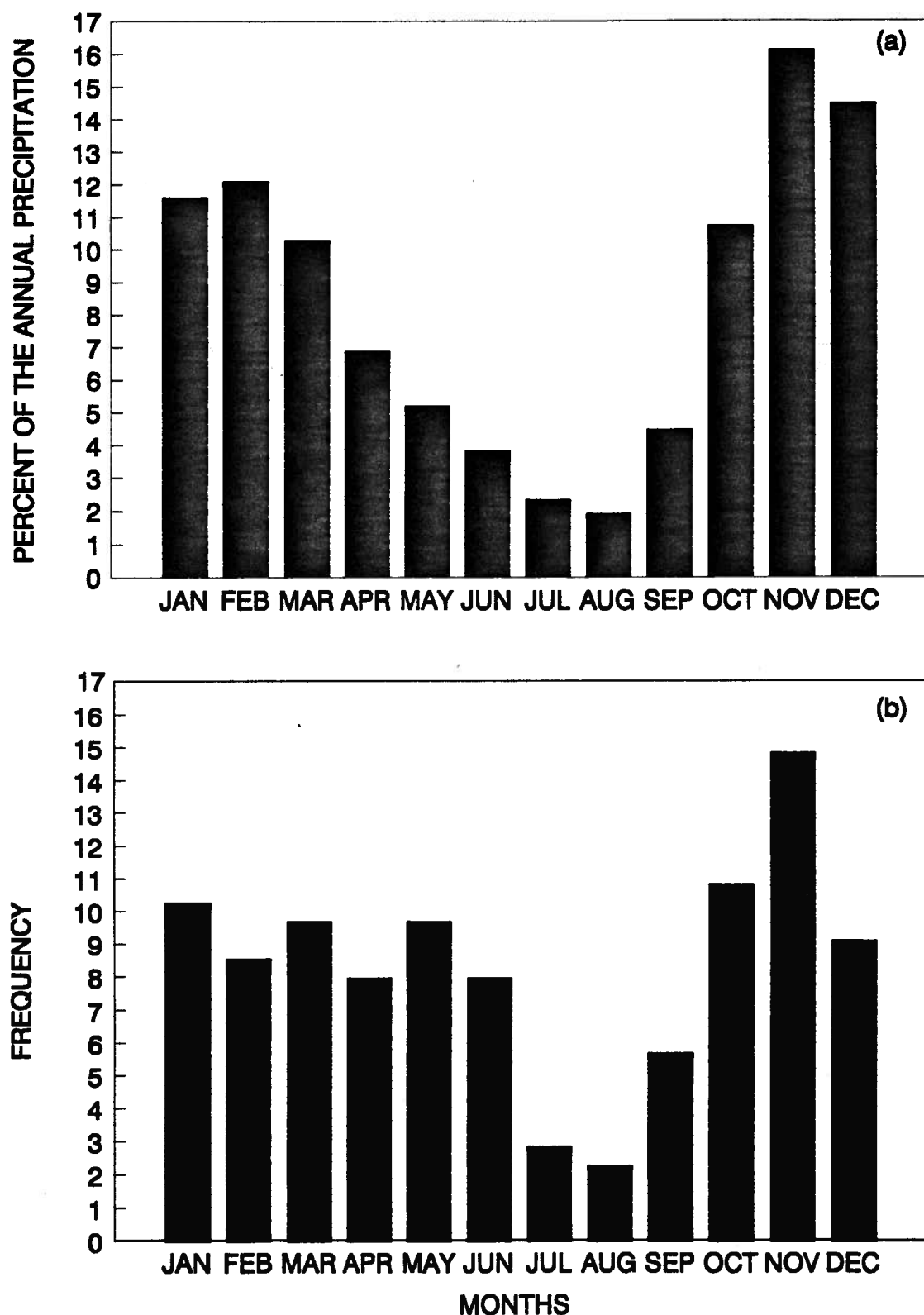


Fig. 4.1 a) Monthly distribution of the average annual precipitation at station S-1 and (b) Monthly distribution of the 175 storms analyzed.

Chapter 4. STORM PRECIPITATION DISTRIBUTION

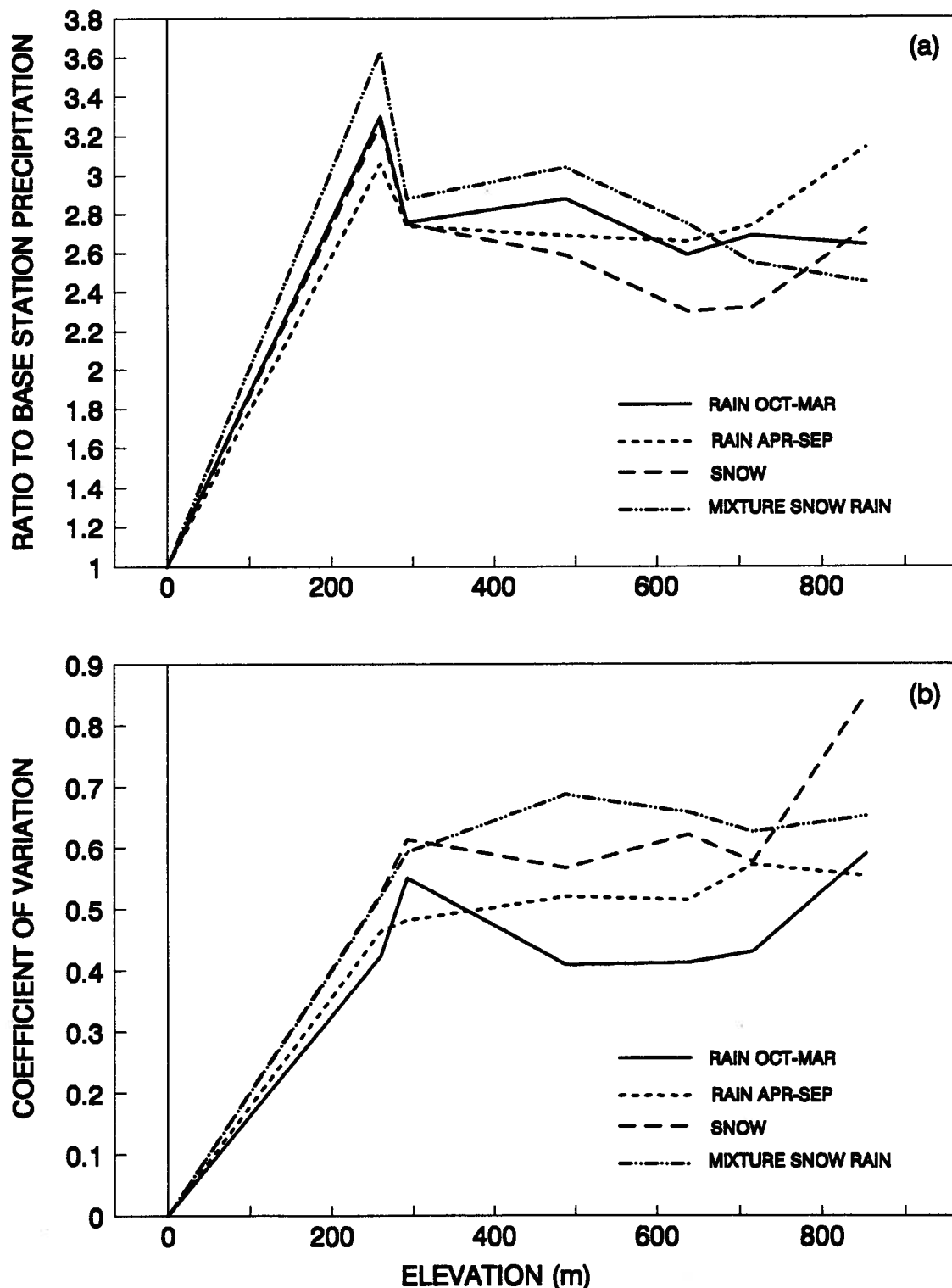


Fig. 4.2 a) Precipitation ratio to base station (Vancouver Harbour) for various stations and types of events and (b) its coefficient of variation.

Chapter 4. STORM PRECIPITATION DISTRIBUTION

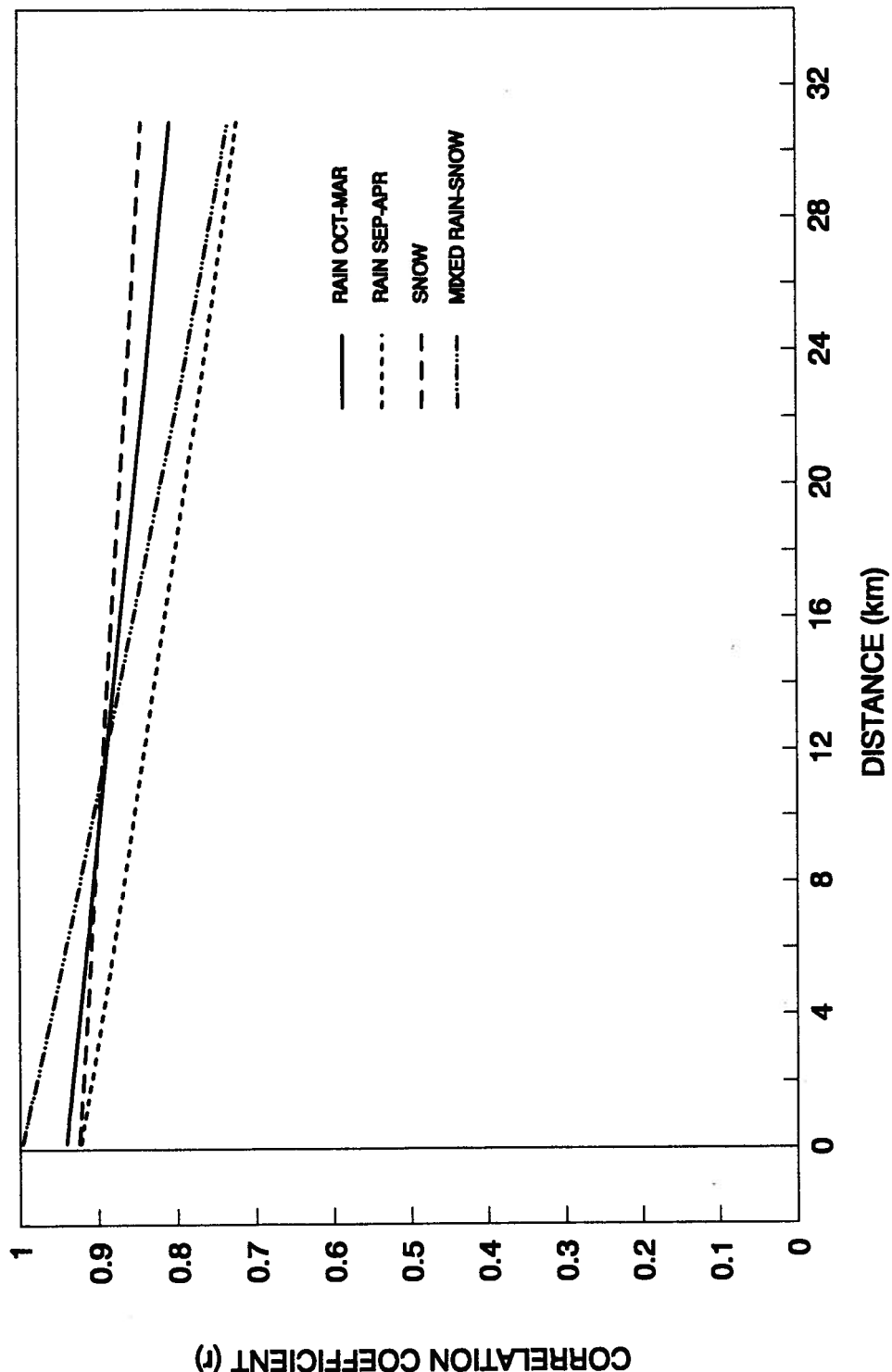
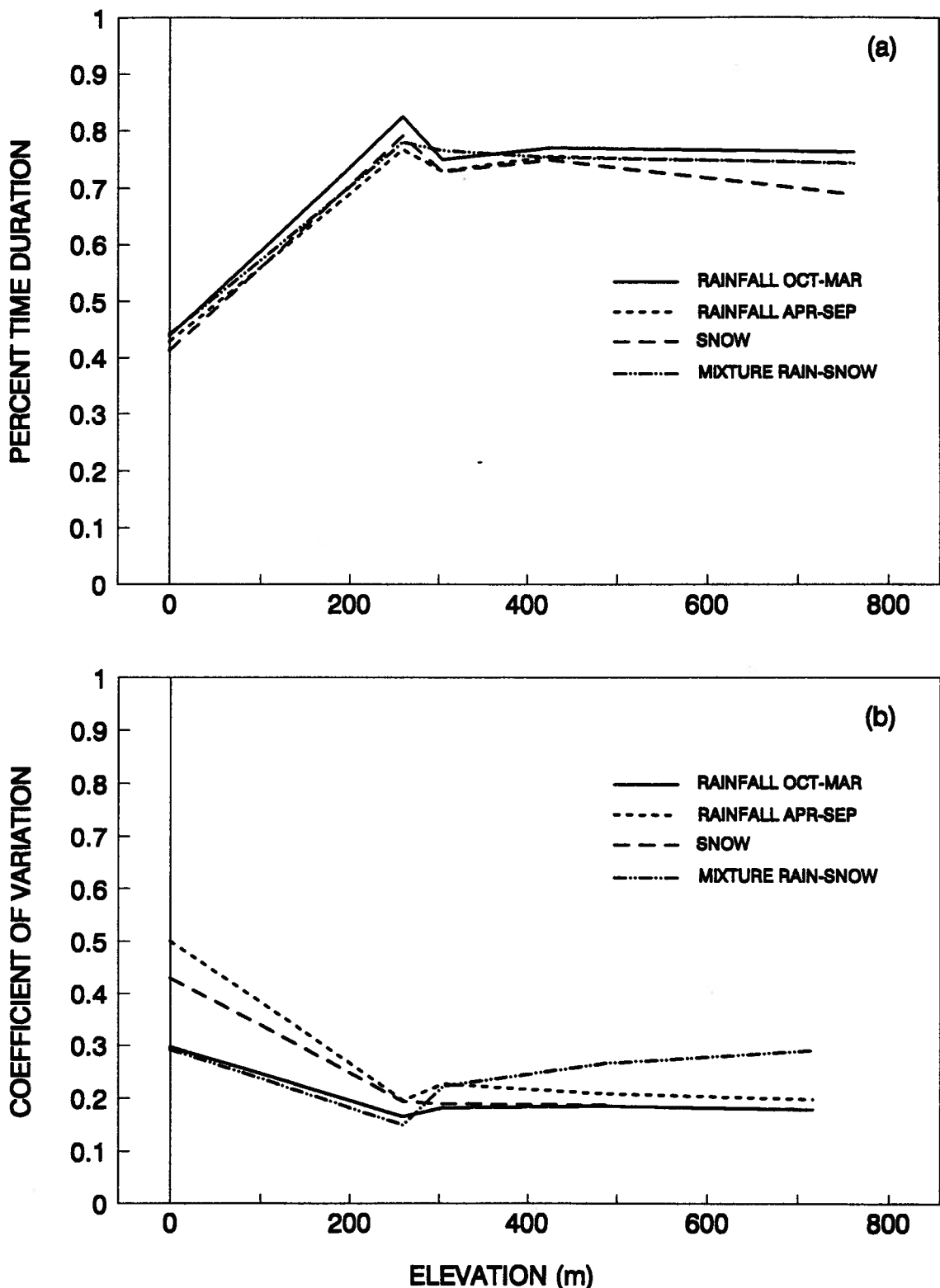


Fig. 4.3. Spatial correlation functions for the various types of storms.

Chapter 4. STORM PRECIPITATION DISTRIBUTION



**Fig. 4.4. (a) Storm continuity at various elevations and types of storms
(b) Coefficient of variation of storm continuity.**

Chapter 4. STORM PRECIPITATION DISTRIBUTION

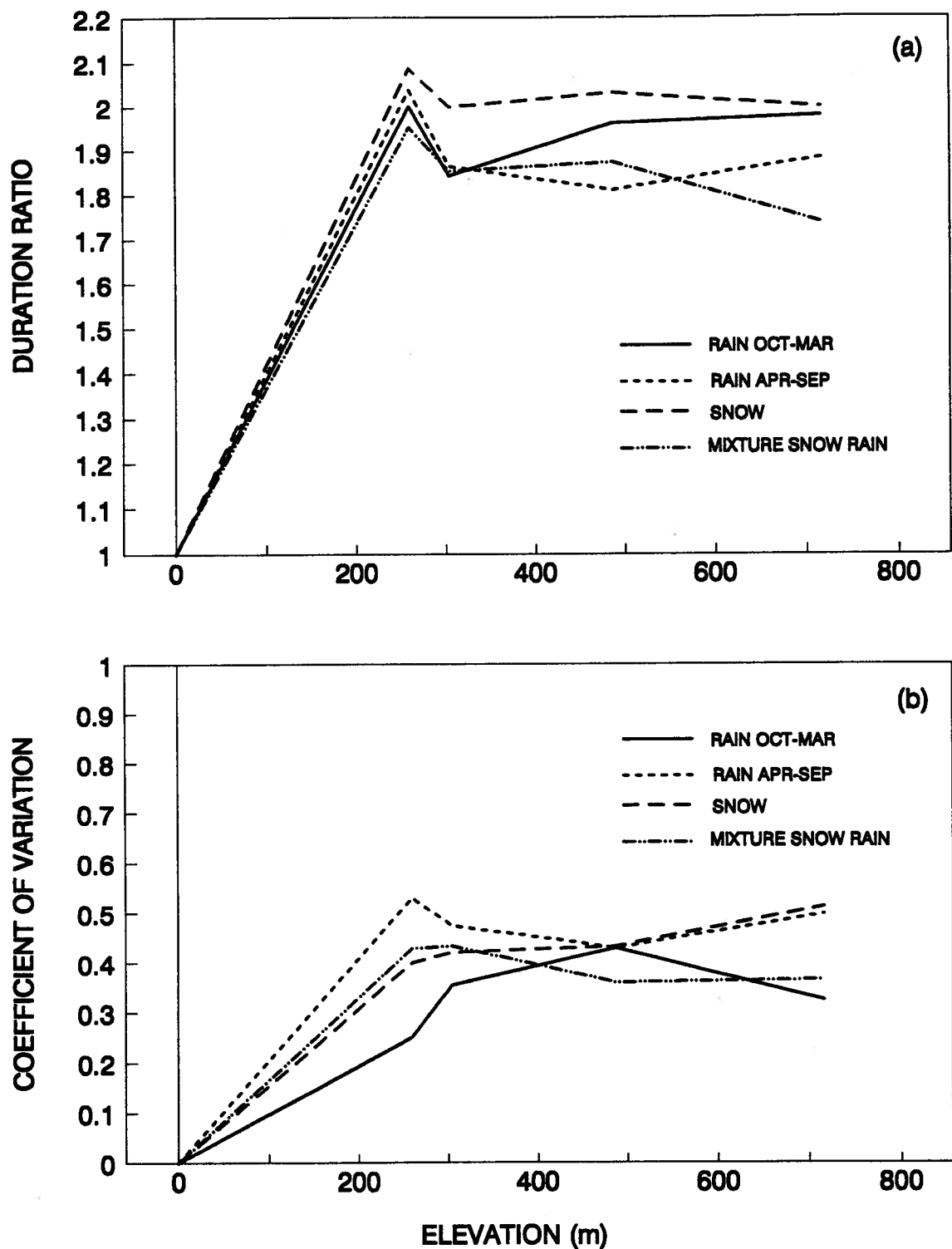


Fig. 4.5. (a) Storm duration ratio to base station for various elevations and types of storms (b) Coefficient of variation of storm duration ratio.

Chapter 4. STORM PRECIPITATION DISTRIBUTION

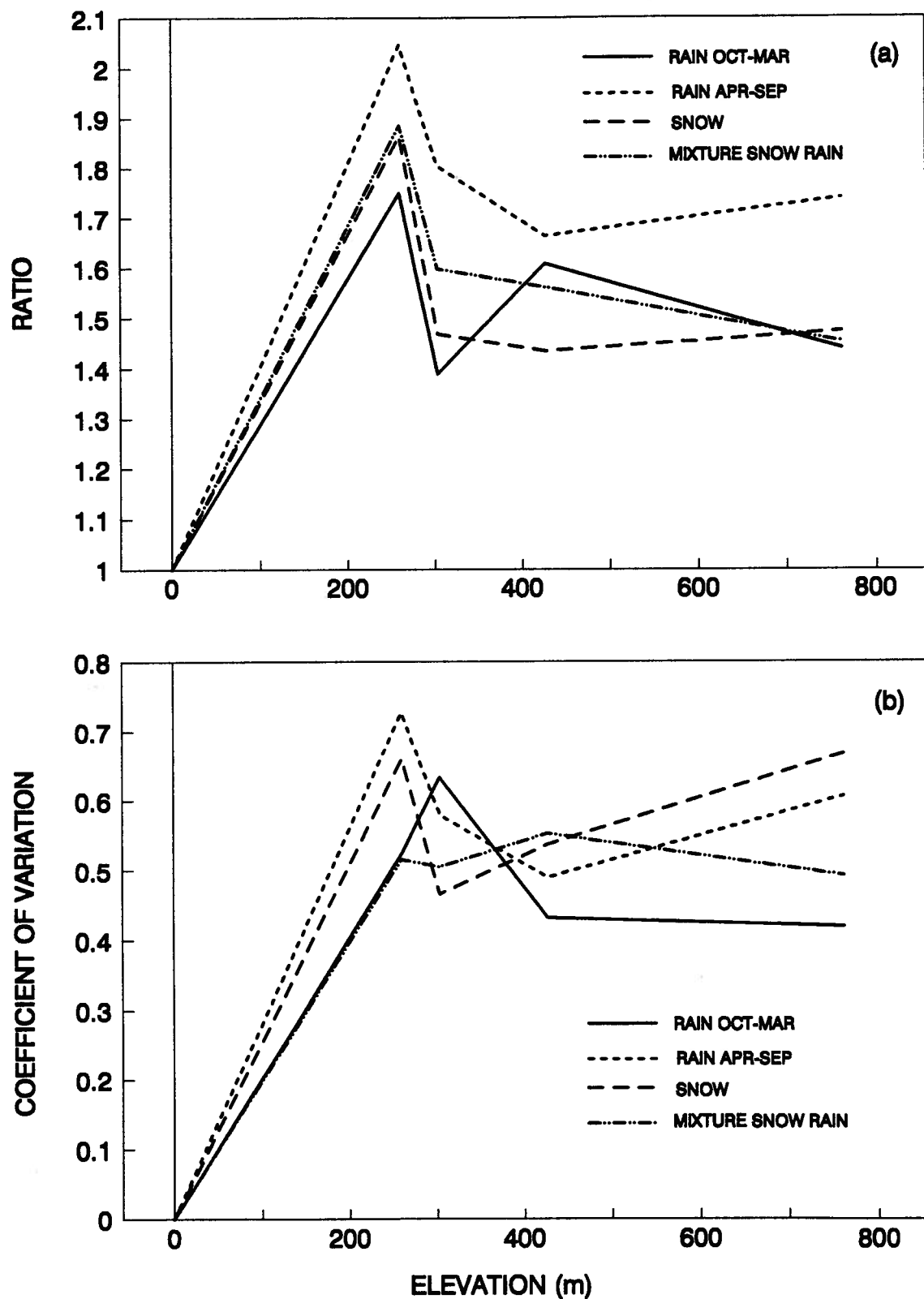


Fig. 4.6. (a) Ratio of the average storm intensity to base station for various elevations and types of storms and (b) its coefficient of variation.

Chapter 4. STORM PRECIPITATION DISTRIBUTION

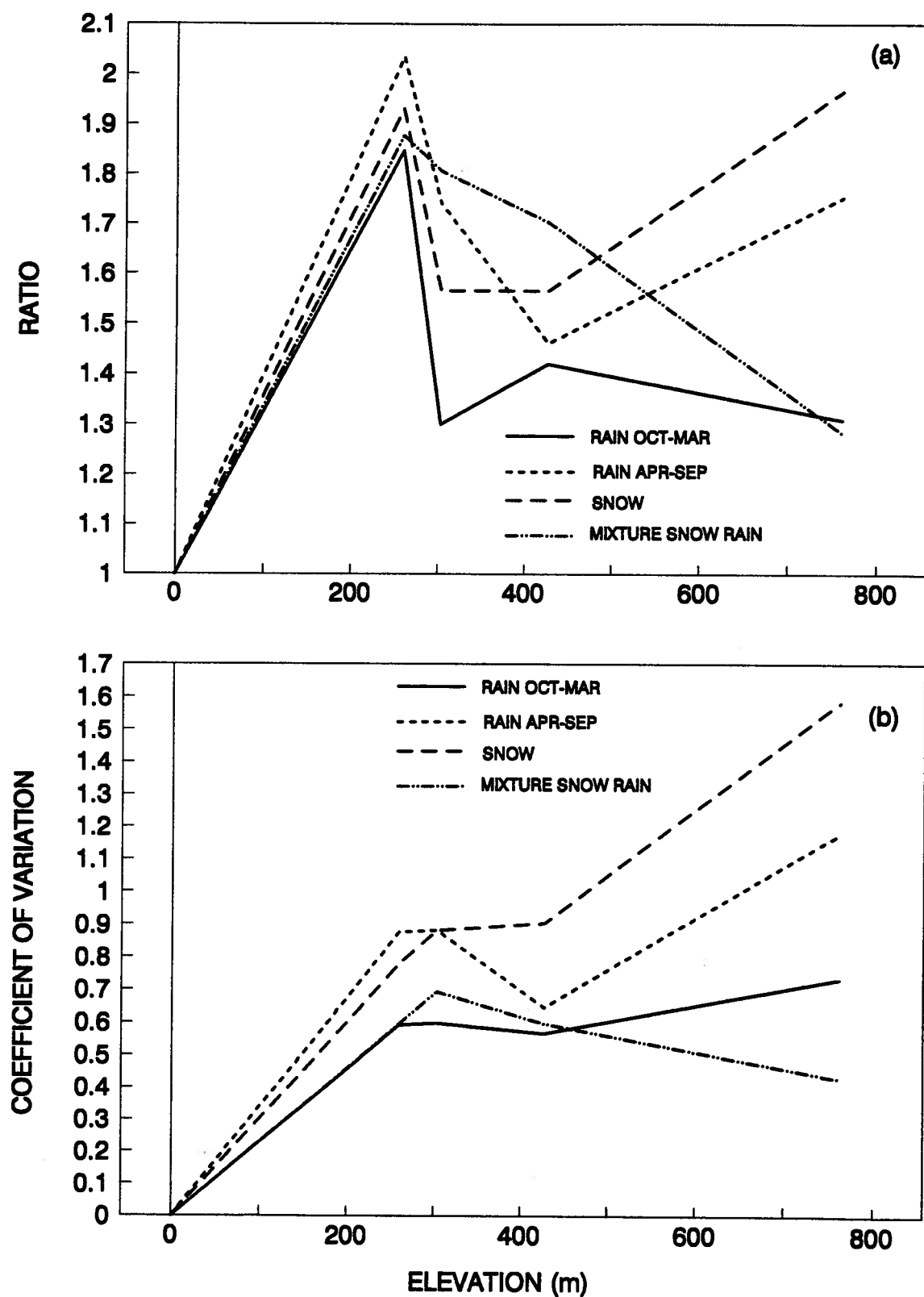


Fig. 4.7. a) Ratio of the maximum hourly intensity to base station for various elevations and types of storms and (b) its coefficient of variation.

Chapter 4. STORM PRECIPITATION DISTRIBUTION

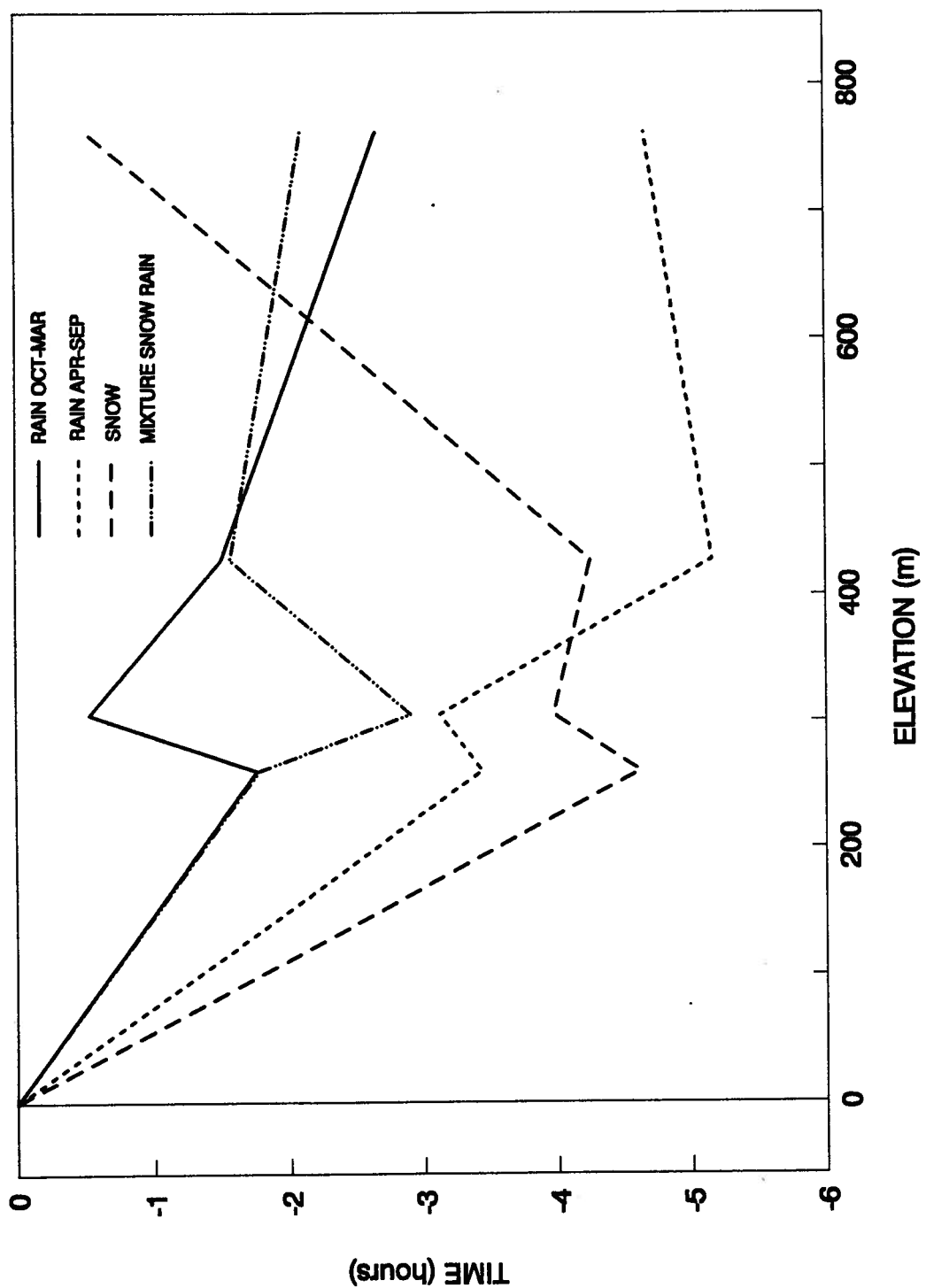


Fig. 4.8. Storm relative start time to the base station at different elevations and type of storm.

Chapter 4. STORM PRECIPITATION DISTRIBUTION

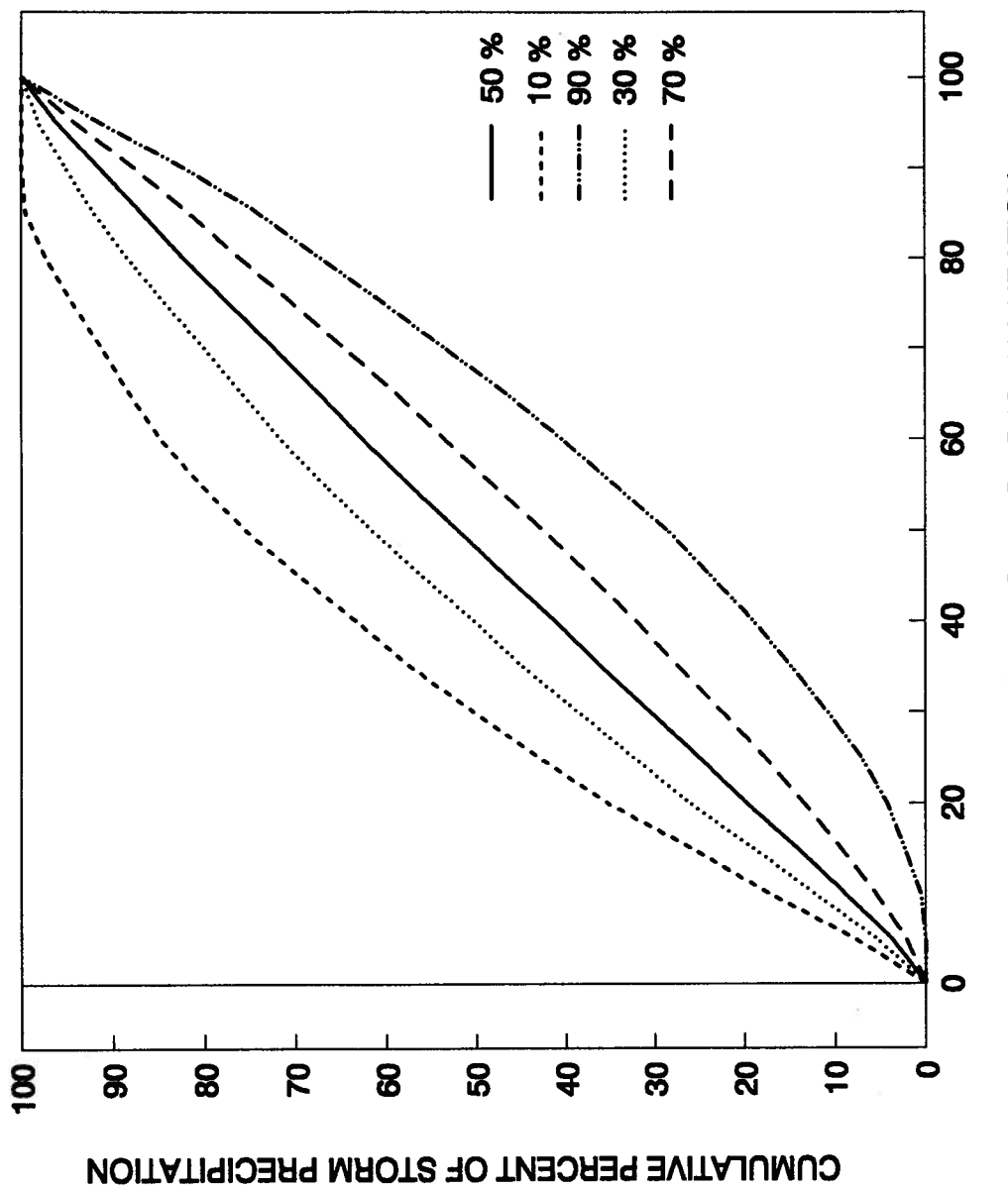


Fig. 4.9. Time distribution probability curves at station 2B.

Chapter 4. STORM PRECIPITATION DISTRIBUTION

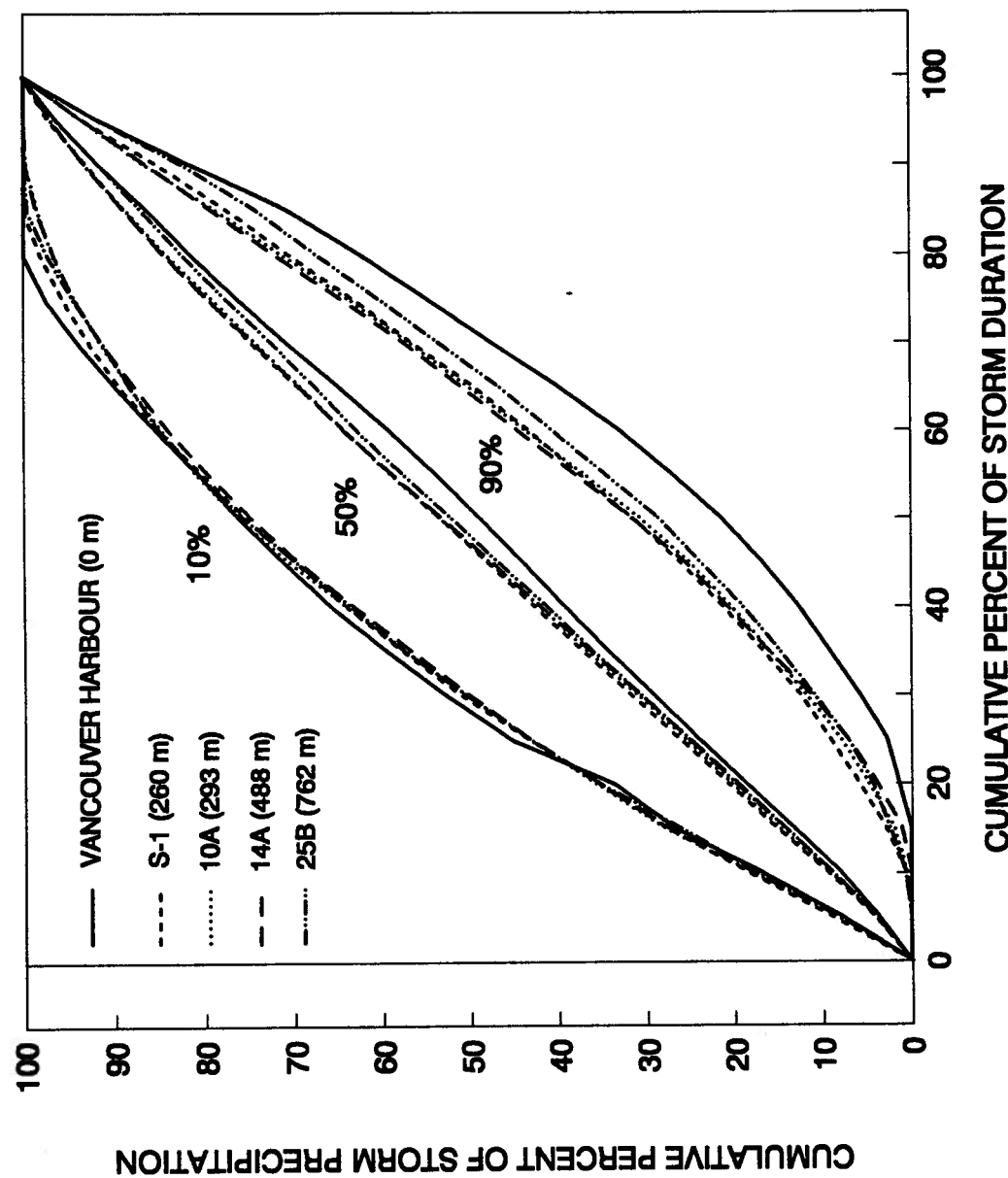


Fig. 4.10. Comparison of the time distribution probability curves for different stations and elevations in the Seymour River watershed

Chapter 4. STORM PRECIPITATION DISTRIBUTION

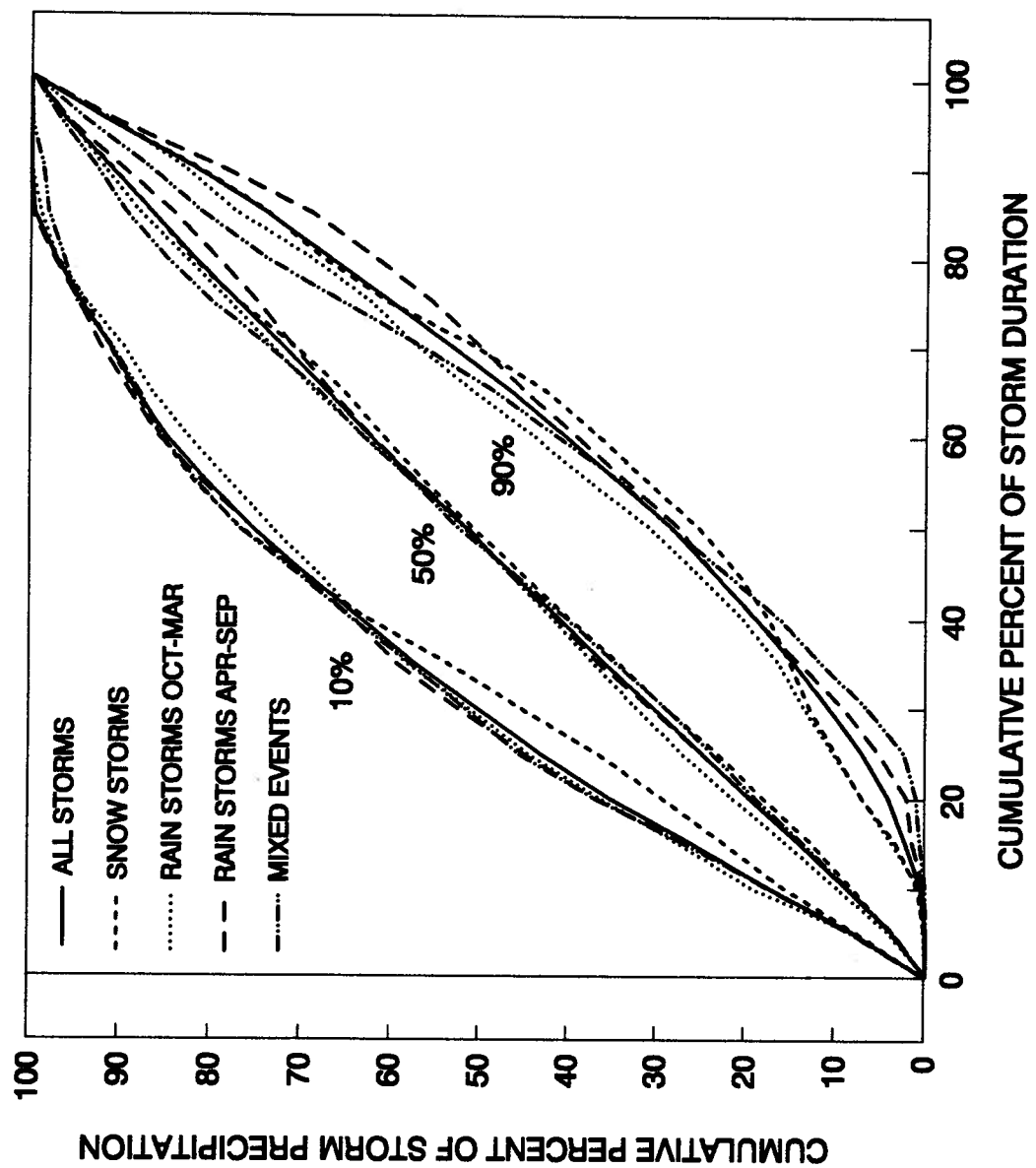


Fig. 4.11. Comparison of the time distribution probability curves for different type of events at the station 25B in the Seymour River watershed.

Chapter 4. STORM PRECIPITATION DISTRIBUTION

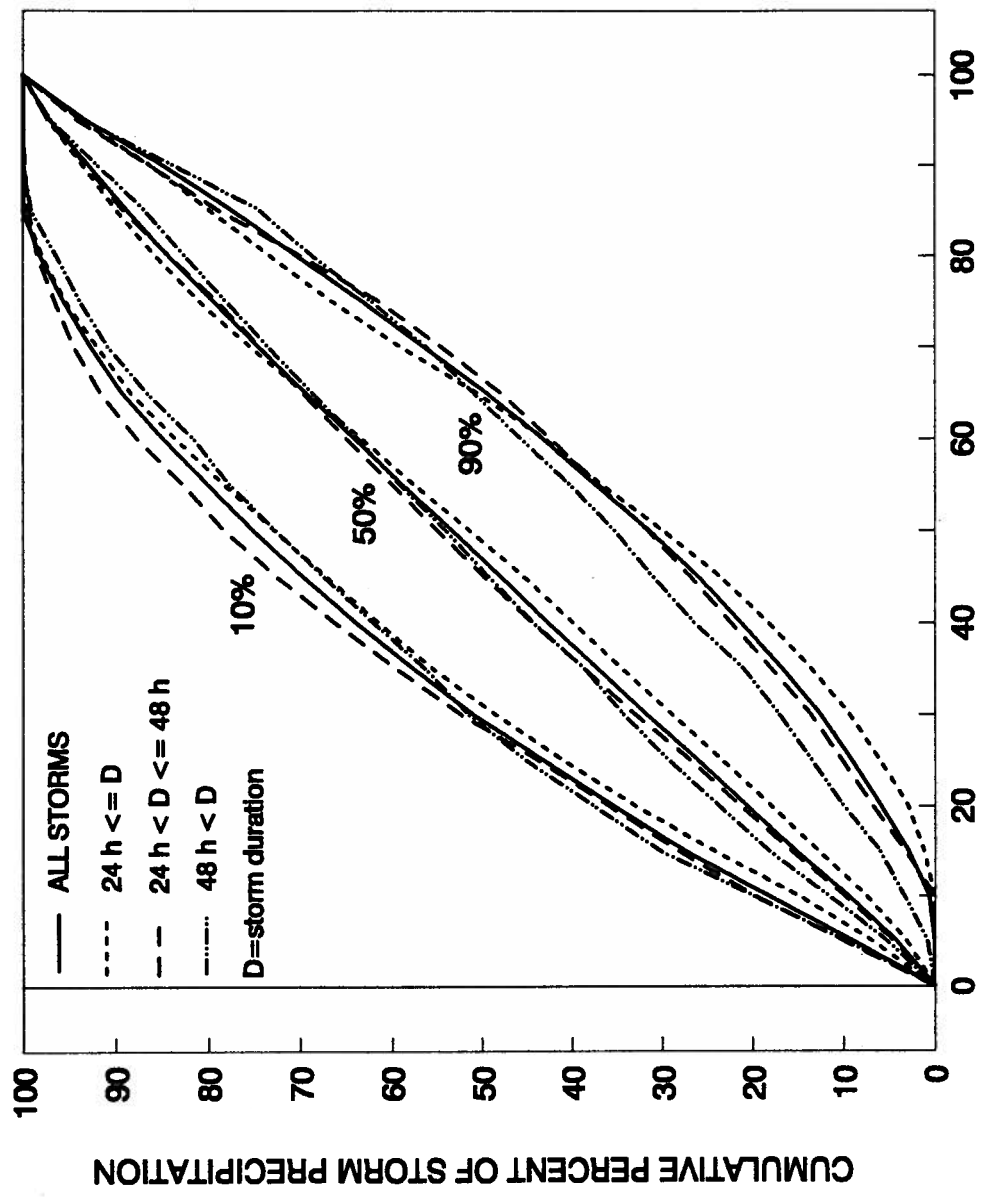
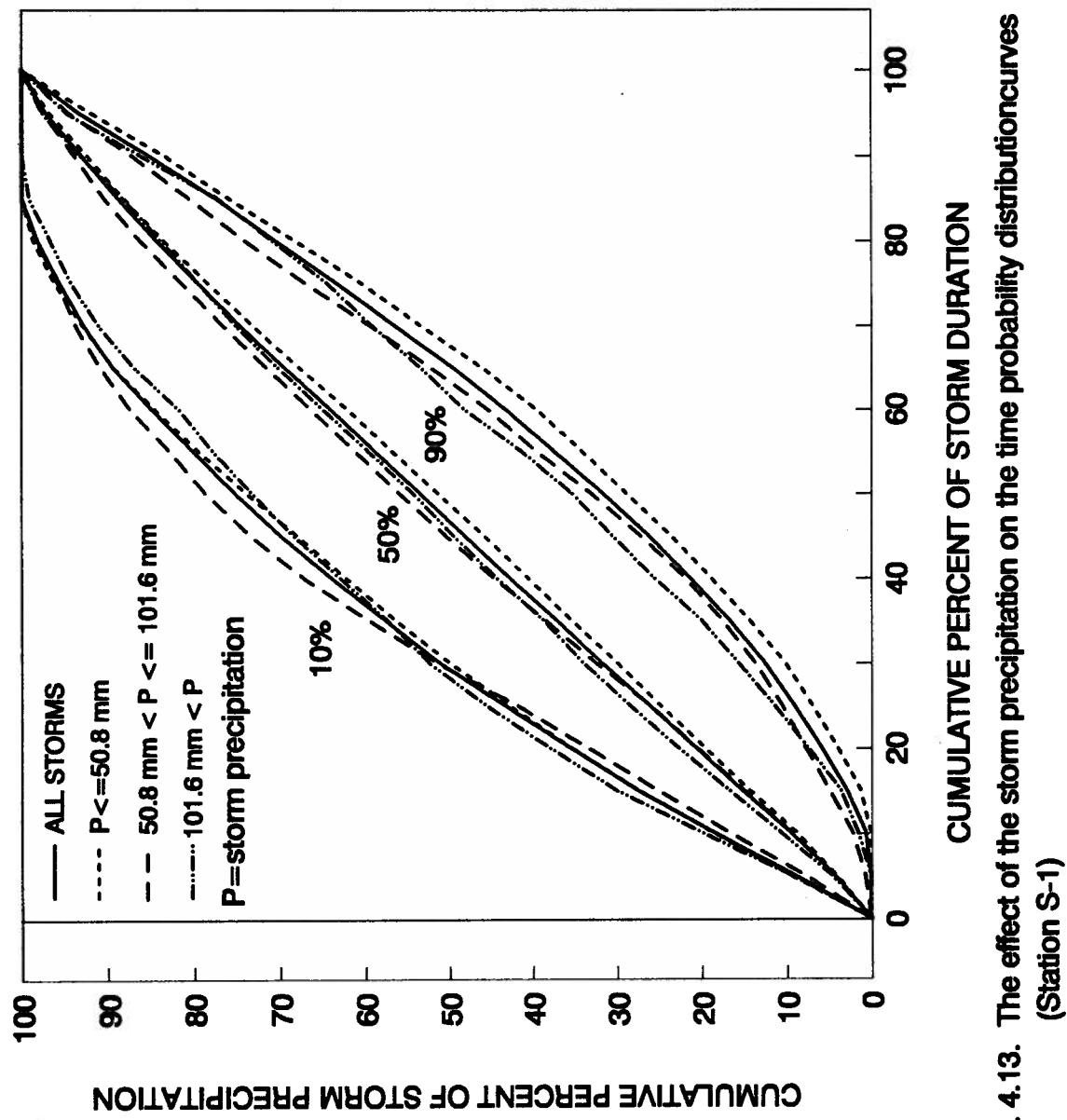


Fig. 4.12. The effect of the storm duration on the time probability distribution curves (Station S-1)

Chapter 4. STORM PRECIPITATION DISTRIBUTION



**Fig. 4.13. The effect of the storm precipitation on the time probability distribution curves
(Station S-1)**

Chapter 4. STORM PRECIPITATION DISTRIBUTION

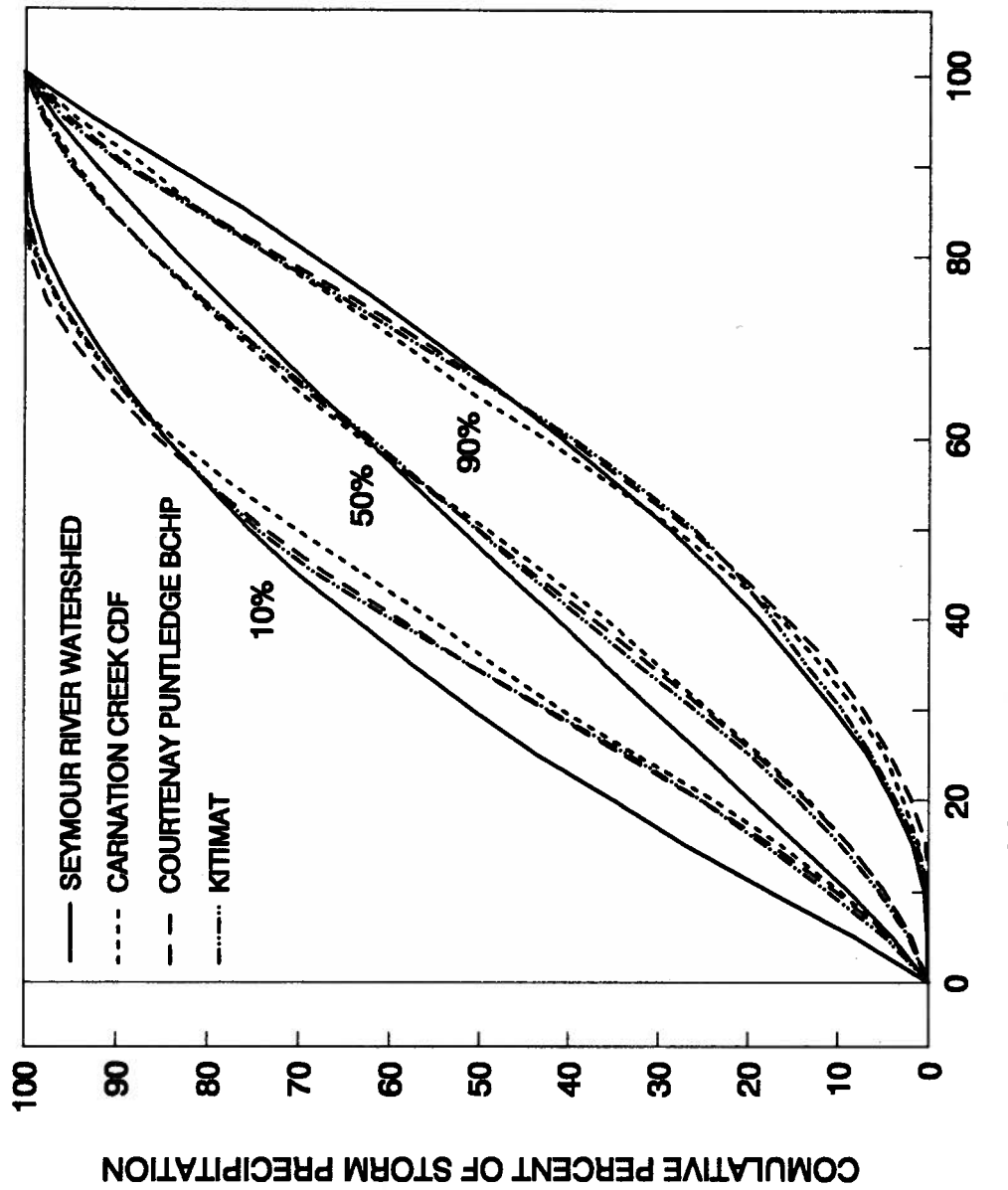


Fig. 4.14. Comparison of the time probability distribution curves for Seymour River watershed and three Coastal British Columbia stations.

Chapter 4. STORM PRECIPITATION DISTRIBUTION

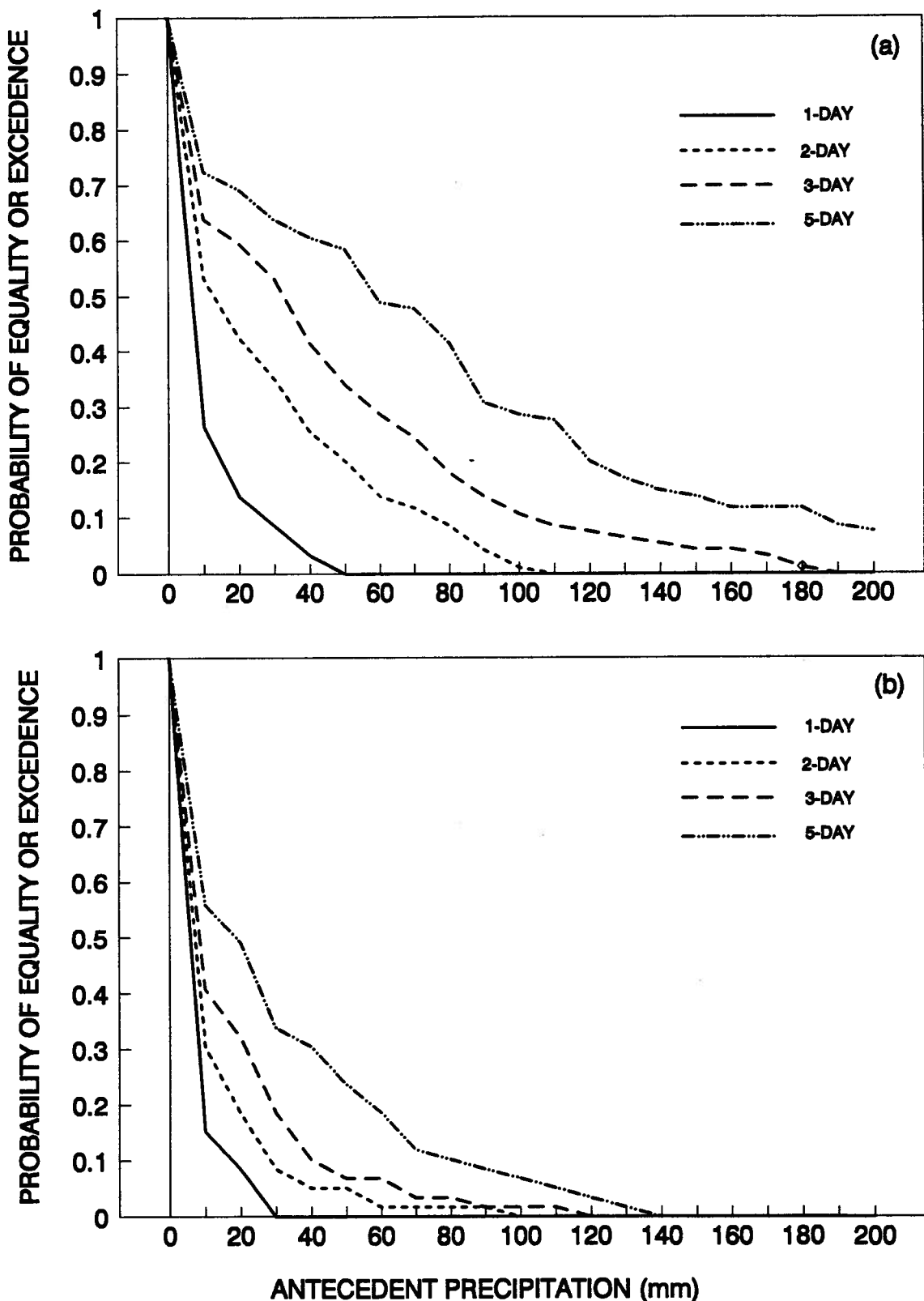


Fig. 4.15. Probability of equality or exceedance of antecedent precipitation at station S-1 for (a) October to March storms and (b) April to September storms

Chapter 4. STORM PRECIPITATION DISTRIBUTION

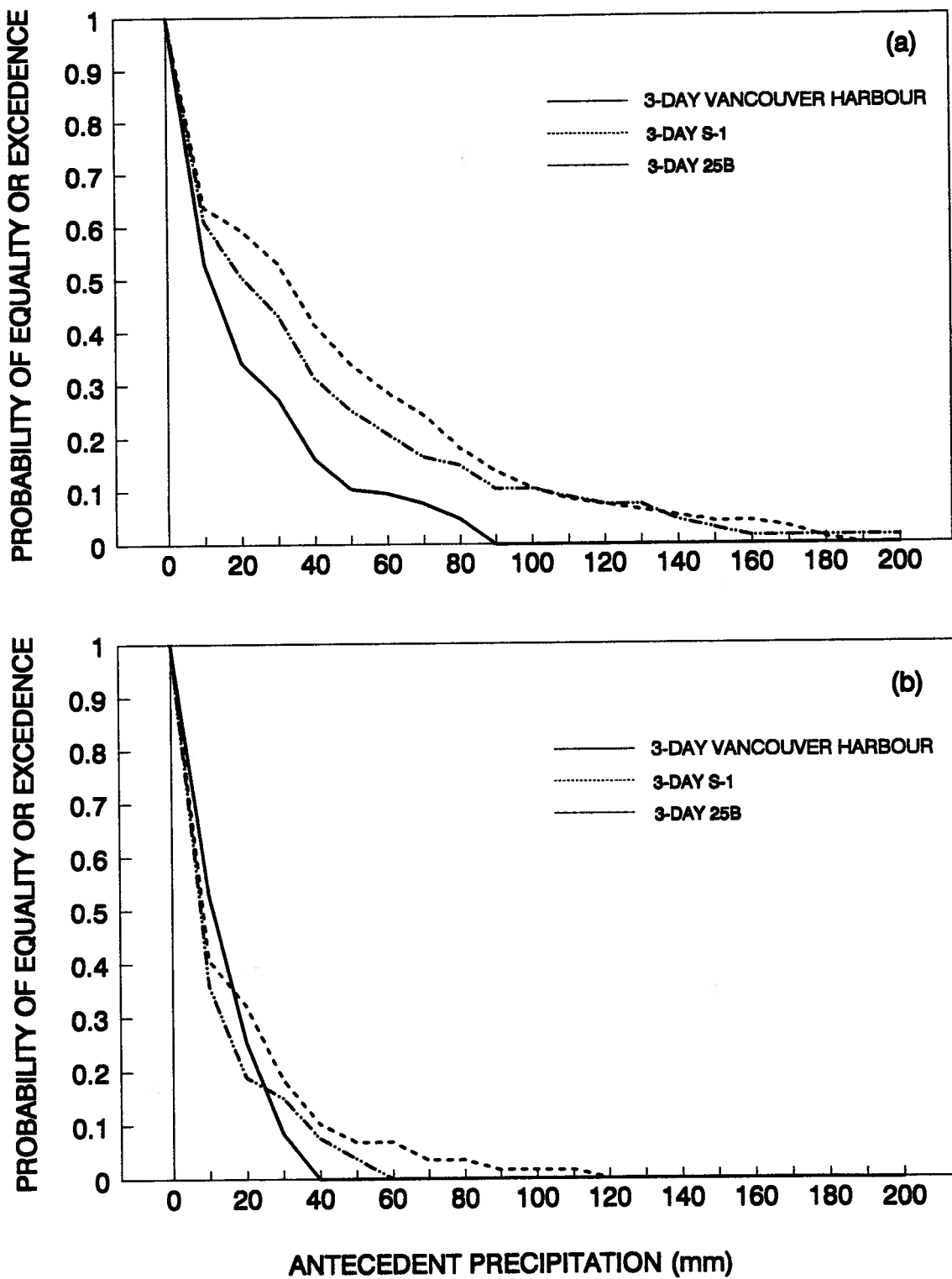


Fig. 4.16. Comparison of the probability of equality or exceedence of the antecedent precipitation for different elevations for (a) winter and (b) summer.

CHAPTER 5

24-HOUR DESIGN STORM FOR COASTAL BRITISH COLUMBIA

5.1 Introduction

The estimation of peak flows is necessary for the design of hydrotechnical structures. If streamflow data are available, a conventional flood frequency technique is applied. Unfortunately there are many streams for which measurements are not available and in these cases many different approaches can be used as will be presented in Chapter 8 of the thesis. One of these methods is the event-based simulation of individual large events, in which a design storm can be derived and used as input to a watershed model for the estimation of the storm runoff hydrograph, which provides estimates of the volume of runoff and the peak flow. The design storm considerations include the return period, the total storm depth, the storm duration, the storm temporal distribution, the storm spatial characteristics, the time response of the watershed and the antecedent soil moisture state of the watershed.

The return period of the storm is selected on the basis of minimizing the cost or assuring a certain level of protection of the hydraulic structure, and consequently of the community. In Canada, the level of protection is determined by the Provinces and depends on the type of structures (Watt et al., 1989). The total precipitation depth at a point is a function of the return period and the storm duration, which is linked to the time of concentration of the watershed. The variation of the rainfall intensity during the storm is an important factor in determining the timing and the magnitude of the peak flows. In addition, the spatial coverage of the storm influences the runoff generation and is especially important for larger basins.

In earlier studies in Canada the focus was on the derivation of the design storm for

Chapter 5. 24-HOUR DESIGN STORM FOR COASTAL BRITISH COLUMBIA

urban watersheds, usually 1-hour to 12-hour storm (Hogg, 1980; Hogg, 1982; Marsalek and Watt, 1984; Watt et al., 1986). This study is concentrated on the derivation and study of the 24-hour design storm for coastal British Columbia mountainous and rural watersheds.

This choice of the 24-hour storm duration has been based on many factors. Firstly, the precipitation in the coastal British Columbia is generated mainly by long duration frontal storms as it has been discussed in Chapter 2. Most of these storms have a duration of about a day as it has been shown from the regional data analyzed in Chapter 4. Secondly, the response of small and medium mountainous watersheds is in the order of several hours so that a long duration storm is required for the generation of peak flows. One might think that a short duration storm may be more adequate for the estimation of peak flow from small steep watersheds of the region. Extensive research in the Jamieson Creek watershed, a small steep watershed which will be used later in the analysis, showed that for rain storms the time lag varied between 5.5 hours to 15 hours with an average of about 8.5 hours (Cheng, 1976). For the most intense and severe storms the time lag decreases down to 2-2.5 hours (Loukas, 1991). These results show that a design storm of longer duration from that of the time lag, like a 6-hour, 12-hour or 24-hour storm could be adequate for the simulation of the peak flow. However, simulation of the peak flows from coastal British Columbia watersheds showed that the 24-hour storm is more suitable, especially for the larger return period floods, as will be shown in Chapter 8 of the thesis (Fig. 8.3). Furthermore, the choice of the 24-hour storm duration is a pragmatic one. Of the 269 precipitation stations located in the coastal British Columbia, an area of about 210,000 km², 173 are storage gauges which are used to measure the daily precipitation. These stations have longer records than the recording stations (Fig. 5.1), which implies more reliable frequency analysis, since the use of the 24-hour design storm can expand the usable data both in space and time resulting in better estimation of flood runoff from ungauged watersheds.

Chapter 5. 24-HOUR DESIGN STORM FOR COASTAL BRITISH COLUMBIA

Since the storm duration of 24 hours is accepted to be adequate for small and medium mountainous and rural watersheds, the time distribution of the storm and its variation in space are the most important parameters of the design storm.

The objective of this Chapter is to present the results of the development of a 24-hour design storm using data from the Seymour River watershed. Important parts of this study will be, firstly, to examine whether the temporal distribution changes with elevation, secondly, to identify the spatial distribution of the precipitation, thirdly, to compare the developed storm with other synthetic storms used in the hydrologic design, and finally to investigate the possibility of transferring the results in other areas of coastal British Columbia. It should be noted that the scarcity of both precipitation and streamflow data in this mountainous region restricts the application of conventional flood frequency analysis and therefore the use of the design storm concept along with rainfall-runoff simulation is one of the methods used in the practical application of hydrology. Also, the study of the 24-hour design storm is different from the analysis of the storm precipitation presented in Chapter 4, since in this Chapter only the extreme rainfall events with duration of 24 hours will be analyzed.

5.2 Data Sets and Method of Analysis

Data from five precipitation recording gauges in the Seymour River watershed will be analyzed. The data sets from the stations Vancouver Harbour, S-1, 10A, 14A and 25B are used. The characteristics of the stations have been shown in Table 2.2 and their location has been presented in Figure 2.3 of Chapter 2. The stations cover an elevation range of about 760 m. The Vancouver Harbour station is the sea-level station and the 25B station is the second highest station of the Seymour watershed located at 762 m elevation (Table 2.2).

The maximum 24-hour rainfall usually occurs in the period from October to January

Chapter 5. 24-HOUR DESIGN STORM FOR COASTAL BRITISH COLUMBIA

(Fig. 5.2) when precipitation is generated by strong frontal systems coming from the North Pacific Ocean. As has been mentioned in Chapter 4, the precipitation during these systems is characterized by long duration and small to moderate intensities.

The selection criteria of the storms have been chosen to identify the 2 or 3 larger storms per year for each station. Hourly rain data were used for the analysis of the storms. The 24-hour storms selected for the analysis have rainfall depths larger than 55 mm for Vancouver Harbour and larger than 90 mm at the other stations. Under these criteria, 21 storms for the period 1976-1990 for the Vancouver Harbour station, 23 storms for the period 1984-1990 for the station S-1, 32 storms for the station 10A for the period 1976-1990, 28 storms for 14A for the period 1980-1990, and 16 storms for the station 25B for the period 1980-1990 were selected.

Analysis of the data for the study of the time distribution is achieved by a method very similar to the one presented by Huff (1967) and used for the analysis of the storm precipitation in Chapter 4. To compare different storms, rainfall for each event was expressed as the cumulative percentage of the total twenty-four-hour rainfall for twenty-four equal time increments through the storm. The resulting values were then used to calculate the time probability distributions which provide quantitative measures of both interstorm variability and the general characteristics of the time sequence of the rainfall. For the few storms which lasted less than 24 hours, the residual time increments were entered as zero rainfall to complete the fixed 24-hour duration event.

The developed time probability curves will be compared both visually and statistically. The statistical test is the Kolmogorov-Smirnov (KS) two sample test (Haan, 1977), which tests for significant differences between two independent cumulative frequency distributions.

The spatial distribution of the maximum 24-hour storms will be analyzed in the study watershed, and then the application of this distribution to other areas of the coastal British

Chapter 5. 24-HOUR DESIGN STORM FOR COASTAL BRITISH COLUMBIA

Columbia region will be investigated in the next paragraphs.

5.3 Time Distribution

Applying the above mentioned method of analysis, time probability distributions were developed for each of the five stations, and an example is shown in Figure 5.3 for station S-1. The percentages are defined such that, for example, for the thirty percent time distribution curve, thirty percent of the storms will have a time distribution above the curve. The time probability distributions of ten, thirty, fifty, seventy, and ninety percent are shown in Figure 5.3.

It is important to know how the time distribution of the storm varies at different elevations. A detailed data base is difficult to find in coastal British Columbia. However for the Seymour River watershed data are available at five stations for an elevation range of about 760 m. The fifty, ten and ninety percent time probability distributions for different elevations are compared in Figure 5.4. From this figure it is observed that the storm time distribution with elevation does not vary significantly and even the extreme time probability curves of ten and ninety percent have similar patterns. The largest deviation of the results is observed for the 90% curves. However, application of the KS test shows no significant differences at the 5% level between the curves from the stations at various elevations. Because of the small differences of the storm time distribution with elevation, average time probability distributions have been developed using the 120 storm distributions from all stations in the study watershed (Fig. 5.5).

It is important to examine whether the 24-hour storm time distribution for the Seymour River watershed can be transferred to other areas of coastal British Columbia. Similarities between the developed time probability curves for the Seymour River watershed

Chapter 5. 24-HOUR DESIGN STORM FOR COASTAL BRITISH COLUMBIA

and the curves developed in other studies for the same region or by using regional data would then indicate that the Seymour River watershed curves could be used for hydrologic design in other areas of the same climatic region. For this reason the time probability distribution curves developed for the Seymour River watershed will be compared firstly with the storm time distributions from other studies in the region and then with the time probability curves using other coastal British Columbia data.

Melone (1986) analyzed the time distribution of the largest 24-hour storm of record observed at each of 58 recording stations across coastal British Columbia, and developed the time probability distributions of the 24-hour storm for the 58 stations. In Figure 5.6 the results of Melone's work are compared with the average time probability distributions for the Seymour River watershed. It is evident from this comparison that the results of this study cover the time distribution of the extreme 24-hour storms in coastal British Columbia stations. Only the ten percent curves deviate, and a possible explanation for this deviation may be that Melone analyzed only the largest 24-hour storm for each of the 58 stations whereas in the present study a large number of storms have been analyzed for each station in the study watershed. However, the general pattern of the rain distribution, at least during the most extreme storms, is similar to the pattern observed in the study watershed. In addition, the statistical KS test showed that there are no significant differences between any of the curves at the 5% level.

The results of this study were also compared to the results that Hogg (1980) reported. Hogg analyzed 119 12-hour events from coastal British Columbia stations. Hogg suggested (Hogg, personal communication) that the time distribution of the 24-hour design storm should be similar to the 12-hour storm. Figure 5.7 shows the comparison of Hogg's results with the results of this study. It is evident from this figure that the 24-hour design storm developed in this study has a similar time distribution to the 12-hour design storm developed by Hogg for

Chapter 5. 24-HOUR DESIGN STORM FOR COASTAL BRITISH COLUMBIA

the British Columbia coast. Also, the statistical KS test showed that there are no significant differences between any of the curves at 5% level.

The findings of this study are also compared with the time distribution of the extreme 24-hour storms from other areas of the same climatic region. Data sets from three stations located in different areas of coastal British Columbia were used to develop time probability distribution curves. The stations used for this analysis are the Carnation Creek CDF station, the Courtenay Puntledge BCHP station, and the Kitimat station (Fig. 2.1) which has been used in Chapter 4 for the comparison of the storm precipitation time distribution. Because of the different microclimates of the areas of the three stations, different criteria were used for the selection of the 24-hour extreme storms analyzed (Table 5.1). The number of years of record is different for these stations and so is the number of the events used for the analysis.

Table 5.1. Characteristics of the coastal British Columbia station used in the analysis of the 24-hour extreme rainfall time distribution.

Station Name	Greatest 24-hour Rainfall (mm)	Mean Annual 24-hour Storm Depth (mm)	Minimum Depth (mm)	Period of Record	Number of Storms
Carnation Creek CDF	230	96.9	70	1975-1986	50
Courtenay Puntledge	124	69.9	55	1964-1991	50
Kitimat	123	92.7	55	1979-1991	31

Chapter 5. 24-HOUR DESIGN STORM FOR COASTAL BRITISH COLUMBIA

The time distribution probability curves developed from the data from the three stations and the average curves developed for the Seymour River watershed are compared in Figure 5.8. The comparison shows that the curves of the three British Columbia stations are similar. Furthermore, these curves are similar to the average Seymour curve shapes. The variability that exists between the time probability curves may be explained by the differences between the microclimates of each site. However, the KS test showed no significant differences between these curves at the 5% level. The above three comparisons suggest that the results of the study can be transferred to other regions of coastal British Columbia without loss of accuracy.

The results of this present work have been compared with some other design storms used by engineers in every day practice. Four such design storms were considered: the Soil Conservation Service Type I and Soil Conservation Service Type IA storms (U.S.D.A., 1986), the Hershfield storm (Hershfield, 1962) and the storms that can be developed using Intensity-Duration-Frequency (IDF) curves, the so-called Alternating Block Method (Chow et al., 1988). The first two design storms were developed by the U.S. Department of Agriculture Soil Conservation Service (SCS). The SCS developed five 24-hour duration storms, and the storms called Type I and Type IA were developed for use on the coastal side of the Sierra Nevada and Cascade mountains of Oregon, Washington and Northern California, and the coastal regions of Alaska. These hyetographs were derived from information presented by Hershfield (1961), by Miller, Frederick, and Tracey (1973) and from additional storm data. These two storms, SCS Type I and IA, are extensively used in coastal British Columbia since the province is located within the greater climatic region for which the storms are designed.

The Hershfield storm (Hershfield, 1962) was developed by analyzing data from 50 widely separated stations with different rainfall regimes across the U.S.A. and an average curve was prepared for all storm durations.

The Alternating Block Method is a popular technique among practicing engineers. This method is a simple way of developing a design hyetograph from Intensity-Duration-Frequency curves. One design hyetograph can be developed for each return period and each storm duration.

These various design storms are compared in Figure 5.9 and the comparison indicates a significantly different rainfall pattern than the observed values. The Alternating Block Method synthetic hyetograph represents a totally different time distribution pattern from the observed. The curve SCS Type IA shows better agreement with the 10% curve developed in this study. It is evident from the above comparison that most of the synthetic hyetographs represent storms with intense periods of rain. On the other hand, the observed pattern is more uniform and does not contain intense bursts of rain.

It is important, however, to identify whether the variations observed between the synthetic hyetographs and the derived time distributions significantly affect the simulation of the runoff. This analysis will be presented at the end of the Chapter after the presentation of the spatial distribution of the extreme 24-hour storms and the analysis of the antecedent rainfall.

5.4 Spatial Distribution

As indicated from the results of the analysis of mean annual precipitation in Chapter 3, the main spatial variation of the precipitation is variation with elevation for medium to small mountainous watersheds. In this part of the Chapter the spatial distribution of the design storm with elevation will be examined.

In the Seymour River watershed the 24-hour maximum storm data have been analyzed and the Extreme Value I (Gumbel) probability distribution has been fitted to the data. The

Chapter 5. 24-HOUR DESIGN STORM FOR COASTAL BRITISH COLUMBIA

results (Fig. 5.10) show that, for all the return periods, the rainfall increases up to the middle position of the watershed (station S-1, at 260 m), and then abruptly decreases (station 10A, at 293 m), before a further slight increase and leveling off at the upper elevations (Fig. 5.10). This particular rain distribution is similar to the distribution of the mean annual precipitation and mean storm precipitation in the study watershed. Both the mean annual precipitation and the extreme 24-hour storms increase by an average factor of about 2.5 between the Vancouver Harbour and S-1 stations and then decrease to a factor of 1.7 at station 10A and then increase and level off to a factor of 2.0 at station 25B. The reason for the abrupt decrease of the rain after the S-1 station is the topography of the area. At the position of station S-1 the Seymour River valley turns to the northwest and the resulting increased convergence of the incoming air mass generates large precipitation at this middle position. Unfortunately, there are not enough recording stations in the area in order to compare the observed rainfall distribution in the study watershed with the precipitation distribution in adjacent watersheds. However, the analysis of the long term annual, seasonal, and monthly precipitation accumulations from the nearby Capilano watershed, presented in Chapter 3, showed that the precipitation distribution in Capilano watershed is similar to that of the Seymour watershed except for the large decrease after the middle of the watershed. Hence, it seems that the rainfall in the study area increases for the first topographical rise and then either levels off or even decreases. The generality of this conclusion for the coastal British Columbia will be examined in the next paragraphs.

Three aspects will be examined. Firstly, it is important to examine the spatial distribution of rainfall over the watershed during the extreme events. The results shown in Figure 5.11 are based on all the extreme events and they have not necessarily occurred at the same time throughout the watershed. However, the analysis of the storm precipitation in the study watershed have shown that the rainfall during a single storm also has a similar

Chapter 5. 24-HOUR DESIGN STORM FOR COASTAL BRITISH COLUMBIA

distribution. Furthermore, a study of the spatial and temporal distribution of extreme historical storms will be presented in Chapter 6 and it will be shown that during an individual storm the precipitation is distributed with a similar pattern to that of the storm and mean annual precipitation found in Chapters 3 and 4. It is also very important to note that the storm rainfall increases and decreases, on average, at a similar rate as the mean annual precipitation. Secondly, it is important to evaluate whether the spatial distribution of the extreme precipitation observed in the Seymour River watershed is transferable to the coastal British Columbia region. Unfortunately, there are not enough recording precipitation stations in the region to analyze the spatial distribution of the short term precipitation. However, there are more storage gauges which could give a good indication of the spatial distribution of the longer term precipitation. The analysis presented in Chapter 3 has shown that the mean annual precipitation in the coastal Pacific Northwest increases up to an elevation of 400-800 m, and then either levels off or even decreases at higher elevations. Hence, the long-term precipitation in the greater region has a spatial distribution pattern with elevation similar to the one observed in the Seymour River watershed except that there is not such a large decrease of the rainfall after the middle position of the watershed. This leads to the third question of whether the extreme 24-hour storm rainfall is a certain percentage of the mean annual precipitation. If this is true then the mean annual precipitation could be used as an index of storm rainfall. The above hypothesis is probably reasonable because most of the annual precipitation is caused by the same type of low pressure systems and most of this rainfall occurs in the fall and winter. This hypothesis will be examined in the next paragraphs.

The analyzed extreme 24-hour rainfall data for return periods of 2-, 5-, 10-, 25-, 50-, and 100-year return period and mean annual precipitation were obtained from Environment Canada, Atmospheric Environment Service for sixty-one recording stations across coastal British Columbia. Thirty-five stations are located in the southwest mainland coast, thirteen on

Chapter 5. 24-HOUR DESIGN STORM FOR COASTAL BRITISH COLUMBIA

the east of Vancouver Island and the Gulf Islands, six on the west of Vancouver Island, and seven are located on the north mainland coast and Queen Charlotte Islands. The sixty-one stations used in the study are listed in Table B1 in Appendix B.

The extreme 24-hour rainfall for the sixty-one British Columbia stations has been plotted against the station mean annual precipitation and regression analysis has also been performed between the extreme 24-hour storm rainfall of the various return periods and the mean annual precipitation. The results of this analysis are shown in Appendix B. Figure 5.11 presents the results for the 10-year 24-hour rainfall and indicates that this storm is, on average, 5.7% of the mean annual precipitation.

However, analyses of this type are biased towards southwestern coastal British Columbia since most of the recording stations are located in that region. For this reason separate analyses have been carried out for the southwest mainland coast, for east Vancouver Island, west Vancouver Island, and the north coast of British Columbia. The results are summarized in Table 5.2 which lists the mean and the range in percentage of the extreme 24-hour precipitation against the mean annual precipitation. There is a significant overlapping between the ranges for the various return periods and sub-regions but it can be observed that the average value increases as the return period increases. Also from this Table can be seen that the ratio of the extreme 24-hour rainfall and the mean annual precipitation has its maximum value for the east coast of Vancouver Island, the dryer of the four sub-regions and also, the variation of the ratio is the largest in this sub-region.

Chapter 5. 24-HOUR DESIGN STORM FOR COASTAL BRITISH COLUMBIA

Table 5.2. Ratio of the 24-hour rainfall and mean annual precipitation for various coastal sub-regions of British Columbia.

Return Period (years)	Southwest Mainland B.C. Coast (%)	East Coast of Vancouver Island (%)	West Coast of Vancouver Island (%)	North B.C. Coast (%)
2	4.1 (3.0-5.3)	5.1 (3.3-7.3)	4.2 (3.3-4.8)	3.8 (3.2-4.3)
5	5.1 (3.6-6.5)	6.6 (3.9-10.3)	5.2 (4.3-6.2)	4.9 (4.0-6.1)
10	5.8 (4.0-7.5)	7.7 (4.4-12.3)	5.9 (5.0-7.2)	5.7 (4.5-7.4)
25	6.7 (4.5-8.6)	8.9 (5.0-14.9)	6.8 (5.8-8.4)	6.6 (5.1-8.9)
50	7.4 (4.9-9.8)	9.9 (5.4-16.7)	7.5 (6.4-9.3)	7.3 (5.6-8.9)
100	8.0 (5.3-10.9)	10.8 (5.8-18.6)	8.1 (7.0-10.2)	7.9 (6.0-11.2)
Mean Annual				
Precipitation (mm)	1968 (982-3600)	1122 (619-1656)	2824 (1870-3943)	2050 (1137-3155)

The above analysis indicates that an estimate of extreme 24-hour rainfall estimate can be made based on mean annual precipitation at a location. Therefore, it is reasonable to suppose that the distribution of long term precipitation with elevation is an index for the distribution of storm rainfall. This conclusion is supported by the results found for the Seymour River watershed, as previously discussed. This means that the largest storm rainfall does not increase linearly with elevation, but increases at the low and middle elevation, and then levels off at the top elevations.

5.5 Antecedent Rainfall

The antecedent rainfall for periods of several days before the design storm is important to the hydrologist, particularly if the problem involves rural or mountainous basins as opposed to highly impervious urban watersheds. The antecedent rainfall characterizes the soil moisture conditions in the watershed prior to the occurrence of the storm and therefore, controls the response of the watershed.

Table 5.3 shows the estimates obtained for the antecedent rainfall at three stations in the Seymour River watershed for five probability levels and for 1- to 5- day periods. It is assumed that the three stations represent the lower, middle and upper watershed (stations Vancouver Harbour, S-1, and 25B, respectively).

These results show that the antecedent rainfall increases with elevation. Furthermore, there is a fifty percent probability that the 1-day antecedent rainfall at the middle and upper watershed will be about 20 mm. This is critical for the generation of the runoff from the steep hillslopes of the watershed and shows that there is a high probability that the soil moisture levels will be high, especially throughout the winter period.

The antecedent rainfall statistics may vary considerably in the same climatic region but the results of this study give a good first approximation.

Chapter 5. 24-HOUR DESIGN STORM FOR COASTAL BRITISH COLUMBIA

Table 5.3. Probability distribution of antecedent rainfall (mm) for the maximum 24-hour storms for various numbers of days.

Probability (%)	1-day	2-days	3-days	5-days
Vancouver Harbour				
10	62.0	81.4	93.4	135.3
30	22.2	43.2	52.4	77.2
50	7.9	22.9	30.1	44.1
70	2.8	12.2	17.0	25.2
90	1.0	6.5	9.7	14.4
S-1				
10	82.2	129.6	158.0	244.4
30	38.4	66.7	83.2	129.3
50	17.9	34.3	43.8	68.4
70	8.4	17.7	23.1	36.2
90	3.9	9.1	12.2	19.1
25B				
10	87.0	154.6	262.9	565.5
30	43.9	85.8	133.0	242.3
50	22.1	47.6	67.3	104.0
70	11.1	26.4	34.0	44.7
90	5.6	14.7	17.2	19.2

5.6 Simulation of Peak Stream Flow at Jamieson Creek Watershed

The observed time distributions and the synthetic hyetographs presented earlier have been used as input to a simple watershed model for the calculation of streamflow runoff. The streamflow data have been taken from the Jamieson Creek watershed. Jamieson Creek is a small tributary of the Seymour River, and is located in the headwaters of the river system. The basin has an area of 2.99 km^2 , and its elevation ranges from 305 to 1310 m above mean sea level so that there is a good variation in elevation. Jamieson Creek is characterized by steep hillslopes having an average gradient of 48%.

Because of the small area of the Jamieson Creek watershed, rainfall data from one station were considered adequate. The station 25B is located in the middle of the watershed, so that it is assumed to represent the average rainfall over the watershed, and its data have been used to estimate the 24-hour rainfall depth. This assumption was confirmed in an earlier, more detailed study (Loukas and Quick, 1993b) in which five stations within the Jamieson Creek watershed were used.

The 24-hour rainfall for various return periods has been distributed in time according to the observed and synthetic hydrographs and the resulting storms have been used as input to an event based watershed model. The watershed model was developed in a previous study and it was shown to give good simulation of the watershed response (Loukas, 1991).

The watershed model is an event model which uses a linear reservoir routing technique and simulates the fast runoff with a series of cascading reservoirs and the slow runoff with one large reservoir (Fig. 5.12). The whole process is infiltration controlled using a power relationship as:

$$P_s = I_f + a \cdot t^{-b} \quad (5.1)$$

where P_s is the rainfall infiltrated and diverted to slow runoff (mm/h), I_f is the final infiltration abstractions (mm/h), and a and b are constants. The remaining rainfall P_f from the total rainfall P_t is diverted to the stream as fast runoff.

In the previous study this model was kept deliberately simple for a first analysis with the intention of adding more complexity to handle soil moisture, but the model was found to perform well, so that no additional complexity was added to it.

An assumption that underlies the application of rainfall-runoff simulation for the estimation of the extreme flows is that the return period of the peak flow is the same as the return period of the 24-hour rainfall depth. This assumption is common in the application of design storms for practical purposes, but it has been challenged (Dickinson et al., 1992). The above assumption should hold if the watershed is small and the only causative factor of floods is the extreme rainfalls which occur at certain periods of the year. The annual floods in the watersheds of coastal British Columbia can be generated by rainfall, rain on snow, and snow melt events (Melone, 1985). In the case of Jamieson Creek watershed, rainfall and rain on snow are the dominant flood producing mechanisms. The annual rain generated floods were identified and separately analyzed from the rain on snow floods.

Generally, there are a number of combinations of watershed conditions, extreme storms of various return periods and time distributions that can produce a flood of a given return period. For example, a 10-year rain storm over dry soil can produce peak flow significantly less than a 10-year flood because of the larger abstractions to the soil storage. However, for this study area, analysis of the time of the occurrence of the largest annual 24-hour rainfall showed that there is about 75% probability that the maximum 24-hour storm will occur in the period from October to January (Fig. 5.2), and during this time period the soil in the study area is wet. More specifically, as already discussed in the previous section, analysis of the antecedent rainfall prior to the extreme events showed that there is fifty percent

chance that the 1-day antecedent rainfall at the upper Seymour River watershed will be larger than 20 mm. Hence, it has been assumed that the soil is saturated at the beginning of the extreme storm and the abstractions to the soil moisture storage have been set to zero.

Using the above assumptions, tests have been made to compare the observed rain generated peak flows with the simulated flows using the various synthetic and derived hyetographs. These analyses have been used to generate the 2-, 5-, 10-, 25-, 50-, and 100-year floods from the Jamieson Creek watershed. Table 5.4 shows the comparison of the simulated peak flows using the various hyetographs with the observed rain generated peak flows for the Jamieson Creek watershed. These results indicate that the 10% time probability distribution curve derived earlier in this Chapter gives results that are close to the observed peak flows. The agreement is better for small return periods. It should be noted that the "observed" 25, 50, and 100-year floods are extrapolations of the observed flows of 16 years using the fitted Extreme Value I (Gumbel) probability distribution. Hence, it is reasonable to expect higher variation between the simulated and the "observed" peak flows for the larger return periods.

Of the various well known rainfall design storms, only the SCS Type IA curve gave reasonably good results. The other synthetic storms produce larger peak flows than the observed flows for all the return periods. The Alternate Block Method hyetograph produces the highest peaks because of the inherent assumption of the method that all the intensities for durations from 1 to 24 hours will occur in the design storm. Furthermore, the arrangement of the intensities in symmetrical fashion around the middle of the storm duration is another reason for the over-maximization of the storm and consequently the peak flow. The SCS Type I and the Hershfield hyetographs produce higher estimates of the peak flow by about 20% and 10%, respectively (Table 5.4).

Table 5.4. Comparison of the simulated peak flows (m³/sec) using various hyetographs with the observed flows of Jamieson Creek watershed.

Hyetograph used	Return Period (years)					
	2	5	10	25	50	100
10% curve	7.01	9.10	10.48	12.25	13.52	14.81
50% curve	5.10	6.62	7.63	8.90	9.84	10.78
90% curve	6.10	7.90	9.12	10.64	11.7	12.81
ABM	11.49	14.49	16.69	19.83	21.83	23.79
Hershfield	8.11	10.53	12.12	14.14	15.64	17.13
SCS Type I	8.73	11.33	13.05	15.22	16.84	18.44
SCS Type IA	7.21	9.35	10.77	12.57	13.90	15.23
Observed	6.20	8.85	10.60	12.82	14.47	16.10

From the derived time distributions only the 10% curve, derived in this study, gives peak flow estimates close to the observed flows. The 50% and the 90% curves produce the lower peak flows of all the hyetographs tested.

In addition to the peak flow itself, two other important considerations for the application of the design storm are the shape of the resulting hydrograph and the timing of the peak flow. Figure 5.13 compares the observed and the simulated 10-year flood hydrographs for the various hyetographs. The SCS Type IA storm and the derived 10% storm gave similar hydrographs to the observed hydrograph. The hydrograph of the 10% storm has higher flows at the beginning of the event and it peaks later than the SCS Type IA hydrograph. However,

the hydrograph volumes are similar. The other synthetic hyetographs produce hydrographs different in shape from the observed hydrograph. The hydrograph generated by the Alternating Block Method curve significantly overestimates the peak flow and has a more symmetrical shape than the other hydrographs. The SCS Type I and Hershfield storms both gave similar hydrographs but the Hershfield storm produced a more delayed peak flow. Finally, the derived curves of 50% and 90% produce the most delayed and flat hydrographs (Fig. 5.13).

The above results show that the design storm derived in this study, using the 10% time probability distribution curve, gave the best results. For the other design storms only the SCS Type IA storm should be used for the estimation of peak flows from mountainous watersheds in the study area, and gives reasonable results provided that attention is paid to the assumptions discussed at the beginning of this section.

5.7 Summary

The distribution of the extreme 24-hour storms in space and time has been analyzed using the rainfall data from the Seymour River watershed. The choice of the 24-hour storm duration was based on meteorological, hydrological and pragmatic reasons. Firstly, the extreme storms are strong winter frontal storms which usually have a duration of about a day. Secondly, the response of rural and mountainous watersheds in the study area is in the order of several hours so that a long duration storm should be used as a design storm. Finally, the use of the 24-hour design storm expands the usable data both in space and time since there are more and longer daily records from storage precipitation gauges and only a few recording gauges in coastal British Columbia.

The analysis showed that the time distribution of the 24-hour storms does not change

Chapter 5. 24-HOUR DESIGN STORM FOR COASTAL BRITISH COLUMBIA

significantly over the elevation range of the data in the Seymour River watershed and therefore, average time probability distributions have been developed. The transferability of the derived storm time distributions was tested against the results of other studies which analyzed rainfall data from coastal British Columbia and actual data from three coastal British Columbia stations. This comparison showed that the 24-hour storm time distributions of this study appear to be transferable to other areas of coastal region of British Columbia.

Examination of other synthetic storms revealed that most of these storms have a time distribution which is characterized by bursts of intense rain which do not appear to be observed in the Seymour River watershed data or in other data from recording rain gauges in the region. Application of the derived and synthetic storms to a real watershed showed that the 10% time probability curve and the SCS Type IA curve gave good estimation of the peak flow. Furthermore, the shape and the time to peak of the hydrograph is similar for these two storms. These results justify the application of either the storm hyetograph derived in this study using the 10% curve, or the SCS Type IA hyetograph, for the estimation of peak flow in coastal British Columbia.

Study of the extreme 24-hour storm rainfall in the Seymour River watershed indicates that the storm rainfall increases up to the middle position of the basin, and then decreases, and levels off at the top elevations. It is very important to note that the extreme 24-hour rainfall is highly correlated with mean annual precipitation. Analysis of the extreme 24-hour rainfall for the four sub-regions of the coastal British Columbia showed that the 24-hour storm depth is a certain percentage of the mean annual precipitation and agrees with earlier findings by Melone (1986). Therefore, the mean annual precipitation can be used as an index for the 24-hour storm depth. The results presented in Chapter 3 have shown that the mean annual precipitation in coastal British Columbia increases up to 400-800 m in elevation, and then levels off or even decreases at the upper elevations. Also, the study of the storm precipitation

presented in Chapter 4 and the analysis of extreme historical storms that will be presented in the next Chapter indicate that the storm distribution across a watershed follows a similar curvilinear pattern, increasing at the lower elevations and then leveling off or even decreasing at elevations above 800 m. Similar results for the annual and seasonal precipitation have been found for the northern Cascade region in Washington State which indicates that the results of this study may be transferable to the greater region of the Pacific Northwest.

The above conclusions together with the results of the analysis of the storm time distribution are significant for the estimation of the peak flows from the coastal watersheds. Furthermore, the result of this study indicates that the extreme 24-hour rainfall can be estimated as a certain percentage of the mean annual precipitation. Of the 269 precipitation stations in coastal British Columbia, 96 are recording gauges, and from these stations only 61 have records long enough to assure a reliable frequency analysis. Therefore, this study indicates that, until more extensive and long-term recording rain gage data are available, the annual data are a valuable guide for design flood estimation.

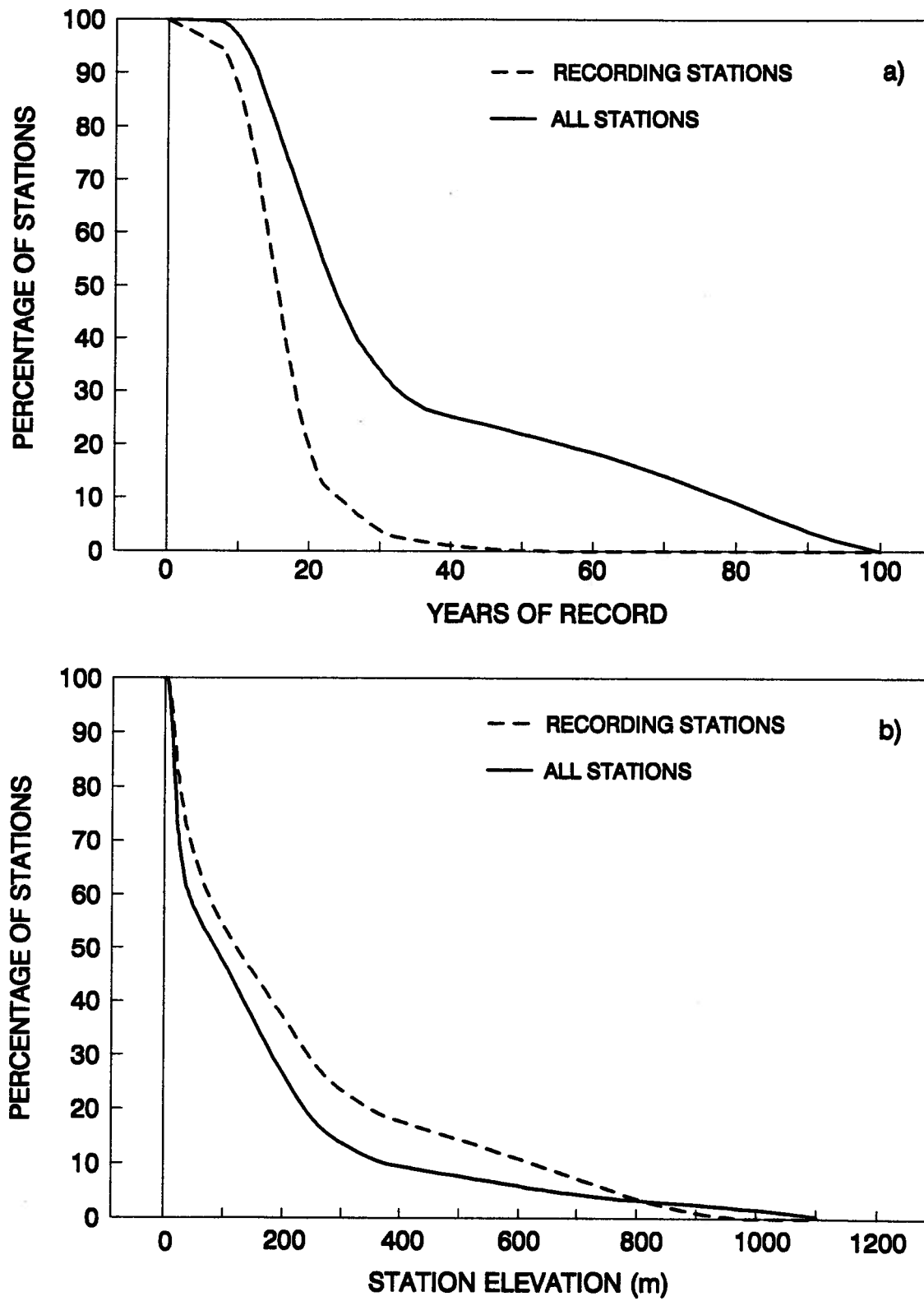


**Fig. 5.1. Distribution of the coastal British Columbia stations with
a) years of record, and b) station elevation.**

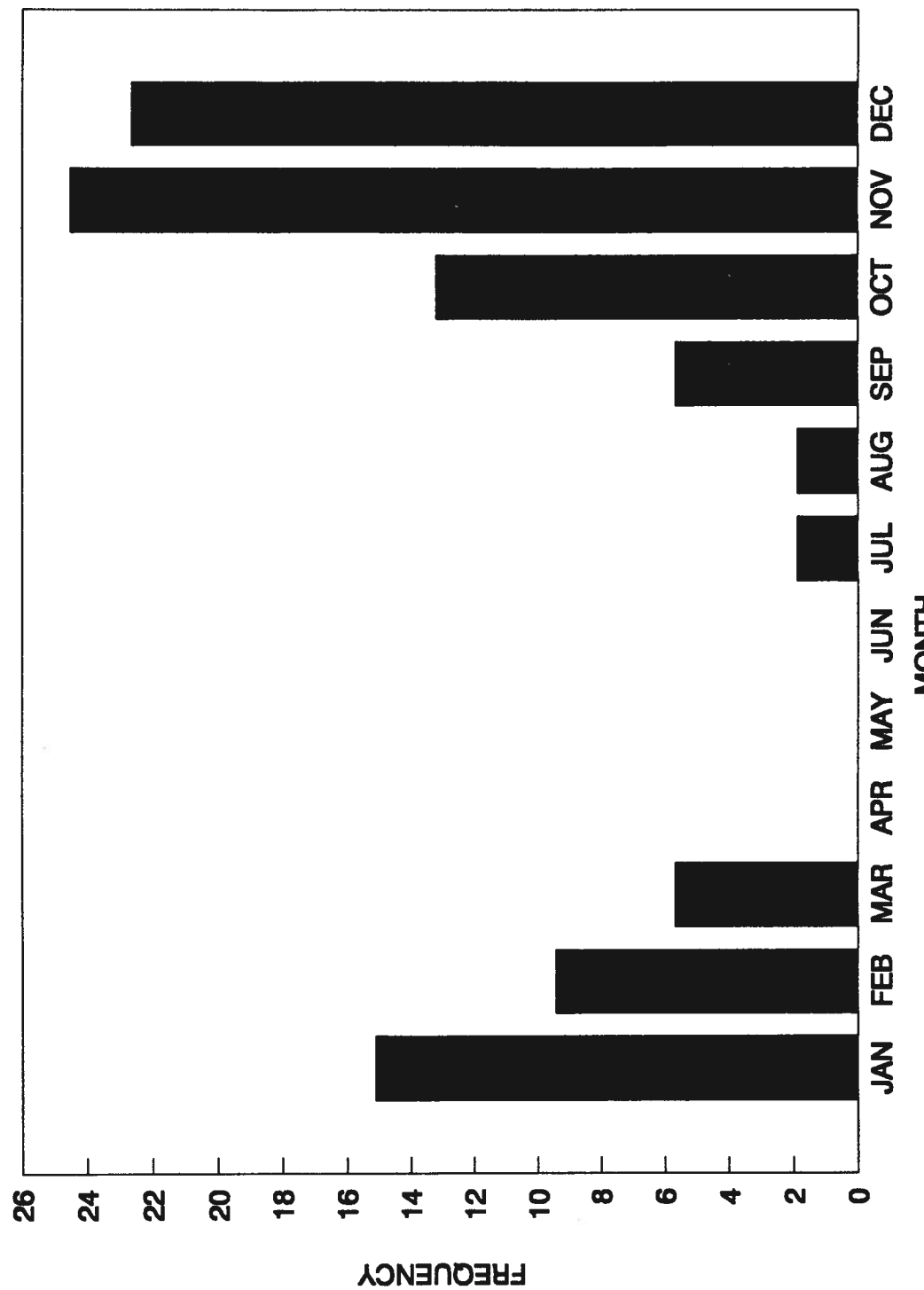


Fig. 5.2. Monthly distribution of the occurrence of the annual maximum 24-hour storms at Vancouver Harbour (53 years).

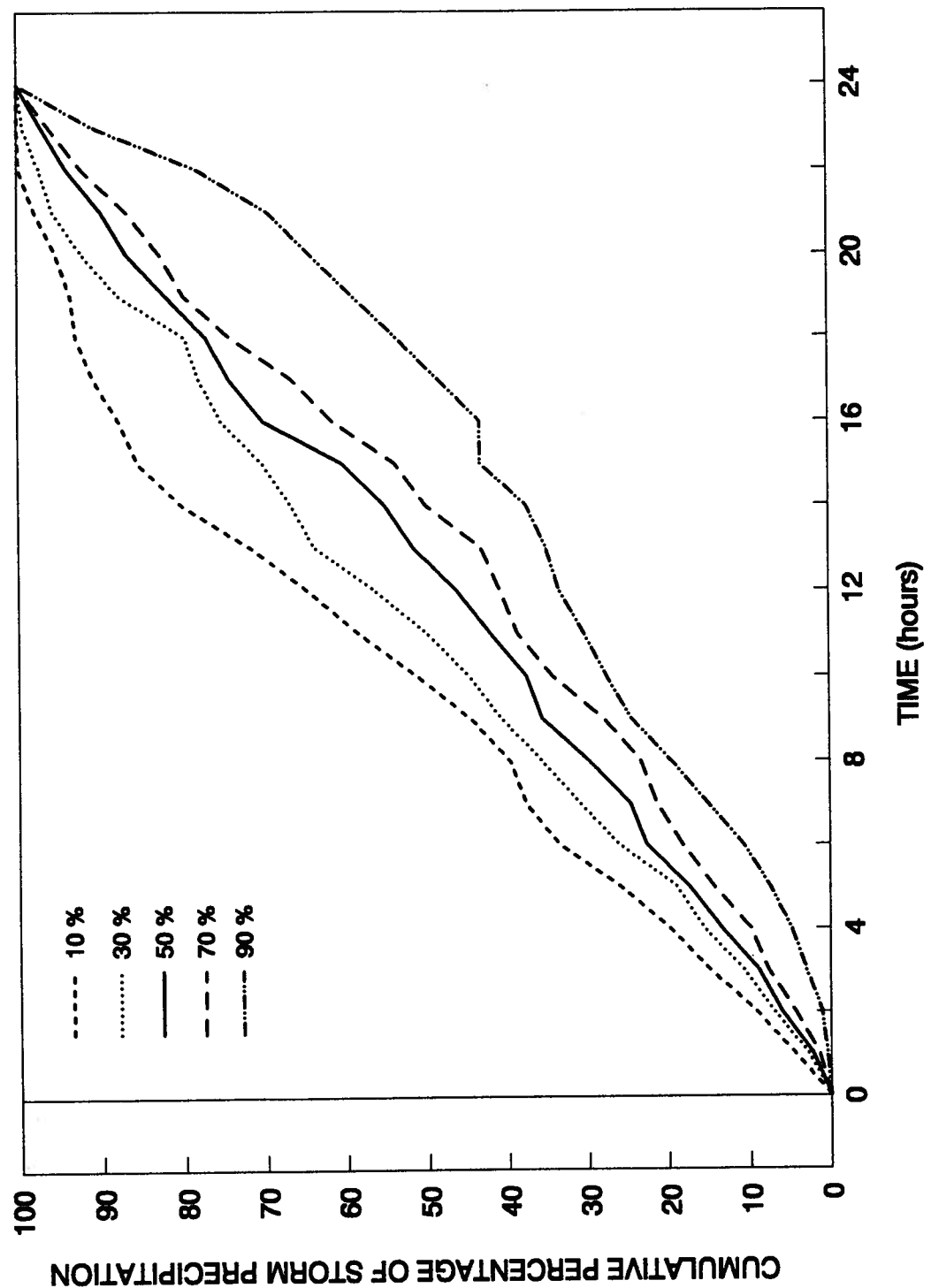


Fig. 5.3. Time probability distributions of 24-hour storms for station S-1.

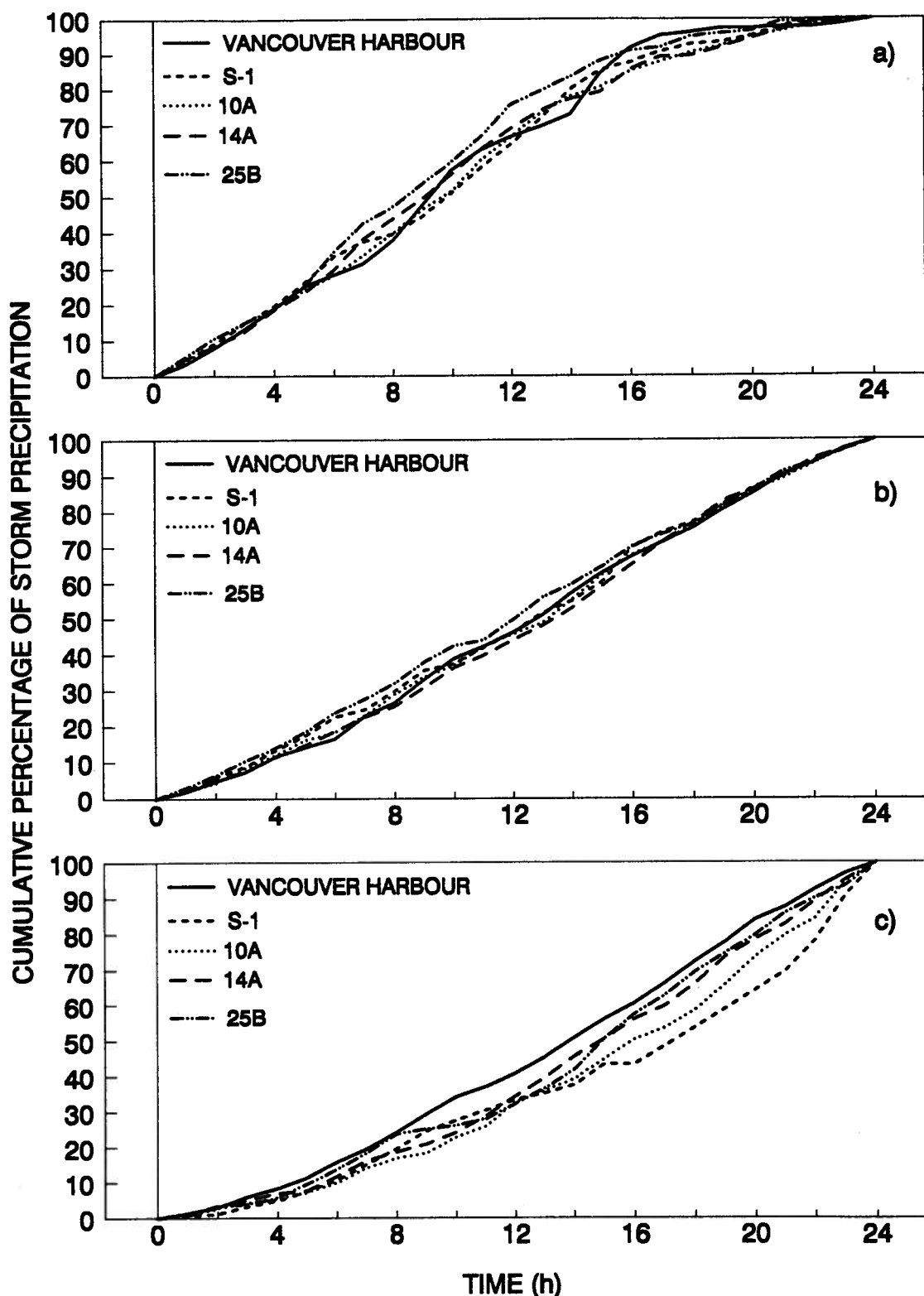


Fig.5.4. Comparison of the time probability distributions for various stations
a) ten percent curves, b)fifty percent curves, and c) ninety percent curves

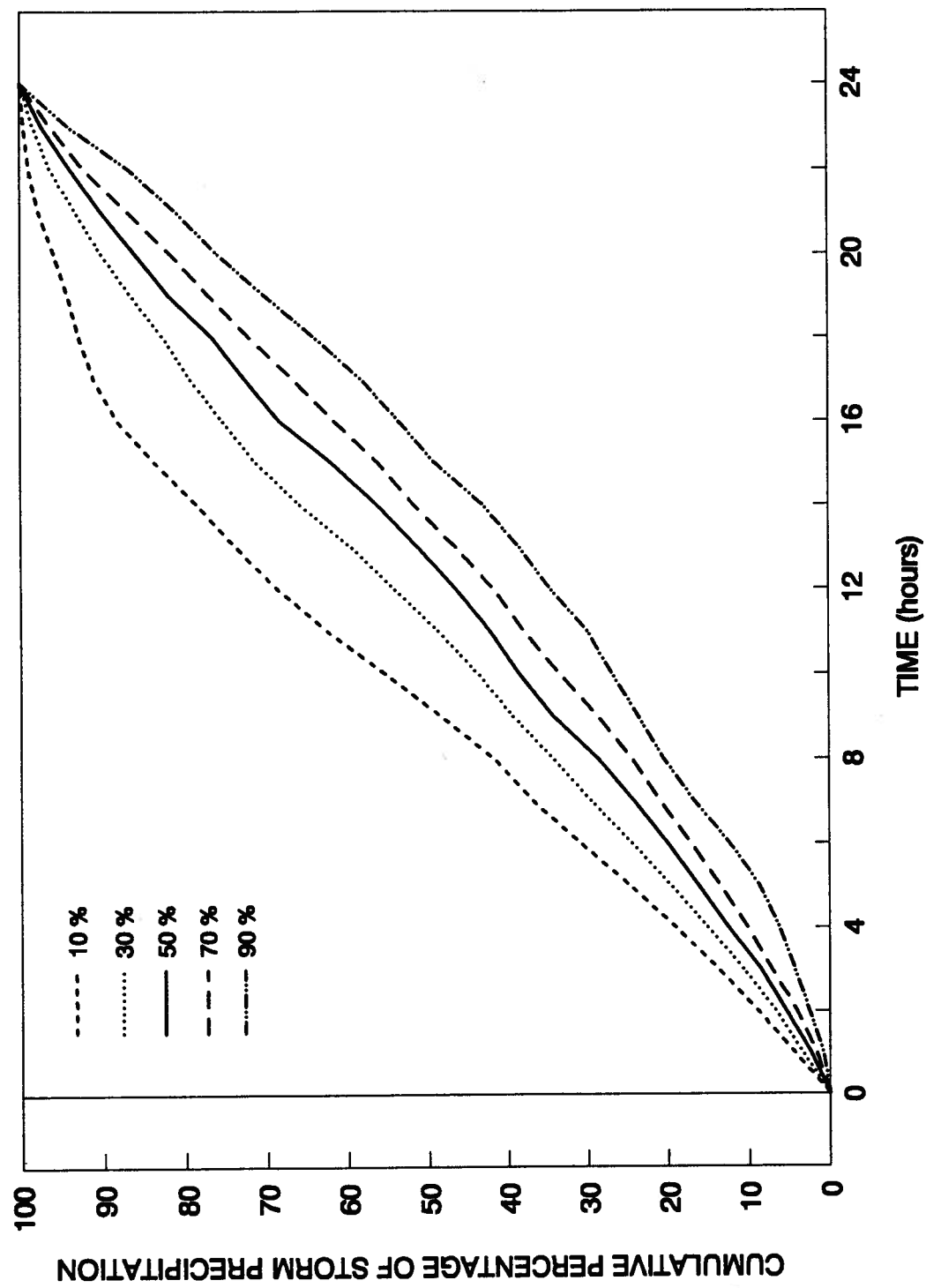


Fig.5.5. Average time probability distributions for the Seymour River watershed.

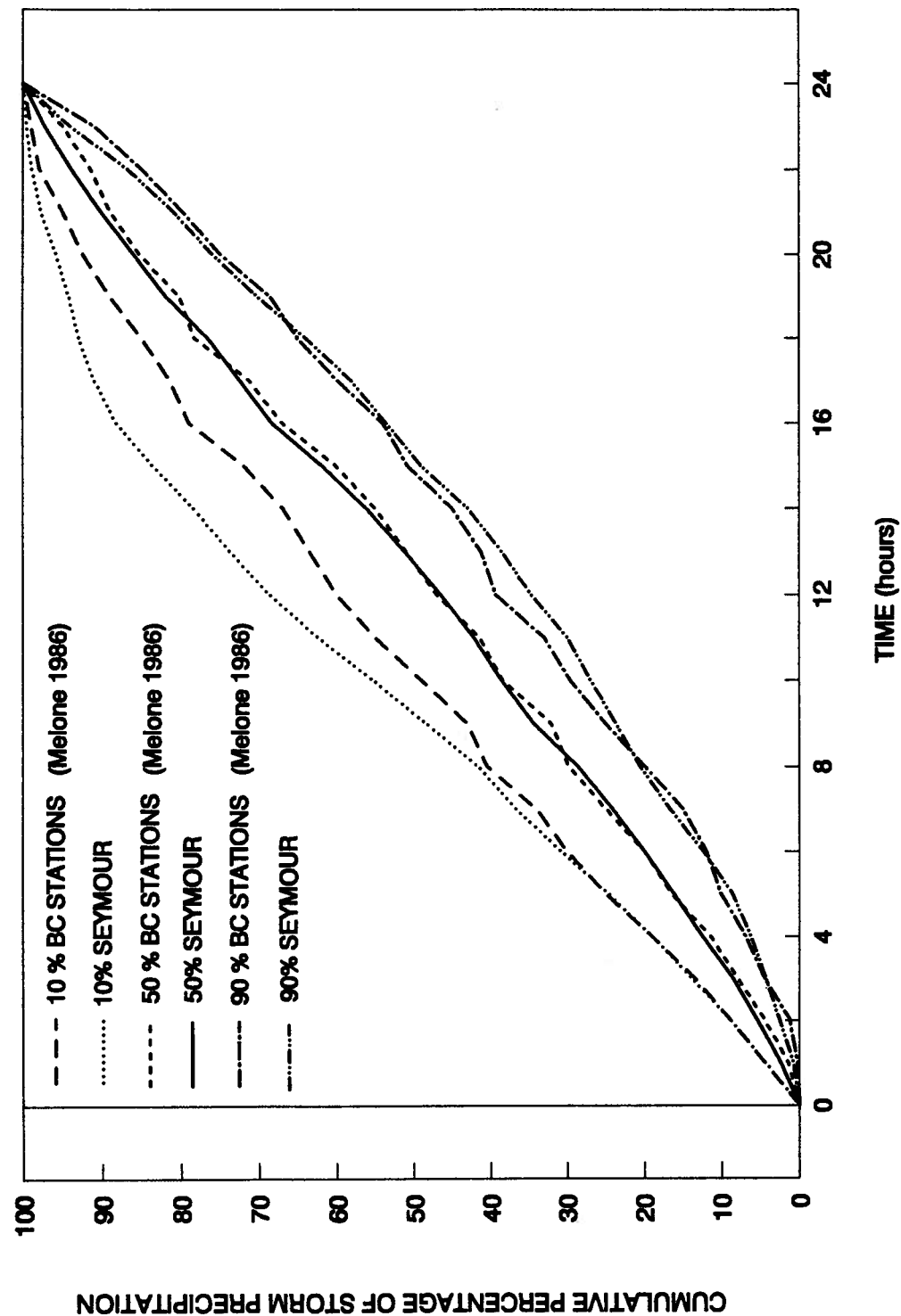


Fig. 5.6 Comparison of the average storm time distribution in the Seymour River watershed with the results of the Melone (1986) analysis for coastal British Columbia.

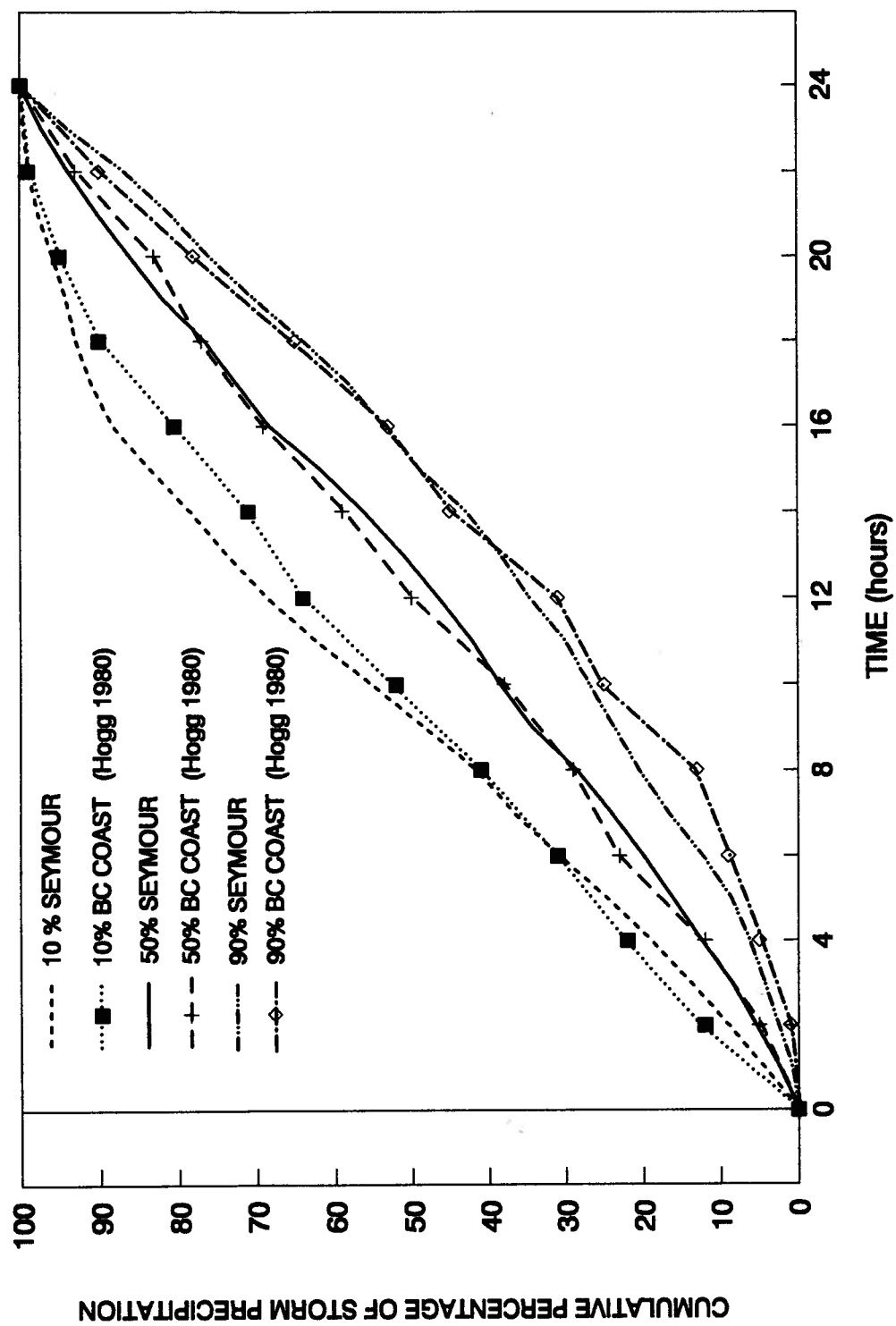


Fig. 5.7 Comparison of the average storm time distributions in the Seymour River watershed with the results of the Hogg (1980) analysis for coastal British Columbia.

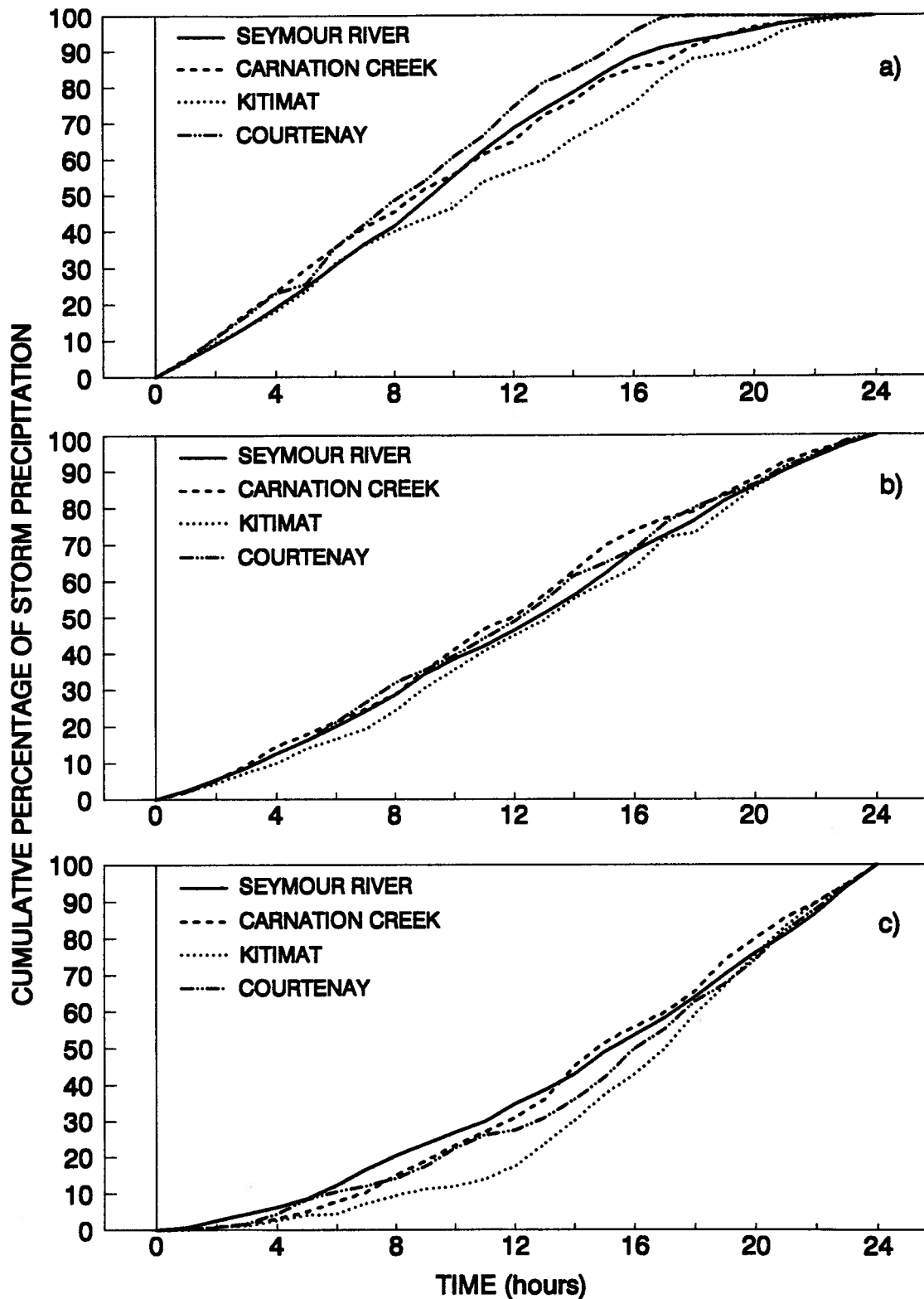


Fig. 5.8. Comparison of the time probability distributions of the Seymour River watershed and three coastal British Columbia stations, a) ten percent curves, b) fifty percent curves, and c) ninety percent curves.

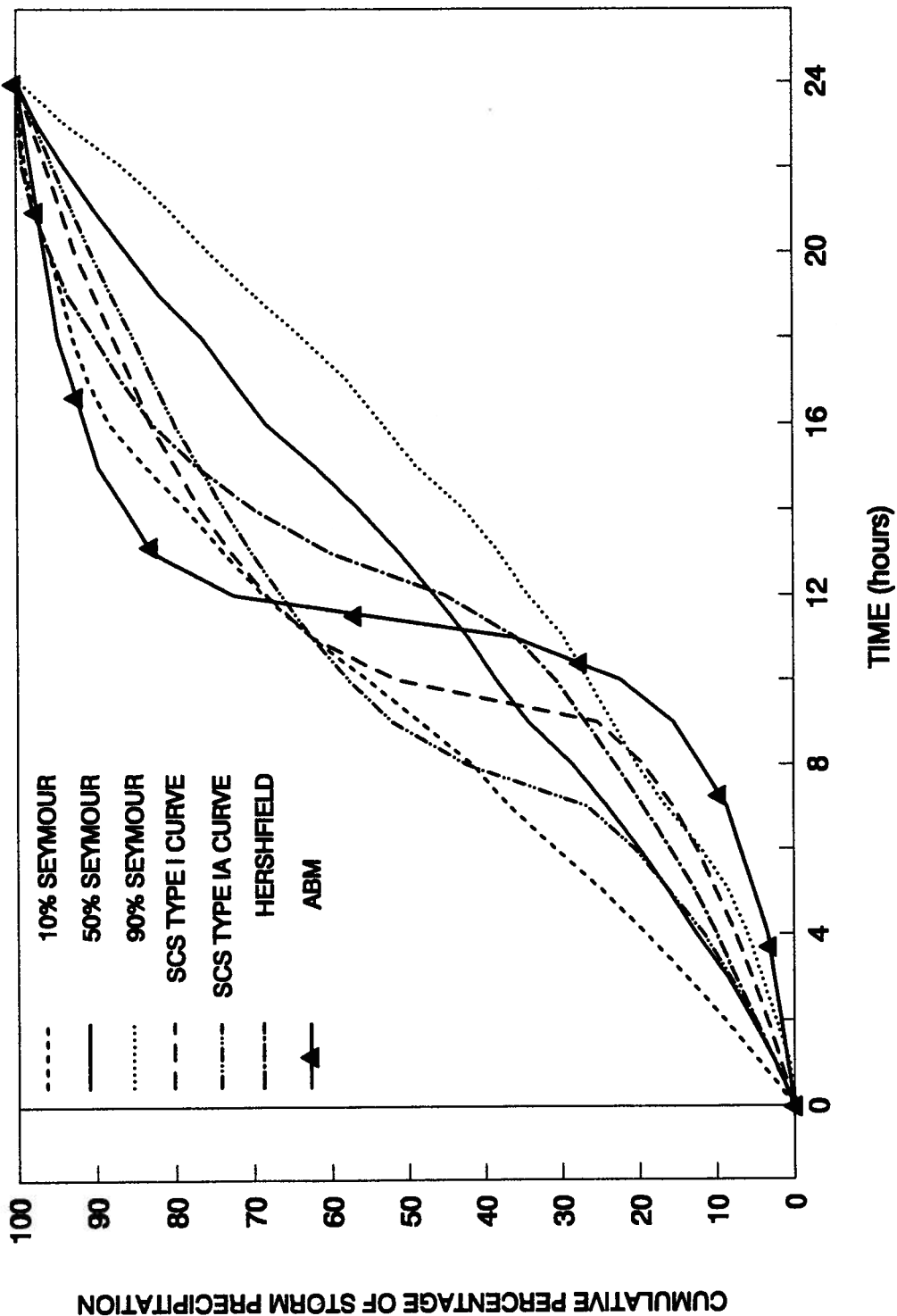


Fig. 5.9 Comparison of synthetic storms with the average time probability distributions in the Seymour River watershed.

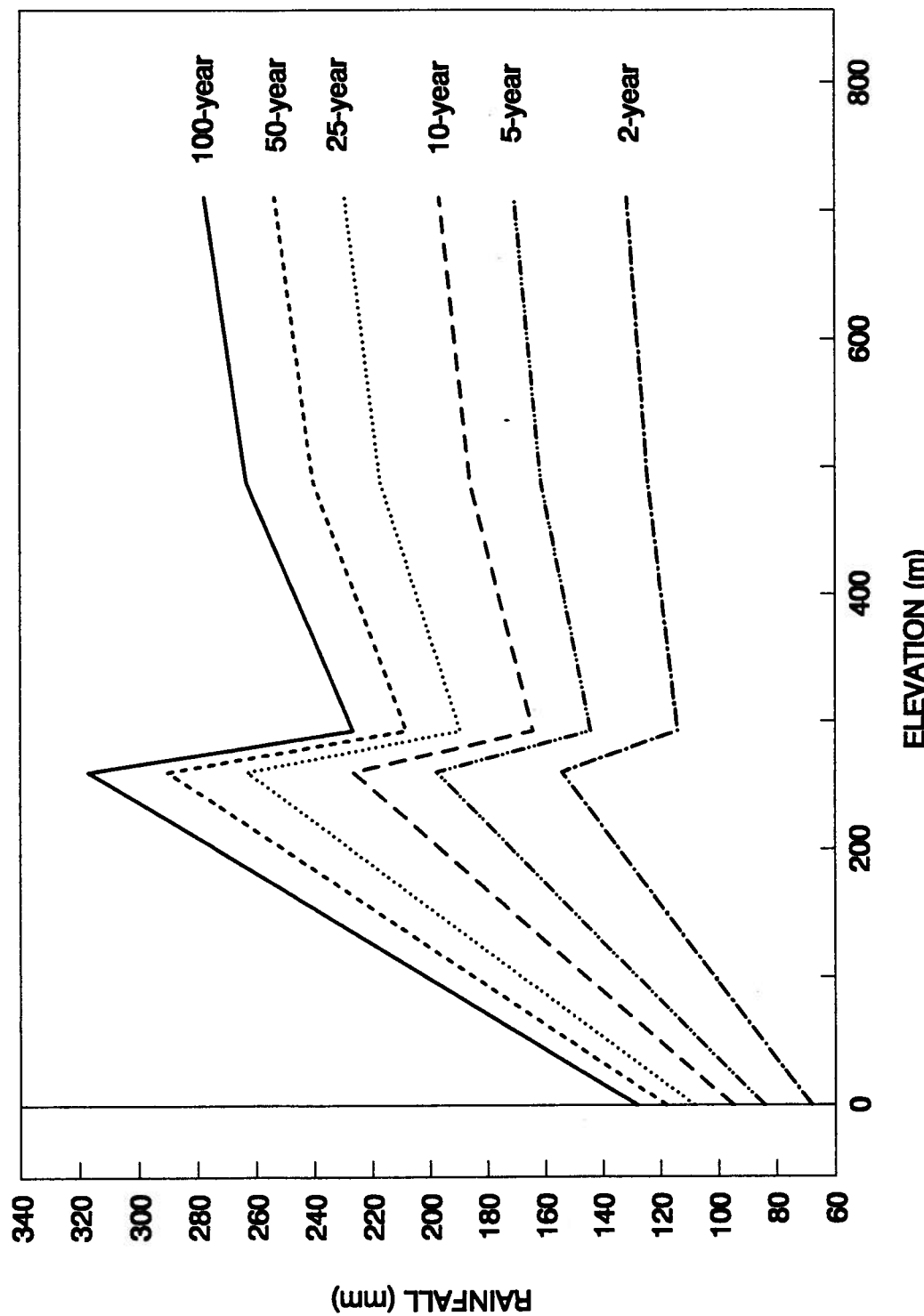


Fig. 5.10. Distribution of rainfall with elevation for extreme 24-hour storms of various return periods in the Seymour River watershed.

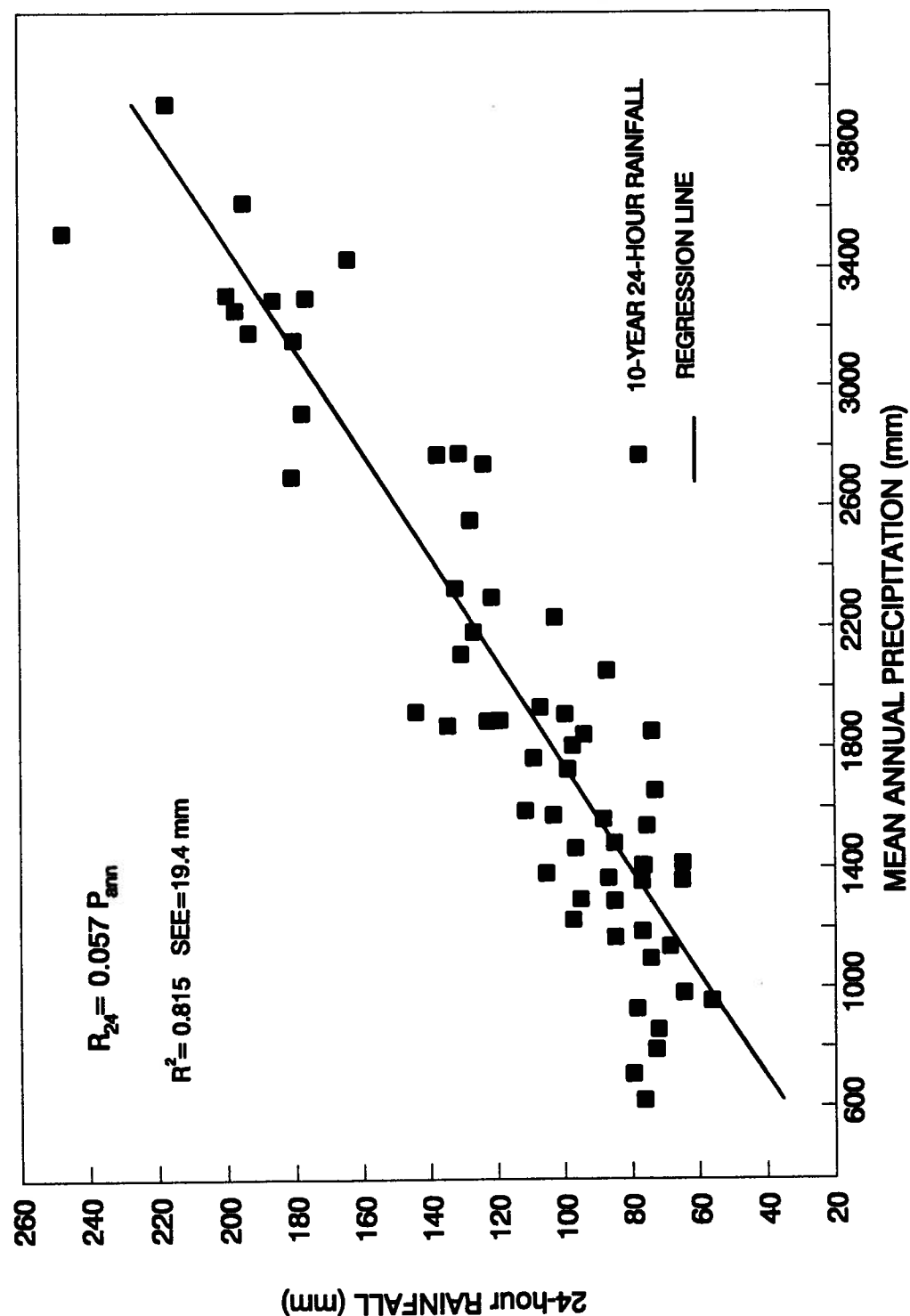


Fig. 5.11. Relationship of the 10-year 24-hour rainfall and mean annual precipitation for the sixty-one recording stations in coastal British Columbia.

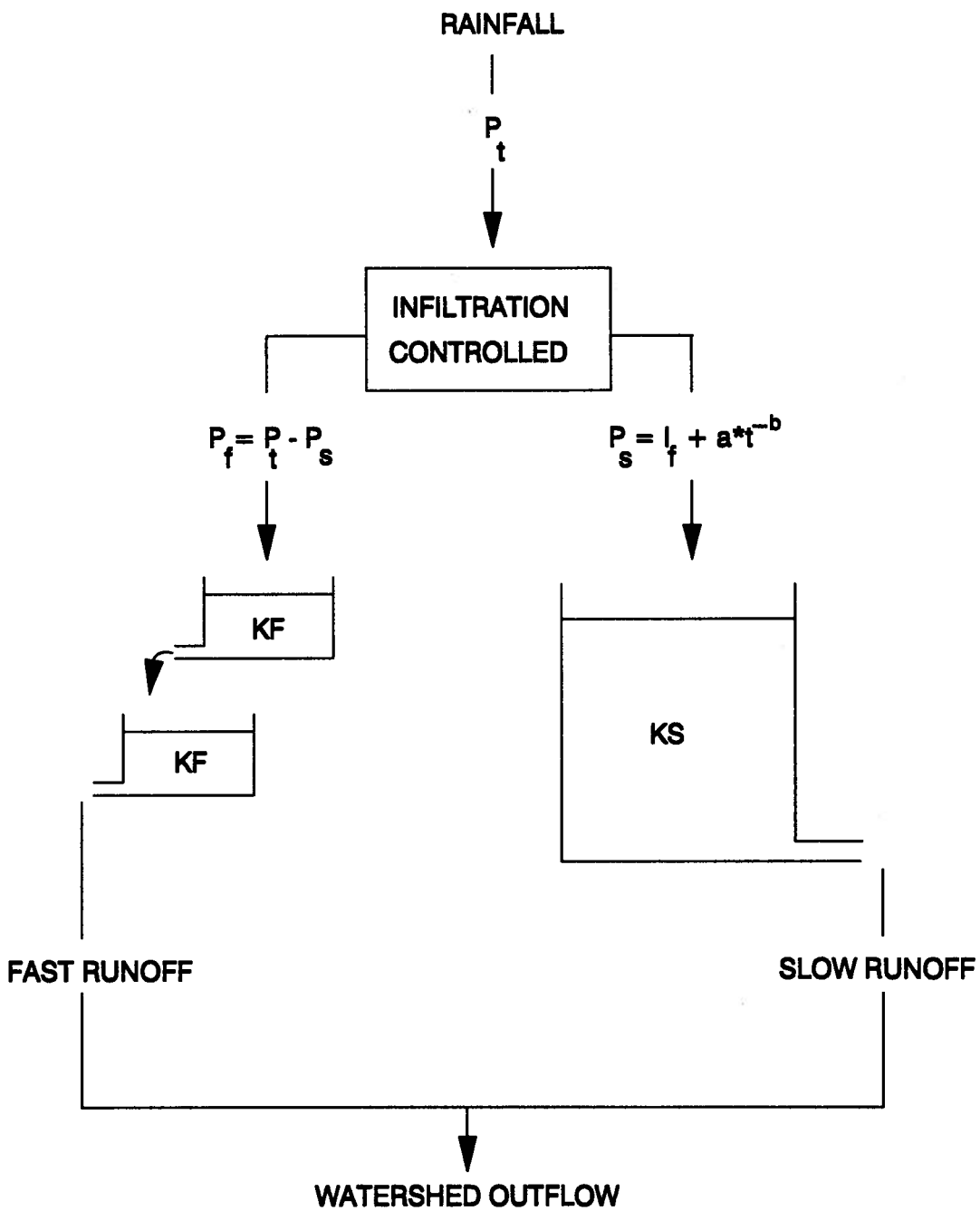


Fig. 5.12. The watershed model flow chart.

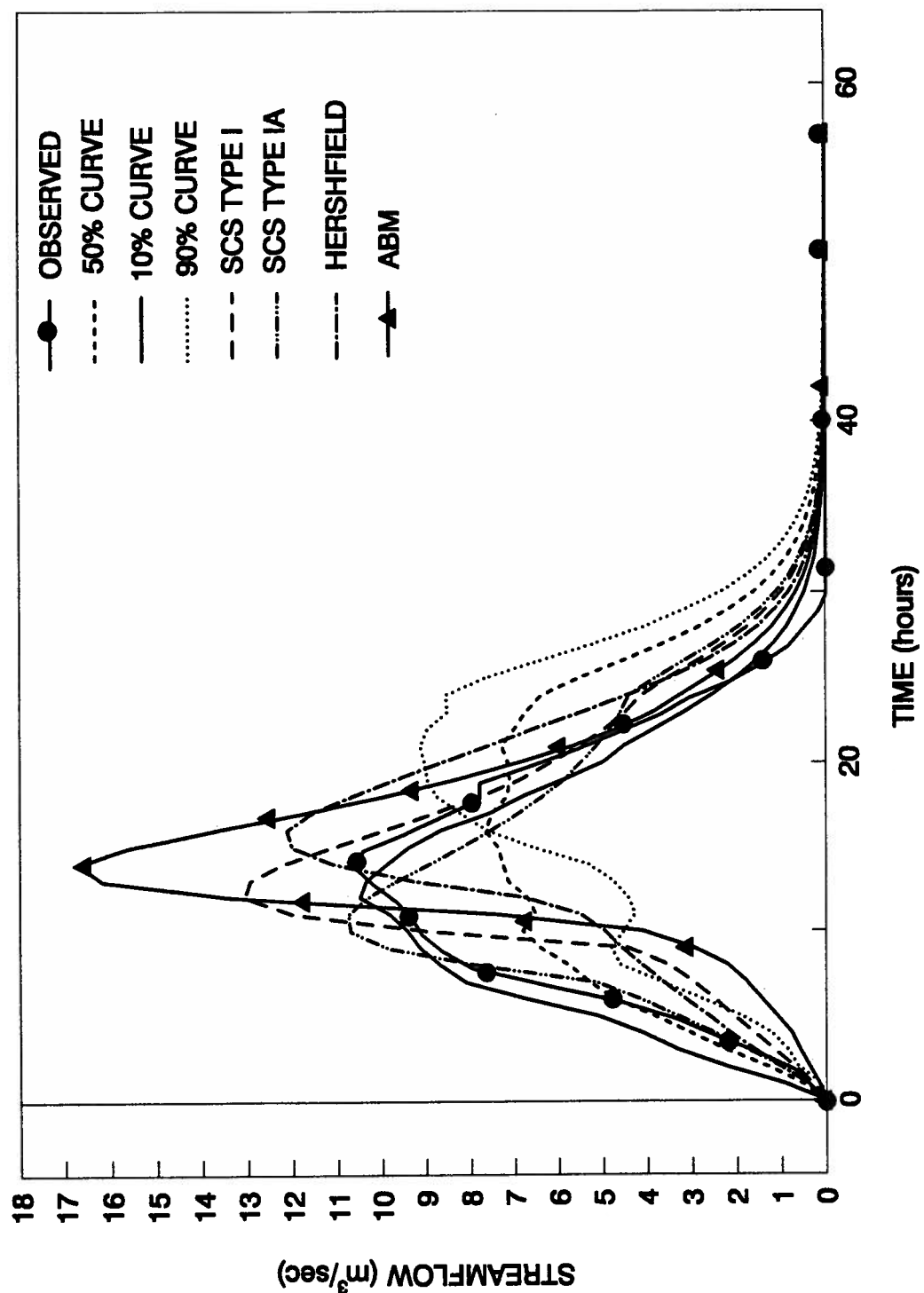


Fig. 5.13 Comparison of the 10-year observed flood hydrograph with simulated hydrographs using synthetic and derived hyetographs, for the Jamieson Creek watershed.

CHAPTER 6

STUDY OF HISTORICAL LARGE STORMS

6.1 Introduction

In Chapters 4 and 5 the spatial and temporal distribution of the storm precipitation and the 24-hour maximum rainfall was analyzed. The storms analyzed were the largest for the record of the stations in the Seymour River watershed. However, it is important to examine historical large storms that have caused flooding in the greater area of Vancouver and the lower Fraser valley. In this Chapter the synoptic meteorological conditions of these severe storms will be presented, their spatial and time distribution will be examined with the available data from the greater Vancouver area and Seymour River watershed, and finally they will be compared with the results of the study of storm precipitation in Chapter 4 and the analysis of the 24-hour rainfall presented in Chapter 5.

Five storm periods that have caused severe flooding will be presented. Summaries of the synoptic conditions of these storms are available from Atmospheric Environment Service storm studies. The storms that will be presented occurred in winter, fall and summer so that their analysis will give an overall description of the meteorological conditions of flood producing mechanisms.

6.2 The July 11-12, 1972 Rainstorm

6.2.1 Synoptic conditions

The first storm occurred in July. July is one of the driest months of the year for the study area. But on July 11-12, 1972 the area was deluged by a rainfall unprecedented for that month. This storm was frontal and occurred under a strong southwesterly flow of warm moist air, not common for the dry season of April to September, and it had many characteristics of the winter storms.

On July 11 at approximately 10 a.m. Pacific Standard Time the leading frontal wave approached Vancouver bringing continuous rainfall. Twenty four hours later the cold front of the second wave passed over the area. Its passage through the lower Fraser Valley abruptly cut off the continuous rainfall, although a few post-frontal showers were observed, especially in the northeast Lower Fraser Valley. Radiosonde soundings from Quillayute, Washington help to explain the development of the strong moist southwesterly upper-air flow over the coast (Schaefer, 1973). On July 11, 1972, an air mass with wet bulb potential temperature of 12-14°C extended up to 500 mb and the layer between 600 and 750 mb was very dry. Above 500 mb the air was near saturation at a wet bulb potential temperature of 18-19°C and warm advection was underway at all levels. By the morning of July 12 the entire air column had warmed by 4-5°C except for the layer just above the cooler surface water. The wet bulb potential temperature ranged from 14°C at surface, to 17°C at 600 mb and 19-20°C at 500 mb. At 500 mb strong west-southwest winds of 60 knots were recorded (Schaefer, 1973). Twelve hours later the winds had increased to 70 knots, the frontal system had passed over the Fraser valley and cold winds swept the area lowering the mean daily temperature by 2°C.

6.2.2 Spatial distribution

Schaefer (1973) compared data from 78 A.E.S. stations. He found that the total storm precipitation increased from 60-77 mm at low elevations to about 150 to 180 mm at the mountains. Schaefer's data for the high elevations were based only on measurements on the North Shore mountain slope stations. Such a station, the Hollyburn Ridge at 910 m recorded an all time record of 167.4 mm. Schaeffer presented no data for the valleys of the North Shore which extended further into the mountain range. Examination of the Seymour valley data shows that the total storm depth was 128.4 for station 10A, 142.2 mm for station 14A, 143.3 mm for station 21A and 173.5 mm for station 28A. These data compared to 148.8 mm at Seymour Falls Dam and 89.7 mm at Vancouver Harbour give a ratio to base precipitation of about 1.6 for the upper and mid-watershed except for the station 28A for which the ratio is 1.93. These values are well below the values found in Chapter 4 which are in the order of 2.8-3.0.

The 24-hour precipitation was not larger than the annual 24-hour maximum for most of the stations in the area. However, the Hollyburn Ridge station, which received the greatest storm accumulation reported by all stations in the area, showed a new record for the daily precipitation of 167 mm. For the upper Seymour watershed the 24-hour precipitation had a return period less than 2 years.

However, the picture changes when these accumulations are compared with the July records. The daily accumulation of 73.7 mm in Vancouver Harbour is the largest for 53 years of record. For Seymour Falls Dam the 103.1 mm is the third largest daily rainfall in 63 years. So, in general this storm was not extreme by annual standards, but by July standards was exceptional.

The duration of the continuous storm increased from 25 hours at low lands to 30-31 hours on the mountain tops (Schaefer, 1973). For the Seymour watershed stations the duration ranged from 46 hours at 10A and 21A to about 60 hours at 28A. Comparing these values with the 29 hours of storm duration at Vancouver Harbour shows a duration ratio of about 1.55 for 10A and 21A and 2.07 for 28A. Schaeffer (1973) pointed out that the mean precipitation rate increased with elevation from 2.5 mm/h at low elevations to 8 mm/h at the mountain tops. However, from the above results we can see that the average precipitation intensity for the upper Seymour remained relatively constant at about 3 mm/h, as much as the low elevation value.

As the Schaefer study (1973) showed, the large precipitation on the mountain slopes was primarily due to greater intensities. However, the results of this study suggest that in the Seymour valley which extends further into the mountainous range, the larger precipitation was totally due to larger duration. As Schaefer (1973) pointed out, the moist but stable air mass forced to rise over the mountain slopes released its moisture at much higher rate than at low elevations. However, the valley convergence was not as efficient as the orographic lifting. But the storm duration was more prolonged at the upper Seymour River watershed and the increased roughness of the mountain range is probably the reason for this.

6.2.3 Time distribution

Figure 6.1 compares the time distribution of the storm with the time probability distribution curves found in Chapter 4. The time distribution of the storm in station 10A is well below the 50 % probability curve whereas the distribution for 14A is below the 50 % curve for the 40 % of the storm duration and then it rises over this curve. These results show that the storm intensity remains relatively constant for most of the duration for 10A whereas the higher

Chapter 6. STUDY OF HISTORICAL LARGE STORMS

intensities occur at the beginning of storm at 14A. However, both curves can be approximated by a line.

6.3 The December 13-18, 1979 Rainstorms

6.3.1 Synoptic conditions

During most of December 1979 much of British Columbia was affected by a mild moist southwesterly flow of air both at the surface and aloft. Throughout the early days of December 1979 usual amounts of precipitation had fallen over the southern coast. On December 13, 1979 the wet southwesterly moisture condition was intensified by the pressure of an almost stationary frontal system which stayed over the lower Fraser valley and southern Vancouver Island. A series of minor depressions and waves which moved constantly northeastward along the front delayed the passage of the front over the area. As a result, southern coastal British Columbia received large amounts of continuous rain, very mild temperatures and strong winds. The rain was intensified as the waves approached the coast (Chilton, 1980). Inspection of the December 13 tephigraph from Quillayute, Washington reveals a stable profile with a warm and moist air mass aloft. The wet bulb potential temperature was 12°C at 500 mb, and the persisting surface dew points reached 10°C for the days of December 13 and 14 (Schaefer, 1980). This situation described the first storm period. The heavy rain during this period resulted in mudslides and local flooding causing widespread inconvenience.

After the heavy rain of December 14, the front and the associated southwesterly flow of moist air were moved to the south. In part this was in response to the strong continental Arctic high pressures centered over the interior of British Columbia. The mean daily

Chapter 6. STUDY OF HISTORICAL LARGE STORMS

temperature at Vancouver Harbour dropped from 6.5°C to 2.6°C on December 15, 1979. Radiosonde sounding revealed mid-level drying and surface cooling (Schaefer, 1980). The southwesterly flow during this time affected southern Washington and Oregon states.

However, on December 16 and 17 the southwesterly flow again moved north and started affecting the southwestern Coastal British Columbia. The tephigraph of December 16 showed a very stable and moist profile with wet bulb potential temperatures reached 16°C for the 600 mb level and above. During this period, the persisting dew points reached 11°C. On December 18 the profile became drier aloft and less stable producing showers that followed the passage of the frontal system over the area.

The synoptic conditions that produced these two storms do not occur every winter on the south coast at least not to the extent of the December 1979 events (Chilton, 1980). However, the resulting storms were very similar to most of the winter storms which occur in the area.

The two distinctive storm periods of December 13-14 and December 16-18 will be analyzed separately. Even though these two storms were generated by the same system their distribution was different.

6.3.2 The December 13-14, 1979 storm

6.3.2.1 Spatial distribution

Schaefer (1980) compiled data from 18 stations in the greater Vancouver area and Vancouver Island. For the first storm larger precipitation fell over Vancouver Island than in the Vancouver area. In the Seymour River watershed the precipitation gradient was lower than the average gradient reported in Chapter 4. The storm precipitation increased from 112.3 mm

Chapter 6. STUDY OF HISTORICAL LARGE STORMS

at Vancouver Harbour to 196.2 mm at Seymour Falls Dam and then decreased to 152.9 mm at 10A and leveled off at 173.2 mm at 14A. These values represent a ratio of 1.75 at Seymour Falls Dam, 1.36 at 10A and 1.54 at 14A. The maximum 24-hour rainfall fallen at Vancouver Harbour (80.5 mm) during the storm had a return period of about 4 years. The return periods decreased at the mountains. The 121.4 mm in 24 hours at 10A had 2.5 years return period whereas the 123.2 mm at 14A was only a 2-year storm. Examination of the data from other stations in the area showed that this pattern of the decrease of return periods with elevation was more general over the southwestern British Columbia (Schaefer, 1980). However, because of the wet period preceding the storm and the heavy 24-hour rainfalls exceeding 120 mm, the chance for landslides had increased. Actually, many landslides were reported during the two-day period between December 13 and 14.

Examination of the duration of the storm showed that the storm had about the same duration at the lower elevations as in the mountainous area, being 41 hours at Vancouver Harbour and only 46 hours at 14A. As a result the larger rainfall at the upper Seymour watershed was the result of higher intensities. The average rainfall intensity increased from 2.73 mm/h at Vancouver Harbour to about 3.75 mm/h at 10A and 14A. These values represent an increase equal to 37%. The same increase has also been observed for the storm precipitation.

The maximum hourly intensity increased by 70% between the lower and upper watershed. Checking the start time of the storm reveals that the storm started 3 hours earlier at the upper watershed. This resulted from the increased roughness of the mountains and the orographic lifting which promote the condensation of the hydrometeors.

6.3.2.2 Time distribution

Figure 6.2 compares the time distribution of the December 13-14 storm with the curves developed from the analysis of the 175 storms presented in Chapter 4. It seems that the distribution of the storm in time changes as the elevation changes (Fig. 6.2). At Vancouver Harbour the largest intensities occurred at the beginning of the storm while the heaviest intensities in the Seymour River watershed occurred at the end of the storm (Fig. 6.2).

6.3.3 The December 16-18, 1979 storm

6.3.3.1 Spatial distribution

The second storm of the December 13-18, 1979 period was more severe for the lower Fraser valley than for Vancouver Island. This is the result of the passage of the front to the northeast and its intensification, as the radiosonde soundings have shown (Schaefer, 1980). This second storm precipitated larger amounts on the mountains and valleys than at the low lands. The total storm depth at Vancouver Harbour was 155.8 mm while 347.4 mm fell at Seymour Falls Dam, 249.7 mm at 10A and 243.1 mm at 14A. These values represent an increase of about 220% at Seymour Falls Dam and about 60% for the upper watershed over the precipitation accumulation at the Vancouver Harbour station.

However the intensification of the rain was greater at the lower elevations. The 24-hour maximum rainfall of 121.1 mm at Vancouver Harbour had a return period of 60 years. The return periods decreased to about 3 years at Seymour Falls Dam (151.8 mm), 4 years at 10A (139.7 mm) and 2 years at 14A (124.5 mm). The 24-hour rainfall accumulations, as the above data show, increased by 25% at the middle of the Seymour valley and leveled off at the

Chapter 6. STUDY OF HISTORICAL LARGE STORMS

upper watershed.

Similar variation of the return periods has also been observed in the greater area of Vancouver. For example, the daily precipitation of 87.5 mm at the Vancouver International Airport had a return period of 70 years while the 136 mm fallen at Coquitlam Lake station were only a 3-year 24-hour storm accumulation.

Examination of the storm duration reveals that the storm lasted 56 hours at Vancouver Harbour and 67 hours at 10A and 14A. These values represent an increase of 20% in duration between the upper and the lower watershed. This means that the larger precipitation at the upper watershed was not only due to the longer storm duration but also due to greater storm intensities. Comparison of the average storm intensities showed that the Vancouver Harbour value of 2.78 mm/h increased by about 30% at the upper watershed. However, the maximum hourly intensity remains relatively constant. In light of these results one can say that, at least for the upper Seymour River watershed, the larger accumulations were due to both longer duration and higher storm intensities.

Examination of the time that the storm started shows that the storm started first at the upper and mid-watershed, namely about 5 hours earlier at 10A and 2 hours earlier at 14A than at Vancouver Harbour.

6.3.3.2 Time distribution

Figure 6.3 shows the time distribution of storm for the stations Vancouver Harbour, 10A and 14A. The storm has different distribution at Vancouver Harbour than it has at the upper watershed. At Vancouver Harbour the highest intensities occurred in the mid-duration of the storm whereas for the two other stations there is intensification of the storm just before its half duration, followed by a lull.

6.4 The October 25-31, 1981 Rainstorms

6.4.1 Synoptic conditions

The weather of October 1981 over the southwestern British Columbia was dominated by three large scale circulation patterns (Schaefer, 1982). These included a low pressure trough (October 1-9), a high pressure ridge (October 10-24), and a southwesterly flow (October 25-31). Frontal storms generated in the North Pacific Ocean and transported by the westerlies impinge on the southwestern coast of British Columbia on October 25. For the first days of the period of October 25-31, the weather systems were similar to the winter systems that produce large precipitation in the area. The wet weather during October 25-27 was accompanied by freezing levels well above 2000 m and at about 1500 m on October 28. However, by that time satellite images showed that tropical moisture generated in the vicinity of Hawaii was swept into the southwesterly flow, ahead of an advancing frontal zone (Horita, 1981). From Quillayute tephigrams, it appears that this injection of tropical moisture in the system created a large scale instability (Horita, 1981). This warm moist air associated with the final heavy rainstorm during October 30-31 brought freezing levels up to 3000 m on October 31.

Two storms can be identified for the period October 25-31, 1981. The first is the storm of October 25 to 28 and the second started on October 28 and lasted until November 1. These two storms were associated with two disastrous events. During the first storm, a landslide occurred just before midnight of October 27 in the small M Creek watershed which flows from the steep mountain slopes into Howe sound (Fig. 2.3). The mixture of mud, tree trunks, water and boulders burst down on the highway, washing out the bridge and killing five people in a car that was on the bridge. Two more cars drove over the edge of the 15 meter

Chapter 6. STUDY OF HISTORICAL LARGE STORMS

drop where the bridge used to be. Also, a small house built near the beach was washed out to sea by the debris torrent while another house was battered by the debris.

The second storm was very severe for the area of North and West Vancouver. The heavy rains on October 30 and 31 resulted in flooding of Seymour River, Lynn Creek and Mosquito Creek in the North Shore mountains. The floods claimed the life of a man swept away by the floodwaters of Mosquito Creek. The roaring waters of the rivers and creeks of the area burst and overtopped their banks flooding residential areas causing millions of dollars in damage. The muddy flood waters of Seymour River eroded the footings of two bridges jeopardizing the stability of the structures. Finally, a mudslide into Capilano Lake reservoir created turbidity problems in the drinking water.

The spatial and temporal distribution of the two storms will be examined separately in the next paragraphs.

6.4.2 The October 25-28, 1981 storm

6.4.2.1 Spatial distribution

The first storm of the period October 25-28 was very severe in the Vancouver area. The storm was intensified by the convergence of the valleys but not by the orographic lifting, as the data show. For example the Hollyburn Ridge station (910 m) on the southern slopes of Hollyburn mountain received only 83.8 mm while the Seymour Falls Dam station in the nearby Seymour River valley, received 158.9 mm in the same period. In the Seymour River watershed the storm exhibited very large increases. The Vancouver Harbour storm precipitation was only 37.6 mm whereas the rainfall increased to 158.9 mm at Seymour Falls Dam, 223 mm at 10A, 223 at 14A and 203.5 at 25B. These values show that the storm

Chapter 6. STUDY OF HISTORICAL LARGE STORMS

rainfall increased by about 4 times between the lower and mid-watershed and then increased and finally leveled off in the upper watershed at a ratio of about 5.5.

The storm was not as large or as severe as the storm depth ratios might indicate. The 24-hour rainfall at Vancouver Harbour had a return period of less than 2 years. But the severity increased to 3.5 years at 10A (134 mm), to 4 years at 14A (149.8) and 2.5 years at 25B (142.2 mm). Station 25B is located 15 km east of M Creek watershed and the 24-hour rainfall accumulation was 142 mm. O'Loughlin (1972) showed that when the 24-hour rainfall exceeds the 120 mm the steep slopes of the area are prone to landslides, and therefore this storm rainfall accumulation is capable of producing landslides in the already wet steep hillslopes.

The storm lasted only 75% longer at the upper watershed. As a result, the large rainfall at the top of the watershed was due to large average storm intensities, which increased by about 200% at the upper Seymour River watershed.

The storm started about 6 hours earlier at the upper Seymour River watershed than at Vancouver Harbour.

6.4.2.2 Time distribution

Figure 6.4 shows the time distribution of the storm for four stations. It seems that the time distribution of the storm did not change with elevation. High intensities occurred for all elevations at the middle of the storm duration and then for the rest of the storm the storm intensities were moderate.

6.4.3 The October 28-31, 1981 storm

6.4.3.1 Spatial distribution

The second storm of the period October 25-31, 1981 was more severe than the first storm. The injection of tropical highly unstable moist air in the frontal system is the causative reason for the severity of the storm. For this storm of October 28-31, as for the October 25-28 storm, the valley convergence was much more efficient than the orographic lifting. Hollyburn Ridge received only 212 mm while Seymour Falls Dam received 486 mm. In the upper Seymour River watershed the storm precipitation dropped to 213.4 mm at 10A, 243.9 mm at 14A and 278.6 mm at 25B. These precipitation accumulations represent a ratio to the Vancouver Harbour precipitation of 4.54 for Seymour Falls Dam, 2.0 for 10A, 2.3 for 14A and 2.6 for 25B. Also, it is significant that the precipitation accumulation at Hollyburn Ridge station is similar to the accumulations observed at the Seymour valley stations located further inwards in the mountainous area.

The severity of the storm increased with elevation in the Seymour River watershed. The return period of the 78.5 mm in 24 hours at Vancouver Harbour had a return period of 3.5 years while the return period increased to 9 years at Seymour Falls Dam (205.5 mm), 10 years at 14A (183.9 mm) and 15 years at 25B (210.9). The return periods of the 24-hour storm in the valleys on the North Shore mountains were larger than on the mountain slopes. For comparison the return period at Hollyburn Ridge was only 4.3 years (136.4 mm) while at Lynn Creek it was 10 years (136 mm).

These extreme storms were dependent on both the higher intensities and the prolonged duration. The duration increased by 50% in the mountains whereas the average storm rate and the maximum hourly intensity increased by 70%. Furthermore, the storm started, on average,

Chapter 6. STUDY OF HISTORICAL LARGE STORMS

5 hours earlier in the upper Seymour watershed than at the Vancouver Harbour station.

6.4.3.2 Time distribution

Figure 6.5 shows that the storm has similar time distribution pattern at all elevations. The larger intensities were observed at the middle of the storm at about October 29.

6.5 The November 8-11, 1990 Rainstorm

6.5.1 Synoptic conditions

November is the wettest month of the year for the southwestern British Columbia. On the evening of November 8, 1990 a strong warm front associated with a large Pacific low pressure system moved into southwestern British Columbia. Satellite images revealed that this warm unstable air mass was generated in the North Pacific close to Hawaii. Highly moist tropical air was injected in the system. The storm was named "Pineapple Express" by the U.S. National Weather Service forecasters.

The storm moved slowly as a number of waves and troughs progressed eastward, causing heavy precipitation. The heavy precipitation started in the early morning hours of November 9th and lasted until the evening of November 10th in the lowland areas and continued until the evening of November 11th in the mountainous areas. The storm coverage extended from northern coastal British Columbia to northern Washington State.

Severe widespread flooding was reported in all the coastal region, but the hardest hit areas were the eastern Lower Mainland and the Whatcom County in Washington State. The strong southwesterly flow of air was associated with high freezing levels and so the flooding

Chapter 6. STUDY OF HISTORICAL LARGE STORMS

was aggravated by the melting of the accumulated snow. In Chilliwack and Sumas Prairie large areas were evacuated when the Chilliwack River rose 2 to 2.5 m, overtopping its banks and flooding large areas. The flooding was estimated to have a return period of 200 years. Poor highway conditions were blamed in the deaths of two people and injuries to four others. The estimated damage approached 10 million dollars. Furthermore, clogging of the drainage systems resulted in flooding of basements and streets in Vancouver. The heavy precipitation resulted in numerous mudslides and rockslides which disrupted traffic on the major highways. In Washington State the damage was comparable to that of the Chilliwack - Sumas areas.

6.5.2 Spatial Distribution

The precipitation amounts varied greatly across the south coast of British Columbia. The southwestern and central Vancouver Island reported amounts of 150 to 200 mm but areas in the Northern Vancouver Island received even larger amounts. In the greater Vancouver area the rain amounts varied around 100 mm, whereas they increased in the north and east lower Fraser Valley due to orographic lifting and valley convergence. For example, in Squamish, north of Vancouver the rainfall accumulation was 310 mm while in the eastern lower Fraser valley the precipitation amounts rose quickly from over 150 mm at Abbotsford to 200 mm at Chilliwack and to 337 mm at Hope.

In the Seymour River watershed the same pattern was observed. The precipitation increased from 108 mm at Vancouver Harbour to 460 mm at Seymour Falls Dam and then leveled off at 339.6 and 354.3 mm at stations 14A and 25B, respectively. These values show that the precipitation increased by more than 4 times between the lower and upper watershed and then decreased and leveled off at a ratio of about 3.2.

The severity of the storm increased in the same pattern as the storm depths. The return

Chapter 6. STUDY OF HISTORICAL LARGE STORMS

period of the 24-hour rainfall increased from about 1 year at Vancouver to 9 years at Abbotsford (79.6 mm), 10 years at Chilliwack (99.4 mm) and to more than 100 years at Hope (173.1 mm).

In the Seymour River watershed the severity of the storm increased up to the middle position and then declined. The return period of the 24-hour rainfall at Vancouver Harbour was 1.2 years (55 mm) and increased to 33 years at Seymour Falls Dam (300 mm) and then decreased to 10-years and 5-years at 14A (173.3 mm) and 25B (170.2 mm), respectively. The 300 mm reported in Seymour Falls Dam is the second largest 24-hour event of record, and the largest value reported during this storm for the whole southwestern British Columbia. The result of the very large precipitation accumulations were that many landslides, mudslides and rockslides occurred in the mountainous area east of Hope.

Examination of the storm duration showed that the storm lasted about 57 hours in Vancouver Harbour and about 80 hours at the upper Seymour River watershed. These values indicated a ratio of storm duration of about 1.40 between the low level areas and the upper study watershed.

The above results reveal that the larger storm precipitation at upper and mid-watershed was mainly due to the larger storm intensities, which increased from 1.89 mm/h at Vancouver Harbour to 4.26 mm/h and 4.51 mm/h at 14A and 25B, respectively. These values show an increase of about 2.3 times between the upper and the lower watershed. Furthermore, the same has been observed for the maximum hourly intensity which increased from 3.8 mm/h at Vancouver Harbour to about 12.0 mm/h at the upper watershed, representing an increase of more than 300%.

The storm started, on average, about 24 hours earlier at the middle and upper watershed than at Vancouver Harbour. These results along with the findings for the storm duration show that the orographic lifting and the valley convergence triggered the intense

Chapter 6. STUDY OF HISTORICAL LARGE STORMS

storm earlier and the mountain roughness delayed the passage of the storm by about 24 hours.

6.5.3 Time distribution

The time distribution at the Vancouver Harbour was uniform and followed the 50% time probability curve (Fig. 6.6a). At the upper watershed the high intensities were observed after the middle of the storm. This pattern remained consistent for the two upper elevation stations 14A and 25B (Fig. 6.6b and c).

6.6 The November 21-24, 1990 Rainstorm

6.6.1 Synoptic conditions

For the second time in November 1990 a strong frontal storm impinged on southwestern British Columbia bringing heavy rain. This system, like the previous one, had been injected with moist subtropical air during its passage over the North Pacific. However, this system did not stay over the area as long as the November 8-11, 1990 system. It moved from a southwesterly direction to the northeast. Heavy rain did fall but was not as continuous or as heavy as the previous storm. Flooding was reported in greater Vancouver and Victoria but the worst flooding occurred in Washington State, north and west of Seattle.

6.6.2 Spatial distribution

This storm was not as severe as the previous November 8-11, 1990 storm. The storm was intensified over the mountain slopes and the valleys as compared to low level areas. The total

Chapter 6. STUDY OF HISTORICAL LARGE STORMS

storm depth increased from about 60 mm in Vancouver to 101.3 mm at Abbotsford, 132.1 mm at Chilliwack and 247.8 mm at Hope. The rain shadow effect was not as strong with this system so that the heavy precipitation extended further east of the Coast Mountains. Large amounts of precipitation in the Victoria area caused flooding (94.8 mm in Victoria Airport).

In the Seymour River watershed, large increases in the valley had occurred. The total storm depth at Vancouver Harbour was 57.4 mm but increased to 439.5 mm at Seymour Falls Dam. At the upper watershed the storm precipitation amount decreased and leveled off at 240 mm. These values represent an increase of about 700% at Seymour Falls Dam and 300% at the upper watershed over the precipitation at Vancouver Harbour.

The intensification of the rain followed a similar pattern to that of the rain distribution. The 24-hour maximum rain at Vancouver Harbour (27.4 mm) had a return period smaller than a year, but increased at Seymour Falls Dam (228.3 mm) to 10.5 years and 4 years at 10A (139.4 mm) and 8 years at 14A (178.1 mm). The same distribution of the return periods has been observed for the greater area. For example the return period of the daily rainfall at Vancouver Airport, Abbotsford and Chilliwack was less than one year while it was 15 years at Hope.

The storm duration increased from 37 hours at Vancouver Harbour to 61 and 71 hours at 10A and 14A, respectively. The above results of duration and precipitation indicate that the higher intensities at the upper watershed are mainly responsible for the increase of precipitation at the higher elevations as compared to the middle and low elevations . Examination of the average storm intensity revealed that the storm intensity increased by 130% between the lower and upper watershed (from 1.55 mm/h to about 3.5 mm/h). Also, the maximum hourly intensity increased by about 170% between the lower and upper watershed.

The storm started about 20 hours earlier at the upper Seymour River watershed than at

Vancouver Harbour.

6.6.3 Time distribution

The storm had different time distribution at Vancouver Harbour station from that at the upper study watershed. At the Vancouver Harbour station the storm was not continuous and two different storm periods can be distinguished (Fig. 6.7a). This resulted in two steep parts of the curve in the beginning and the end and a flat area at the middle of the storm duration. At the upper watershed the time distribution is similar at 10A and 14A stations. The larger increase after the middle duration represents the heavy rainfall on November 23, 1990. One can observe that this part of the time distribution curve is reasonably linear (Fig. 6.7b, c).

6.7 Summary

Examination of five storms showed that the main flood-producing mechanism in the area is the frontal systems that developed over the North Pacific Ocean and moved eastward until they impinge on the coastal British Columbia. The warm, wet flow of air is occasionally intensified with the injection of humid tropical air, and, as a result, very large precipitation accumulations are generated in the study area.

These frontal systems are capable of producing more than one storm as the meteorological conditions change and the systems move away north or south and then again move over the study area. These systems occur mainly during the winter and fall months and rarely during summer. The importance of this for the hydrology of the region is that the soil moisture storage is mostly filled during the wet winter and fall months and combined with the heavy precipitation results in large floods and slope instability.

Chapter 6. STUDY OF HISTORICAL LARGE STORMS

From the examination of the limited data in the Seymour River watershed, it is evident that, in general, the severe storms have a spatial distribution similar to the distribution found in the analysis of the 175 storms in Chapter 4 and the results of the 24-hour maximum rainfall in Chapter 5. Furthermore, the increased roughness and the orographic lifting and the valley convergence cause the severe storms to start earlier at the upper Seymour River watershed than at the low-level Vancouver area. Also, for the same reasons the duration of the storms is significantly increased in the mountainous area. As a result, the larger accumulations at the upper study watershed are due to the high intensities and the long durations. The time distribution of the storms analyzed varied for the same station from storm to storm but it was within the range of the results presented in Chapter 4.

The comparison of the severe storms with the findings of the analysis of the storm precipitation in the Seymour River watershed shows that, in general, the severe storms have similar spatial and temporal distribution characteristics to the less severe storms analyzed in Chapter 4 of the thesis. This is significant because it confirms that the previous results can be used for the estimation of extreme storms that produce flooding and other related problems in the area. Furthermore, similar storm studies by Atmospheric Environment Service (Schaefer, 1979a; Schaefer, 1979b) indicate that flood producing storms in other areas of coastal British Columbia have similar characteristics as those observed in the greater Vancouver area. This is not surprising since the same large-scale atmospheric circulation produces storms that impinge in the north or south coast of British Columbia depending of the regional circulation patterns.

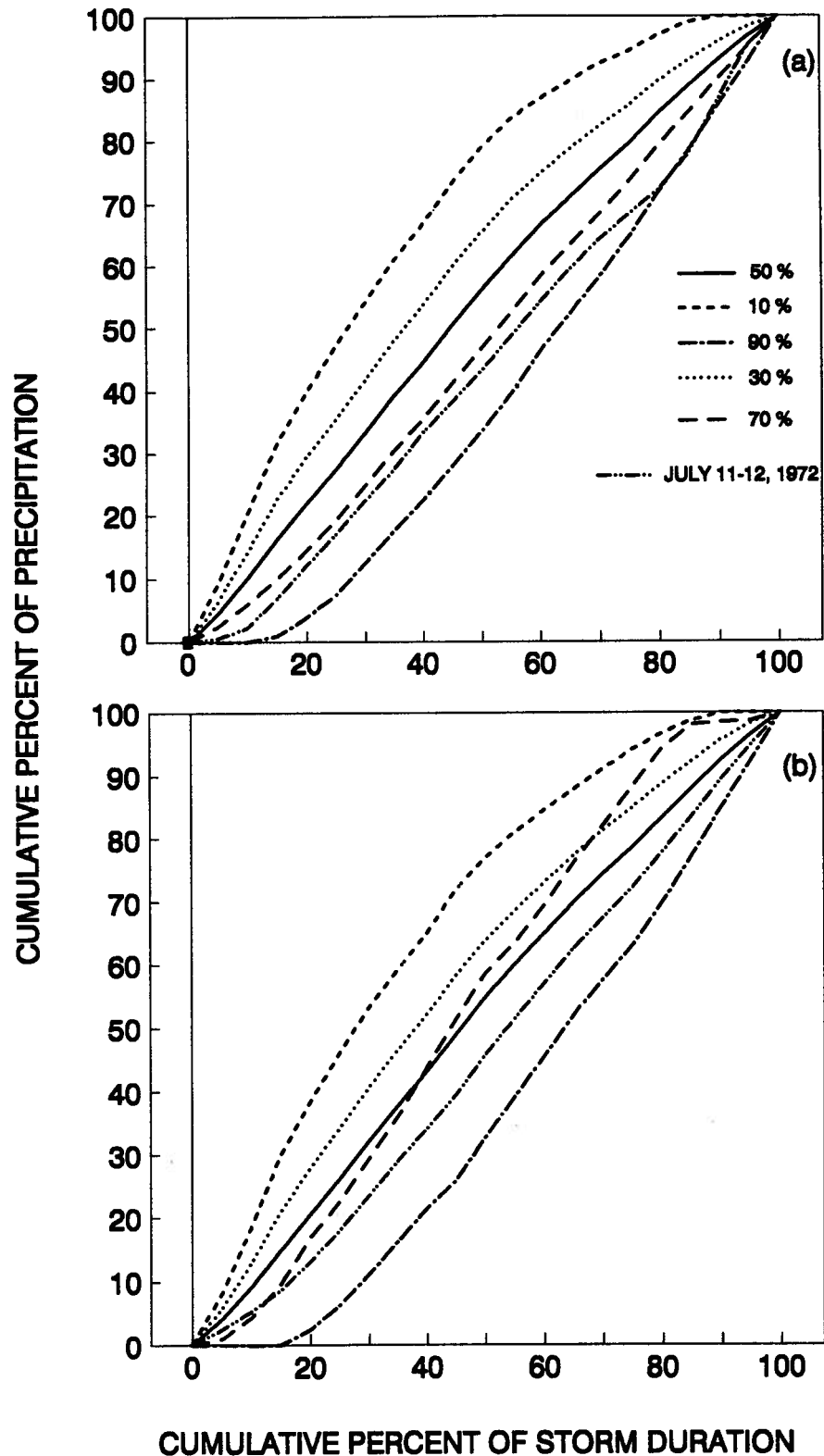


Fig. 6.1 Comparison of the time distribution of the July 11-12, 1979 storm with time probability distribution curves at (a) station 10A and (b) station 14A

Chapter 6. STUDY OF HISTORICAL LARGE STORMS

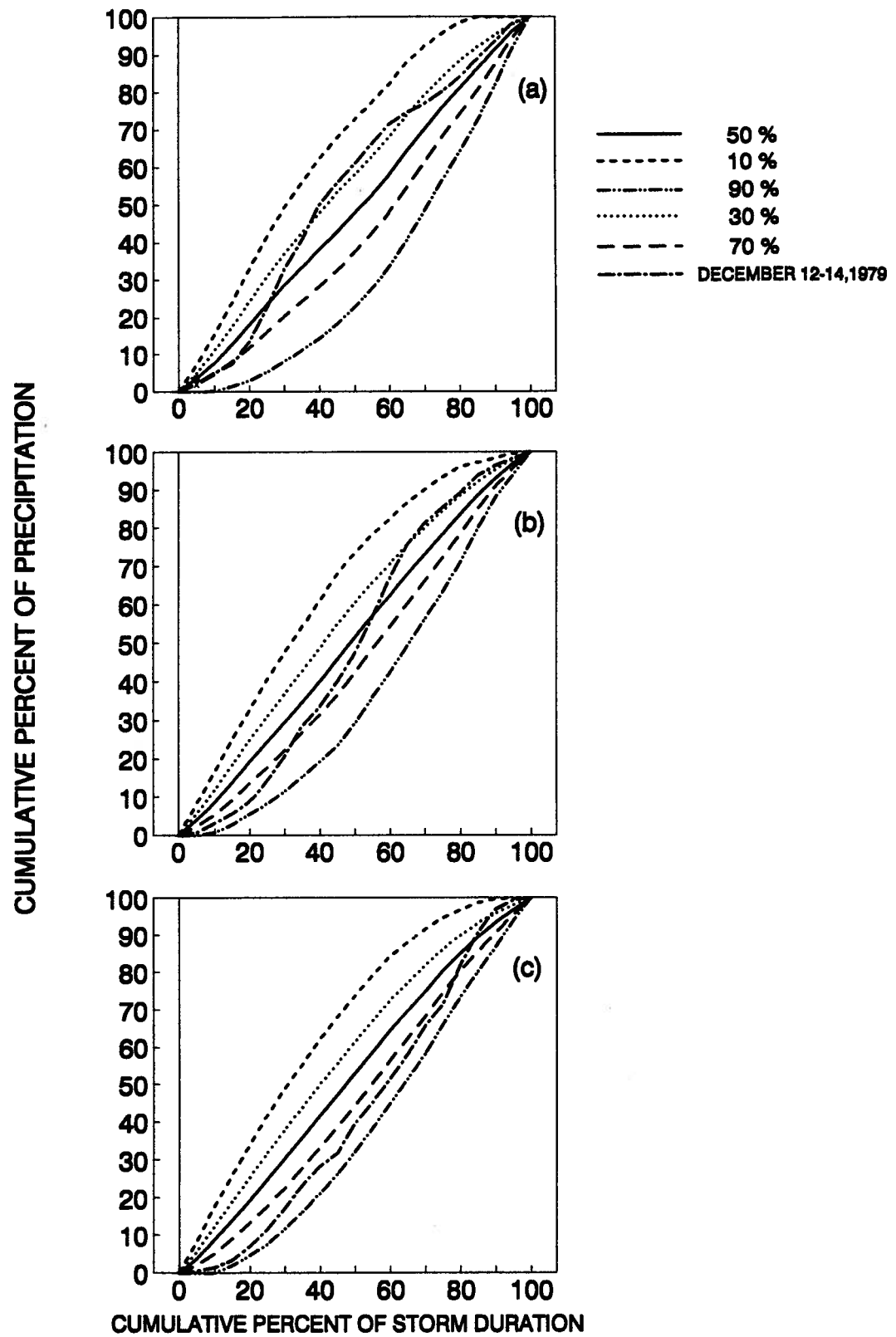


Fig. 6.2 Comparison of the time distribution of the December 12-14, 1979 storm with time probability distribution curves at (a) station Vancouver Harbour (b) station 10A and (c) station 14A

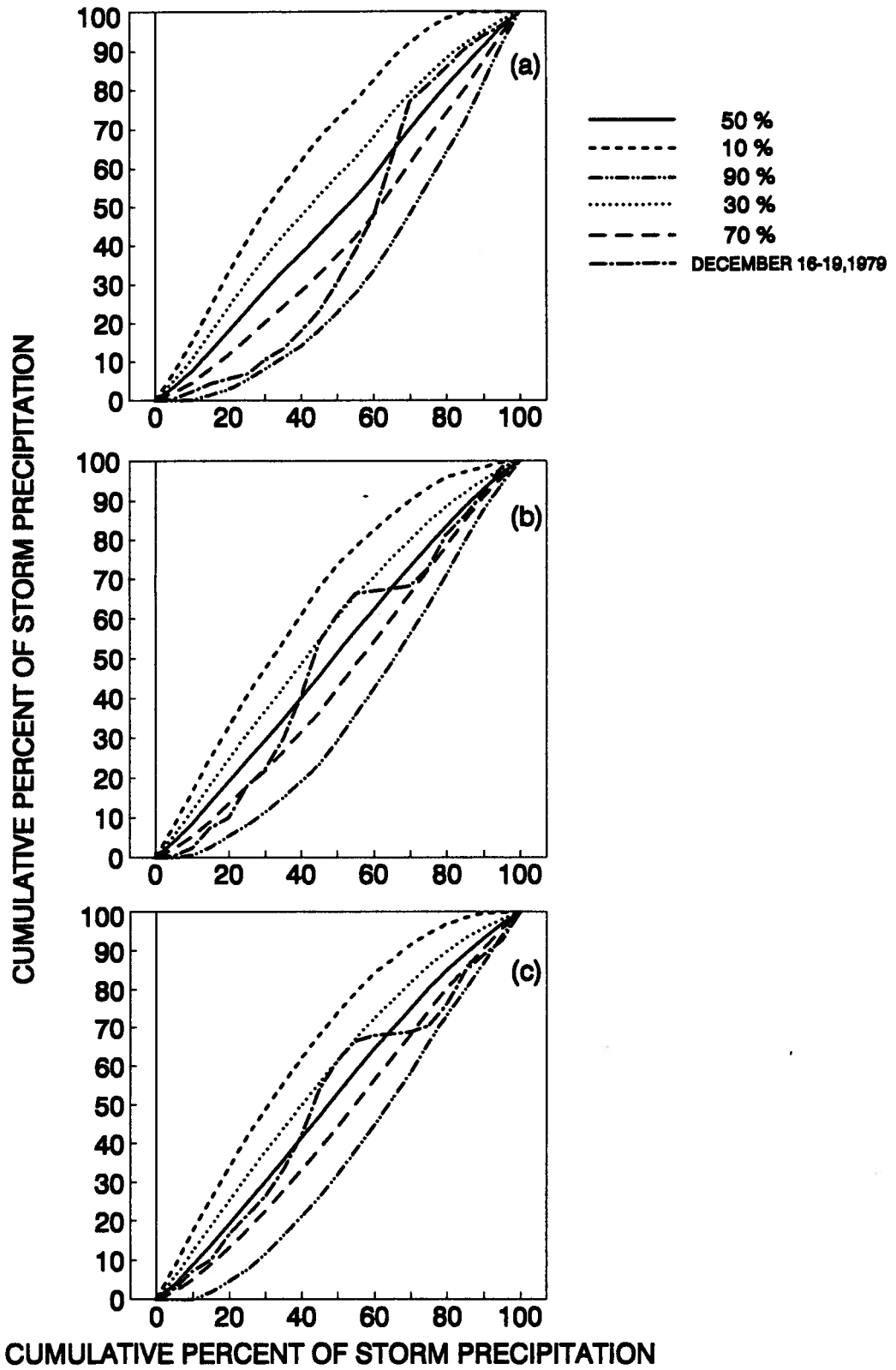


Fig. 6.3 Comparison of the time distribution of the December 16-19, 1979 storm with time probability distribution curves at (a) station Vancouver Harbour (b) station 10A and (c) station 14A

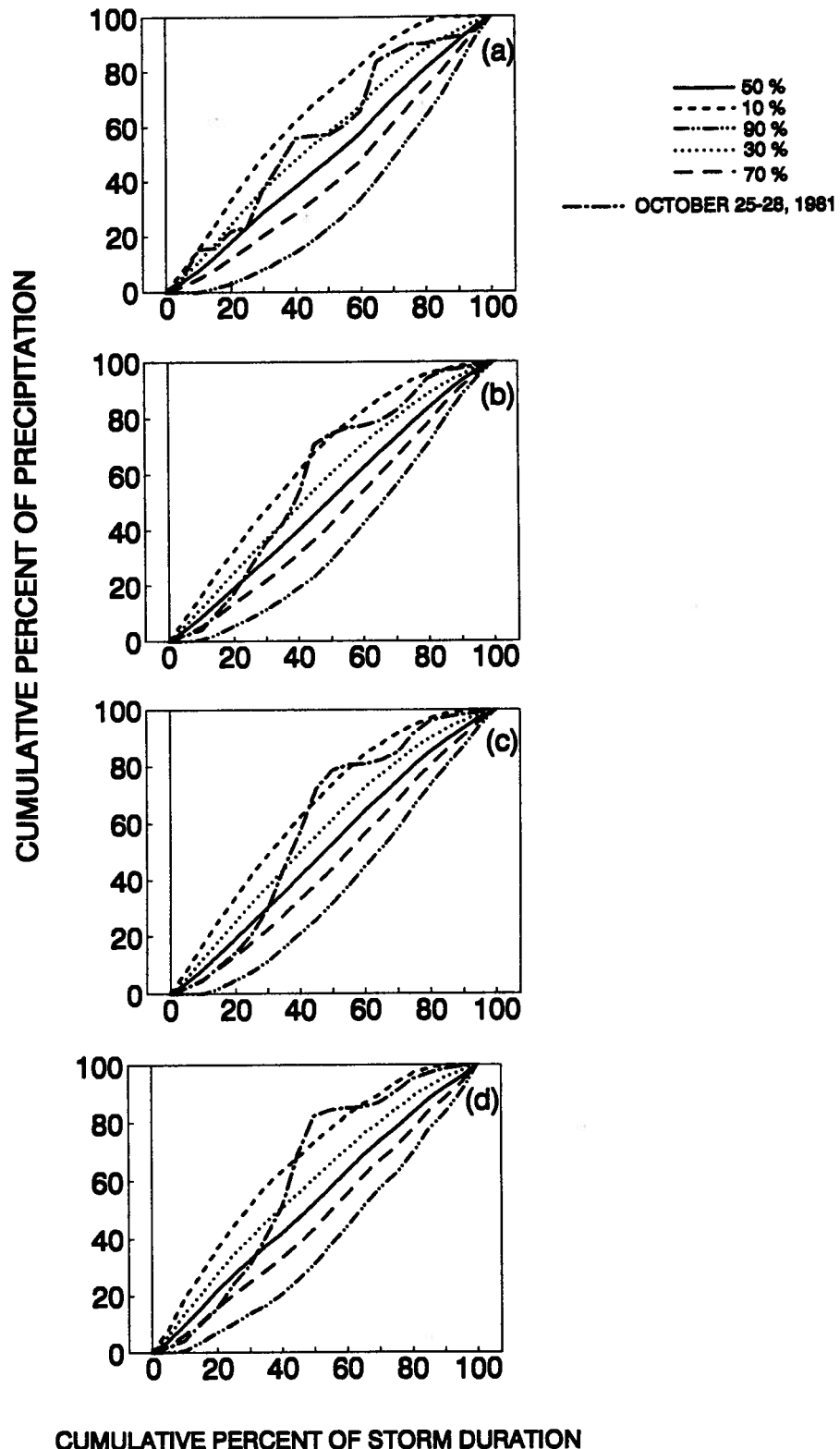


Fig. 6.4. Comparison of the time distribution of the October 25-28, 1981 storm with time distribution probability curves at (a) station Vancouver Harbour (b) station 10A, (c) station 14A and (d) station 25B

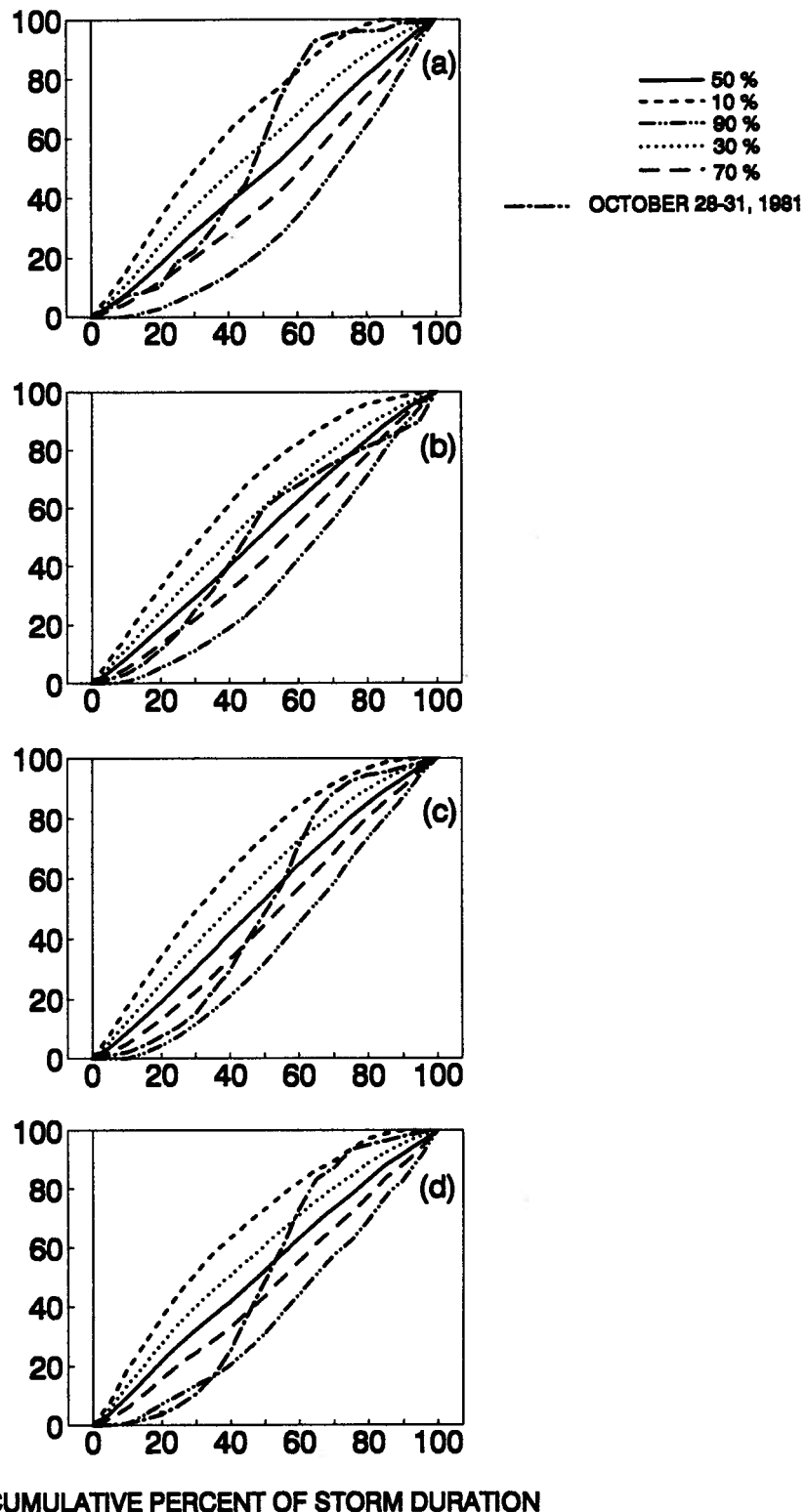


Fig. 6.5. Comparison of the time distribution of the October 28-31, 1981 storm with time distribution probability curves at (a) station Vancouver Harbour (b) station 10A, (c) station 14A and (d) station 25B

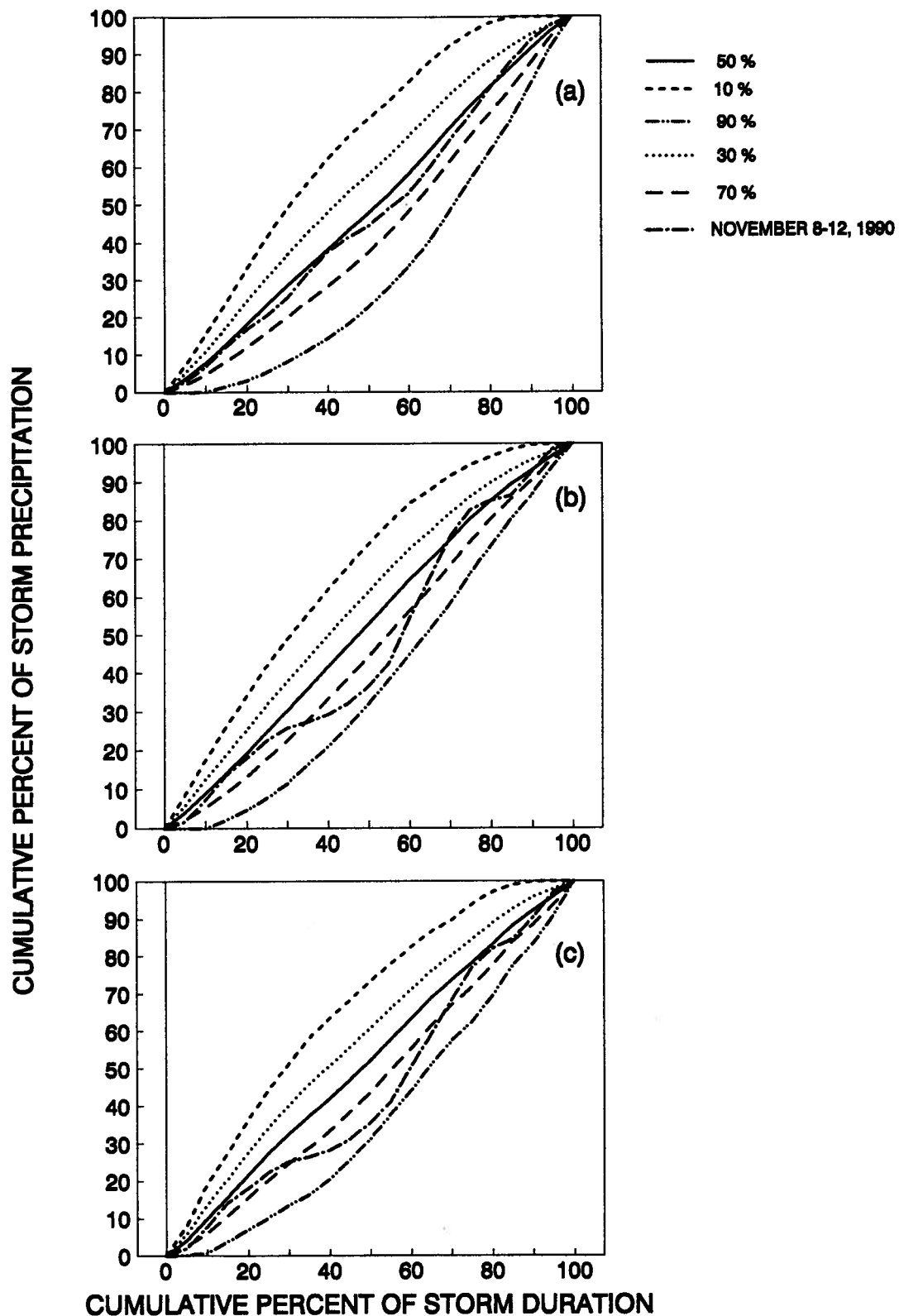


Fig. 6.6 Comparison of the time distribution of the November 8-11, 1990 storm with time probability distribution curves at (a) Vancouver Harbour (b) station 14A and (c) station 25B

Chapter 6. STUDY OF HISTORICAL LARGE STORMS

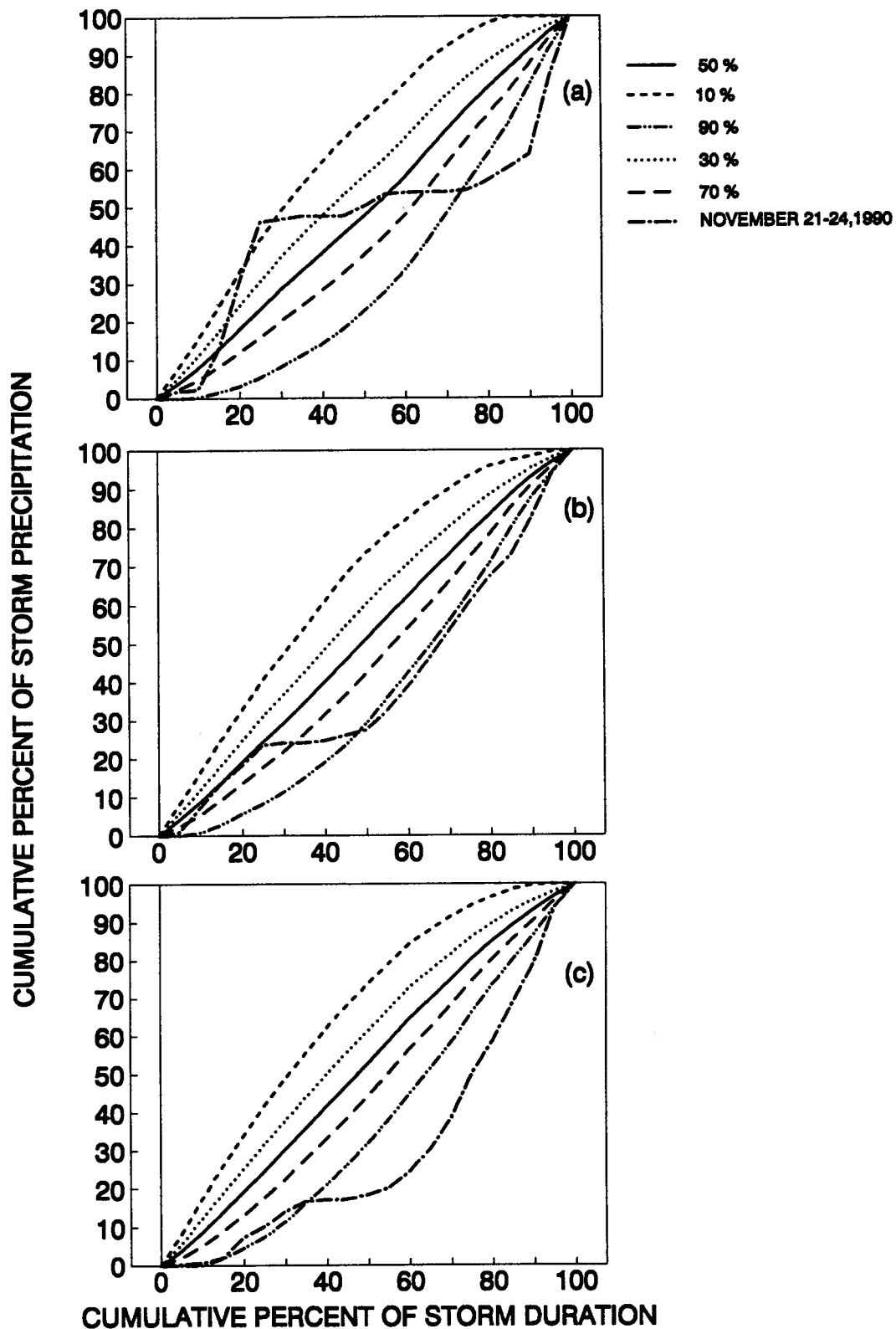


Fig. 6.7 Comparison of the time distribution of the November 21-24, 1990 storm with time probability distribution curves at (a) Vancouver Harbour (b) station 10A and (c) station 14A

CHAPTER 7

APPLICATION OF A METEOROLOGICAL MODEL

7.1 Introduction

In the previous Chapters, the study of precipitation was carried out by statistical analysis of the existent database. The findings of this analysis are then generalized over the coastal region of British Columbia and relationships between the short-term and the long-term precipitation were identified to extend the application of the results over the region. Another way to estimate precipitation is by using meteorological models. Several theoretical meteorological models have been proposed which can evaluate the short-term precipitation considering the appropriate meteorological and topographic parameters and terrain-atmospheric interactions. The basic approach uses a wind model to calculate the horizontal and vertical air motions induced by the mountain terrain. This wind model is then used to drive the rain model which estimates the condensation from the moist air mass as it passes over the mountain regions.

The wind field can be regarded as the combined effect of three major factors: synoptic-scale forcing, topographic blocking or channeling, and thermal effects. The synoptic-scale pressure field itself can be greatly modified by the dynamic and thermodynamic effects of large-scale topography. Relatively simple models suitable for the diagnosis or forecasting of the wind field have been used and can be grouped into three types according to the approach adopted: mass conservation models, models using one-layer vertically integrated primitive equations of motion and models using one-level primitive equations. Mass conservation models (Dickerson, 1978; Ross et al., 1988) assume a well-mixed, constant density layer beneath a low-level inversion where mass is conserved. The second simplified model

approach uses the equations of motion, vertically integrated for a well-mixed boundary layer (Lavoie, 1974; Overland et al., 1979). In these models mass is conserved in the mixed layer but not the layers above. The third type of model uses the primitive equations for one level without a continuity equation. For example, Danard (1977) proposed a model which requires the geostrophic wind at the surface and at 850 mb, the lower tropospheric lapse rate and surface air temperature. It integrates to a steady state the tendency equations at the surface only for wind, pressure and potential temperature. Mass and Dempsey (1985) extend that approach to calculate surface wind and temperature using equations for horizontal momentum and temperature tendency in sigma coordinates. The wind field is determined by the vertical temperature structure. Thermally-induced circulations due to diabatic forcing can also be included. The model has been applied at southwestern coastal British Columbia, western Washington and north-western Oregon.

The above types of wind models require a modest amount of initial data and computing resources and are useful for analysis and forecasting of wind for engineering purposes. However, the current trend is to embed mesoscale models capable of resolving regional detail in general circulation models (Giorgi and Bates, 1989; Giorgi, 1990). This type of approach will be useful for climate assessments and scenarios of changed forcings.

The estimated wind field is used as input to a precipitation model for the estimation of precipitation field over complex terrain. Modeling of orographic precipitation has followed two broad lines of approach. Some analytical studies (Elliot and Shaffer, 1962; Danard, 1971; Rhea, 1978) have used a combination of the Bernoulli equation, the continuity equation and hydrostatic flow for mountains of arbitrary shape. Other analyses (Walker, 1961; Wilson, 1978) have been based on the perturbation method and idealized barriers. In this approach the motion in a (x, z) plane can be expressed as a perturbation superimposed on a steady basic current of velocity.

The essential components of any type of orographic precipitation models include measures of the adiabatic ascent or descent, condensation or evaporation, and precipitation of the condensate. The treatment of water substance in the above models is quite variable. In some models, all of the condensed moisture is precipitated, others use various precipitation efficiency factors (Marwitz, 1974). In some models (Young, 1974 and Nickerson et al., 1978) cloud microphysics is also incorporated.

Both the wind models and the precipitation models can be set up in three dimensions but in most cases a vertical cross section can reasonably represent the storm's flow pattern into a project basin. This reduction to two dimensions simplifies the calculations and reveals the relevant factors in storm precipitation (Wiesner, 1970). Furthermore, the meteorological models can simulate the physical processes over the full-atmosphere or just in the boundary-layer of the atmosphere which extends a few kilometers over the terrain. Even though precipitation is generated several kilometers above the earth's surface, the horizontal variations of precipitation should be correlated to horizontal variations of the physical processes in the Atmospheric Boundary Layer (ABL). These models are flexible, and more simple and suitable for engineering design than the full-atmosphere models. In addition to the simplicity another advantage of boundary-layer models compared to full-atmosphere models is that the former appear to be relatively free of truncation errors associated with using the sigma coordinates in steep terrain (Danard and Jorgensen, 1992). Hence boundary-layer models can, hypothetically, be used with very small grid sizes in a mountainous terrain.

This Chapter presents the results of the application of a boundary-layer meteorological model in the study area north of Vancouver. The model is the BOUND_P model and it is tested in an area which has a highly variable topography. Furthermore, an additional test of the model is the small grid size. The model will be used to simulate historic storms, and then to predict the precipitation over the area for particular storms. The purpose of this testing of

Chapter 7. APPLICATION OF A METEOROLOGICAL MODEL

the model is to evaluate its performance and to identify whether it is suitable for the forecasting of runoff from mountainous watersheds of the region if it is combined with a hydrological model or whether it can be used for the estimation of the Probable Maximum Precipitation and consequently, the Probable Maximum Flood.

Firstly, a brief description of the model will be given. Then, the input data necessary for the application of the model will be discussed. The results of the application of the model will be presented in the next section. Finally, the concluding remarks will be stated.

7.2 General Description of the BOUND_P Model

7.2.1 Overview

The meteorological model BOUND_P was designed by Danard and Jorgensen (1992). The model was used in this study because it was readily available with advice and help from Dr. Danard and it has been used in hydrological applications by the British Columbia Hydropower Authority. The test of the model is the first independent test of the model against observed data.

The model consists of two main parts, the calculation of surface winds and the computation of the vertical flux of water at the top of the Atmospheric Boundary Layer (ABL). These two parts will be briefly described in the next paragraphs.

7.2.1.1 The wind model

The wind model is adapted from the models designed for British Columbia Ministry of Forests (Danard and Galbraith, 1991) and the U.S. National Weather Service (Danard and Galbraith, 1989) and has been presented in detail in two papers (Danard, 1988 and Danard, 1989). The wind model calculates the geostrophic wind V_g which is the air movement resulting when the pressure force and the Coriolis force are in balance. The geostrophic wind is the result of the pressure gradient and the rotation of the earth assuming no friction and no topography.

From the geostrophic wind V_g the model calculates the large-scale velocity u^* using the expression:

$$u^* = C_s V_g \quad (7.1)$$

where

$$C_s = \frac{k}{\sqrt{\left[\ln\left(\frac{h}{z_0}\right) - A \right]^2 + B^2}}$$

is the geostrophic momentum transfer coefficient (square root of the conventional drag coefficient), k is the von Karman's constant (0.35), h is the height of the atmospheric boundary layer (ABL), z_0 is the roughness length, and A and B are universal generalized similarity functions.

The height of the Atmospheric Boundary Layer is calculated from the formula proposed by Brown (1981):

$$h = c_b \frac{u^*}{f} \quad (7.2)$$

where f is the Coriolis parameter and c_b is a dimensionless factor less than 0.3 for stable conditions ($L>0$) and greater than 0.3 for unstable conditions ($L<0$).

The universal generalized similarity functions, A and B, are calculated using the method of Danard (1988).

The component wind which is necessary for the calculation of the vertical water flux is the balanced surface wind \vec{V}_b . \vec{V}_b is the unaccelerated wind for which the large-scale pressure gradient, the Coriolis and the frictional forces are in balance. The balanced surface wind speed is estimated by:

$$V_b = \frac{u^*}{k} \left[\ln \left[\frac{z_a}{z_0} \right] + f_2 \left[\frac{z_a}{L} \right] \right] \quad (7.3)$$

where u^* is the large-scale wind velocity, z_0 is the roughness length over water L is the Monin-Obukhov length, z_a is the anemometer height and $f_2(z_a/L)$ is a stability correction term and k is the von Karman's constant ($k=0.35$).

The first law of thermodynamics is applied to the surface in the form:

$$\frac{\partial \theta_s}{\partial t} = -\vec{V} \cdot \nabla \theta_s + K_t \nabla^2 (\theta_s - \theta_i) + Q - C_n (\theta_s - \theta_{sl}) \quad (7.4)$$

where θ_s is the surface potential temperature, K_t is the horizontal thermal diffusivity, θ_i is the initial surface potential temperature, Q is the diabatic heating rate, C_n is a nudging coefficient,

and θ_s is the large-scale potential temperature. The diabatic heating rate, Q, can be found assuming that the surface pressure tendency is hydrostatic.

Then, the equation of motion is integrated in the form:

$$\frac{\partial \vec{V}}{\partial t} = -\vec{V} \cdot \nabla \vec{V} - (g \nabla Z_s + RT_s \nabla \ln p_s) - f \vec{k} \times \vec{V} + \vec{F}_s + K_m \nabla^2 \vec{V} + \frac{\partial \vec{V}_b}{\partial t} - C_n (\vec{V} - \vec{V}_b) \quad (7.5)$$

where \vec{V} is the surface wind at any level in ABL, Z_s is the terrain elevation, R is the gas constant, T_s is the surface air temperature, g is the acceleration of gravity, p_s is the surface pressure, f is the Coriolis parameter, k is the von Karman's constant, \vec{F}_s is the frictional force per unit mass in the surface layer and it is assumed $\vec{F}_s = C_f \cdot \vec{V}^2$, K_m is the momentum horizontal diffusivity, C_n is a nudging coefficient, and \vec{V}_b is the balanced wind the speed of which is given in Equation 7.3.

The estimated wind field around and over the mountains is estimated solving Equations 7.4 and 7.5 and then, this wind is used as input to the water flux model which approximates the condensation processes in the ABL. The water flux model will be briefly presented in the next paragraphs.

7.2.1.2 The water flux model

The basic predictor is the vertical flux of the water at the top of the Atmospheric Boundary Layer (ABL). The vertical flux can be written as:

$$W = W_b + E \quad (7.6)$$

Chapter 7. APPLICATION OF A METEOROLOGICAL MODEL

where $W_b = (r + r_l)\rho V_p$ is the non-turbulent flux of water (or undisplaced flux), r is the water vapour mixing ratio, r_l is the mixing ratio of condensed water (having a value of 5×10^{-4}), ρ is the air density, V_p is the vertical velocity relative to an isobaric surface and E is the evaporation from the earth's surface. W_b is usually larger than E .

It can be proven (Danard and Jorgensen, 1992) that the vertical velocity can be written as :

$$V_p = V_t + V_0 + V_c \quad (7.7)$$

with:

$$\begin{aligned} V_t &= -\frac{1}{g\rho} \frac{\partial p_s}{\partial t} \\ V_0 &= -\frac{1}{g\rho} \sigma_H V_H \nabla p_s \\ V_c &= -\frac{1}{g\rho} \int_{\sigma_H}^1 \nabla p_s V d\sigma \end{aligned}$$

where g is the acceleration of gravity, ρ is the air density, p_s is the surface pressure, σ_H is the value of the sigma coordinate $\sigma = \frac{P}{P_s}$, at the top of the ABL ($\sigma_H \approx 0.9$), and V_H is the wind at

the top of the ABL.

The term V_t of the above equation represents the effect of the surface pressure tendency and it is usually small. The term V_0 is the effect of the orography (upslope, and downslope motion) and it is positive as air is moving from high pressure (low elevation) to low pressure (high elevation). Finally, the term V_c represents the effect of convergence due to friction or orography.

When the atmospheric water vapour is displaced vertically upwards, it takes some time for it to condense and to grow to precipitation size and begin falling. Precipitation droplets are carried with the winds as they fall. Furthermore, the precipitation is initially in the form

of ice at the top layers of ABL even for summer storms. The ice particles can be transported over a very large distance by the wind. The vertical water flux estimated by the Equations 7.6 and 7.7 is the undisplaced water generated at each grid ignoring the movement of the droplets due to horizontal wind. In order to account for the horizontal movement of the precipitation droplets, a routine for the estimation of the downwind displacement of the water flux has been incorporated in the model (displaced water flux).

7.2.2.3 Estimation of precipitation

Once the values of the displaced vertical water flux W are calculated, they are then fitted to the observed precipitation P at a number of stations, through regression. Various relationships could be used. The first is:

$$P = A_1 + A_2 W \quad (7.8)$$

where A_1 and A_2 are regression coefficients. The coefficient A_1 represents the precipitation that occurs over a horizontal smooth surface with no topography.

Another relationship is :

$$P = A_1 + A_2 W + A_3 W^2 \quad (7.9)$$

which has been shown to account for the effects of W on duration as well as on the intensity (Danard, 1971).

Another alternative relationship is:

$$P = A_1 + A_2W + A_3W^2 + A_4Z \quad (7.10)$$

where Z is the terrain elevation. This equation also accounts for the small topographic variations. The efficiency of the above equations will be tested in the application of the model.

The meteorological input data are available every 6 hours from the Canada Meteorologic Centre. However, the model averages the vertical water flux over a 24-hour period for each of the four 6-hour time steps. The average 24-hour vertical water flux is used in Equations 7.8, 7.9, and 7.10.

Finally, the model uses an objective analysis procedure in order to minimize the discrepancies between the estimated and observed precipitation (Danard and Jorgensen, 1992). The result is called objectively analyzed precipitation and it should be similar to the observed precipitation.

7.3 Data Sets

The meteorological model BOUNDP has been applied to the North Shore mountain area which covers the two study watersheds, the Seymour River and Capilano River watersheds. The data sets required by the model for its application will be presented in the next paragraphs.

Two types of data are required by the model: a) data that are necessary to initialize the model run and b) data that are used throughout the running of the model. The initial data requirements include: i) terrain elevation (mean elevation of each grid cell), ii) water percentage of each grid cell, iii) water temperature, iv) ice percentage of each grid cell. Topographical data have been digitized for the whole Province of British Columbia by the

Chapter 7. APPLICATION OF A METEOROLOGICAL MODEL

British Columbia Department of Environment, Land and Parks. The terrain elevations are supplied for a grid 30"x30", and then are averaged for the model grid cells. The water fraction is digitized from topographical maps of 1:50,000 scale. The water temperature is not necessary input data and is calculated by the model. The ice-fraction is considered to be zero for the storms simulated in this study.

Data used throughout the running of the model are: i) height and temperature at 700, 800, and 1000 mb, pressure levels and ii) boundary-layer relative humidity. The heights and temperatures at 700, 850, and 1000 mb were retrieved from the Canada Meteorological Centre (CMC) for a grid of $1^{\circ}\times 1^{\circ}$. These data are the output of the CMC finite element model. This model accepts radiosonde measurements usually every 24 hours from a very sparse radiosonde network across Canada. The model then interpolates and forecasts the meteorological elements every 6 hours for the next 24 hours for a grid of $1^{\circ}\times 1^{\circ}$. When a new set of measurements are available the model updates the forecasts of these data. The 24:00 UTC (Universal Coordinated Time) data for each day are the updated data and the 06:00 UTC, 12:00 UTC, and 18:00 UTC data are the forecast data. These data are available for 5 days a week, from Monday to Friday. For the weekends, only the forecast output of the CMC finite element model is used.

The meteorological data of $1^{\circ}\times 1^{\circ}$ needs to be interpolated, once more, to the BOUND_P model grid. In this study, the interpolation is achieved by using B-splines (IMSL, 1989). Fourth order polynomials are used for both latitude and longitude for the interpolation.

The meteorological data, retrieved from CMC, contained no information about relative humidity. To compute the relative humidity, the Equation 7.11 is used (Linsley et al, 1982):

$$RH = 100 \left(\frac{112 - 0.1T + T_d}{112 + 0.9T} \right)^8 \quad (7.11)$$

where T is the air temperature, and T_d is the dew point temperature.

The mean daily temperature of the Vancouver Harbour A.E.S. station is used as the air temperature. The dew point temperature cannot be smaller than the minimum temperature for humid air. Quick (1987) has used the minimum daily temperature as the dew-point temperature for the calculation of snowmelt with success. This assumption has been adopted in the present study.

The Equation 7.11 approximates the relative humidity to within 0.6% in the range of -25°C to 45°C (Linsley et al, 1982). Furthermore, the value used in the simulation is the surface value whereas the average relative humidity of ABL is required. However, it is assumed that Equation 7.11 gives an average value over the domain since upslope areas have larger relative humidity than downslope areas. Moreover, testing of the model with various values of relative humidity showed that the model is insensitive to the humidity and its variations.

7.4. Application

7.4.1 Complications

The precipitation was initially simulated for an area covering a latitude range from 49° 15' to 49° 35' and a longitude range from 123° 18' to 122° 48'. The calculation domain consisted of 20x20 grids each having dimensions 1'x1' or 1.2x1.8 km, approximately. The model calculates the water flux in the grids located at the edge of the calculation domain, using the values of water flux from grids outside the calculation domain. Hence, five grid widths around the calculation domain have been added increasing it to the model domain, which covered an area from 49° 10' to 49° 40' latitude and from 123° 10' to 122° 50' longitude.

The model for this very fine grid mesh gave very large values of vertical water flux. The water flux was in the range of 10,000-100,000 mm/day. The water flux should be in the range of hundreds of mm/day. In view of these unreasonable results, the number of the border grids was increased from five to fifteen grids increasing the distance of the border around the calculation domain from 9 km to 27 km in the longitudinal direction and from 6 to 18 km in the latitudinal direction. This was done because the model interpolates outside the model domain resulting in very large vertical fluxes. However, application of the model to the increased model domain gave similar results. No further attempt was made to increase the border grid size because the model then would have become inefficient, having a model domain about twice the calculation domain.

The small grid size gives a much better description of the topography of the area but results in very steep slopes. It is believed that these steep slopes resulted in numerical instability and consequently, in unreasonable results. The elevation from one grid to the next could be increased by more than 1000 m. This large elevational increase is, for the model, like an infinite increase in elevation between grids. In this case, the model produces very large values of the water flux.

The next step was to increase the grid size. Increasing the grid size results in smoothing of the topography, giving smaller slopes. The grid size was increased to 2'x3', which is 3.6x3.6 km, approximately. The precipitation was then simulated for an area covering a latitude range from 49° 15' to 49° 35' and a longitude range from 123° 18' to 122° 48'. The new calculation domain consisted of 10x10 grids. Six grids around the calculation domain have been added, increasing it to the model domain, which covers an area from 49° 03' to 49° 47' latitude and from 123° 36' to 122° 30' longitude.

The application of the model to the new model domain gave more reasonable water flux values. The above problems in the application of the BOUND_P model prove that the

Chapter 7. APPLICATION OF A METEOROLOGICAL MODEL

model is affected by the grid size and consequently, the steepness or smoothness of the model domain is a very important factor. Small grid size results in numerical instabilities giving unreasonable results.

Figures 7.1 and 7.2 are the three dimensional topographical maps of the calculation and model domain for the grid size (2'x3') used in the modeling, respectively. The topographical contour maps are shown in figures 7.3 and 7.4.

The results that will be discussed in the next paragraphs are the results obtained from the application of the model to the domain of 2'x3' grid size which gave the acceptable results.

7.4.2 Results

The meteorological data necessary for the application of the model where readily available for the years 1990-1992. Seven large historical storms from this period were selected for the application of the model BOUNDP. The storms used are: August 29-30, 1990, October 24-27, 1990, November 8-13, 1990, November 21-24, 1990, April 3-4, 1991, August 26-30, 1991, November 16-18, 1991. The daily accumulations at 33 stations in the area (Table 7.1) during these storms where used to compare the computed to the observed precipitation. The first four storms were used to estimate the regression coefficients of the Equations 7.8, 7.9, 7.10 (**Calibration**). The next three storms were used for the application of the model in full prognostic mode, using the analyzed regression coefficients of the historic storms (**Verification**).

Care is needed when comparing the modeled and observed precipitation because the meteorological input data and the modeled precipitation are referred to Universal Coordinated Time (UTC) whereas the observed precipitation is referred to Pacific Standard Time (PST). Observed climate day for class 1 A.E.S. station begins at 08:00 PST (16:00 UTC) and ends at

Chapter 7. APPLICATION OF A METEOROLOGICAL MODEL

08:00 PST (16:00 UTC) of the next morning. To compute the vertical flux for A.E.S. stations, the model is run with input data for 12:00 UTC of the day and 00:00 UTC of the next day. The resulted displaced vertical water fluxes were averaged to produce climate day values.

7.4.2.1 Calibration of the model

Although four storms were used for the calibration of the model, only the results for the simulation of the November 10, 1990 will be shown. These results are the best results achieved throughout the calibration procedure. The storm impinged on the area on November 8-13, 1990 causing severe floods in the Greater Vancouver Area as has been discussed in Chapter 6. The largest daily precipitation was observed on November 10, 1990 at the Seymour Falls Dam station. The 300 mm recorded is the second largest daily accumulation in 64 years of record.

Figures 7.5 and 7.6 show the undisplaced vertical water flux for November 10 (12:00 UTC) and November 11 (00:00 UTC), respectively. The undisplaced vertical water flux for these two days has a similar pattern but larger values of water flux are observed for November 11 (00:00 UTC). Figures 7.7 and 7.8 show the downwind displaced water flux for November 10 (12:00 UTC) and November 11 (00:00 UTC). The distribution patterns of the downwind displaced water flux for these two days are totally different and the values of the flux increase considerably on November 11 (00:00 UTC). Around that time the heaviest precipitation was recorded.

Chapter 7. APPLICATION OF A METEOROLOGICAL MODEL

Table 7.1. Precipitation stations used in the application of the BOUND P model

Station Name	ID number*	Latitude	Longitude	Elevation (m)
BURNABY CAPITOL HILL	1101146	49 17'	122 59'	183
BURNABY METROTOWN	110A1ND	49 13'	123 00'	125
BURNABY MTN TERMINAL	1101155	49 16'	122 56'	137
BURNABY SIMON FR. UNIV.	1101158	49 17'	122 55'	366
IOCO REFINERY	1103660	49 18'	122 53'	53
COQUITLAM COMO LAKE AV.	1101889	49 16'	122 52'	160
PORT MOODY GLENAYRE	1106CL2	49 17'	122 53'	130
VANCOUVER HARBOUR	1108446	49 18'	123 07'	0
VANCOUVER KITSILANO	1108453	49 16'	123 10'	12
VANCOUVER UBC	1108487	49 15'	123 15'	87
N.VANC.DOLLARTON	110NFNF	49 19'	122 57'	52
N.VANC.GRAND BOUL.	110EF57	49 19'	123 03'	111
N.VANC.GROUSE MTN RES.	1105658	49 23'	123 05'	1128
N.VANC.HIGHLANDS	110EFNN	49 21'	123 07'	130
N.VANC.CLEVELAND DAM	110EF56	49 22'	123 06'	157
N.VANC.LONSDALE	1105665	49 19'	123 04'	308
N.VANC.REDONDA DR.	110N6F5	49 22'	123 05'	229
N.VANC.WHARVES	1105669	49 19'	123 07'	6
N.VANC.2ND NARROWS	1105666	49 18'	123 01'	4
N.VANC.SONORA DR.	110N6FF	49 22'	123 06'	183
N.VANC.SEYMOUR HATCH.	110N666	49 26'	122 58'	210
N.VANC.SEYMOUR FALLS	1107200	49 26'	122 58'	244
W.VANC.CYPRESS PARK	1108828	49 21'	123 15'	155
W.VANC.MILLSTREAM	1108840	49 22'	123 08'	381
LIONS BAY	1104634	49 28'	123 14'	137
S-1	UBC	49 28'	122 57'	240
10A	UBC	49 32'	123 00'	293
14A	UBC	49 32'	123 01'	488
21A	UBC	49 32'	123 01'	640
25B	UBC	49 33'	123 02'	716
28A	UBC	49 33'	123 03'	853
C-1	UBC	49 26'	123 11'	610
C-2	UBC	49 27'	123 06'	320

*Official A.E.S. Station Number

The downwind displaced vertical water flux is used for the estimation of precipitation. The daily observations of 33 stations in the greater study area were used for the fitting of Equations 7.8, 7.9, 7.10. Table 7.1 shows the stations used and their topographical and geographical characteristics.

Each one of the Equations 7.8, 7.9, 7.10 were used for all four historic storms. The results showed that Equation 7.10 gives a better explanation of the variation of precipitation in space, so that it was decided only to use this equation for the verification of the model.

Figure 7.9 shows the model estimated precipitation using Equation 7.10 for November 10, 1990. Figure 7.10 shows the objectively analyzed precipitation for the same day. Figure 7.11a is the scatter graph of the observed and calculated precipitation for November 10, 1990. Figure 7.11b is the scattergraph of the total observed and calculated precipitation for the storm November 8-13, 1990.

It is clear, from Figure 7.11, that the model underestimates the high precipitation and overestimates the smaller precipitation which is observed at the lower elevations. The high values of precipitation for November 10, 1990 were observed in Seymour valley, where increased convergence generates large amounts of precipitation. The model precipitation for this particular position is underestimated by more than 100%. Correlation analysis between the estimated and observed precipitation for November 10, 1990 showed that the correlation coefficient is 0.807. However, the regression line is flat and its slope and intercept is statistically significantly different from the line of perfect agreement (1:1 line) at 5% level (Fig. 7.11a). The results improved when the total storm precipitation of November 8-13, 1990 is considered (Fig. 7.11b). The correlation coefficient between the observed and the estimated precipitation increased to 0.905, but still the slope and the intercept of the regression line is significantly different from the line of perfect agreement at 5% level. The

improvement is the result of the overestimation of precipitation by the model during the lower precipitation days.

The application of the model to the historic storms shows that the best possible prediction is achieved for the larger storms and the storms that result in considerable accumulations in the lowlands. These storms were deep frontal storms and cause severe flooding in the greater Vancouver area. On the other hand, the model gave very poor results for the smaller storms. The correlation coefficients between the simulated and the observed precipitation are very low, being between 0.10-0.20.

Another general observation is the underestimation of the large precipitation in the middle Seymour and Capilano valleys, which reaches 100%, and the overestimation of the lower precipitation at the low elevations. This large precipitation results from the increased convergence of the incoming air. The topography of the area is so variable that the grid size smoothed out the critical topographical features, and so eliminated the causative factors of the increased precipitation.

As a result of the underprediction of the precipitation in the middle valleys, the model does not depict the precipitation distribution pattern found from the analysis of the observed storm precipitation in the Seymour River watershed. That analysis, in Chapter 4 showed that the precipitation always increases up to the mid-position of the valley and then either decreases or levels off.

7.4.2.2 Analysis of the regression coefficients

The coefficients found from the application of the model for the four historic storms were analyzed in order to find appropriate values for the use of the model in the prognostic mode.

The coefficients A_1 , A_2 , A_3 , and A_4 of Equation 7.10 are plotted against the average precipitation over the area. Figure 7.12 shows the variation of A_1 and A_2 with the average precipitation. The values of A_1 increase linearly, except for three values which are lower than expected. Coefficient A_2 ranges about a constant value.

The next figure (Fig. 7.13) shows that, except for three cases, the value of A_3 ranges around zero for all the values of the average precipitation. The values of coefficient A_4 increase with the average precipitation over the study area but they do not show a consistent linear relationship. The coefficient A_4 was then plotted against the precipitation difference between the Grouse mountain resort station and the U.B.C. station and this caused the relationship to become linear. This might be expected, since A_4 is the multiplicator of elevation in Equation 7.10 and, thus, indicates the effect of the orography on the precipitation.

From the above relationships, it is clear that the regression coefficients can be predicted knowing or estimating the average precipitation over the greater area and the precipitation difference between the mountains and the lowlands. The values of coefficient A_1 were correlated against the average precipitation except for the three outlier values. The resultant equation is,

$$A_1 = 0.980 P_{av} \quad (7.12)$$

with $R^2=0.867$ (Fig. 7.14). If the average precipitation P_{av} is available from some other source such as satellite or radar data, the value of the A_1 coefficient can be estimated from Equation 7.12.

An average value of $A_2=0.293$ is used for coefficient A_2 . The coefficient A_3 is put equal to zero. Danard (1971) showed that the quadratic term W^2 of Equation 7.10 accounts for the effect of W on the duration as well as on the intensity. In the study area strong frontal

systems generate the large storms. These storms cover large areas having small to moderate intensity and large duration. The areal variation of the intensity and the duration is not as large as it is in convective storms. This probably explains the average value of zero of the coefficient A_3 .

The values of A_4 were correlated with the precipitation difference between Grouse mountain resort station and U.B.C. station. The resultant equation is:

$$A_4 = -4.06 + 0.962 P_{Grouse-UBC} \quad (7.13)$$

with $R^2=0.870$ (Fig. 7.15).

7.4.2.3 Verification of the model

The storms of April 3-4, 1991, August 26-30, 1991, and November 16-18, 1991 were used for the application of the model in prognostic mode. The results of the best simulation, that of August 26-30, 1991 storm will be presented in the next paragraphs.

Figures 7.16 and 7.17 show the undisplaced flux of August 29, 1991 (12:00 UTC) and August 30, 1991 (00:00 UTC). It seems that the general pattern is the same in both figures. Figures 7.18 and 7.19 show the downwind displaced vertical water flux for both the above dates. The pattern is different in these two figures. With the use of the predicted values of the regression coefficients, the precipitation is predicted and compared to the observed values. Figures 7.20a and 7.20b show the scatter graphs between predicted and observed precipitation for August 29, 1991 and for the storm period August 26-30, 1991. Correlation analysis between the observed and simulated precipitation showed that the correlation coefficient for August 29, 1991 is 0.589. Furthermore, the regression line between the observed and

Chapter 7. APPLICATION OF A METEOROLOGICAL MODEL

modeled precipitation is flat and significantly different from the line of perfect agreement at the 5% level. The model overpredicts the lower precipitation and underpredicts the high precipitation that occurred in the mountain valleys by about 50% (Fig. 7.20a).

The results improve when the total storm precipitation from August 26 to August 30, 1991 is considered. The correlation coefficient between the predicted and observed precipitation takes a value of 0.690. The improved correlation for the total storm period is the result of the overprediction of precipitation during the low precipitation days and underprediction of the high precipitation days. Hence, the total storm precipitation is better estimated by the model. However, again the regression line is significantly different from the line of perfect agreement at the 5% level (Fig. 7.20b).

From the results of the application of the model for the prognosis of storms, it is clear that the results compare better to the observed precipitation amounts for the high precipitation days than for the low precipitation days. The correlation coefficients between the observed and simulated precipitation for the high precipitation days are, on average, about 0.600. The simulation of the low precipitation days gave poor results with r values around 0.100. However, the regression line even for the high precipitation days was statistically different from the line of perfect agreement. The regression line was usually flat which shows that the model severely underpredicts the high precipitation accumulations in the valleys and overpredicts the low precipitation in the lowlands. Hence, the model fails to reproduce the general spatial distribution pattern of precipitation over the greater area that has been observed and described in Chapter 4.

Application of another meteorological model, similar to the BOUND_P model, by Rhea (1978) in the Rocky Mountains of Colorado showed that the model gives the best results for ridges and high plateaux, but overestimates amounts in narrow mountain valleys and underestimates for broad intermontane basins. These findings show that this type of model

does not at present describe the complex meteorological conditions which are needed to accurately simulate the mountainous precipitation.

7.5 Summary

The application of the model BOUNDP in the study area showed that the model is very sensitive to the grid size of the calculation domain. Small grid size causes numerical instability because of the steepness of the terrain. The numerical instability was eliminated when the grid size was increased from 1.2x1.8 km to 3.6x3.6 km. This increased grid size smoothed out the critical features of the topography which are responsible for the generation of the precipitation in the valleys. As a result the model underpredicts the high precipitation which occurs in the mountain valleys. This large accumulation of precipitation is the result of the funneling of the incoming air mass and the resultant increased convergence. Furthermore the model overpredicts the low precipitation in the lowlands so that it fails to reproduce the areal precipitation distribution over the area.

The model overpredicts also the precipitation during the low precipitation days and underpredicts the precipitation during significant accumulations. When the total storm precipitation over a number of days is considered the overprediction of the low precipitation and the underprediction of the high precipitation are partially compensated.

The real test of the model for hydrologic applications will be to use the model in conjunction with a hydrologic watershed model for the simulation of the runoff from the mountainous areas. However, the very large underprediction of high precipitation, by even 100%, and the misrepresentation of the areal precipitation pattern negate this testing. The underprediction of the large storms reduces the reliability of the model for flood modeling.

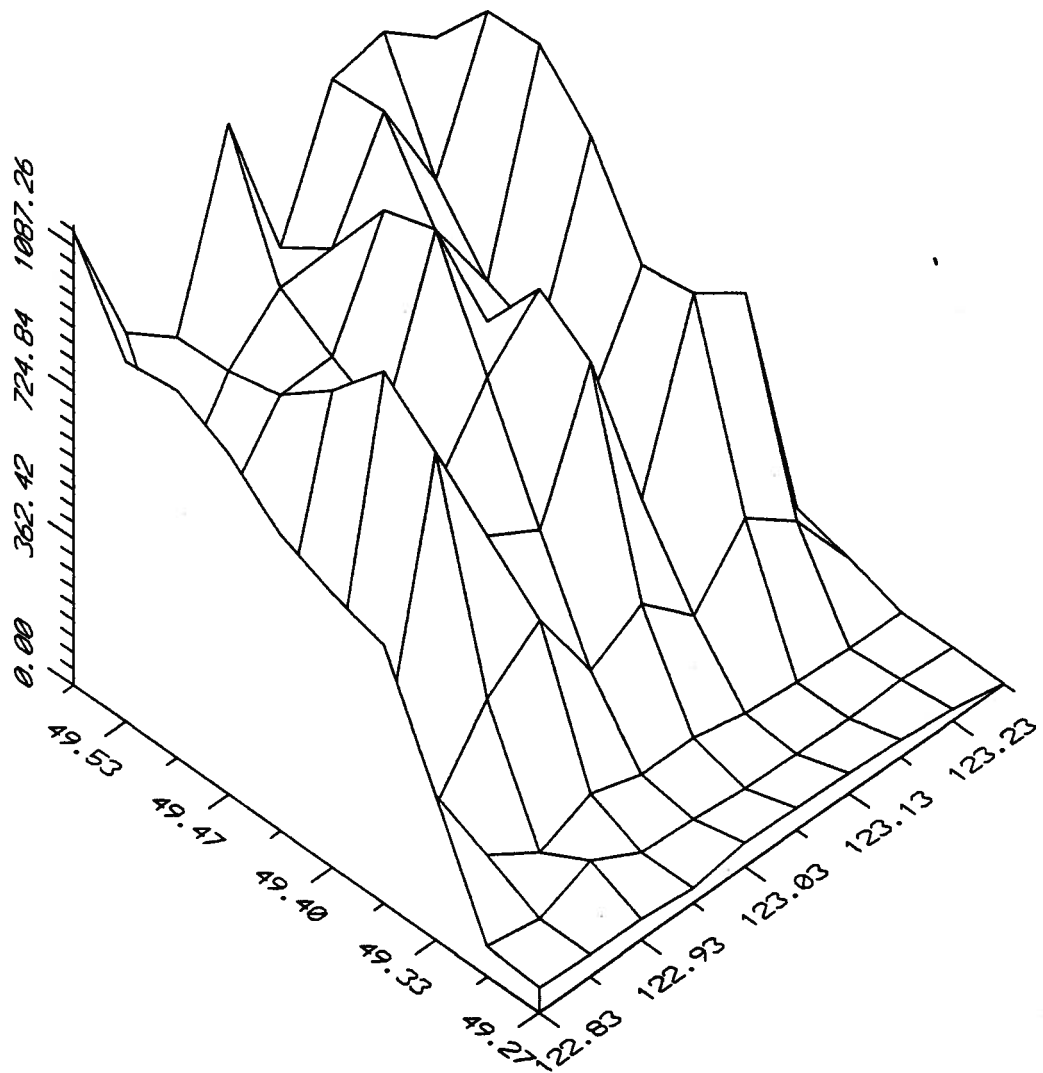
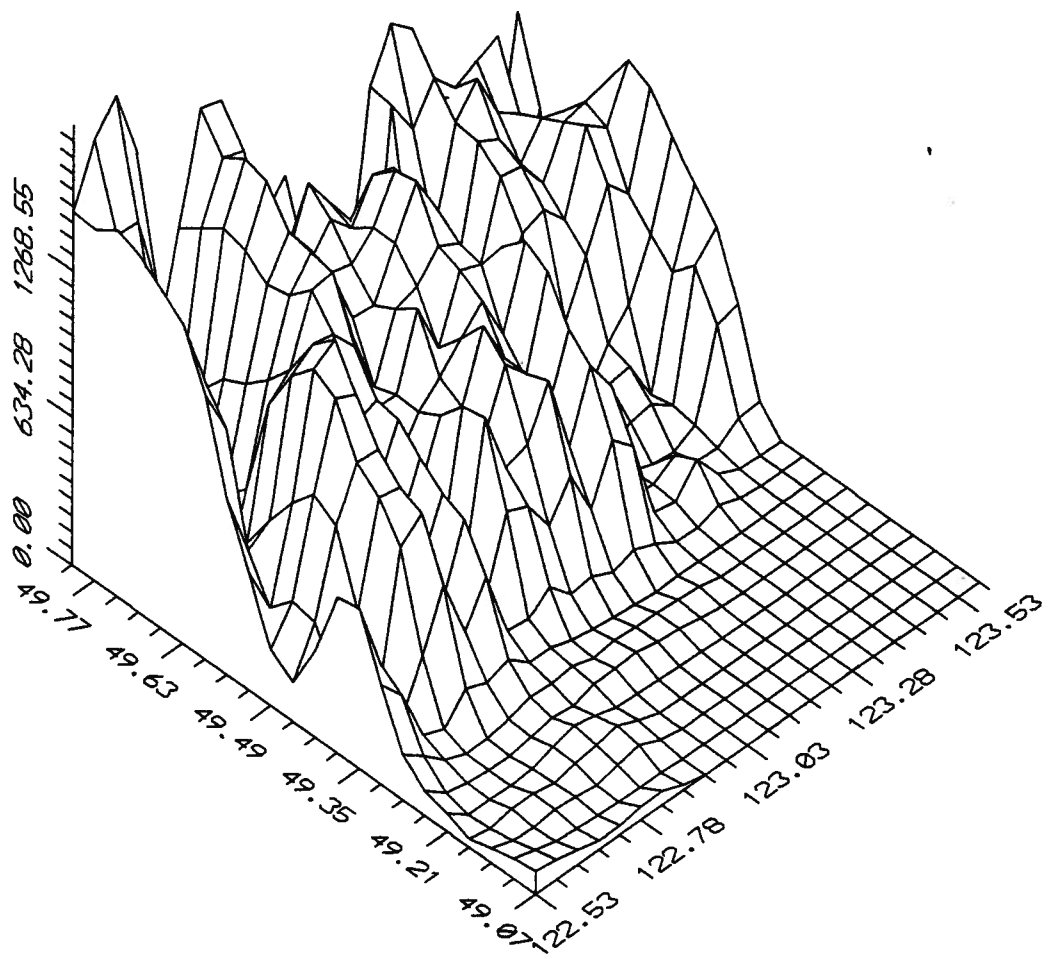


Fig. 7.1. Three dimensional map of the calculation domain (latitude and longitude in degrees and elevation in meters with vertical scale 1:17,500)



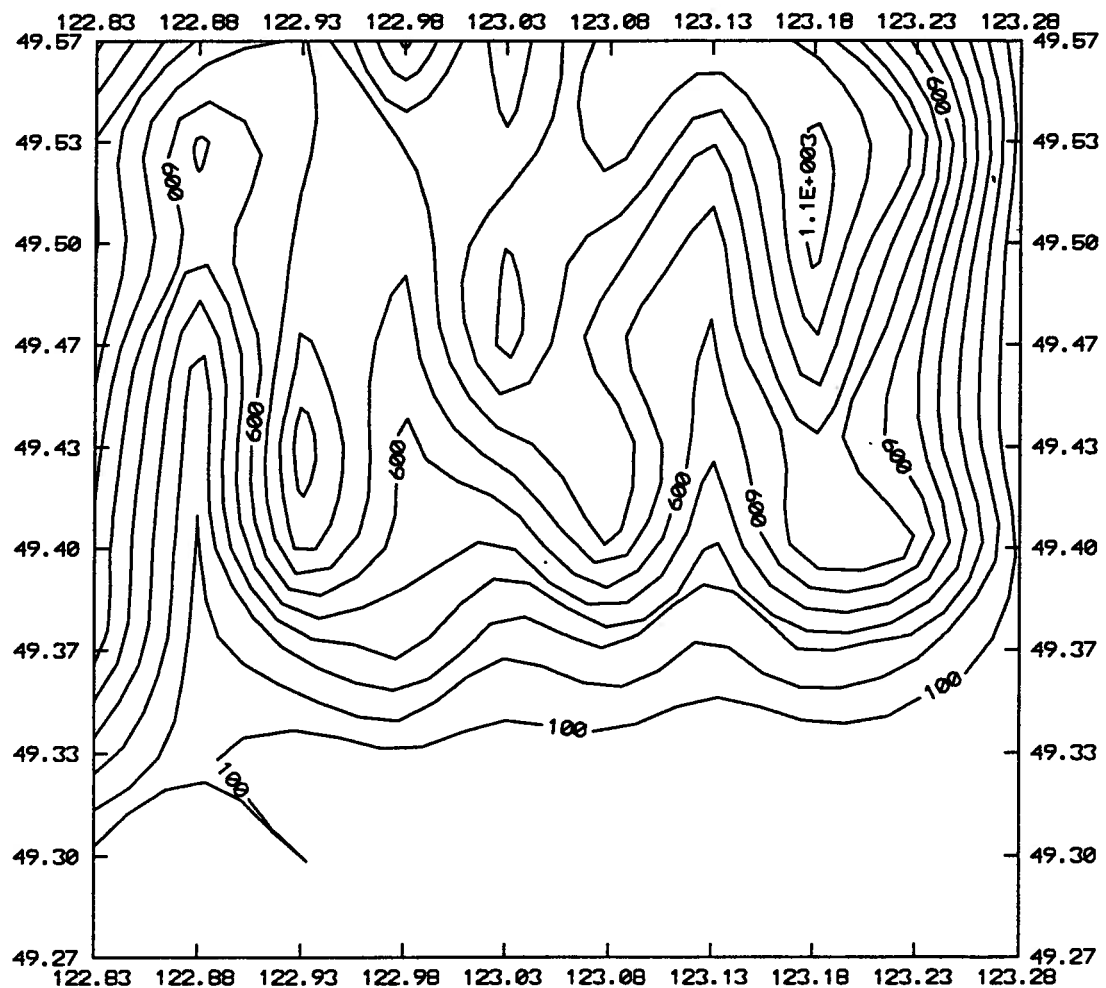


Fig. 7.3. Topographical contour map of the calculation domain (latitude and longitude in degrees)

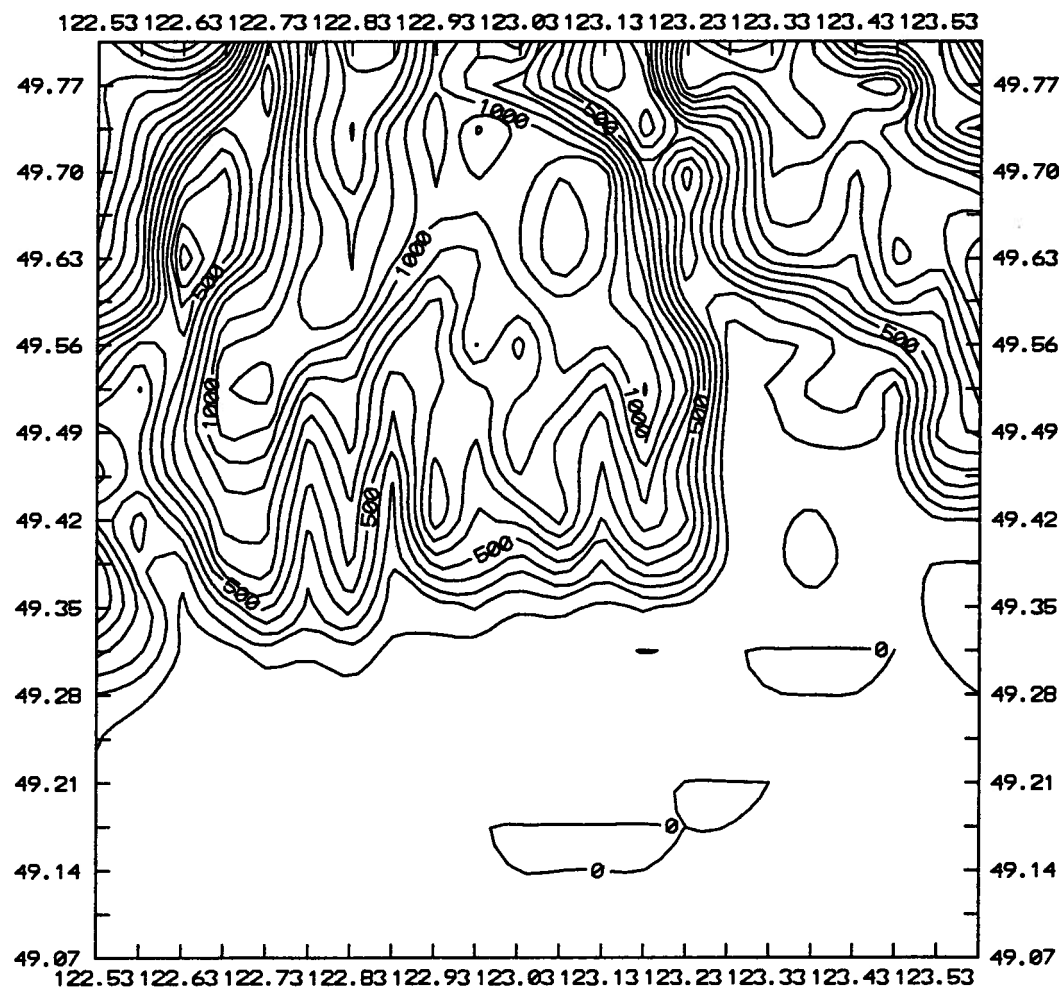


Fig. 7.4. Topographical contour map of the model domain (latitude and longitude in degrees)

Chapter 7. APPLICATION OF A METEOROLOGICAL MODEL

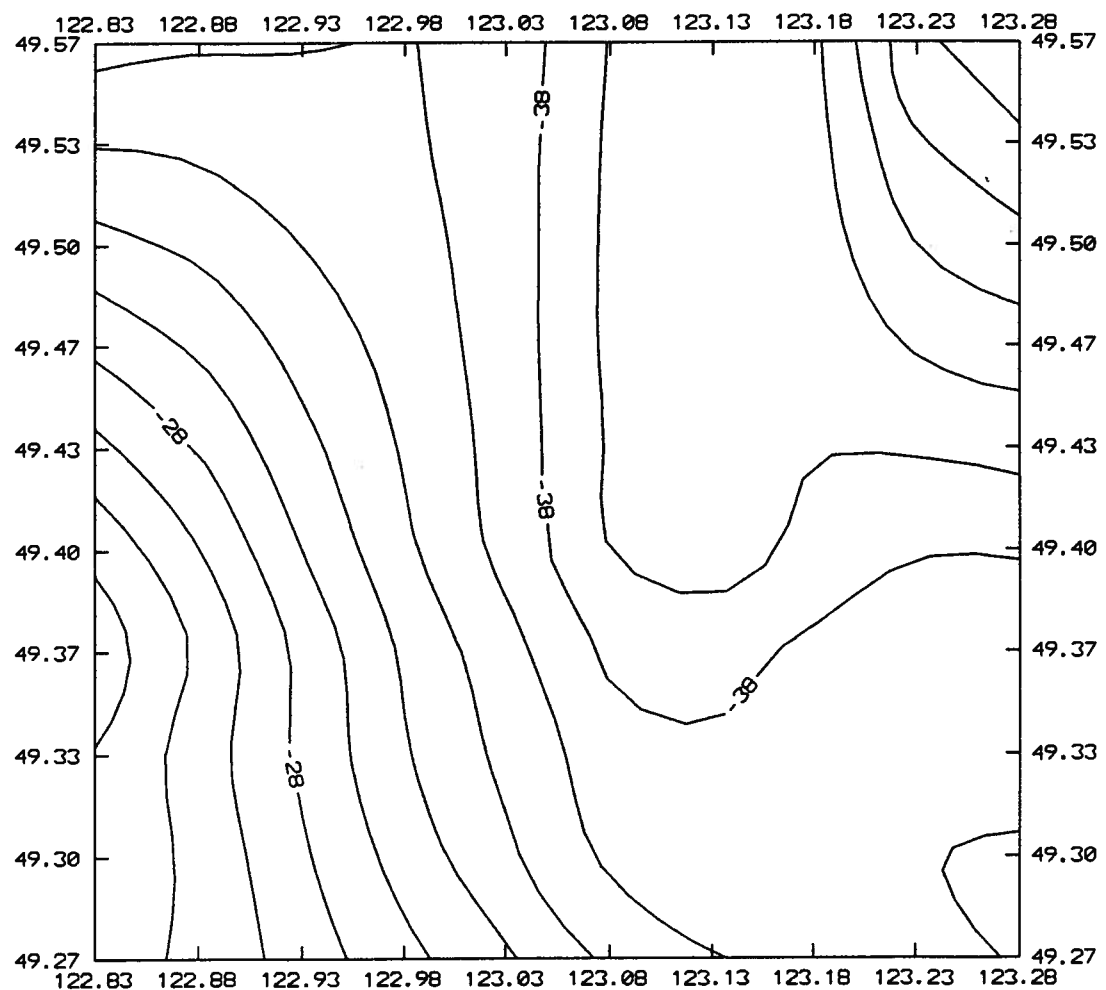


Fig. 7.5. Undisplaced water flux (mm) for November 10, 1990 (12:00 UTC)

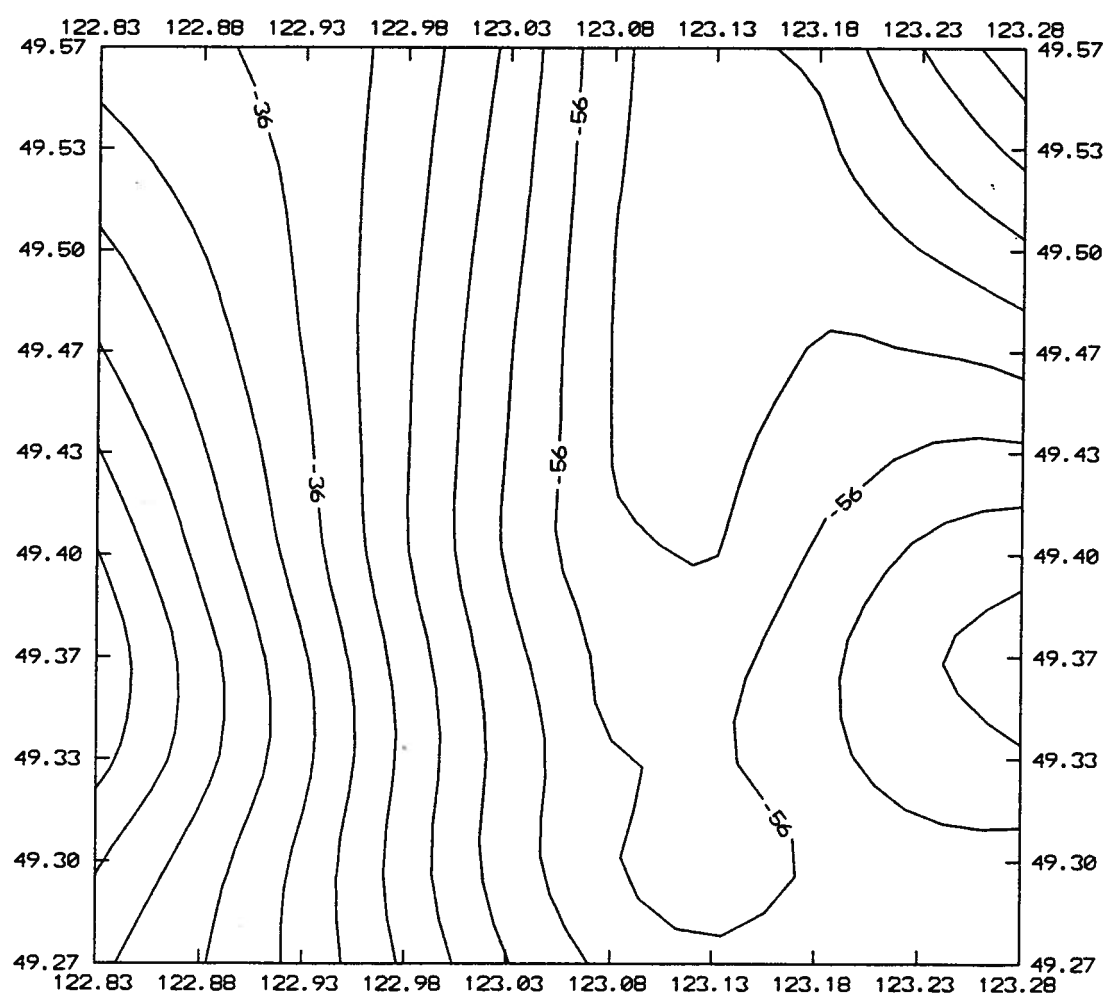


Fig. 7.6. Undisplaced water flux (mm) for November 11, 1990 (00:00 UTC)

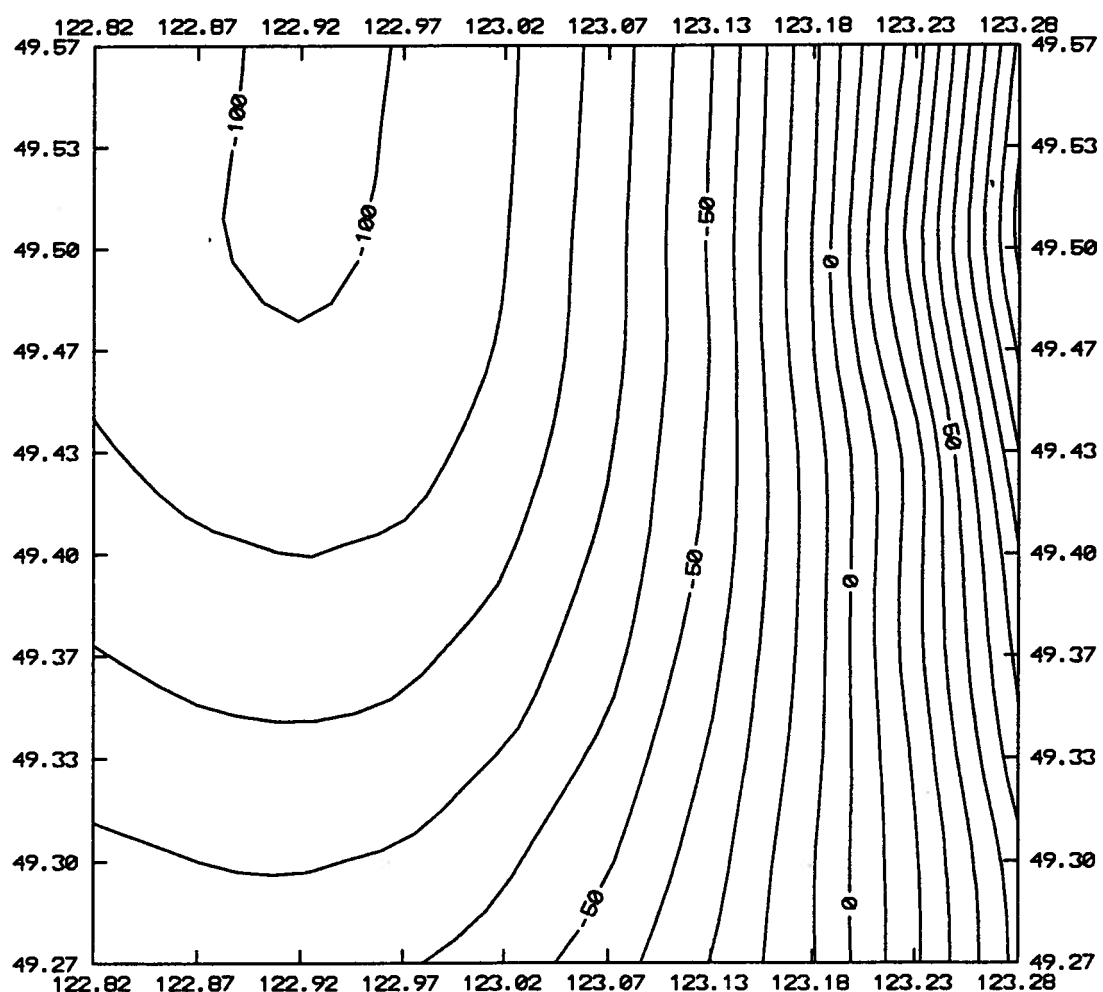


Fig. 7.7. Displaced water flux (mm) for November 10, 1990 (12:00 UTC)

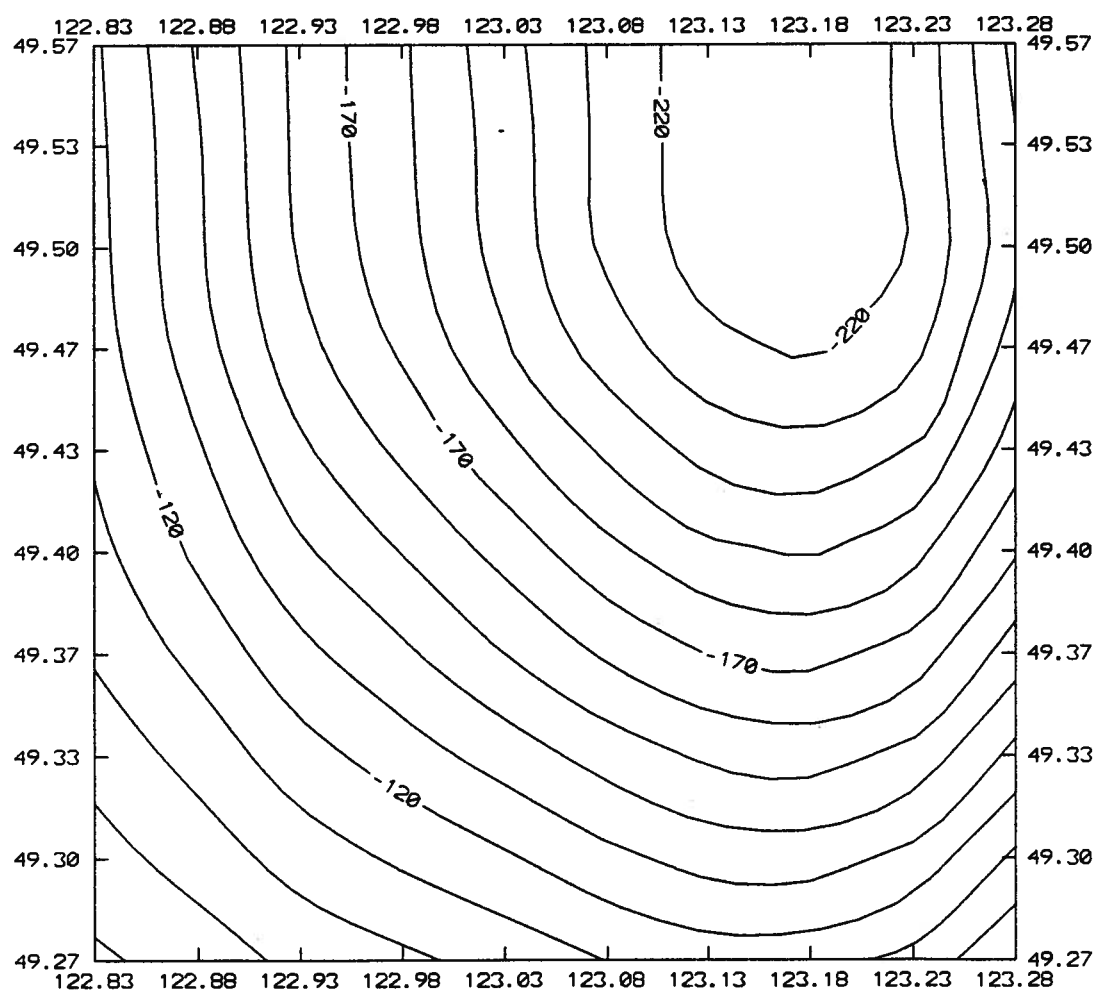


Fig. 7.8. Displaced water flux (mm) for November 11, 1990 (00:00 UTC)

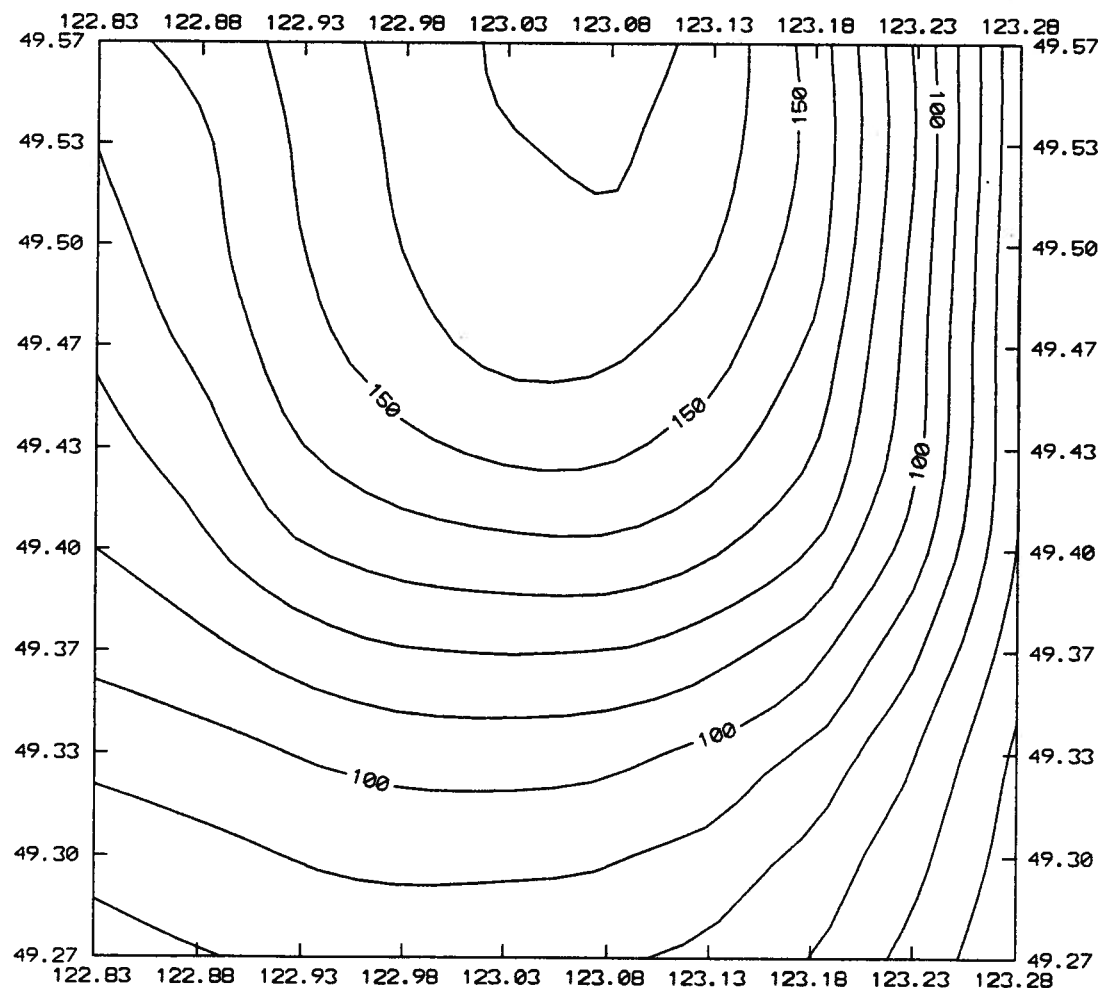


Fig. 7.9. Predicted precipitation (mm) for November 10, 1990

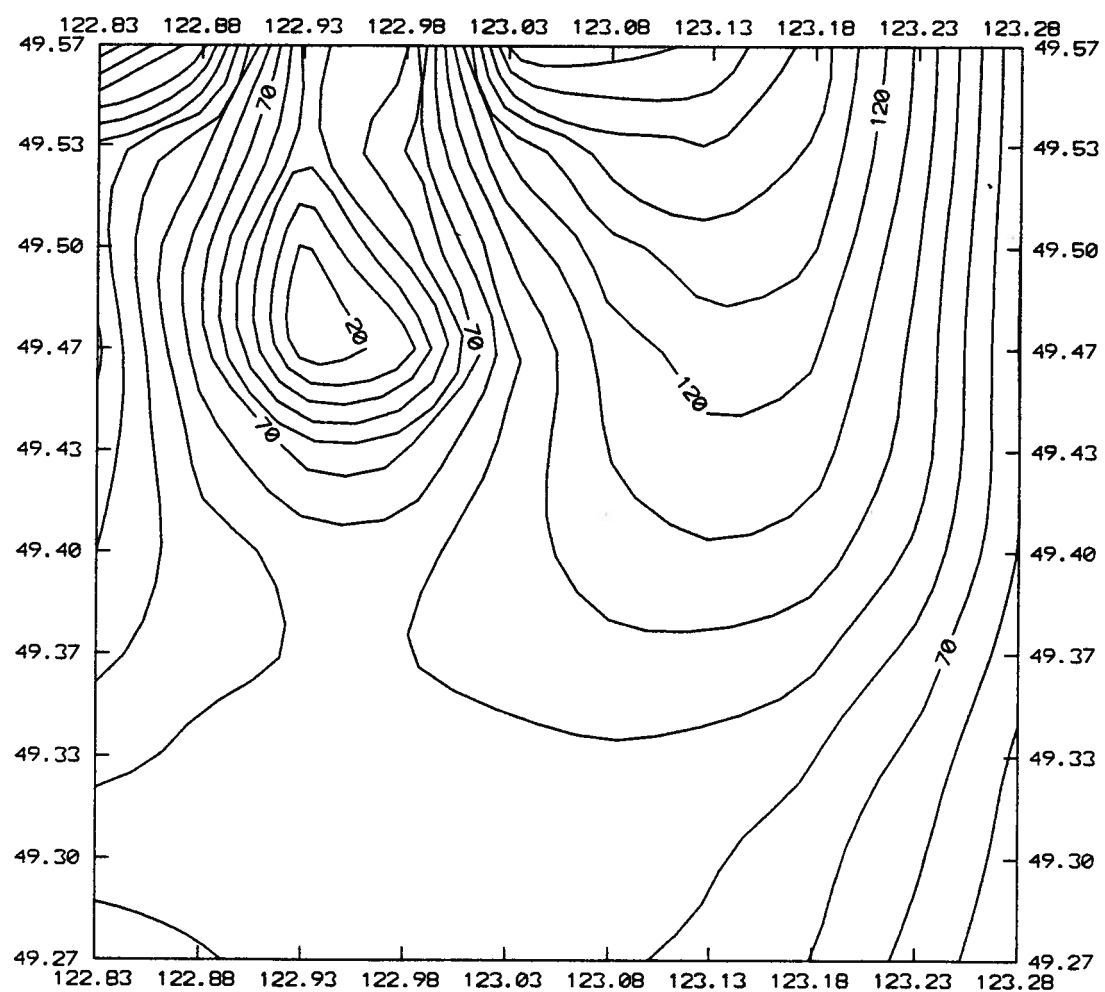


Fig. 7.10. Objectively analyzed precipitation (mm) for November 10, 1990

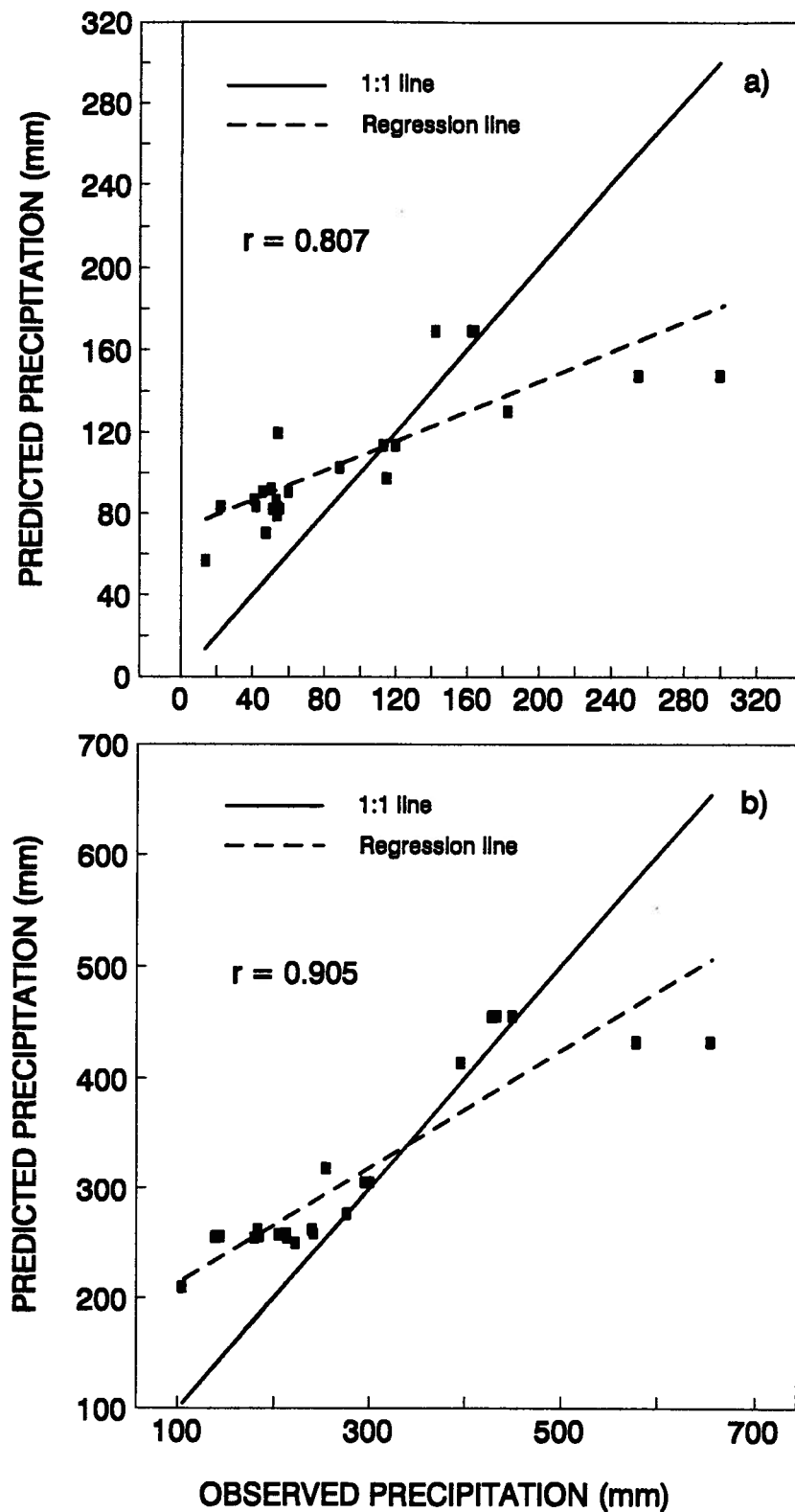


Fig. 7.11. Scattergraphs of observed and predicted precipitation for calibration for a) November 10, 1990 and b) total storm period between November 8-13, 1990

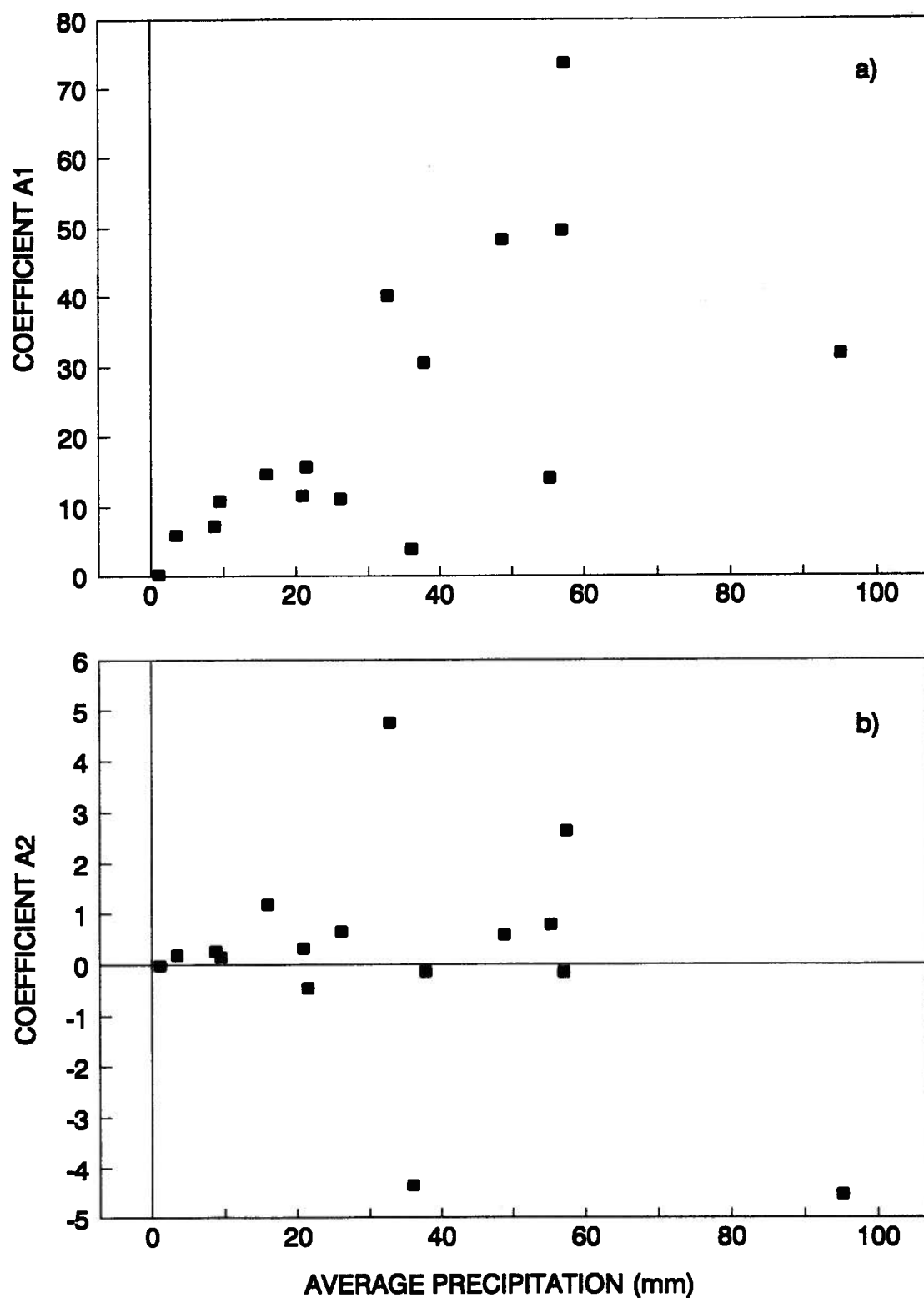


Fig. 7.12. Regression coefficients versus the average domain precipitation
a) A1 and b) A2

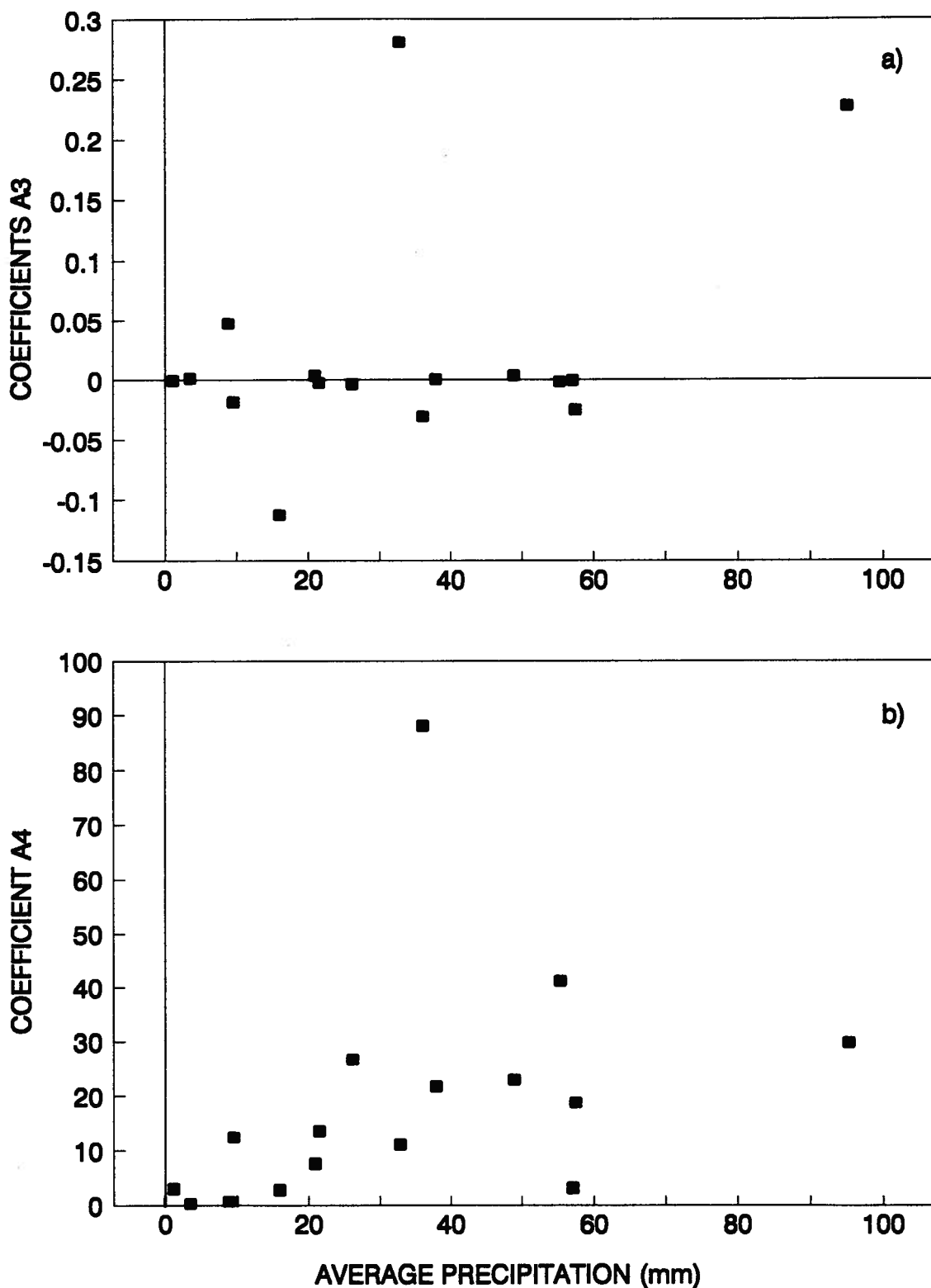


Fig. 7.13. Regression coefficients versus the average domain precipitation
a) A3 and b) A4

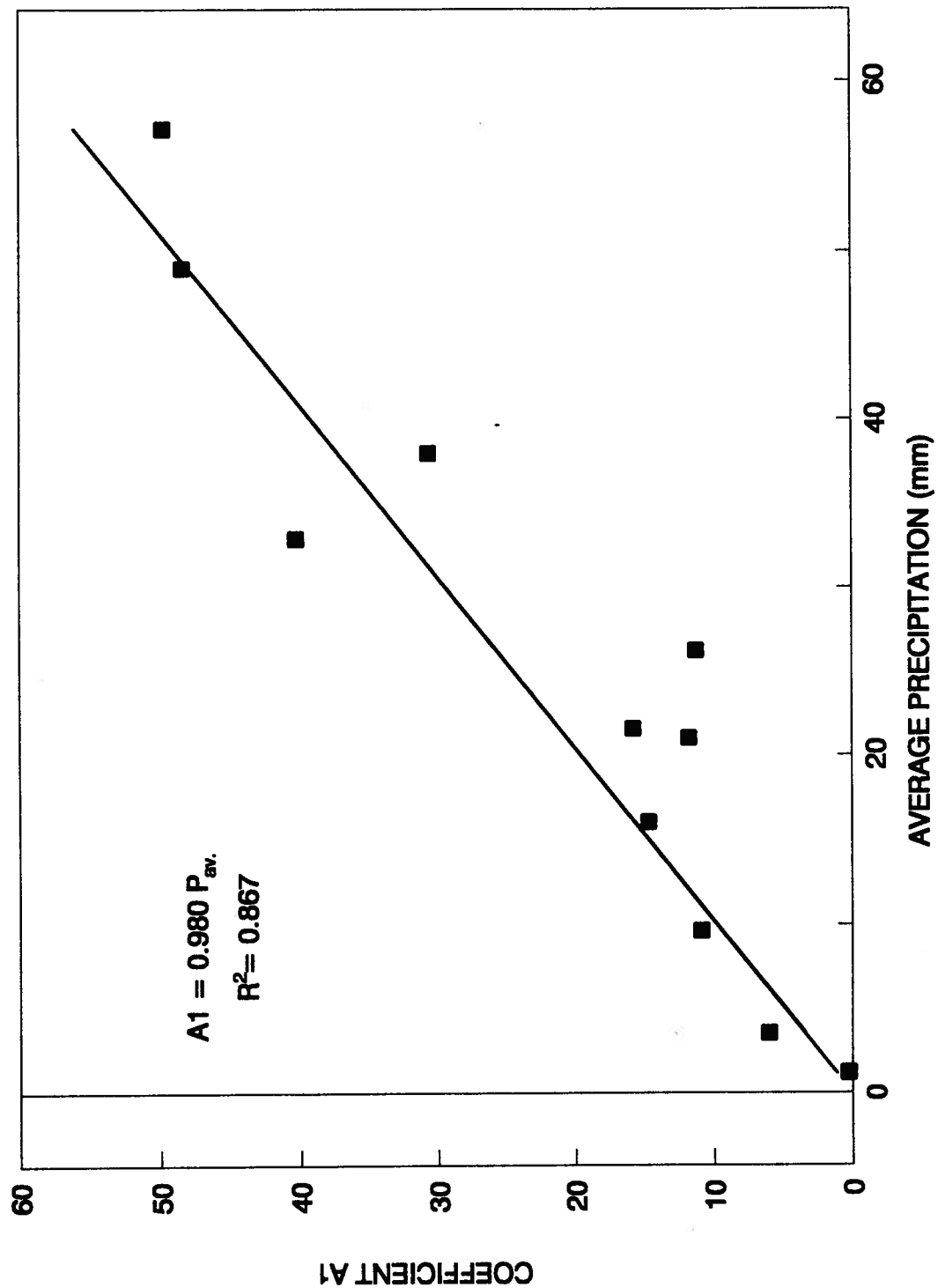


Fig. 7.14. Regression between the average domain precipitation and the coefficient A1

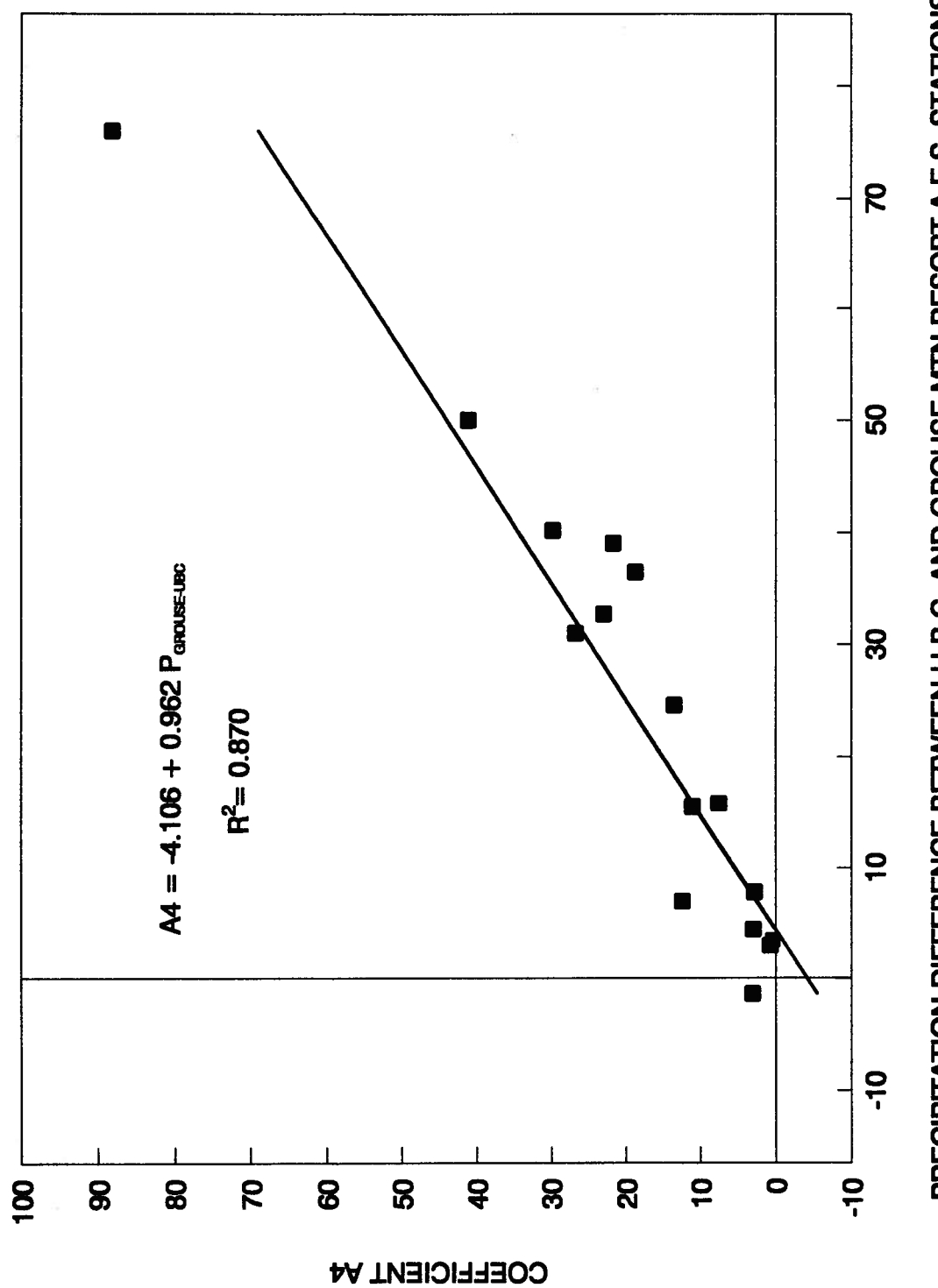


Fig. 7.15. Regression between the precipitation difference between U.B.C. and Grouse mountain resort and the coefficient A4

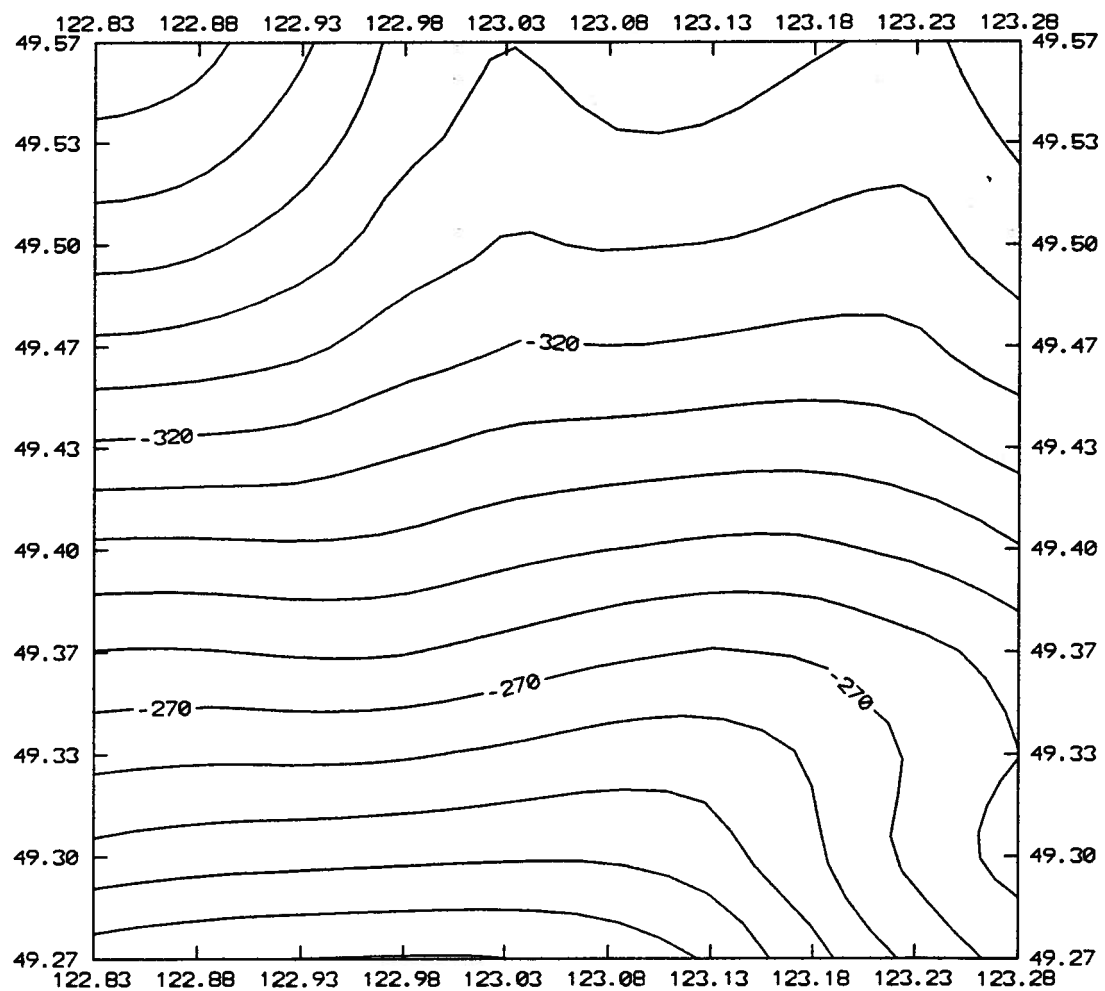


Fig. 7.16. Undispersed water flux (mm) for August 29, 1991 (12:00 UTC)

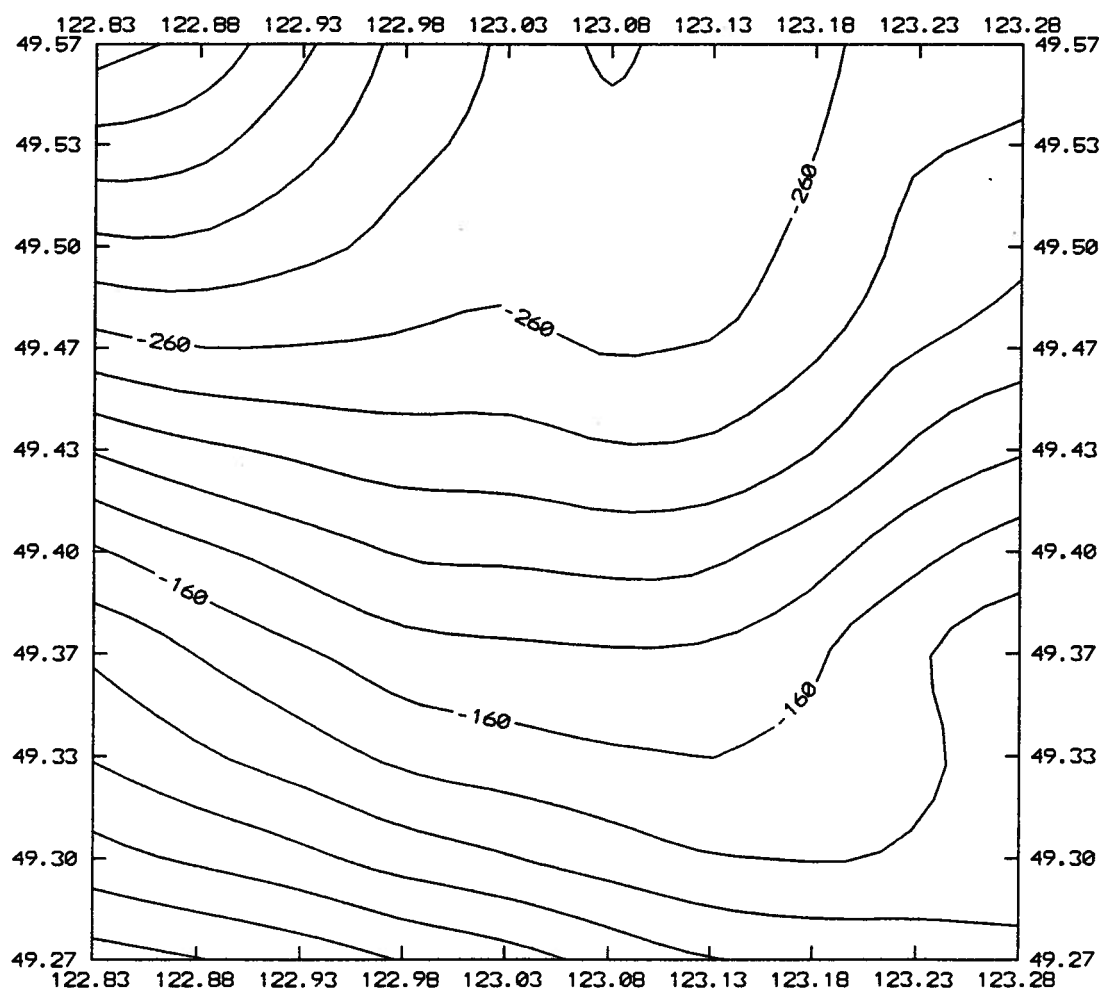


Fig. 7.17. Undisplaced water flux (mm) for August 30, 1991 (00:00 UTC)

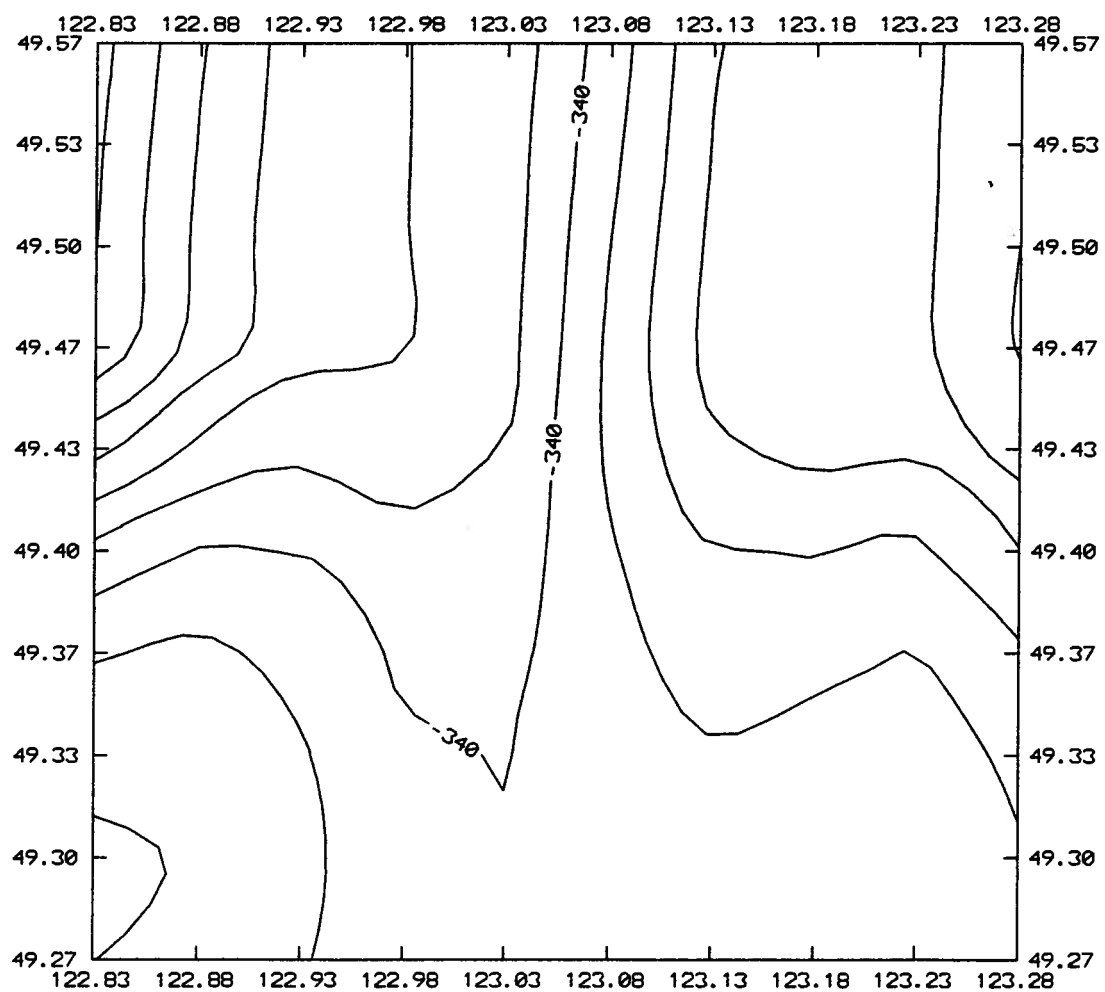


Fig. 7.18. Displaced water flux (mm) for August 29, 1991 (12:00 UTC)

Chapter 7. APPLICATION OF A METEOROLOGICAL MODEL

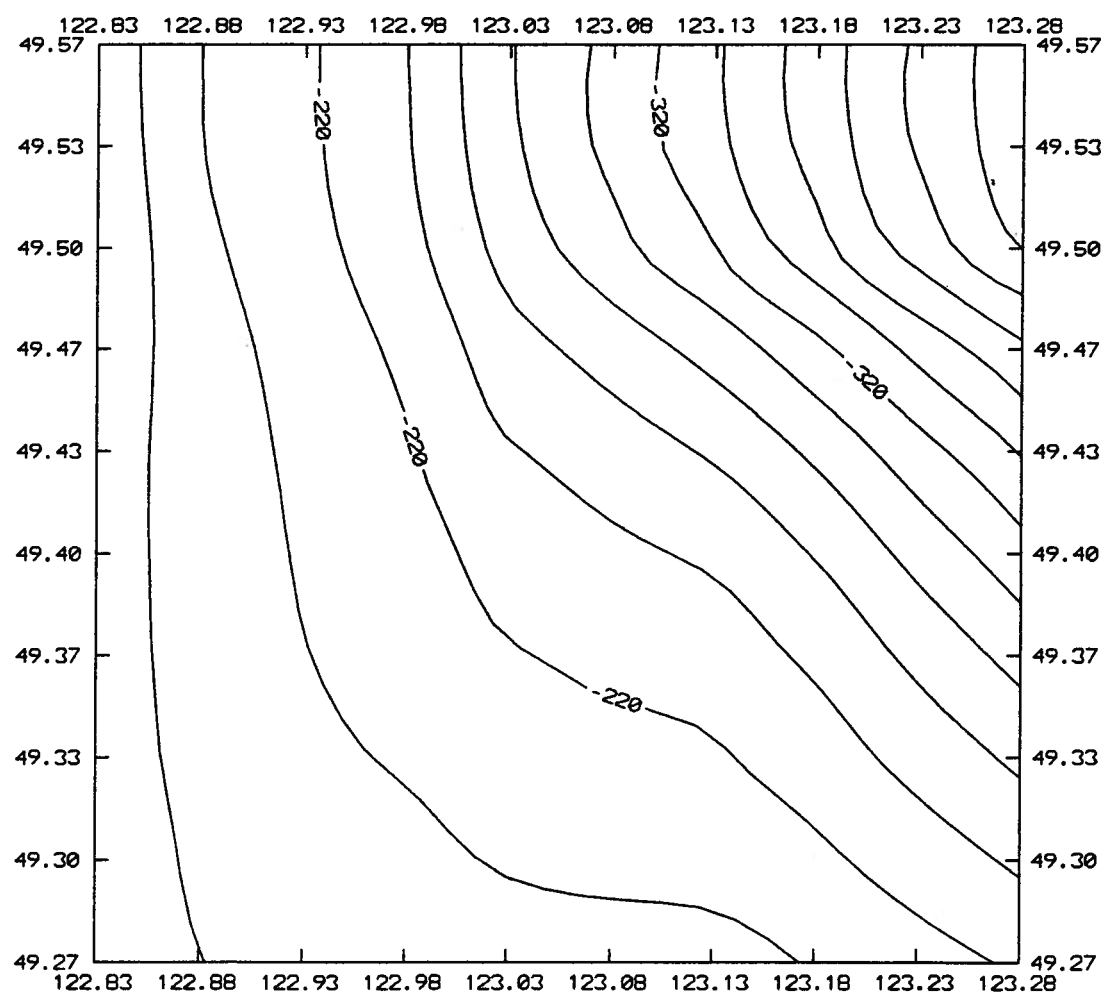


Fig. 7.19. Displaced water flux (mm) for August 30, 1991 (00:00 UTC)

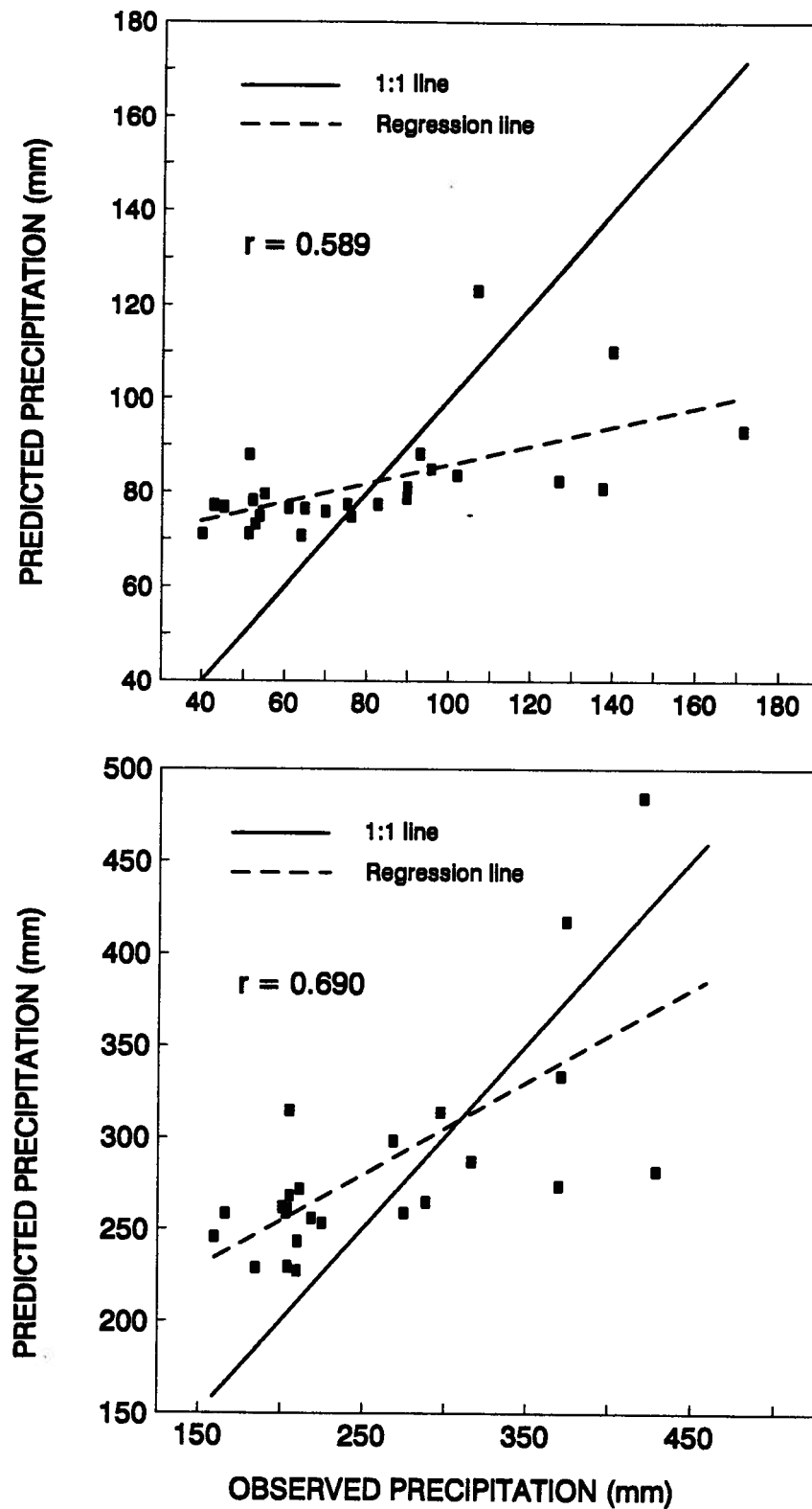


Fig. 7.20. Scattergraphs of observed and predicted precipitation for verification for a) August 29, 1991 and b) total storm period between August 26-30, 1991

CHAPTER 8

A PHYSICALLY BASED STOCHASTIC-DETERMINISTIC PROCEDURE FOR THE ESTIMATION OF FLOOD RUNOFF

8.1 Introduction

In the previous Chapters the distribution of precipitation in space and time has been analyzed with statistical methods. However, the estimation of the precipitation is, for hydrologists, just the first of many stages of the analysis of the watershed response and the estimation of the runoff. An important practical application of hydrology is the estimation of extreme flood events since the planning and design of water resources projects depend on the frequency and magnitude of peak discharges. In this Chapter the findings on precipitation distribution and previous results on watershed modeling will be integrated into a physically based procedure for the estimation of flood frequency from ungauged watersheds of coastal British Columbia.

The approaches used to analyze extreme events can be classified as purely statistical, simulation, and derived distribution techniques. The purely statistical methods attempt to fit extreme value probability distributions to measured peak flow records. The method is extremely data intensive and can be applied only to gauged watersheds. For ungauged watersheds two other statistical methodologies can be applied. The first methodology includes the regional techniques (Watt et al, 1989; Chapman et al, 1992) namely the Index Flood Method, the method of Direct Regression of Quantiles, and the method of Regression for Distribution Parameters. The second method is the combination of single site and regional data. This can be done either analytically (Watt et al, 1989) or numerically using the Bayes'

Chapter 8. A PHYSICALLY BASED STOCHASTIC-DETERMINISTIC PROCEDURE FOR THE ESTIMATION OF FLOOD RUNOFF

theorem (Russell, 1982). More details about the regional and combination techniques will be given in a later section of this Chapter.

Simulation techniques use rainfall-runoff models of varying degrees of complexity to generate synthetic discharges knowing the precipitation. For ungauged watersheds the rainfall-runoff models should be calibrated with regional data. Furthermore, the simulation can be either continuous when long time-series of rainfall are available or event-based when only certain large rainfall events are simulated. In the case of continuous simulation the peak discharges are ranked and the flood frequency is estimated. In the event rainfall-runoff simulation, it is assumed that the return period of a flow is the same as the return period of the rainfall producing the flow. This assumption is often criticized and has occasionally been studied (Reich, 1970; Larson and Reich, 1972; Dickinson et al, 1992). An event rainfall-runoff simulation has been applied in Chapter 5 for the estimation of the peak runoff from the Jamieson Creek watershed, where the assumptions underlying the application of the method have been discussed.

The derived distribution approaches are based on relatively simple rainfall-runoff models that are used to derive the cumulative distribution function of the flood runoff and subsequently obtain a relationship between discharge and recurrence interval. The method of derived distributions uses a model for the rainfall generation which is usually stochastic, an infiltration model and a watershed response model. The derivation of the Cumulative Distribution Function (CDF) of the peak flow can be found either analytically or numerically. In the next paragraphs detailed information about this relatively new method of the derived distributions will be presented.

Hebson and Wood (1982) and Diaz-Granados et al. (1984) derived analytically the CDF of the peak flow. These two methods use the same rainfall model of Eagleson (1972). According to this model the intensity and duration of the storm are assumed to be independent

Chapter 8. A PHYSICALLY BASED STOCHASTIC-DETERMINISTIC PROCEDURE FOR THE ESTIMATION OF FLOOD RUNOFF

random variables and their joint probability is exponential. Hebson and Wood (1982) used the geomorphologic instantaneous unit hydrograph developed by Rodriguez-Iturbe and Valdes (1979). Diaz-Granados et al. (1984) used the geomorphoclimatic instantaneous unit hydrograph proposed by Rodriguez-Iturbe et al. (1982). Both methods were applied to real watersheds and obtained reasonable results when compared to observed data.

Moughamian et al. (1987), however, applied the above two methods to the same watersheds and reported that the two methods perform poorly when compared to the Log-Pearson type III extreme value analysis of 40 years of data. Sensitivity analysis showed that the two models are extremely sensitive to small variations in the parameters of the rainfall generation model as well as to the variation of the infiltration parameters. Furthermore, Moughamian et al. (1987) showed that the models of Hebson and Wood (1982) and Diaz-Grenados et al (1984) performed poorly even when the infiltration parameter values were estimated by least squares optimization. Finally, Moughamian et al. (1987) concluded that "...the results indicate that fundamental qualitative improvements are needed before derived flood frequency methods can be applied with any confidence."

Another attempt to analytically estimate flood frequency using the derived distributions was performed by Cadavid et al. (1991). Their method incorporates the Eagleson's (1972) rainfall model, Philip's infiltration equation (Philip, 1960), and kinematic overland flow mechanics. They applied their method to two urban watersheds, where overland flow is the predominant runoff mechanism and found that their method estimated the high frequency flows (lower flows) better than the most extreme flows. They identified the inaccurate values of the rainfall model parameters as a possible reason for the poor performance of the method.

Haan and Edwards (1988) analytically derived the peak flow probability distribution using the Extreme Value type I (EVI) distribution to describe the rainfall probabilities and the

Chapter 8. A PHYSICALLY BASED STOCHASTIC-DETERMINISTIC PROCEDURE FOR THE ESTIMATION OF FLOOD RUNOFF

U.S. Soil Conservation Service (1972) Curve Number (CN) model to simulate the infiltration and watershed response. They tested the method on seven small agricultural watersheds and they found that when the U.S. Weather Bureau TP 40 (Hershfield, 1961) 2-year and 100-year 24-hour rainfall depths were used for the estimation of the EVI distribution, the method overestimated the peak flow. However, when the parameter values of the EVI distribution were estimated by observed rainfall data the results improved significantly.

The most recent attempt to analytically estimate the flood probability distribution with the derived distributions methodology is by Raines and Valdes (1993). Raines and Valdes (1993) used Eagleson's (1972) rainfall model, the CN model to estimate the infiltration and geomorphoclimatic instantaneous unit hydrograph to simulate the watershed response (Rodriguez-Iturbe et al, 1982). They applied their method to four small watersheds and they showed that their method is an improvement over the earlier methods of Hebson and Wood (1982) and Diaz-Grenados et al. (1984). However, they concluded that "the parameter estimation procedure needs to be improved to provide more reproducible parameters to yield more consistent results. However, the estimation of rainfall parameters is the most subjective task and seems to be responsible for major source of error..."

All attempts for the analytical derivation of the flood probability distribution showed that although the method gives a physical insight in the flood generation process, the assumptions needed to simplify the problem usually result in poor performance of the method. The oversimplifications are mainly done in the rainfall generation model since the temporal and spatial distribution of rainfall are not considered. To overcome these problems the flood probability distribution can be derived numerically. Consuegra et al. (1993) used regional data to derive storm patterns, the CN method to estimate the infiltration, and the geomorphologic unit hydrograph to describe the watershed response. They fitted the storage parameter of the CN model to an Antecedent Precipitation Index (API) and, considering the

Chapter 8. A PHYSICALLY BASED STOCHASTIC-DETERMINISTIC PROCEDURE FOR THE ESTIMATION OF FLOOD RUNOFF

probability of the rainfall and API, they simulated a large number of scenarios for the generation of the peak flow. Then they were able to calculate the frequency of a given flow by integrating the probability of the flow for all possible scenarios. They applied their method to a 51 km² Swiss mountainous watershed and compared the results with the results of a statistical analysis of simulated flows by a continuous deterministic model for a period of 20 years. The comparison showed that their method could reproduce the simulated flows. They made, however, no attempt to compare the estimated peak flows with observed data.

Another recent attempt to analytically derive the distribution of the flood flow was made by Muzik (1993). He used Monte Carlo simulation to generate the rainfall depth, duration, and time distribution and the parameters of the CN model were used to model the infiltration process. Muzik used a regionally derived dimensionless unit hydrograph to simulate the watershed response. This regional unit hydrograph was developed from an analysis of flows from 30 watersheds in the Alberta foothills (Muzik and Chang, 1993). Application of the method to two Alberta watersheds showed that the method can simulate the flood probability distribution fairly well.

The above results showed that the numerical derivation of the flood probability distribution gives better results than the analytical method. The reason for the poor performance of the analytical method is the poor representation of the rainfall characteristics as has already been mentioned. In the numerical method, the storm time and space distribution, the storm duration and the storm depth can be simulated, whereas the Eagleson model, used in most of the analytical studies, considers only the duration and the intensity of the storm and assumes that these two parameters are independent.

This Chapter presents an improved method for the estimation of design flood parameters for mountainous and rural ungauged watersheds. The proposed procedure uses the numerical derivation of the flood probability distribution approach and incorporates the

Chapter 8. A PHYSICALLY BASED STOCHASTIC-DETERMINISTIC PROCEDURE FOR THE ESTIMATION OF FLOOD RUNOFF

findings of the research on the rainfall spatial and temporal distribution as well as the response of the watersheds of the region. The procedure is based on a rainfall simulator, and the watershed response model developed in an earlier study (Loukas, 1991) and applied in Chapter 5. Firstly, the proposed procedure will be presented and its components, the rainfall simulator and the watershed response model, and their parameters will be discussed in detail. Then, the procedure will be applied to eight representative catchments located in coastal British Columbia with varying basin characteristics and compared with historical streamflow data. The sensitivity of the procedure to the variation of its parameters will be analyzed next and finally, the procedure will be compared with regional techniques and conclusions will be stated.

8.2 Procedure

This section describes the derived flood frequency procedure. As has been noted above, the procedure is based on a rainfall simulator, and a watershed model which simulates the infiltration process and the watershed response. The intention in developing this procedure is to provide hydrologists with a method for the estimation of flood frequency that requires very limited data. The problem of data limitation is especially evident in the mountainous area of coastal British Columbia and the coastal region of Pacific Northwest where the hydrologist usually has to estimate the flood frequency with very limited precipitation and runoff data. In the next paragraphs the rainfall and watershed response models will be discussed.

Chapter 8. A PHYSICALLY BASED STOCHASTIC-DETERMINISTIC PROCEDURE FOR THE ESTIMATION OF FLOOD RUNOFF

8.2.1 Rainfall model

A rain storm is characterized by its duration, depth, time and space distribution. It is important to incorporate all these characteristics in a simulation to have a reliable representation of the rainfall process. The minimum data for the rainfall depth can be found in the Rainfall Frequency Atlas for Canada (Hogg and Carr, 1985). This publication by Environment Canada contains maps for all the Canadian Provinces showing the isopleths of the mean and the standard deviation of the annual extreme rainfall of various durations (Fig. 8.1 and 8.2). These storm durations range from 5 minutes to 24 hours. The shorter storm durations are more important for the generation of floods in small, highly impermeable urban watersheds. Since this study is focused on the mountainous and rural watersheds the larger storm durations of 6, 12 and 24 hours should be more suitable. Simulation has been performed using the 6-hour, the 12-hour and the 24-hour extreme storms and the watershed model proposed in an earlier study (Loukas, 1991) and used in Chapter 5 for the simulation of the peak flow from the Jamieson Creek watershed. The simulation has been performed for the Carnation Creek watershed, which will be presented later in this Chapter, and the results show that the 6-hour and the 12-hour storm durations are adequate for the generation of the small return period and more frequent floods but they are incapable of producing the more extreme peak flows (Fig. 8.3). On the other hand, the 24-hour storm gave reasonably good simulation of the low and high frequency floods (Fig. 8.3). This result is in accordance with the flood producing mechanisms in the coastal British Columbia. The most severe floods in this region are generated by frontal storms that have durations that range around 24 hours as already discussed in Chapters 4 and 6. Furthermore, the choice of the 24-hour storm duration is a pragmatic one. Of the 269 precipitation stations located in the coastal British Columbia, 173 are storage gauges which are used to measure the daily precipitation. These stations have

Chapter 8. A PHYSICALLY BASED STOCHASTIC-DETERMINISTIC PROCEDURE FOR THE ESTIMATION OF FLOOD RUNOFF

longer records than the recording stations (Fig. 5.1), which implies more reliable frequency analysis, and hence, the use of the 24-hour design storm can expand the usable data both in space and time resulting in better estimation of flood runoff from ungauged watersheds. As a result the 24-hour storm was selected as the representative storm.

The storm depth of the 24-hour storm is assumed to follow the Extreme Value type I (EVI) distribution. This extreme value distribution has been extensively used for the analysis of rainfall in Canada (Watt et al., 1989). Furthermore this probability distribution is two parameter distribution and so it limits the number of the parameters required.

The mean and the standard deviation of the annual extreme 24-hour rainfall, the two parameters required for the estimation of the EVI, are estimated either from the records of existing data stations or from the Rainfall Frequency Atlas for Canada (Hogg and Carr, 1985) or from mean annual precipitation data because as has been shown in Chapter 5 this can be used as an index of the 24-hour rainfall of various return periods. Especially, the values derived from the Rainfall Frequency Atlas for Canada are representative only for the low level areas. The study of long-term and storm precipitation in Chapters 3 and 4 showed that in the coastal British Columbia the precipitation increases up to an elevation of about 400-800 m and then either decreases or levels off. This particular spatial distribution is evident even for the most extreme storms, as shown in Chapter 6.

The average increase of the rainfall over the watershed from the lower to the higher level areas was estimated to be about 1.5 times. This average increase will be used in the simulation procedure and no attempt has been made to describe the rainfall spatial distribution in more detail since the watershed response model used in this procedure is a lumped model and only the average rainfall over the watershed is needed. It is important to mention that judgment is necessary at this point to better estimate the rainfall over the watershed. Also, this average fudge factor of 1.5 seems to be representative for watersheds that have an

Chapter 8. A PHYSICALLY BASED STOCHASTIC-DETERMINISTIC PROCEDURE FOR THE ESTIMATION OF FLOOD RUNOFF

elevation range similar to that of the Seymour River and Capilano River watersheds which is 0-1800 m. For higher level basins a larger factor may be used and a value of 2 may be representative whereas for low level basin a lower value may be used. However, for the watersheds tested the average value of 1.5 seems to be reasonably representative because all have an elevation range similar to that of the two study watersheds.

In Chapter 5 another useful way to estimate the rainfall over the watershed has been proposed. It has been shown that the extreme 24-hour rainfall of various return periods is a certain percentage of the mean annual precipitation. Hence, if there are any long-term precipitation data in the region the hydrologist can easily estimate the rainfall depth parameters.

The time distribution is another important characteristic of a storm. A way of modeling the variability of rainfall within the 24-hour rainy periods is through the cumulative dimensionless hyetograph. Such an analysis has been presented in Chapter 5 where time probability curves have been proposed for the coastal British Columbia. For this cumulative dimensionless hyetograph, the rain at each of the twenty four time steps is the cumulative percentage of the total storm rainfall from the beginning of the storm, $R(t)$. A statistical model for the cumulative dimensionless hyetograph has to take into account, in addition to the random nature of $R(t)$, that its successive values are dependent and constrained to:

$$0 = R(0) \leq R(1) \leq \dots \leq R(24) = 100\% \quad (8.1)$$

It is proposed to model $R(0), \dots, R(24)$ as a random sample of size 24 from a continuous distribution. Since $R(t)$ ranges between zero and one or 100%, any continuous density distribution in this interval could be an appropriate choice. The triangular distribution is proposed because it is simple and fits our data reasonably well, as will be shown later. The

Chapter 8. A PHYSICALLY BASED STOCHASTIC-DETERMINISTIC PROCEDURE FOR THE ESTIMATION OF FLOOD RUNOFF

quantiles of 10%, 50% and 90% are necessary to define the density function of the triangular distribution. These quantiles, for the simulation of the 24-hour storm time distribution, can be estimated from the results of the analysis of the time distribution of the 24-hour design storm as presented in Chapter 5.

Under the assumption of an ordered sample from a continuous random sample ranging between zero and one, all the conditions stated above are fulfilled because dependence is also a property of order statistics and no extra parameters are necessary to fit correlations. A similar model has recently been developed and tested in Spain with very good results (Garcia-Guzman and Aranda-Oliver, 1993).

The proposed model is tested against observed data. As mentioned above the results of the previous analysis of the time distribution of the 24-hour storm for the coastal British Columbia are used in the proposed model to define the triangular distribution. The simulated time distribution probability curves are compared to the observed curves in Figure 8.4. The observed and simulated 10% cumulative probability curves are in good agreement whereas the simulated 50% and 90% curves deviate from the observed ones. Probably a more sophisticated model should be more suitable. However, application of the non-parametric Kolmogorov-Smyrnov test (Haan, 1978) showed that observed and simulated time probability curves are not significantly different at the 5% level. Hence, for each one of the 24 hourly time steps the rainfall is distributed according to the triangular probability distribution with increasing order.

The most important characteristics of a storm, precipitation amount, duration, and time distribution, have been incorporated in the procedure. This increases the reliability of the storm estimation and is an improvement over the popular Eagleson's method (1972), which considers only the average intensity of the storm for a given duration. The proposed method incorporates the time distribution of the storm and up to a certain degree the storm spatial

Chapter 8. A PHYSICALLY BASED STOCHASTIC-DETERMINISTIC PROCEDURE FOR THE ESTIMATION OF FLOOD RUNOFF

distribution. In the next paragraphs the other component of the procedure, the watershed response model will be considered.

8.2.2 Watershed response model

The watershed response model used in the procedure has been developed in a previous study (Loukas, 1991). The same model has been applied to the Jamieson Creek watershed for the estimation of peak flow in Chapter 5. This particular model is used because it requires very little information about the watershed and its parameters can be estimated from the geomorphology of the catchment. Furthermore, it was found that the model gives a good simulation of the watershed response. The model has been presented in Chapter 5 and reference will be made to that Chapter of the Thesis whenever necessary.

The above model has been applied to the Jamieson Creek for the study of its hydrologic behaviour and response (Loukas and Quick, 1993a). This application showed that the storage factor of the slow runoff (K_S) (Fig. 5.13) is constant and equal to 750 hours. This value is consistent with the value used in the simulation of runoff from watersheds of the region using the U.B.C. watershed model (Quick, 1993), which uses a similar linear routing technique.

Another result of the previous application of the model was that the infiltration abstractions (Fig. 5.13) were constant ($P_s=I_f$) for most of the events. The only exception was the rainfall-runoff events during intense summer storms over dry soil conditions. However, these events are not capable of producing the highest annual flows since large volume of rain water is infiltrated into the dry soil so, flow significantly delayed. Excluding these events, the parameter I_f was found to be normally distributed with a mean value of 1.37 mm/h and a coefficient of variation of 30%. Furthermore, it was also found that the storage factor of the

Chapter 8. A PHYSICALLY BASED STOCHASTIC-DETERMINISTIC PROCEDURE FOR THE ESTIMATION OF FLOOD RUNOFF

fast runoff is normally distributed around a mean value KF_m and a coefficient of variation of 30%.

From the Nash theory of linear routing, the storage factor, KF , is related to the time lag of the watershed as:

$$t_l = n \cdot KF \quad (8.2)$$

where n is the number of the linear reservoirs or the shape parameter of the Nash unit hydrograph.

Recent research (Rosso, 1984; Chutha and Dooge, 1990) has shown that the shape parameter, n , of the Nash model is a function only of the geomorphology of the watershed and it is related to Horton order ratios. Hence, for a given watershed the shape parameter remains the same for all types of storm events and is independent of the storm characteristics.

On the other hand, Rosso (1984) and Chuptha and Dooge (1990) showed that the scale parameter or storage factor, KF , is a function not only of the geomorphology of the watershed but also of the precipitation characteristics. So, the parameter KF changes from storm to storm. As a result and according to Equation 8.3 the time lag of the watershed will change as well. Furthermore, Sarino and Serrano (1990) and Yang et al (1993) showed that the most uncertain parameter of the Nash cascade of linear reservoirs model is the storage parameter KF . Sarino and Serrano (1990) expressed the uncertainty of the hydrograph only to the uncertainty of the storage factor KF using Stochastic Differential Equations. They also found that either the Normal or the Log-normal probability distributions can be fitted to the values of KF , but they used the Normal distribution in their study. As a secondary result of this work Sarino and Serrano (1990) found that the scale parameter, n , ranged around a mean value of

Chapter 8. A PHYSICALLY BASED STOCHASTIC-DETERMINISTIC PROCEDURE FOR THE ESTIMATION OF FLOOD RUNOFF

2.24. A similar result has been found in the analysis of the runoff from a Czechoslovakian watershed (Blazkova, 1992). For this reason a value of n equal to 2 was used.

Yang et al. (1993) used the Bootstrap sampling method to study the uncertainty of the hydrograph and they found that this uncertainty can be accounted for if only the uncertainty of the storage factor KF is considered. Also, from the simulations, they found that the KF parameter is normally distributed around a mean value.

From the above discussion, it is possible to assign certain probability distributions and values to the parameters of the model. In the application of the procedure, it is assumed that KS is constant and equal to 750 hours, the infiltration abstractions to slow runoff can be described only by a parameter If which is constant for a certain event but is normally distributed around a mean equal to 1.37 mm/h with a coefficient of variation equal to 30%. Furthermore, it is assumed that two reservoirs for the simulation of the fast runoff are adequate. This is in accordance with the previous application of the model (Loukas and Quick, 1993a) and the results of the other studies mentioned above. Finally, the storage factor of the fast runoff KF is assumed to follow the Normal distribution with a mean of KF_m and coefficient of variation of 30%.

The mean of the storage factor of fast runoff, KF_m , can be found using Equation 8.2. The time lag of the watershed, t_l , can be estimated by the modified Snyder method (Linsley et al, 1986),

$$t_l = C \cdot \left[\frac{L \cdot L_c}{S^{0.5}} \right]^m \quad (8.3)$$

where C and m are coefficients, L is the length of the main stream (km), L_c is the distance from the mouth of the watershed to the centroid of the watershed (usually is taken as $L_c=L/2$) (km), S is the mean slope of the main stream (m/m).

Chapter 8. A PHYSICALLY BASED STOCHASTIC-DETERMINISTIC PROCEDURE FOR THE ESTIMATION OF FLOOD RUNOFF

The value of the coefficient C depends on the average resistance to flow through the drainage network. The U.S. Bureau of Reclamation (Cudworth, 1989) recommends $C=18.2K_n$ and the U.S. Army Corps of Engineers (1990) uses $C=16.8K_n$ where K_n is the average resistance to flow through the drainage network. There is not a definite value of C that can be used. For this reason, the value of C is assumed equal to 0.42. According to U.S. Army Corps of Engineers relationship this value of C represents an average resistance over the watershed of about 0.025 which seems reasonable for rural and mountainous watersheds.

The value of the exponent, m, in Equation 8.3 generally has been assigned within the range of 0.30 to 0.38 (Sabol, 1993). The U.S. Army Corps of Engineers (1990) typically uses $m=0.38$. This value has been used in this study.

Equation 8.3 has been tested against an independent sample of 44 basins. These data were taken from a paper of Watt and Chow (1985). The data cover a wide range of basin sizes from 0.5 ha to 5,840 km². The basins are located across North America from the midwest United States to Quebec in Canada. The characteristics of the basins used in the analysis are shown in Table C1 in Appendix C.

The modified Snyder method, as given by Equation 8.3, is found to perform very well except for the largest basin (5,840 km²). This basin is flat and has a time lag of 40 hours. Figure 8.5 shows the scattergraph between the observed and estimated time lag for the remaining 43 basins. The regression line is very close to the line of perfect agreement (1:1 line) and their slopes and intercepts are not significantly different at the 5% level. The statistical parameters R² and Standard Error of Estimate (SEE) show that Equation 8.3 fits the data well and so it is used for the estimation of the parameter KF_m.

In summary the proposed method requires very little information about the hydrology of the watershed area. The only necessary input parameters of the procedure are the mean and the standard deviation of the extreme 24-hour storm depth over the watershed and the mean

Chapter 8. A PHYSICALLY BASED STOCHASTIC-DETERMINISTIC PROCEDURE FOR THE ESTIMATION OF FLOOD RUNOFF

value of the storage parameter KF which can be found by the Equations 8.2 and 8.3 and topographical data. Figure 8.6 shows the flow chart of the procedure. Monte Carlo simulation is used to generate the large number of parameters (5,000). At the end of every simulation a flood hydrograph is estimated and from that the hydrograph parameters are calculated. The 5,000 values of the flood hydrograph parameters are then ranked and plotted on probability paper as synthetic frequency curves.

The above procedure has been programmed in a 123-Lotus (Lotus Development Co., 1989) spreadsheet. A recently developed attached-in program, the @RISK (Palisade Co., 1991), is used to generate the large number of the parameters by using a random number generator.

The application of the procedure to coastal British Columbia watersheds will be presented next.

8.3 Application and Results

The proposed procedure has been applied to eight coastal British Columbia watersheds (Fig. 8.7). The watersheds used in the simulation had to meet the following criteria:

- they must be mainly rain-fed watersheds,
- they should have natural flow and no man-made storage impoundment should exist in their area,
- they should have negligible natural lake storage, and
- they should have long enough flow records to allow statistical analysis.

Table 8.1 shows the topographical characteristics of the eight watersheds used in the simulation. For these watersheds, the hourly peak discharge, the daily peak discharge and the flood volume are simulated. It is considered that these parameters of the flood hydrograph are

Chapter 8. A PHYSICALLY BASED STOCHASTIC-DETERMINISTIC PROCEDURE FOR THE ESTIMATION OF FLOOD RUNOFF

the most important and can be used for the estimation of other design parameters as river flood stage, reservoir level, etc.

The mean and the standard deviation of the annual extreme 24-hour rainfall are mainly estimated using the Rainfall Frequency Atlas for Canada (Hogg and Carr, 1985). Where rainfall gauges were located in the area of the watershed the estimates from the Atlas were compared with the actual data and, after engineering judgment, the best estimate of the rainfall was used. More specifically, for the Capilano River watershed the results of the analysis of the rainfall data from the adjacent Seymour River watershed are transposed and used. In the case of the Carnation Creek, the data from a station at the lower elevations were analyzed and then extrapolated according to observed long-term precipitation distribution at the higher elevations (Hetherington, personal communication). For Chapman Creek no actual data are available so the mean and the standard deviation of the 24-hour rainfall are estimated from the Rainfall Frequency Atlas for Canada and then are increased by a factor of 1.5 to represent the average rainfall over the watershed. The isopleths of both mean and standard deviation of the 24-hour extreme rainfall in the Rainfall Frequency Atlas for Canada are wide apart in the area around Zeballos River watershed because of the very limited number of stations. The nearest rainfall station to the watershed is the Tahsis station which is a storage gauge. In Chapter 5 it was shown that the 24-hour rainfall depth of various return periods is a certain percentage of the mean annual precipitation of the location. Hence, estimates of the rainfall parameters are made from the Tahsis station data which compare well with the estimates from the Rainfall Frequency Atlas for Canada. For the other four watersheds, the North Allouette River, the Oyster River, the Hirsch Creek and the San Juan River, the mean and the standard deviation of the 24-hour extreme annual rainfall are estimated using the Rainfall Frequency Atlas for Canada. Finally, the estimates are increased by 1.5 times to represent the average watershed rainfall and are used for the simulation.

Chapter 8. A PHYSICALLY BASED STOCHASTIC-DETERMINISTIC PROCEDURE FOR THE ESTIMATION OF FLOOD RUNOFF

The topographical characteristics of the watersheds necessary for the estimation of the mean value of the time lag from Equation 8.3, were measured from 1:50,000 scale topographic maps.

The observed flows were obtained in hourly time steps from the Water Survey of Canada, Environment Canada. From these data, the annual maximum hourly and daily peak flows and the flood volumes were estimated. The Extreme Value type I (Gumbel) and the Log-normal probability distributions are fitted to the observed data. These two probability distributions have been extensively used for flood flows in Canada, the United States and Great Britain (Watt et al, 1989).

Chapter 8. A PHYSICALLY BASED STOCHASTIC-DETERMINISTIC PROCEDURE FOR THE ESTIMATION OF FLOOD RUNOFF

Table 8.1. The characteristics of the eight watersheds used in the study.

Watershed	Location	Area (km ²)	Stream Length (km)	Stream Slope (m/m)	Land Use
Capilano	South Mainland	175	26.0	0.040	Forested
Carnation	West Vancouver Island	10.1	7.8	0.085	Forested
Chapman	South Mainland	64.5	20.7	0.052	Forested
Zeballos	West Vancouver Island	181	22.0	0.022	Forested
North Allouette	South Mainland	37.3	13.0	0.035	Forested
Oyster	East Vancouver Island	298	37.6	0.022	Forested
Hirsch	North Mainland	347	36.5	0.053	Forested
San Juan	South-West Vancouver Island	580	41.97	0.010	Forested

Figures 8.8-8.15 show the results of the simulation for the eight study watersheds. The results are, in general, very good except for some simulations of the flood volume. For the flood volume the simulated frequency curve deviates more than the frequency curves of the hourly and daily peak flow from the observed data and the fitted probability distributions. This does not necessarily mean that the method gives poor simulation of the flood volume

Chapter 8. A PHYSICALLY BASED STOCHASTIC-DETERMINISTIC PROCEDURE FOR THE ESTIMATION OF FLOOD RUNOFF

frequency because the estimation of the peak flood volume from the hydrograph record is highly judgmental and subjective. The overall performance of the method is very good as can be seen from these figures.

8.4 Sensitivity Analysis

To have a better understanding the effects of the parameter uncertainties, a sensitivity analysis was performed on the impact of the parameter variation on the resulting flood frequencies. To quantify the sensitivity of the flood frequency curves to parameters a sensitivity index, SI, similar to that of Raines and Valdes (1993) was defined as,

$$SI = \frac{Q_{pn} - Q_{po}}{Q_{po}} \times 100 \quad (8.4)$$

where Q_{po} and Q_{pn} are the old and new 100-year peak discharges, respectively. Furthermore, the sensitivity analysis results have been plotted on probability paper along with the observed data and the base simulation results. The sensitivity analysis is performed for the Carnation Creek watershed.

The sensitivity analysis is first performed for the uncertainty of the model parameter values (parameter value sensitivity). The effect of assuming that the parameters follow a different probability distribution from the one initially used is examined next (parameter form sensitivity).

For the parameter value sensitivity the mean annual rainfall depth and its standard deviation, the mean of storage parameter of the fast runoff (KF_m) and the rainfall abstractions (I_f) were increased and decreased by 10% and 20% of their values used in the simulation

Chapter 8. A PHYSICALLY BASED STOCHASTIC-DETERMINISTIC PROCEDURE FOR THE ESTIMATION OF FLOOD RUNOFF

above. Furthermore, the coefficients of variation of KF_m and I_f were varied from 20% to 40% instead of the assumed value of 30% used in the base simulation.

For the sensitivity of the method to the form of the parameters the storage factor KF and the rainfall abstractions I_f are assumed constant and equal to their mean value, instead of normally distributed around their mean values. The parameter KF is also assumed to vary according to a Log-normal probability distribution with the same mean and standard deviation.

The results show that the sensitivity of the procedure to the variation of the parameter values and form is usually small (Tables 8.2-8.8 and Figures 8.16-8.22). The simulated hourly and daily peak flow and the flood volume vary less than the model parameters. The most insensitive model parameter seems to be the rainfall abstractions, I_f , and the most sensitive parameter is the mean rainfall depth of the 24-hour annual extreme storm. Hourly peak flow is most sensitive to the variations of the mean annual extreme 24-hour rainfall and to the variation of the mean value of the storage parameter of the fast runoff, KF_m , and is affected by the form of KF , as well (Table 8.8). The daily peak flow and the flood volume are less sensitive to the parameter variations and their form. These two parameters of the flood hydrograph are the most sensitive to the variations of the mean annual 24-hour rainfall and its standard deviation (Fig. 8.16 and 8.17).

The above sensitivity of the procedure is significantly less than the sensitivity of the method of Raines and Valdes (1993) for which 13% variation of the Curve Number parameter resulted in a maximum 180% underestimation of the 100-year discharge.

Chapter 8. A PHYSICALLY BASED STOCHASTIC-DETERMINISTIC PROCEDURE FOR THE ESTIMATION OF FLOOD RUNOFF

Table 8.2. Sensitivity Index values (SI, %) for the mean annual extreme 24-hour rainfall (R_m) for Carnation Creek.

Hydrograph Parameter	$R_m - 20\%$	$R_m - 10\%$	$R_m + 10\%$	$R_m + 20\%$
Hourly Peak Flow	-14.2	-7.1	10.2	16.1
Daily Peak Flow	-12.9	-8.3	4.1	10.5
Flood Volume	-11.8	-8.0	5.2	11.6

Table 8.3. Sensitivity Index values (SI, %) for the standard deviation of the annual extreme 24-hour rainfall (σ_R) for Carnation Creek

Hydrograph Parameter	$\sigma_R - 20\%$	$\sigma_R - 10\%$	$\sigma_R + 10\%$	$\sigma_R + 20\%$
Hourly Peak Flow	-4.0	-2.5	4.0	4.0
Daily Peak Flow	-9.0	-6.0	1.1	5.6
Flood Volume	-10.2	-4.8	5.7	6.7

Chapter 8. A PHYSICALLY BASED STOCHASTIC-DETERMINISTIC PROCEDURE FOR THE ESTIMATION OF FLOOD RUNOFF

Table 8.4. Sensitivity Index values (SI, %) for the mean of storage factor (KF_m) for Carnation Creek

Hydrograph Parameter	$KF_m - 20\%$	$KF_m - 10\%$	$KF_m + 10\%$	$KF_m + 20\%$
Hourly Peak Flow	10.9	6.7	-7.4	-5.2
Daily Peak Flow	-4.3	-2.9	-2.5	-0.03
Flood Volume	0.03	-1.5	-1.9	-0.09

Table 8.5. Sensitivity Index values (SI, %) for the coefficient of variation of KF (CV_{KF}) for Carnation Creek

Hydrograph Parameter	$CV_{KF} = 20\%$	$CV_{KF} = 25\%$	$CV_{KF} = 35\%$	$CV_{KF} = 40\%$
Hourly Peak Flow	-7.8	-7.1	7.3	32.1
Daily Peak Flow	-0.8	-1.5	-0.7	-0.8
Flood Volume	-1.0	0.4	-0.3	-0.2

Chapter 8. A PHYSICALLY BASED STOCHASTIC-DETERMINISTIC PROCEDURE FOR THE ESTIMATION OF FLOOD RUNOFF

Table 8.6. Sensitivity Index values (SI, %) for the mean of infiltration abstractions parameter (I_f) for Carnation Creek

Hydrograph Parameter	$I_f - 20\%$	$I_f - 10\%$	$I_f + 10\%$	$I_f + 20\%$
Hourly Peak Flow	4.2	-2.5	0.2	-1.7
Daily Peak Flow	-1.7	-2.0	-0.9	-1.3
Flood Volume	-0.3	-2.4	-3.9	-2.0

Table 8.7. Sensitivity Index values (SI, %) for the coefficient of variation of I_f (CV_{I_f}) for Carnation Creek

Hydrograph Parameter	$CV_{I_f} = 20\%$	$CV_{I_f} = 25\%$	$CV_{I_f} = 35\%$	$CV_{I_f} = 40\%$
Hourly Peak Flow	-4.8	1.2	0.5	-1.4
Daily Peak Flow	-3.3	-5.4	-2.2	-2.3
Flood Volume	0.1	-3.2	0.6	-1.8

Chapter 8. A PHYSICALLY BASED STOCHASTIC-DETERMINISTIC PROCEDURE FOR THE ESTIMATION OF FLOOD RUNOFF

Table 8.8. Sensitivity Index values (SI, %) for the form of the parameters for Carnation Creek

Hydrograph Parameter	KF constant	I _f constant	KF and I _f constants	KF Log-normal
Hourly Peak Flow	-14.2	1.7	-13.5	-10.1
Daily Peak Flow	-2.6	-2.4	-1.3	-3.5
Flood Volume	-1.9	-2.3	-1.6	-3.0

8.5 Comparison with Regional Techniques

Regional techniques have been broadly used for the estimation of peak runoff in Canada (Watt et al., 1989), Great Britain (Hoskings et al., 1985) and elsewhere (Inna et al., 1993). In this section the proposed method will be compared with the most popular regional techniques. Furthermore, regional equations relating floods and physiographic and climatic variables, will be developed for the coastal British Columbia. Finally the results of the various methods will be compared with observed data from a real watershed.

8.5.1 Methods

The methods of flood frequency estimation that will be compared with the proposed procedure, are presented in this section. These methods fall into the categories of regional techniques, statistical methodologies as they have been classified in the Introduction section of this Chapter. The methods used are the Index Flood method, method of Direct Regression of Quantiles, method of Regression for Distribution Parameters, the B.C. Environment methodology (regional methods), and Russell's Bayesian methodology (statistical method). A brief description of each one of these methods will be presented next.

8.5.1.1 Index flood method

The Index Flood method involves the development of a regression equation expressing the "index" flood - usually the mean annual - in terms of independent physiographic and/or climatic variables. Then, the index flood is related to the floods of various return periods for the whole region. It implies that within a region, all frequency curves can be approximated with the same shape curve, or in other words the regional flood frequency curve is an average over the region. As a result a dimensionless regional frequency curve is determined.

When the flood frequency of an ungauged watershed is to be found the index flood is estimated by the regional equation, knowing the characteristics of the area and then it is multiplied with the dimensionless regional frequency curve to give the flood frequency curve for the ungauged watershed.

The physiographic factors used as predictor variables for the index flood are usually the basin area, basin surface storage by lakes and swamps, main channel slope, main channel

Chapter 8. A PHYSICALLY BASED STOCHASTIC-DETERMINISTIC PROCEDURE FOR THE ESTIMATION OF FLOOD RUNOFF

length, mean basin elevation, drainage density, basin shape factor, soil and cover type. The climate of the area is of major consideration and it can be represented as a predictor in the regression equation by the mean annual precipitation, mean annual extreme rainfall or other parameters.

The index flood method is very popular among hydrologists. In Canada for example there are twelve studies for the various regions of the country that use the index flood method (Watt et al., 1989).

8.5.1.2 Method of direct regression of quantiles (DRQ)

Within a hydrologically and climatically homogeneous region the floods of various return periods can be assumed that depend on physiographic and climatic characteristics of the individual watersheds. With the DRQ method not only the index flood is related to the characteristics of the watershed but also all the flood quantiles. This method is the second most popular regional technique in Canada (Watt et al., 1989).

8.5.1.3 Method of regression for distribution parameters (RDP)

The RDP method assumes that a standardized flood frequency distribution can be applied over a homogeneous region. It is hypothesized that the parameters of the flood frequency distribution for each individual watershed will change according to the physiographic characteristics. Usually a two parameter probability distribution is assumed to fit the floods of the region. The mean and the standard deviation or the coefficient of variation of the floods for the gauged watersheds are related through regression to physiographic and climatic

Chapter 8. A PHYSICALLY BASED STOCHASTIC-DETERMINISTIC PROCEDURE FOR THE ESTIMATION OF FLOOD RUNOFF

parameters. Then, using the predictor equations it is possible to estimate the probability distribution parameters and so, the flood frequency for an ungauged watershed.

8.5.1.4 B.C. Environment method

The British Columbia Ministry of Environment, Lands and Parks proposed a method for the flood frequency estimation based on the Index Flood method (Reksten, 1987). The whole province was separated into homogeneous subregions, and the mean annual daily flood, Q_{md} , of the watershed in these subregions was plotted against the basin area. No attempt was made to relate the mean annual flood to other physiographic and climatic parameters because these data were not available (Reksten, 1987).

The ratios of the floods for various return periods to the mean annual daily flood, C_t , were calculated for the gauged watersheds of the subregions. Knowing the area of an ungauged watershed the mean annual daily flood, Q_{md} , can be estimated from graphs and then is multiplied by the values of C_t to give an estimation of the daily flood for various recurrence intervals.

The B.C. Environment method also estimates the instantaneous flood. In each subregion of British Columbia the mean ratio of instantaneous to daily flood, I/D, is estimated for the gauged watersheds and plotted against the area of the watersheds. So, the I/D value for a given area multiplied by the daily flood gives the instantaneous flood of the same return period. The above method averages the response of each watershed, and so the I/D ratio, to only one value which is questionable since the response of the same watershed even for the largest floods can vary significantly.

8.5.1.5 Russell's Bayesian methodology

Russell (1982) proposed a procedure which involves the use of a compound distribution which is a weighted combination of individual probability distributions. The initial values are assigned to the parameters of the component distributions and their weights on the basis of subjective or regional estimates of the mean and the standard deviation of flood peaks. The weights of the component distribution can be updated using the Bayes' theorem in light of any additional measurements or even subjective information, such as the largest flood in a number of years or a flow which was not exceeded in a given number of years. The method requires the low, probable, and high estimates of the mean and the standard deviation. The low value is the one for which there is 90% probability that it will be exceeded, probable is the best estimate and high is the estimate with 90% probability that will not be exceeded.

The model developed based on the above procedure estimates the values of the mean and the standard deviation half way between the low and the probable estimates, and the probable and the high estimates. The marginal probabilities assigned for each one of these values are 0.169, 0.206, 0.250, 0.206, 0.169 for the low to the high estimates.

The compound distribution is made up of 25 component distributions each specified by a mean and a standard deviation and a weight or marginal probability. The probability of any particular combination of mean and standard deviation is obtained by multiplying the individual probabilities and normalizing to make the sum of all the weights equal to 1.0. The frequency of a given flood is simply the weighted sum of all the component distributions. If further information is available the weights or marginal probabilities of the component distributions are updated by using the Bayes' theorem.

8.5.2 Application

In this section the application of the various methods to a coastal British Columbia watershed will be presented. The study watershed is the Sarita River watershed on the west coast of Vancouver Island and its area is 162 km². The majority of the flow is generated as for the rest of the coastal watersheds by strong frontal systems formed above the North Pacific Ocean. The west coast of the Vancouver Island is actually in the path of these frontal systems. As a result, the highest values of the unit discharge (discharge over area) in British Columbia have been observed in that area (Environment Canada, 1982). The results of the various techniques are compared with twelve years of instantaneous peak flow data and thirty seven years of peak daily flow.

The various methods are applied to rainfed watersheds, because the majority of the floods recorded at about 74% of the coastal British Columbia streamflow stations are rainfall-induced floods (Melone, 1986). Also the rainfall-induced floods should be separated from the snowmelt-induced floods because snowmelt-induced floods have much flatter frequency curve than the rainfall-induced floods (Jarrett, 1987). Also, in watersheds where both rainfall and snowmelt induce peak flows the rainfall usually produces the larger flood for the most extreme conditions. The application of each one of the methods will be presented next.

Although the coastal British Columbia has distinct climatic and physiographic features from the rest of the province, a homogeneity test is applied to eliminate non-conforming stations. The homogeneity test described in Hydrology of Floods in Canada (Watt et al., 1989) has been applied. This homogeneity test has been proposed by Gumbel (1958), and is based on the assumption that the EVI (Gumbel) distribution fits all the regional data and involves the following procedural steps.

Chapter 8. A PHYSICALLY BASED STOCHASTIC-DETERMINISTIC PROCEDURE FOR THE ESTIMATION OF FLOOD RUNOFF

- The ratio of the 10-year flood to the mean annual flood is computed for all stations and averaged over the region.
- Each station mean annual flood is multiplied by the regional average ratio to yield a regionally estimated 10-year flood. The return period of this flood is then estimated from the stations frequency curve.
- This estimated return period of each station's flood is plotted against the station length of record. The 95% confidence bands approximated (Kite, 1978) by $y_e = 2.25 \pm \frac{6.33}{\sqrt{n}}$, where y_e is the reduced variable equal to $y_e = -\ln\left[-\ln\left(1 - \frac{1}{T_e}\right)\right]$, n is the years of station record and T_e is the estimated return period of the flood.

Twenty eight stations are used to test the homogeneity of the instantaneous peak flow records and thirty seven stations are used for the daily peak flows (Table 8.9). All stations used have passed the test as can be seen from Figures 8.23 and 8.24.

In this study, the Index Flood method and the DRQ and RDP methods are used to develop regional equations. The Index Flood method presented in this study, is different from the B.C. Environment methodology even though they both use the same technique. The Index Flood method of this study includes only the rainfall generated flows of rivers that have no man-made impoundment. Furthermore, the regional equations developed, use not only the basin area as a predictor but also other physiographic as well as climatic parameters. Also, separate equations have been developed for the instantaneous and daily peak flow.

The physiographic parameters used for the development of the regional equations are basin area, A, main stream length, L, main stream slope, S, mean basin elevation, E, and lake storage, S_t . These physiographic parameters were measured from maps of 1:50,000 scale. The mean annual 24-hour rainfall, R_m , is used for the representation of the climatic characteristics and it is estimated from the Rainfall Frequency Atlas for Canada (Hogg and Carr, 1985). The watershed characteristics can be seen in Table 8.9.

Chapter 8. A PHYSICALLY BASED STOCHASTIC-DETERMINISTIC PROCEDURE FOR THE ESTIMATION OF FLOOD RUNOFF

Table 8.9. Characteristics of coastal British Columbia watersheds used in the study.

Watershed	Area (km ²)	Stream Length (km)	Stream Slope (m/m)	Mean Elevation (m)	Lake Area (km ²)	Mean Annual 24-h Storm (mm)	Mean Annual Instant. Flow (m ³ /sec)	Mean Annual Daily Flow (m ³ /sec)
Capilano	172	25.97	0.040	782	-	120	317.8	224.1
Carnation	10.1	7.80	0.085	765	-	135	31.2	13.7
Chapman	64.5	20.65	0.044	680	-	78	80.0	47.5
Hirsch	347	36.47	0.020	820	-	80	350.5	207.1
N.Allouette	37.5	13.00	0.035	478	-	110	76.0	44.3
Oyster	298	37.60	0.022	701	-	60	180.3	145.1
San Juan	580	41.97	0.010	414	-	120	776.4	619.6
Sumas	149	32.91	0.005	414	-	55	25.93	23.3
Zeballos	181	22.00	0.022	725	-	190	552.1	338.5
Exchamiskis	370	47.98	0.005	785	-	80	491.2	354.9
Zymagotitz	376	35.77	0.016	772	-	70	272.8	178.2
Pallant	76.7	15.60	0.012	519	8.63	90	70.3	49.4
Canaka	47.7	15.16	0.045	732	-	90	77.8	41.2
Lit. Wedeena	188	23.33	0.022	855	-	70	192.0	127.1
Mackay	3.63	2.45	0.105	497	-	110	6.95	3.61
Murray	26.2	9.00	0.0095	60	-	55	22.8	10.8
Noons	2.59	5.47	0.131	409	-	85	7.46	4.02
Yakoun	477	62.82	0.0025	351	8.50	75	291.1	270.6
Ucona	185	28.50	0.052	834	4.88	160	394.01	233.9
Stawamus	40.4	13.53	0.032	785	-	140	63.51	37.7
Bings	15.5	5.40	0.045	359	-	60	-	6.93
Browns	86	24.25	0.039	626	-	70	-	77.2
Chemainus	355	55.90	0.0105	644	-	80	-	243.9
Englishman	324	34.40	0.019	828	-	80	-	228.8
Haslam	95.6	16.54	0.036	451	-	60	-	38.6
Koksilah	209	35.80	0.011	493	-	60	-	133.7
Tstable	113	25.30	0.037	681	-	70	-	143.2
Kokish	290	36.20	0.0185	799	-	80	130.9	96.9
Tsitika	360	37.15	0.018	792	-	80	412.0	249.6
Jacobs	12.2	3.50	0.025	483	-	75	17.83	10.96
Mashiter	38.9	12.20	0.084	872	-	100	43.7	22.1
Salloomt	161	22.10	0.030	883	-	100	90.6	62.2
Mamquam	334	30.95	0.036	911	-	110	223.3	152.01
Nusatsum	269	32.00	0.029	897	-	100	151.4	100.4
Kemano	583	30.55	0.018	912	-	85	502.1	323.1
Anderson	27.2	13.50	0.0075	47	-	60	-	10.4
Yorkson	5.96	10.6	0.003	35	-	60	-	2.88
Sarita	162	20.32	0.0175	442	-	190	357.7	313.7

Chapter 8. A PHYSICALLY BASED STOCHASTIC-DETERMINISTIC PROCEDURE FOR THE ESTIMATION OF FLOOD RUNOFF

The stepwise multiple regression analysis is conducted as linear analysis using log-transformed data. Only the statistically significant parameters at the 95% level were included in the equations. For all the equations only the basin area, A, the mean stream slope, S, and the mean annual extreme 24-hour storm depth, R_m , are included.

For the index flood method the mean instantaneous flood is given from the equation:

$$Q_{m,in} = 0.011 \cdot A^{0.823} \cdot S^{0.039} \cdot R_m^{1.226} \quad (8.5)$$

with $R^2=0.91$ and $See=9.01\%$.

The respective equation for the mean daily peak flood is:

$$Q_{m,d} = 0.014 \cdot A^{0.934} \cdot S^{0.089} \cdot R_m^{0.987} \quad (8.6)$$

with $R^2=0.91$ and $See=19.3\%$.

Data from all the stations are used to develop dimensionless regional frequency curves for instantaneous and daily peak flows. The ratio of the flows for various return periods to the mean annual flood Q_m are calculated using the EVI distribution. Figures 8.25 and 8.26 show the dimensionless frequency curves for the instantaneous and daily flows, respectively. Multiplication of the mean annual flood with the dimensionless frequency curves gives the frequency curves for a given watershed.

The regional equations for the floods of the 2, 5, 10, 25, 50, and 100 years recurrence interval are developed for the DQR method. The EVI distribution has been used. The equations for the instantaneous flow are shown in Table 8.10. The equations for the daily floods are shown in Table 8.11.

Chapter 8. A PHYSICALLY BASED STOCHASTIC-DETERMINISTIC PROCEDURE FOR THE ESTIMATION OF FLOOD RUNOFF

Table 8.10. Regional equations of instantaneous peak flow for the method of Direct Regression of Quantiles ($Q_T = K \cdot A^c \cdot S^d \cdot R_m^e$).

Return Period T (years)	K	c	d	e	R ²	See
100	0.0648	0.861	1.085	0.171	0.90	8.1
50	0.0518	0.856	1.106	0.157	0.90	8.1
25	0.0422	0.853	1.119	0.144	0.90	8.2
10	0.0252	0.841	1.178	0.110	0.90	8.4
5	0.0186	0.835	1.196	0.085	0.91	8.6
2	0.0097	0.819	1.237	0.084	0.90	9.2

Chapter 8. A PHYSICALLY BASED STOCHASTIC-DETERMINISTIC PROCEDURE FOR THE ESTIMATION OF FLOOD RUNOFF

Table 3. Regional equations of daily peak flow for the method of Direct Regression of Quantiles ($Q_T = K \cdot A^c \cdot S^d \cdot R_m^e$).

Return Period T (years)	K	c	d	e	R ²	See
100	0.0483	0.9442	0.9374	0.11214	0.93	8.3
50	0.0424	0.9439	0.9407	0.1085	0.93	8.4
25	0.0364	0.9434	0.9453	0.1035	0.93	8.5
10	0.0275	0.9369	0.9583	0.0847	0.93	8.7
5	0.0223	0.9413	0.9614	0.0844	0.93	8.8
2	0.0134	0.9378	0.9818	0.0574	0.94	9.4

For the RDP method the regional equations for the mean instantaneous and the mean daily flows are the Equations 8.5 and 8.6 developed for the Index Flood method. The EVI distribution was tested for the estimation of the flow. The equation for the standard deviation of the instantaneous peak flow is:

$$\sigma_{Q_m} = 0.0156 \cdot A^{0.872} \cdot S^{0.248} \cdot R_m^{1.059} \quad (8.7)$$

with $R^2=0.87$ and See=12.8%.

The equation of the standard deviation of the daily peak flow is:

Chapter 8. A PHYSICALLY BASED STOCHASTIC-DETERMINISTIC PROCEDURE FOR THE ESTIMATION OF FLOOD RUNOFF

$$\sigma_{Q_d} = 0.0113 \cdot A^{0.946} \cdot S^{0.146} \cdot R_m^{0.905} \quad (8.8)$$

with $R^2=0.91$ and $\text{See}=114.1\%$.

The B.C. Environment method (Reksten, 1986) has been applied to the various subregions in which the province of British Columbia has been divided. In this study, the results of the analysis for the Vancouver Island subregion (Chapman et al., 1992) are used.

Two watersheds located in the west coast of the Vancouver Island have similar characteristics to the Sarita River. The Zeballos River and the Ucona River watersheds have similar areas, 181 and 185 km², respectively. From the diagrams provided in the B.C. Environment report (Chapman et al., 1992) the mean annual flood is estimated as 300 m³/sec if the Zeballos River is used and 210 m³/sec if the Ucona River is considered.

The ratios of the floods of the various return periods to the mean annual flood are estimated from the results of the analysis of peak daily flows using Log-Pearson type III distribution. The values of the ratios, C_t , for the 2-, 5-, 10-, 25-, 50-, 100-year floods are 0.89, 1.28, 1.58, 1.95, 2.28, and 2.55, respectively if the Zeballos River is used and 0.81, 1.34, 1.75, 2.27, 2.65, 3.09, respectively if the Ucona River is used.

The daily floods of various return periods then can be estimated from the equation:

$$Q_{t,d} = Q_{m,d} \cdot C_t \quad (8.9)$$

The average ratio of the instantaneous to daily flow, I/D is estimated from the B.C. Environment report using the Zeballos River as 1.32 and 1.7 when the Ucona River is used. The instantaneous flood can then be found if the daily flow is multiplied by the I/D factor as:

$$Q_{t,in} = Q_{t,d} \cdot I / D \quad (8.10)$$

Chapter 8. A PHYSICALLY BASED STOCHASTIC-DETERMINISTIC PROCEDURE FOR THE ESTIMATION OF FLOOD RUNOFF

The results for Sarita River watershed are shown in Tables 8.12 and 8.13.

In order to use the Russell's Bayesian method, it is necessary to determine the low, probable, and high estimates of mean annual flow and its coefficient of variation. Only the watersheds located on the west coast of the Vancouver Island (Zeballos, Ucona, Carnation, San Juan in Table 8.9) are used. The low, probable, and high values of the mean annual flood and its coefficient of variation are estimated as the smaller, the average and the larger values of these parameters for the above four watersheds. The estimated low, probable, and high values of the mean annual instantaneous flow and its coefficient of variation are: $340 \text{ m}^3/\text{sec}$, $447 \text{ m}^3/\text{sec}$, $502 \text{ m}^3/\text{sec}$ and 0.3 , 0.5 , 0.7 , respectively. The estimates for the mean annual daily flood and its coefficient of variation are: $194 \text{ m}^3/\text{sec}$, $243 \text{ m}^3/\text{sec}$, $308 \text{ m}^3/\text{sec}$ and 0.35 , 0.50 , 0.65 , respectively. The results for the Sarita River watershed using the Bayesian methodology are shown into the Tables 8.12 and 8.13.

Finally, for the proposed stochastic-deterministic procedure, the mean and the standard deviation of the mean annual 24-hour storm are estimated from the Rainfall Frequency Atlas for Canada (Hogg and Carr, 1985). The mean of the storage factor of fast runoff, K_{Fm} , is found by using Equations 8.3 and 8.4 and topographical data. After estimating the parameter values and 5,000 Monte Carlo simulations the flood frequency of the hourly peak flow and daily peak flow are estimated for the Sarita River watershed (Tables 8.12 and 8.13). It should be noted that the other techniques estimate the frequency of the instantaneous peak flow whereas the proposed procedure estimates the frequency of the hourly peak flow. The hourly peak flow is similar to instantaneous peak flow for large and medium size basins but for small catchments it could be substantially different from instantaneous. Examination of the ratio of hourly to instantaneous peak flow for the Sarita River watershed (162 km^2), showed that this ratio is close to one so that the hourly peak flow of the proposed procedure is compared with

Chapter 8. A PHYSICALLY BASED STOCHASTIC-DETERMINISTIC PROCEDURE FOR THE ESTIMATION OF FLOOD RUNOFF

the observed and estimated instantaneous peak flows for the Sarita River watershed in Table 8.12 and Figure 8.27.

8.5.3 Results

The results of the various techniques are compared in Tables 8.12 and 8.13 and are shown in Figures 8.27 and 8.28. The comparison shows that for the instantaneous peak flow all the techniques give flows larger than the observed flows. This incompatibility is the result of the small number of years of record. It should be mentioned that the largest daily peak flow of 37 years of record is 677 m³/sec and the largest instantaneous peak flow of 12 years of record is only 486 m³/sec. Examination of the data of the Sarita River showed that the ratio of the instantaneous peak flow to the daily peak flow ranges between 1.11 to 1.55 with a mean of 1.35. Applying these ratios to the largest daily flow in record indicates that the instantaneous peak flow of the same day should have been between 750 to 1050 m³/sec. If these flows were extrapolated then the 100-year instantaneous flood should range between 1000 and 1300 m³/sec. As can be seen from Table 8.12 and Figure 8.27, only three techniques have estimated flows that are close to these values. These techniques are the proposed stochastic-deterministic procedure presented earlier, the Bayesian method, and the B.C. Environment method. In Figure 8.27 and Table 8.12 the estimate using the upper 95% confidence level of the regional dimensionless frequency curve (Fig. 8.25) is also presented. This estimate is within the above range of 1000 to 1300 m³/sec for the 100-year flood. This is not surprising since the west coast of Vancouver Island receives large amounts of rain from the Pacific Ocean storms and so the watersheds located in that area exhibit a response that is higher than the average response of the coastal British Columbia watersheds.

Chapter 8. A PHYSICALLY BASED STOCHASTIC-DETERMINISTIC PROCEDURE FOR THE ESTIMATION OF FLOOD RUNOFF

The estimates of the 100-year flood using the other regional techniques are well below the range of 1000 to 1300 m³/sec. This is mainly because the regional equations developed in this study average the watershed response over the coastal region of British Columbia whereas as it has been mentioned above the watersheds located on the west coast of the Vancouver Island respond at a much higher rate than the rest of the coastal watersheds.

The results of the analysis of the peak daily flow are compared with the estimates derived from the fitted Extreme Value type I distribution to the observed data in Table 8.13 and Figure 8.28. As it can be seen the estimates of the proposed procedure, the Bayesian method and the B.C. Environment methodology are closer to the estimates of the fitted EVI distribution. The estimates of the Index Flood method, RDP and DRQ methods are below the observed values. The discussion presented above for the peak instantaneous flow is also valid for the daily peak flow as well.

Chapter 8. A PHYSICALLY BASED STOCHASTIC-DETERMINISTIC PROCEDURE FOR THE ESTIMATION OF FLOOD RUNOFF

Table 8.12. Comparison of estimated instantaneous peak flow (m^3/sec) for various return periods using various methods for Sarita River.

	Return Period (years)					
	2	5	10	25	50	100
Stochastic-Deterministic Simulation	470	646	773	946	1100	1256
Bayesian Method	497	688	816	945	1095	1213
B.C. Environment Method-Ucona	289	478	626	811	947	1103
B.C. Environment Method-Zeballos	352	523	626	811	947	1103
Index Flood Method	369	505	596	710	795	880
Index Flood Method - 95%	381	593	755	960	1110	1259
RDP	374	484	557	650	718	786
DRQ	372	495	564	641	708	769

Chapter 8. A PHYSICALLY BASED STOCHASTIC-DETERMINISTIC PROCEDURE FOR THE ESTIMATION OF FLOOD RUNOFF

Table 8.13. Comparison of estimated daily peak flow (m^3/sec) for various return periods using various methods with the fitted Extreme Value type I distribution to the observed flows for Sarita River.

	Return Period (years)					
	2	5	10	25	50	100
Fitted EVI	275	399	481	584	662	738
Stochastic-Deterministic Simulation	315	424	496	591	679	773
Bayesian Method	282	391	463	551	622	690
B.C. Environment Method-Ucona	170	281	368	477	557	649
B.C. Environment Method-Zeballos	267	396	474	585	684	765
Index Flood Method	194	271	322	387	435	483
Index Flood Method - 95%	199	294	371	466	533	604
RDP	191	270	321	387	435	483
DRQ	216	296	350	415	463	512

Chapter 8. A PHYSICALLY BASED STOCHASTIC-DETERMINISTIC PROCEDURE FOR THE ESTIMATION OF FLOOD RUNOFF

8.6 Summary

Flood frequency curves for ungauged watersheds are very difficult to obtain. This is especially important for coastal British Columbia where both rainfall and streamflow data are limited both in space and time. The physically based stochastic-deterministic procedure proposed in this study provides an alternative to the more traditional methods. The procedure uses the derived distributions method and incorporates the findings of the research on rainfall and watershed response in the region of coastal British Columbia. The input data requirements are minimum and can be derived from a topographical map and the Rainfall Frequency Atlas for Canada.

The application of the procedure to eight coastal British Columbia watersheds and comparison with the observed data and the fitted EVI and Log-normal probability distributions showed that the method is reliable and efficient. Especially, the estimation of the frequency of instantaneous and daily peak flow is very good, whereas the estimation of the frequency of flood runoff volume is not as good as the estimation of the frequency of the other two flood hydrograph parameters. The subjective derivation of the peak flood volume from the hydrograph record is a probable reason for the poor estimation of its frequency.

Sensitivity analysis also showed that the proposed procedure is not very sensitive to the uncertainty in the values and form of the model parameters. The analysis showed that the method is the most sensitive to the variation of the mean annual extreme 24-hour rainfall and less or not sensitive at all to the variation of the other parameters.

The proposed procedure was applied to a real watershed, the Sarita River watershed, along with the most popular regional techniques that were either developed in the course of this study or proposed in the literature. The frequency of the hourly and daily peak flows are compared. The results show that the proposed procedure, the B.C. Environment regional

Chapter 8. A PHYSICALLY BASED STOCHASTIC-DETERMINISTIC PROCEDURE FOR THE ESTIMATION OF FLOOD RUNOFF

methodology (Reksten, 1987), and the Bayesian methodology (Russell, 1982), give good results which fit the observed flow well. It should be mentioned that the other regional techniques, the Index Flood, RDP, and DRQ methods, failed to give good results mainly because they have been developed for the whole coastal British Columbia but they were applied to a watershed on the west coast of Vancouver Island. The response of the watersheds located in that area is much higher than the response of the other coastal British Columbia watersheds because they receive large amounts of rainfall from the highly moist frontal storms. Hence, for this region, probably the equations developed for the extreme conditions should be applied. This has been shown with the use of the 95% confidence limit of the dimensionless frequency curve for the Index Flood method. It would be helpful if regional equations could be developed for the west coast of the Vancouver Island but this is not feasible because there are only four watersheds in the area with long enough records.

In summary, on the basis of the comparison made in this Chapter, it has been shown that the proposed procedure can be applied to ungauged watersheds in coastal British Columbia with very limited data and give results that either are better or comparable to other regional procedures. The value of this procedure is that it utilizes the results on precipitation distribution and incorporates these results along with previous results on watershed modeling for the estimation of flood frequency so that it integrates the findings of the Thesis.

Chapter 8. A PHYSICALLY BASED STOCHASTIC-DETERMINISTIC PROCEDURE FOR THE ESTIMATION OF FLOOD RUNOFF

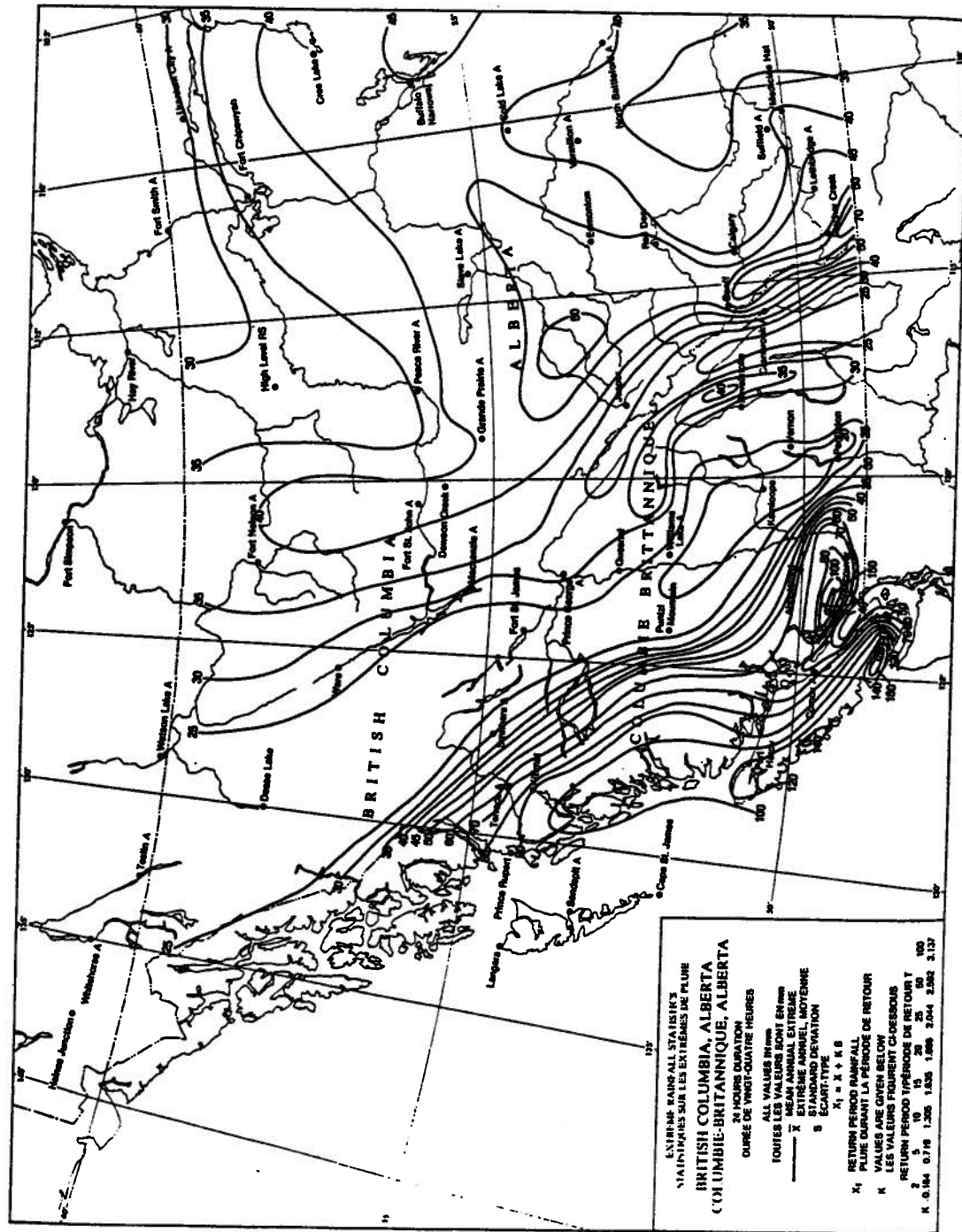


**Fig. 8.1. Isopleths of the mean annual 24-hour rainfall in British Columbia.
(After Rainfall Frequency Atlas for Canada, Hogg and Carr, 1985)**

Chapter 8. A PHYSICALLY BASED STOCHASTIC-DETERMINISTIC PROCEDURE FOR THE ESTIMATION OF FLOOD RUNOFF

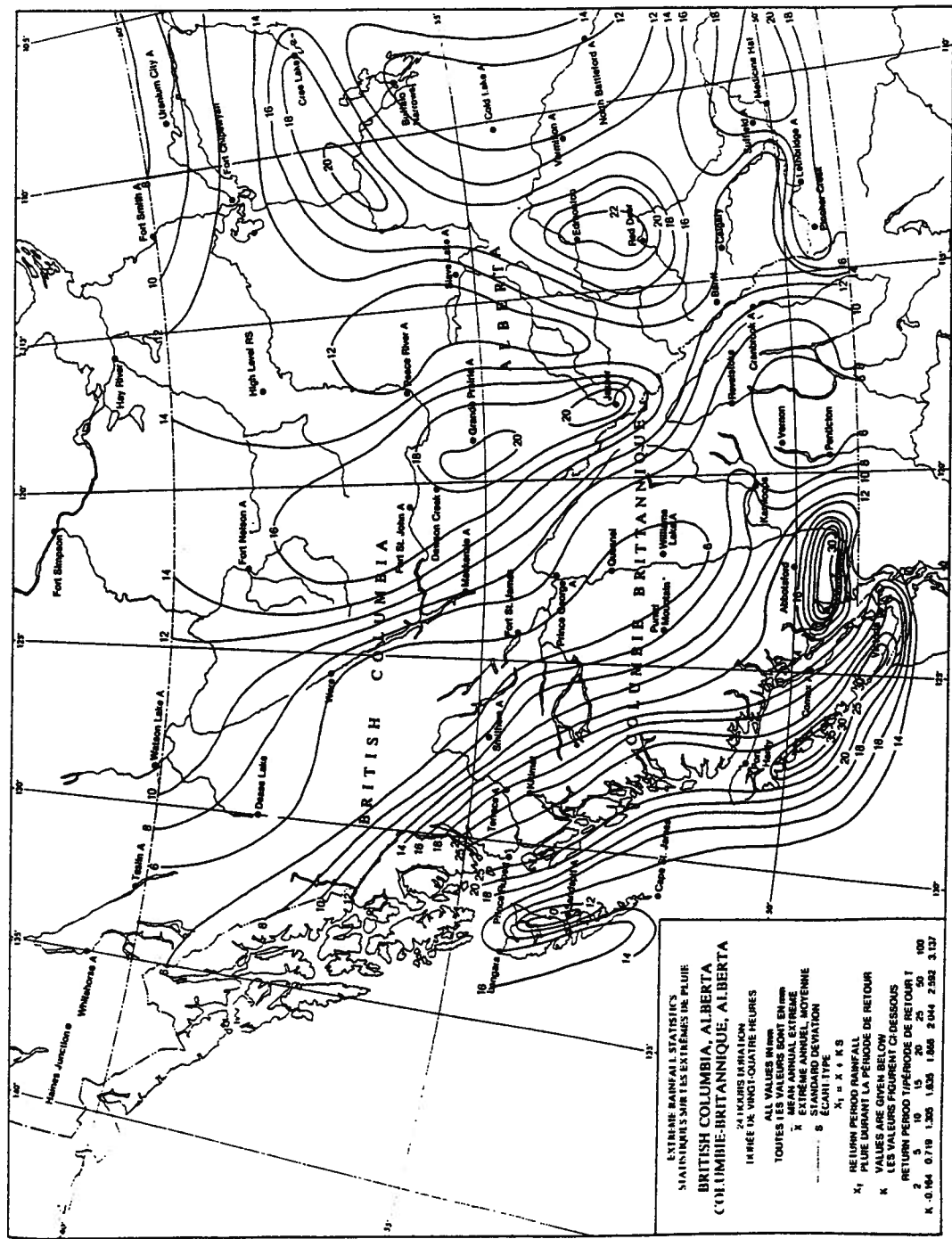


Fig. 8.2. Isopleths of the standard deviation of the mean annual 24-hour rainfall in British Columbia.
 (After Rainfall Frequency Atlas for Canada, Hogg and Carr, 1985)

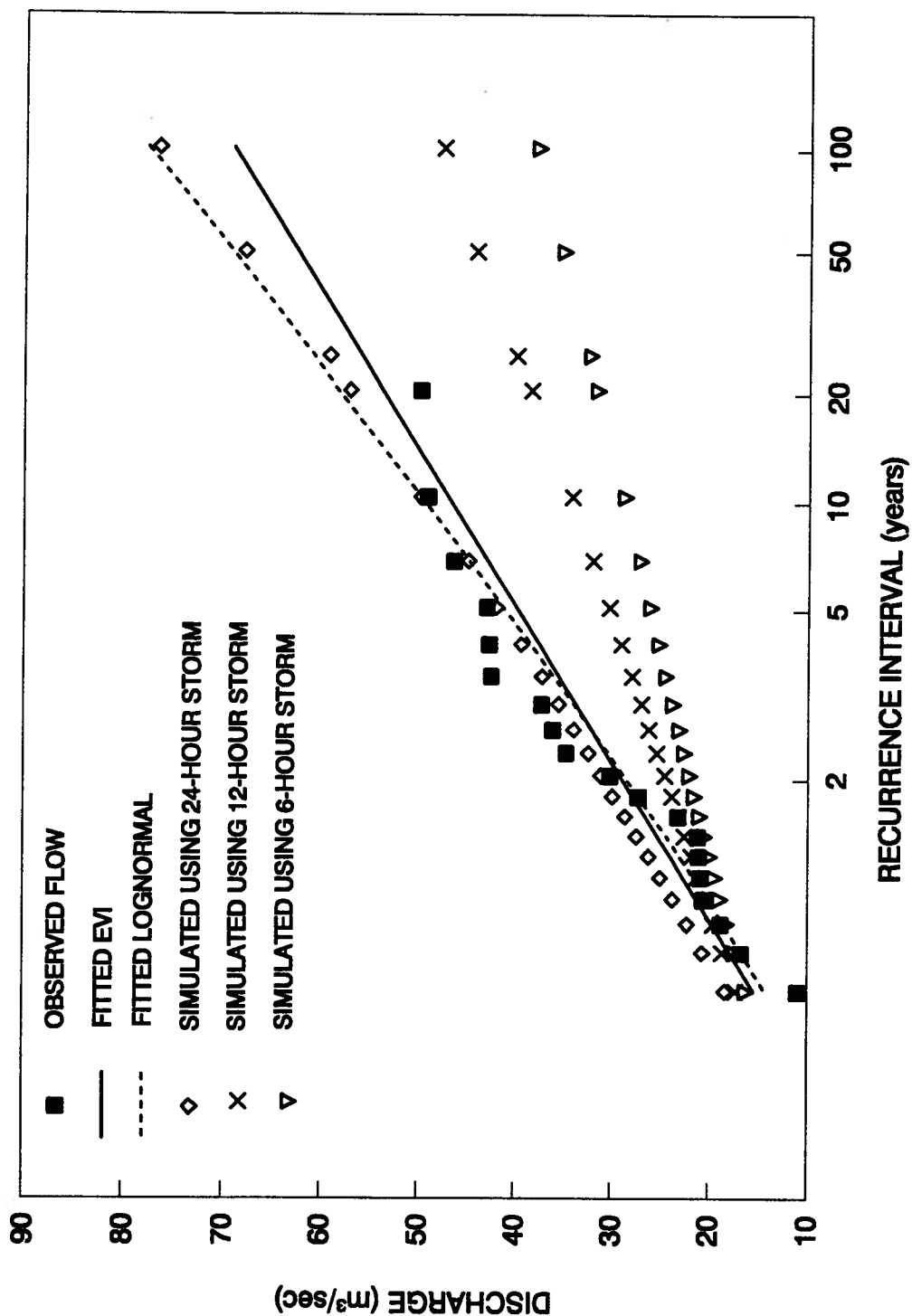


Fig. 8.3 Comparison of the frequency of the observed and simulated hourly peak flow using the 24-hour, the 12-hour and the 6-hour storms for the Carnation Creek watershed

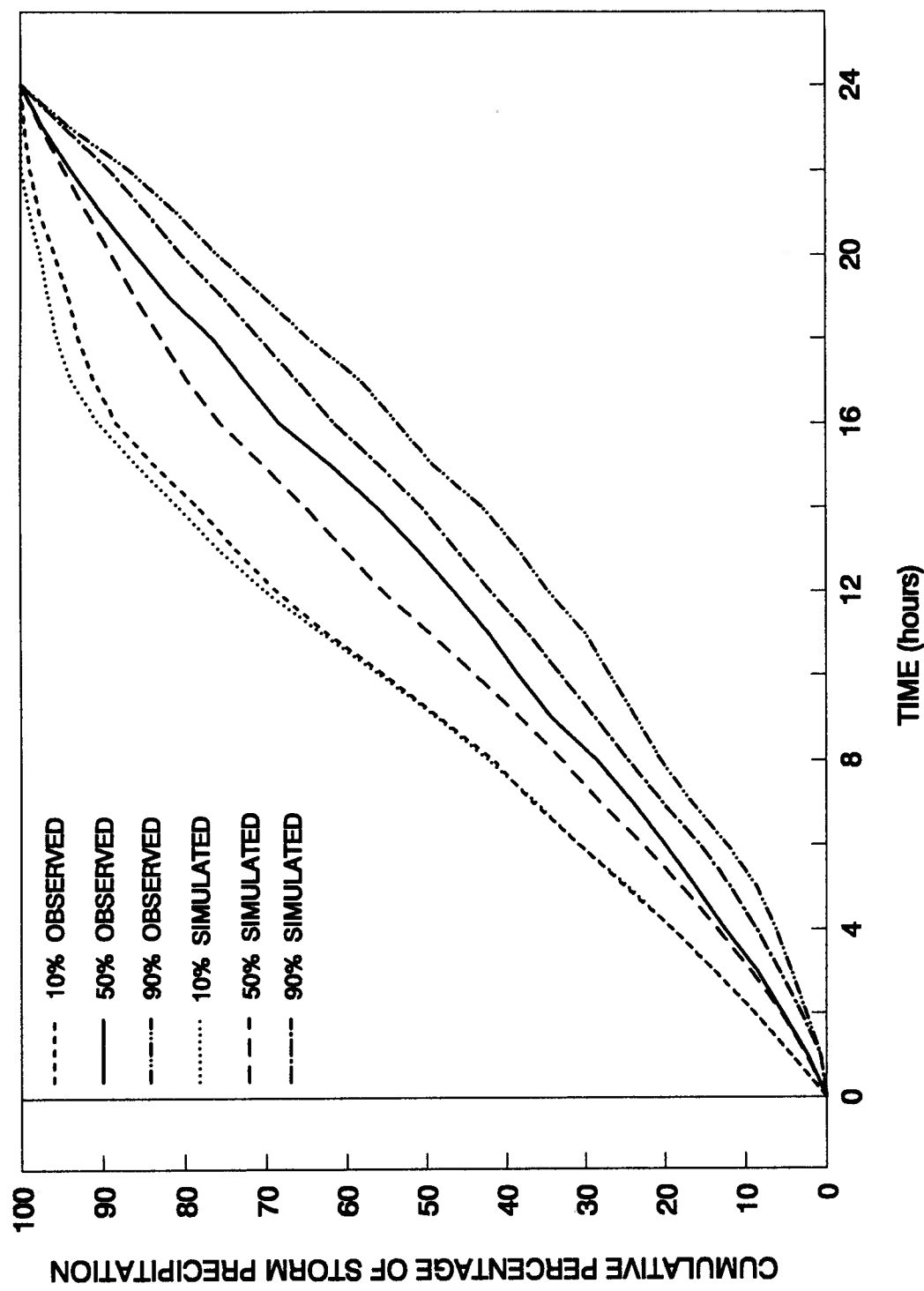


Fig. 8.4. Comparison of the observed and simulated cumulative time probability distributions for the coastal British Columbia.

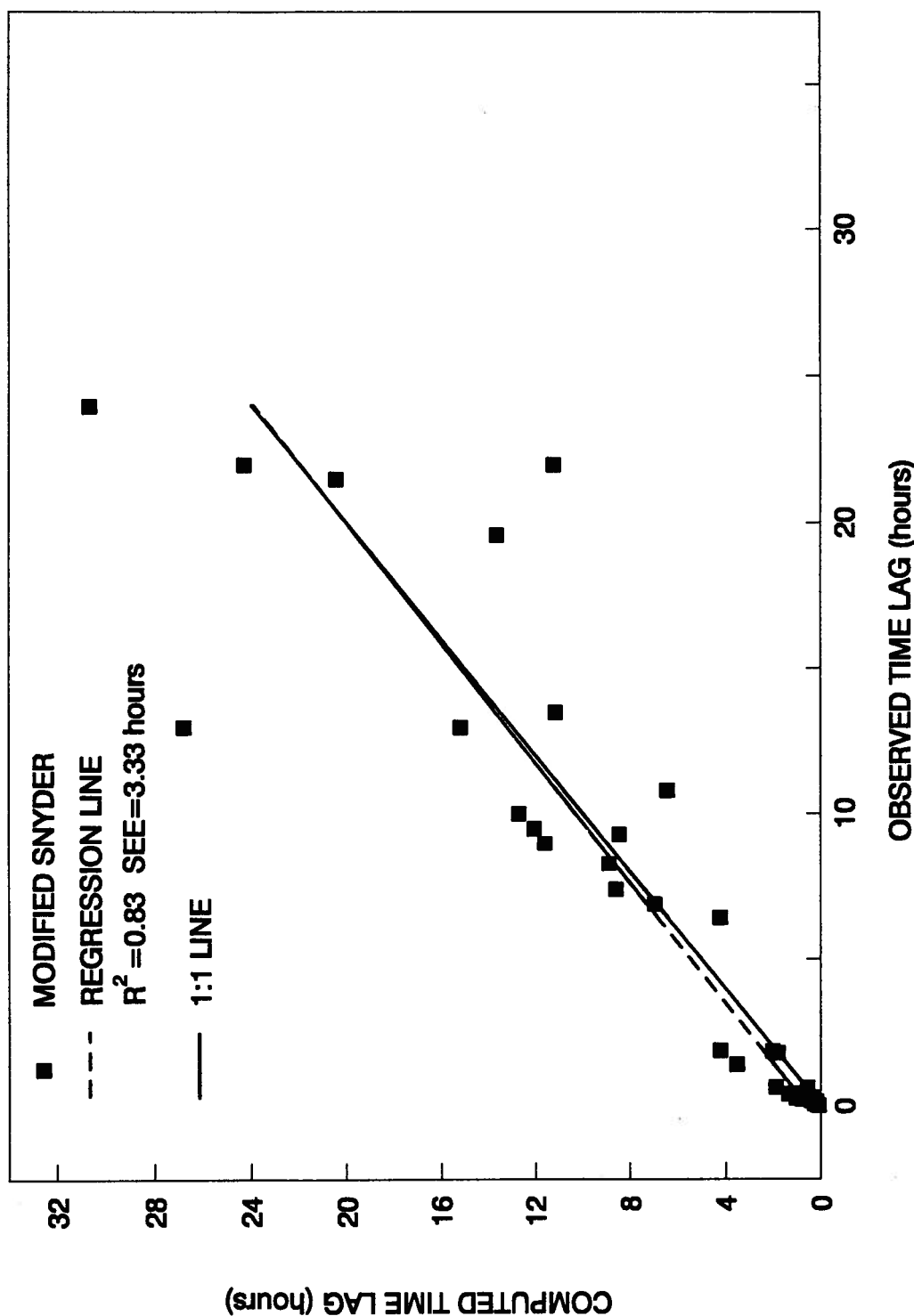


Fig. 8.5. Scattergraph between computed and observed time lag for 43 North America basins.
(Data after Watt and Chow, 1985)

Chapter 8. A PHYSICALLY BASED STOCHASTIC-DETERMINISTIC PROCEDURE FOR THE ESTIMATION OF FLOOD RUNOFF

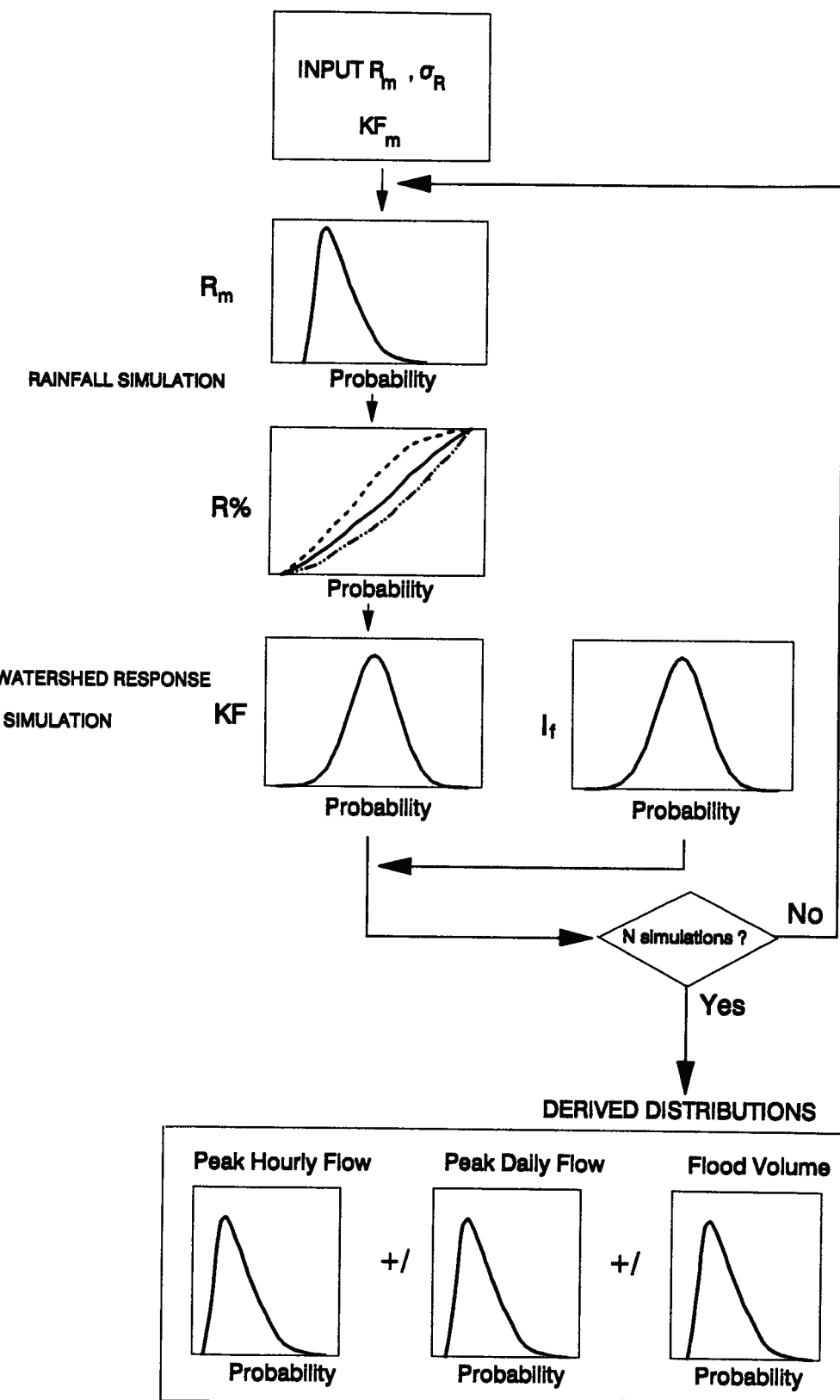


Fig. 8.6. Flow chart of the Monte Carlo simulation.

Chapter 8. A PHYSICALLY BASED STOCHASTIC-DETERMINISTIC PROCEDURE FOR THE ESTIMATION OF FLOOD RUNOFF

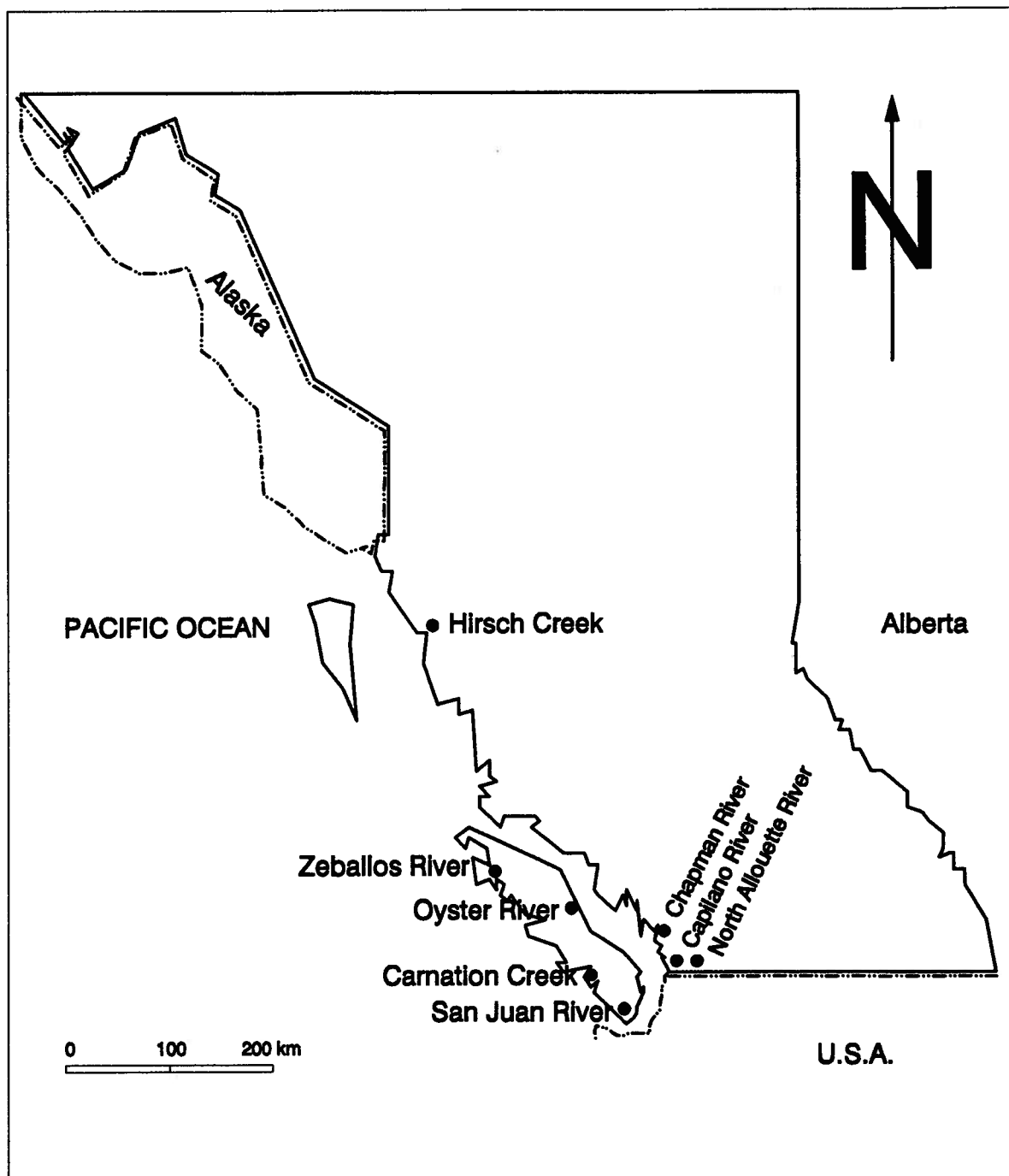


Fig. 8.7. Map showing the location of the eight coastal British Columbia where the proposed procedure has been applied.

Chapter 8. A PHYSICALLY BASED STOCHASTIC-DETERMINISTIC PROCEDURE FOR THE ESTIMATION OF FLOOD RUNOFF

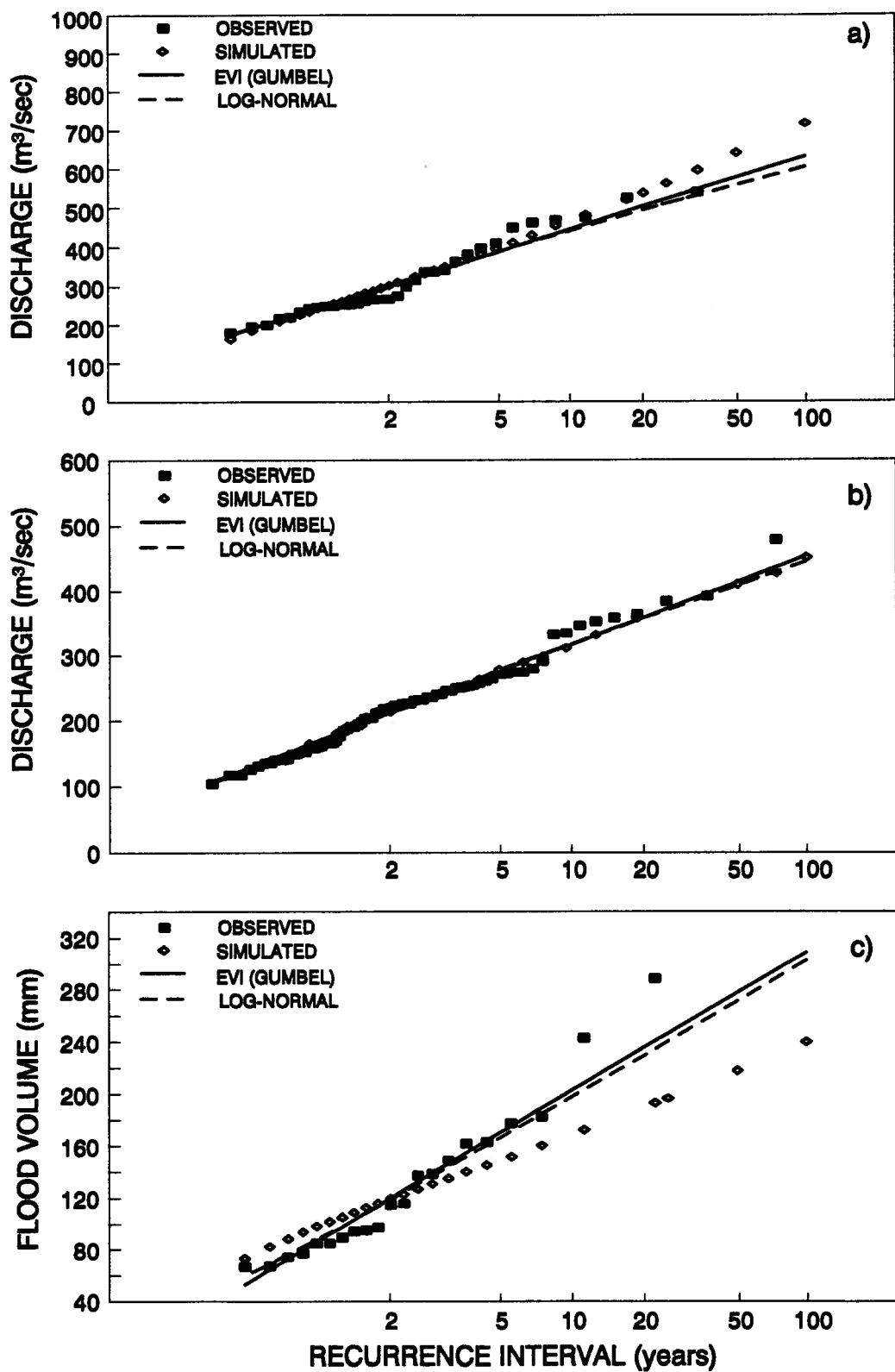


Fig. 8.8. Flood frequency curves for Capilano River watershed.
a) hourly flows b) daily flows and c) flood volume.

Chapter 8. A PHYSICALLY BASED STOCHASTIC-DETERMINISTIC PROCEDURE FOR THE ESTIMATION OF FLOOD RUNOFF

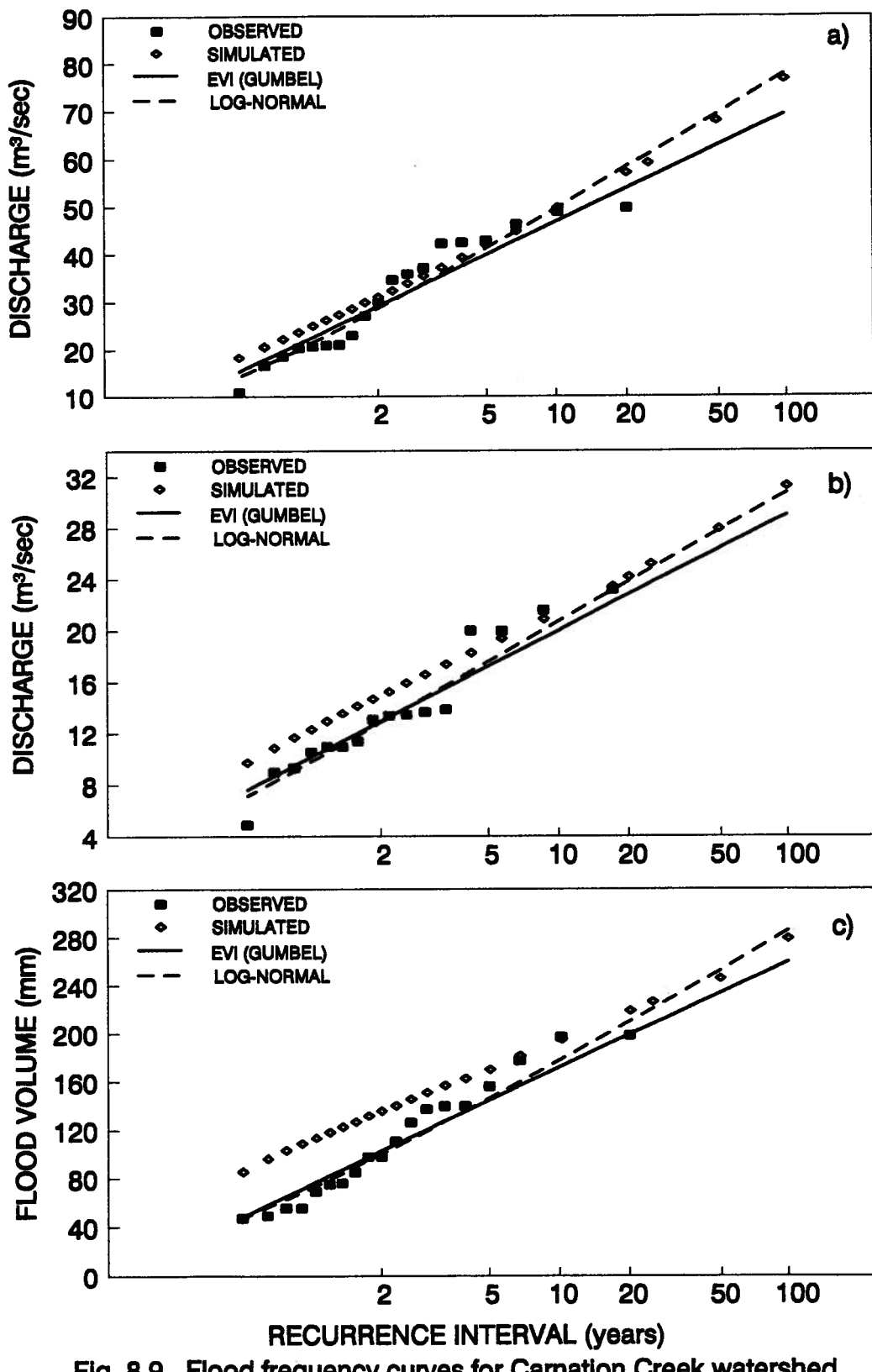


Fig. 8.9. Flood frequency curves for Carnation Creek watershed
a) hourly flows b) daily flows and c) flood volume.

Chapter 8. A PHYSICALLY BASED STOCHASTIC-DETERMINISTIC PROCEDURE FOR THE ESTIMATION OF FLOOD RUNOFF

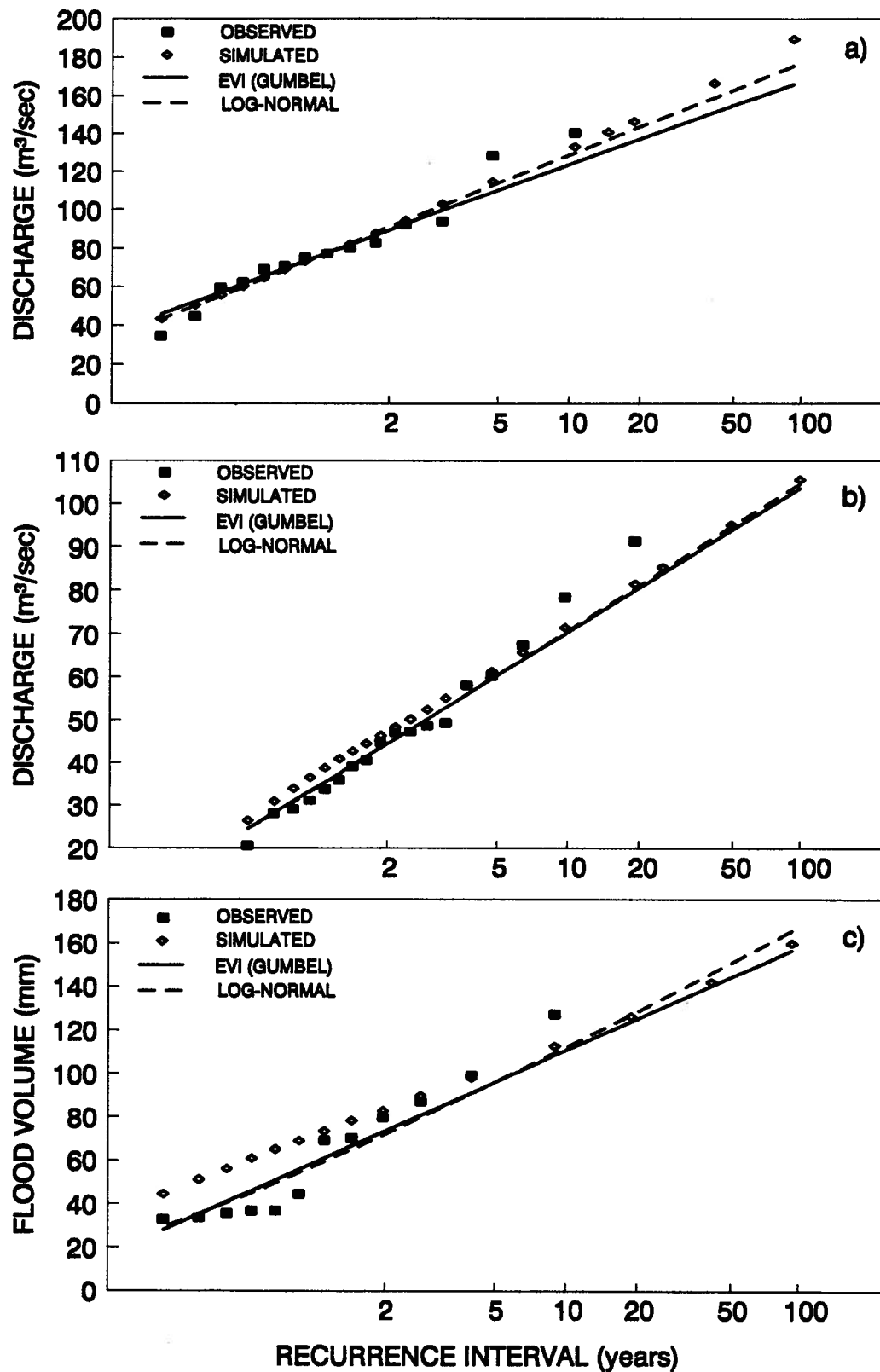


Fig. 8.10. Flood frequency curves for Chapman Creek watershed
a) hourly flows b) daily flows and c) flood volume.

Chapter 8. A PHYSICALLY BASED STOCHASTIC-DETERMINISTIC PROCEDURE FOR THE ESTIMATION OF FLOOD RUNOFF

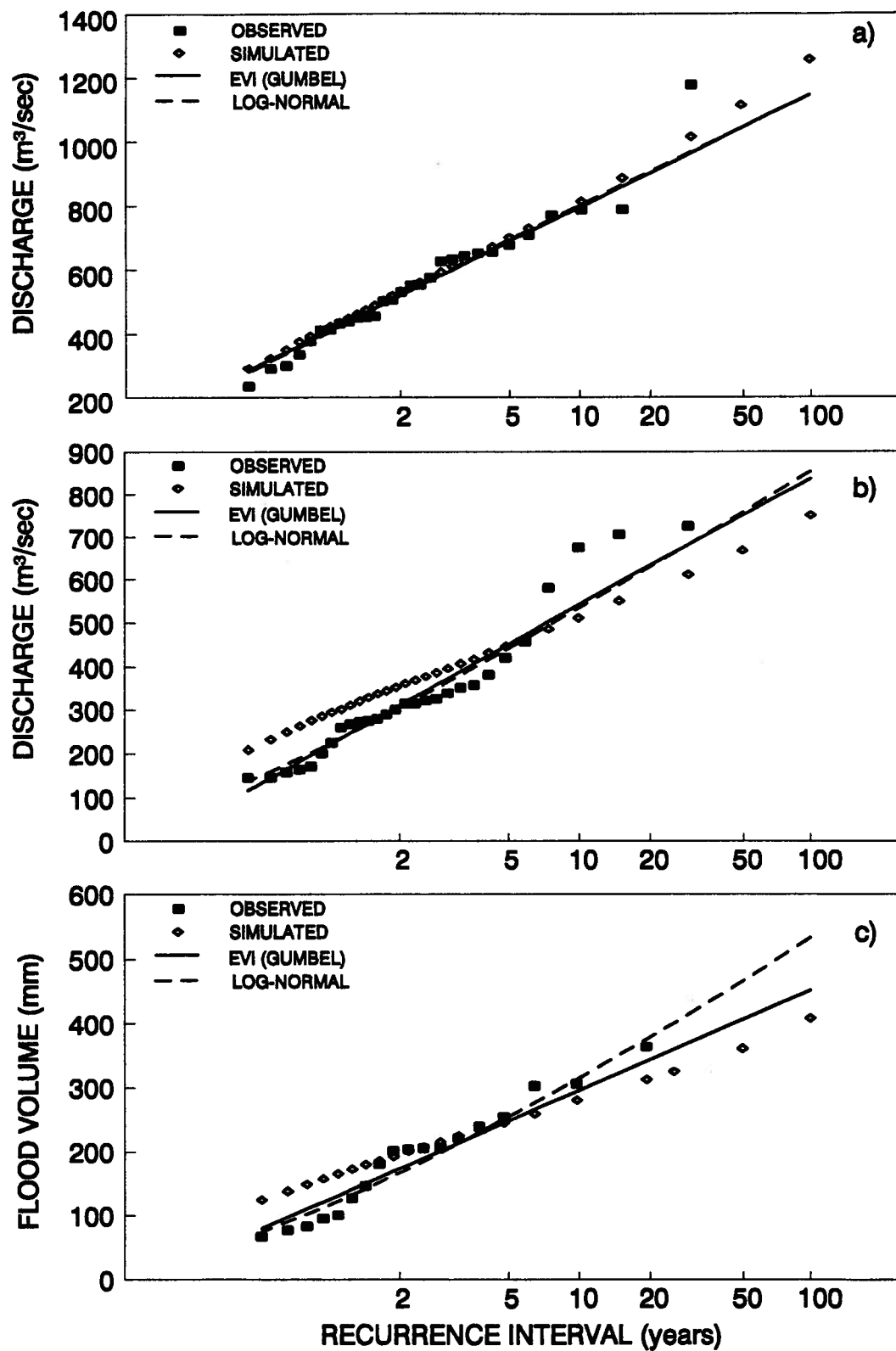


Fig. 8.11. Flood frequency curves for Zeballos River watershed.
a) hourly flows b) daily flows and c) flood volume.

Chapter 8. A PHYSICALLY BASED STOCHASTIC-DETERMINISTIC PROCEDURE FOR THE ESTIMATION OF FLOOD RUNOFF

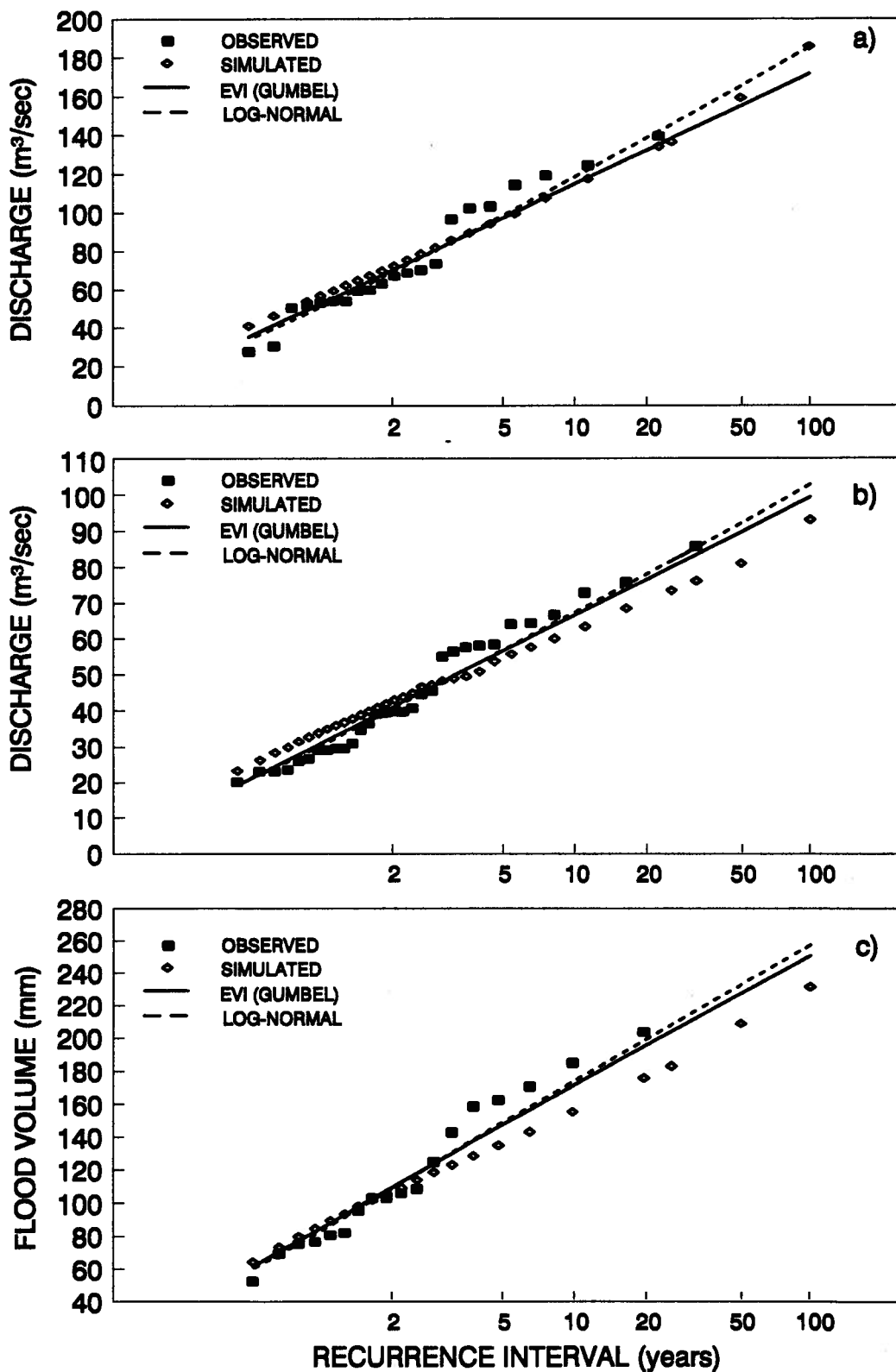


Fig. 8.12. Flood frequency curves for North Allouette River watershed.
a) hourly flows b) daily flows and c) flood volume.

Chapter 8. A PHYSICALLY BASED STOCHASTIC-DETERMINISTIC PROCEDURE FOR THE ESTIMATION OF FLOOD RUNOFF

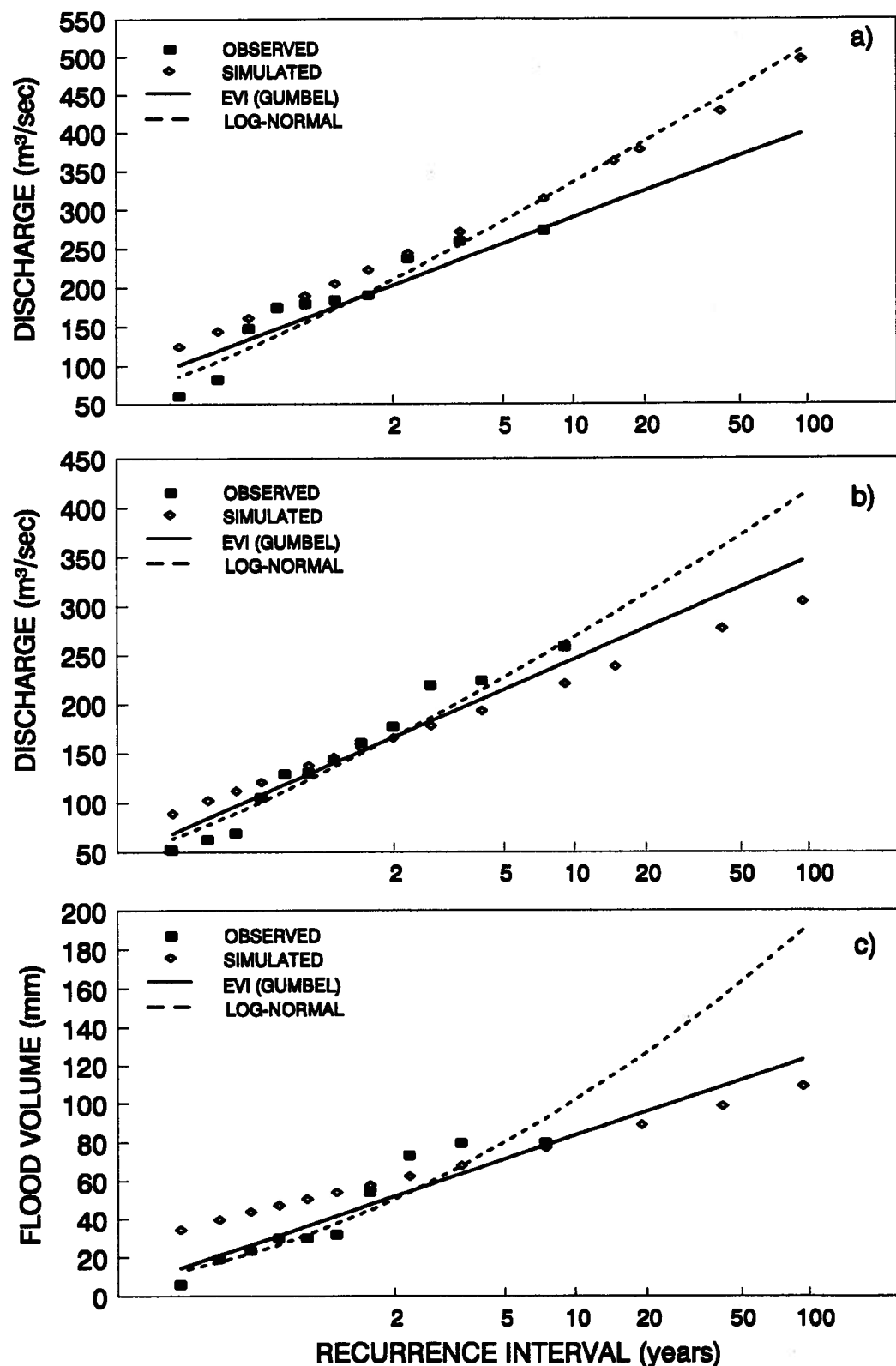


Fig. 8.13. Flood frequency curves for Oyster River watershed.
a) hourly flows b) daily flows and c) flood volume.

Chapter 8. A PHYSICALLY BASED STOCHASTIC-DETERMINISTIC PROCEDURE FOR THE ESTIMATION OF FLOOD RUNOFF

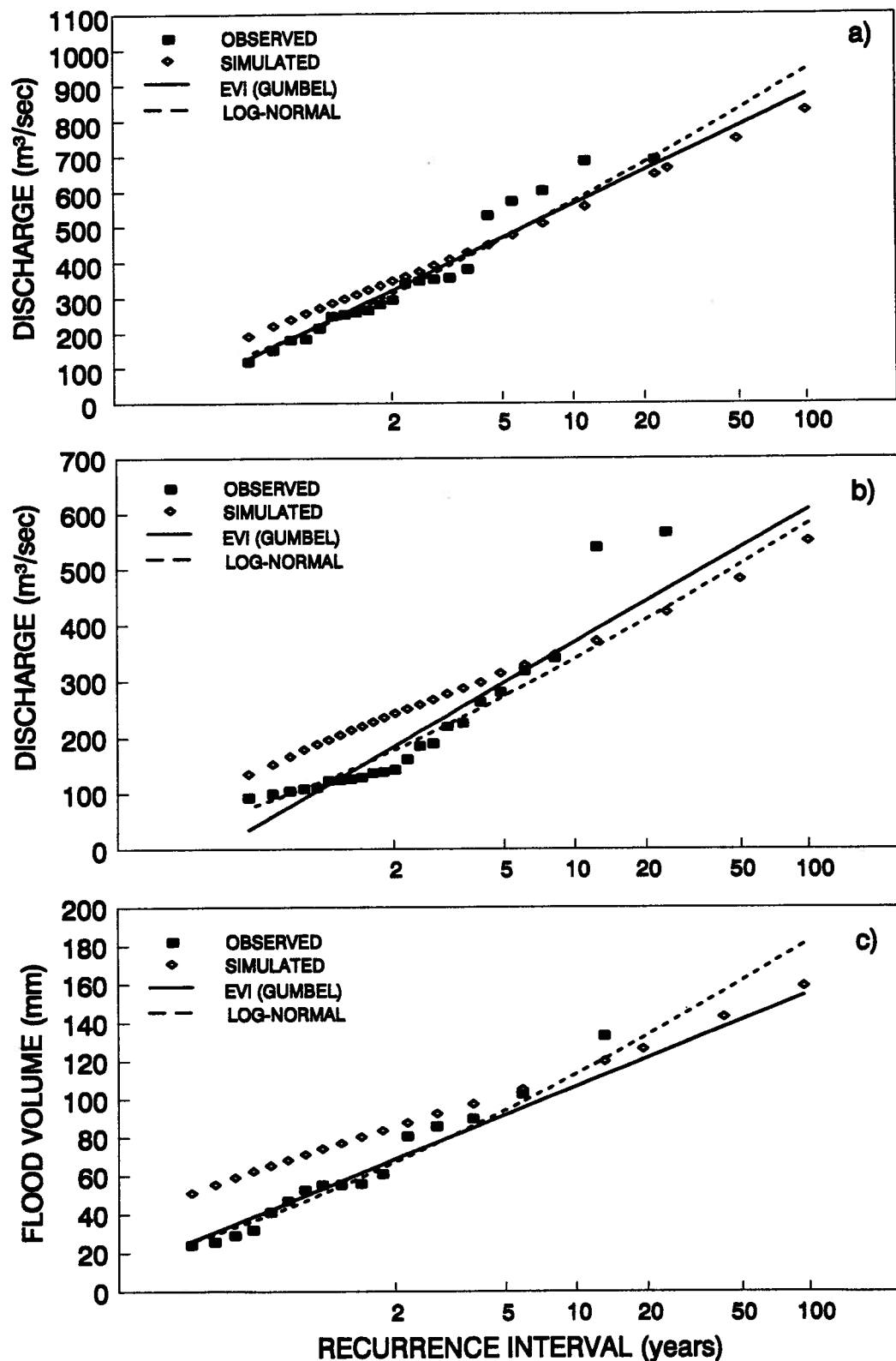


Fig. 8.14. Flood frequency curves for Hirsch Creek watershed.
a) hourly flows b) daily flows and c) flood volume.

Chapter 8. A PHYSICALLY BASED STOCHASTIC-DETERMINISTIC PROCEDURE FOR THE ESTIMATION OF FLOOD RUNOFF

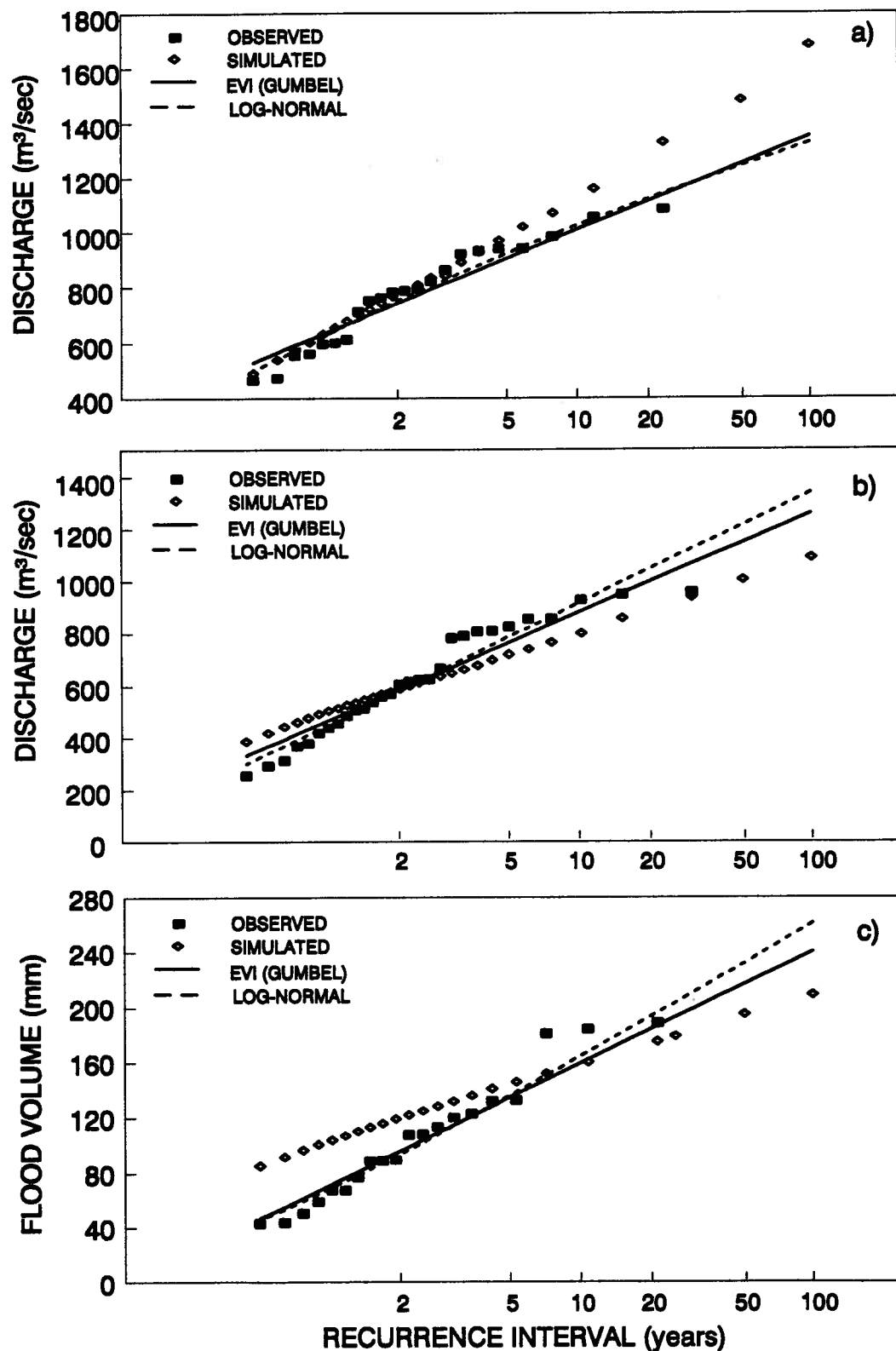


Fig. 8.15. Flood frequency curves for San Juan River watershed.
 a) hourly flows b) daily flows and c) flood volume.

Chapter 8. A PHYSICALLY BASED STOCHASTIC-DETERMINISTIC PROCEDURE FOR THE ESTIMATION OF FLOOD RUNOFF

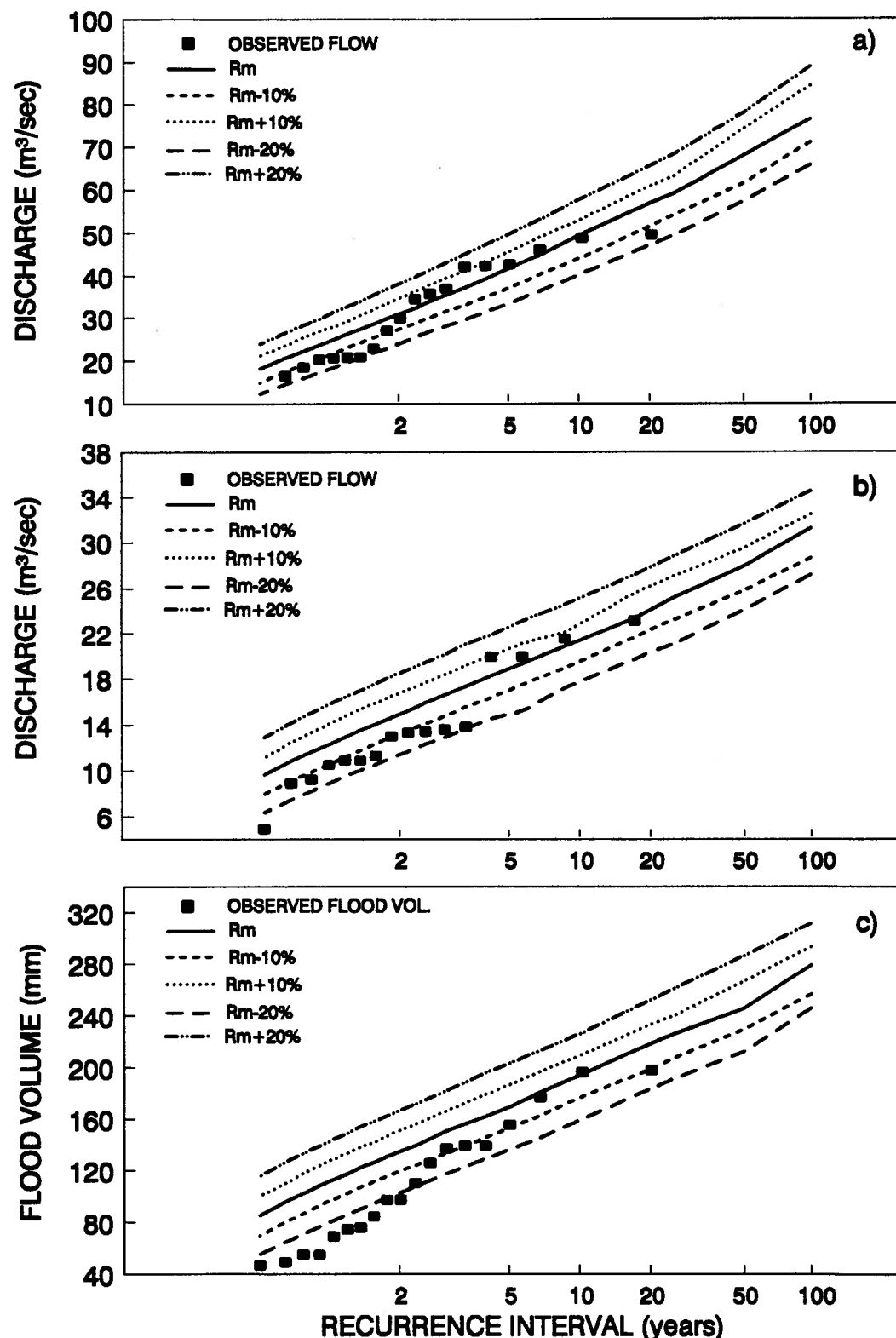


Fig. 8.16. Sensitivity of the procedure to the change of mean 24-hour rainfall depth (R_m) for a)hourly flow, b)daily flow and c) flood volume for Carnation Creek watershed.

Chapter 8. A PHYSICALLY BASED STOCHASTIC-DETERMINISTIC PROCEDURE FOR THE ESTIMATION OF FLOOD RUNOFF

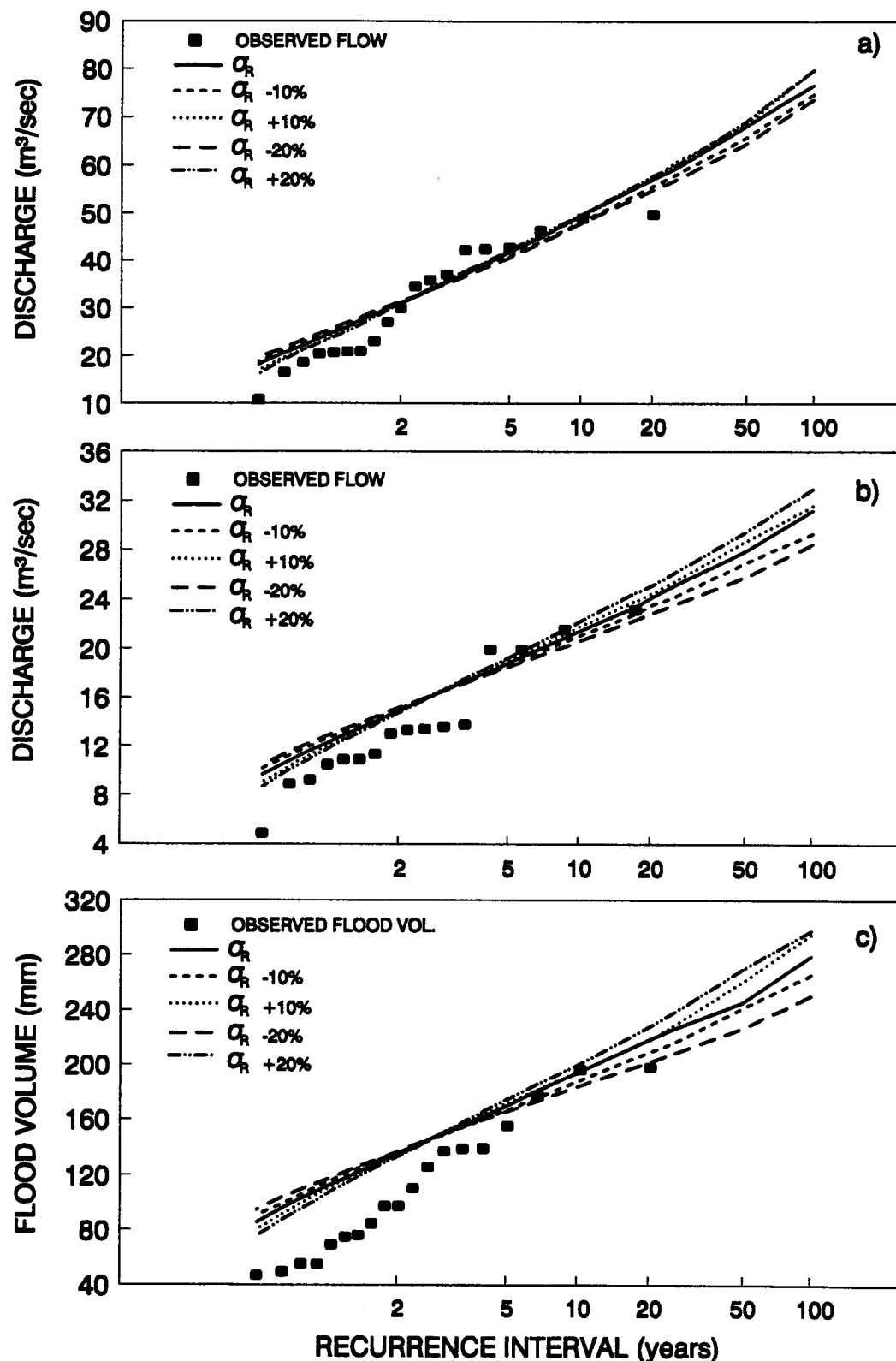


Fig. 8.17. Sensitivity of the procedure to the change of standard deviation of the 24-hour annual rainfall (σ_R) for a)hourly flow, b)daily flow and c) flood volume for Carnation Creek watershed.

Chapter 8. A PHYSICALLY BASED STOCHASTIC-DETERMINISTIC PROCEDURE FOR THE ESTIMATION OF FLOOD RUNOFF

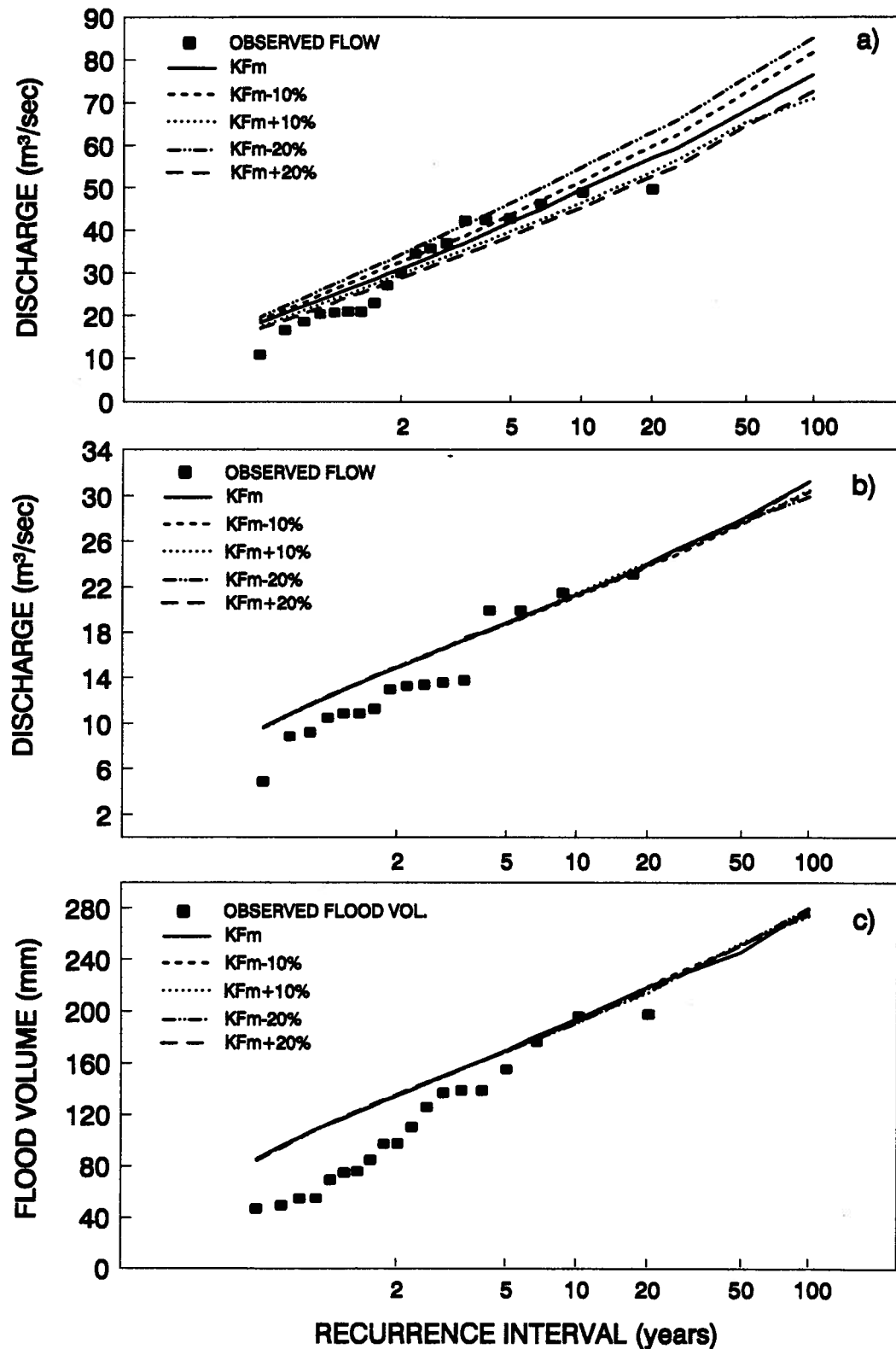


Fig. 8.18. Sensitivity of the procedure to the change of mean storage factor of fast runoff (KFm) for a) hourly flow, b) daily flow and c) flood volume for Carnation Creek watershed.

Chapter 8. A PHYSICALLY BASED STOCHASTIC-DETERMINISTIC PROCEDURE FOR THE ESTIMATION OF FLOOD RUNOFF

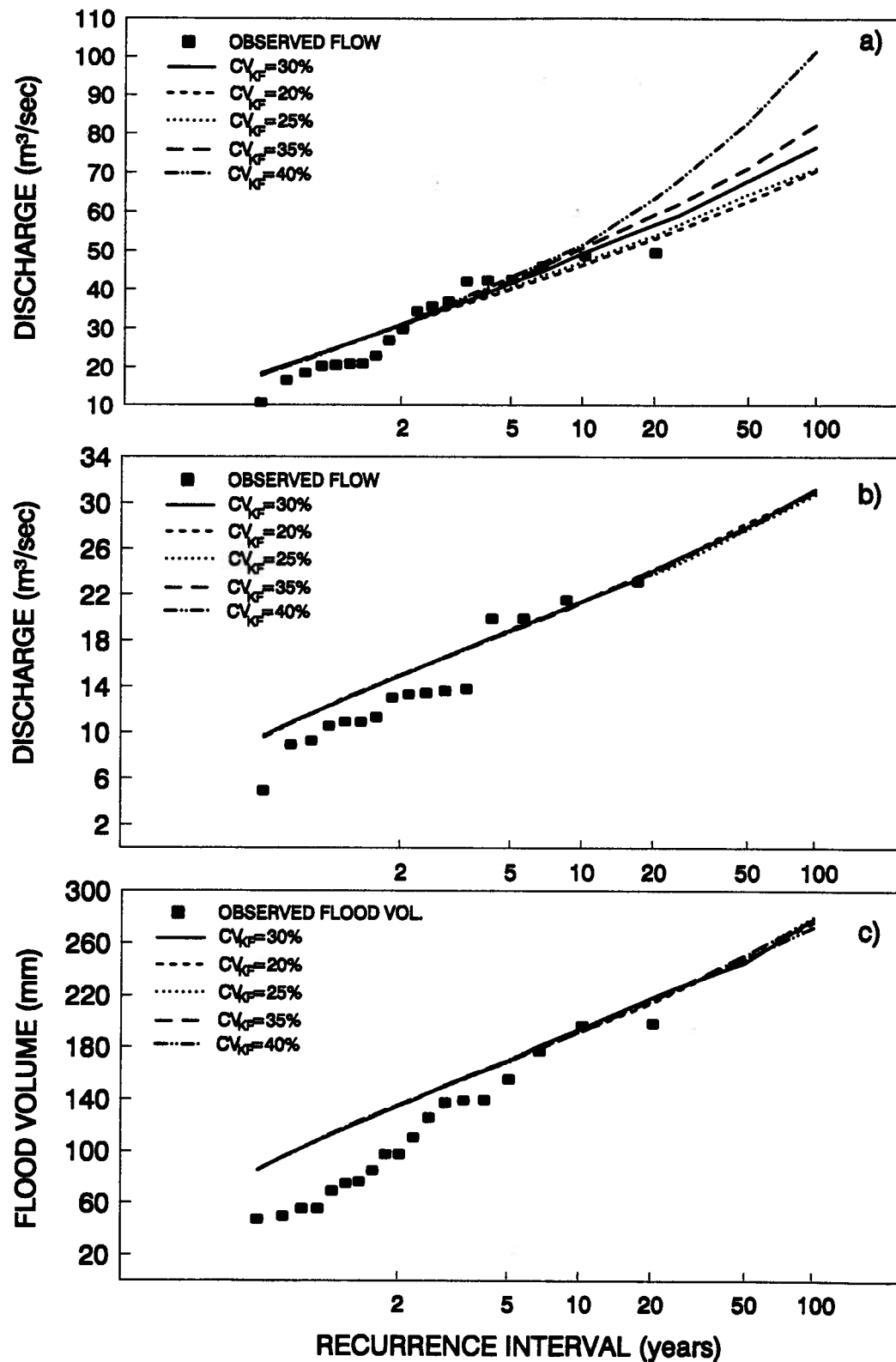


Fig. 8.19 Sensitivity of the procedure to the change of coefficient of variation of storage factor (CV_{KF}) for a) hourly flow, b) daily flow and c) flood volume for Carnation Creek watershed.

Chapter 8. A PHYSICALLY BASED STOCHASTIC-DETERMINISTIC PROCEDURE FOR THE ESTIMATION OF FLOOD RUNOFF

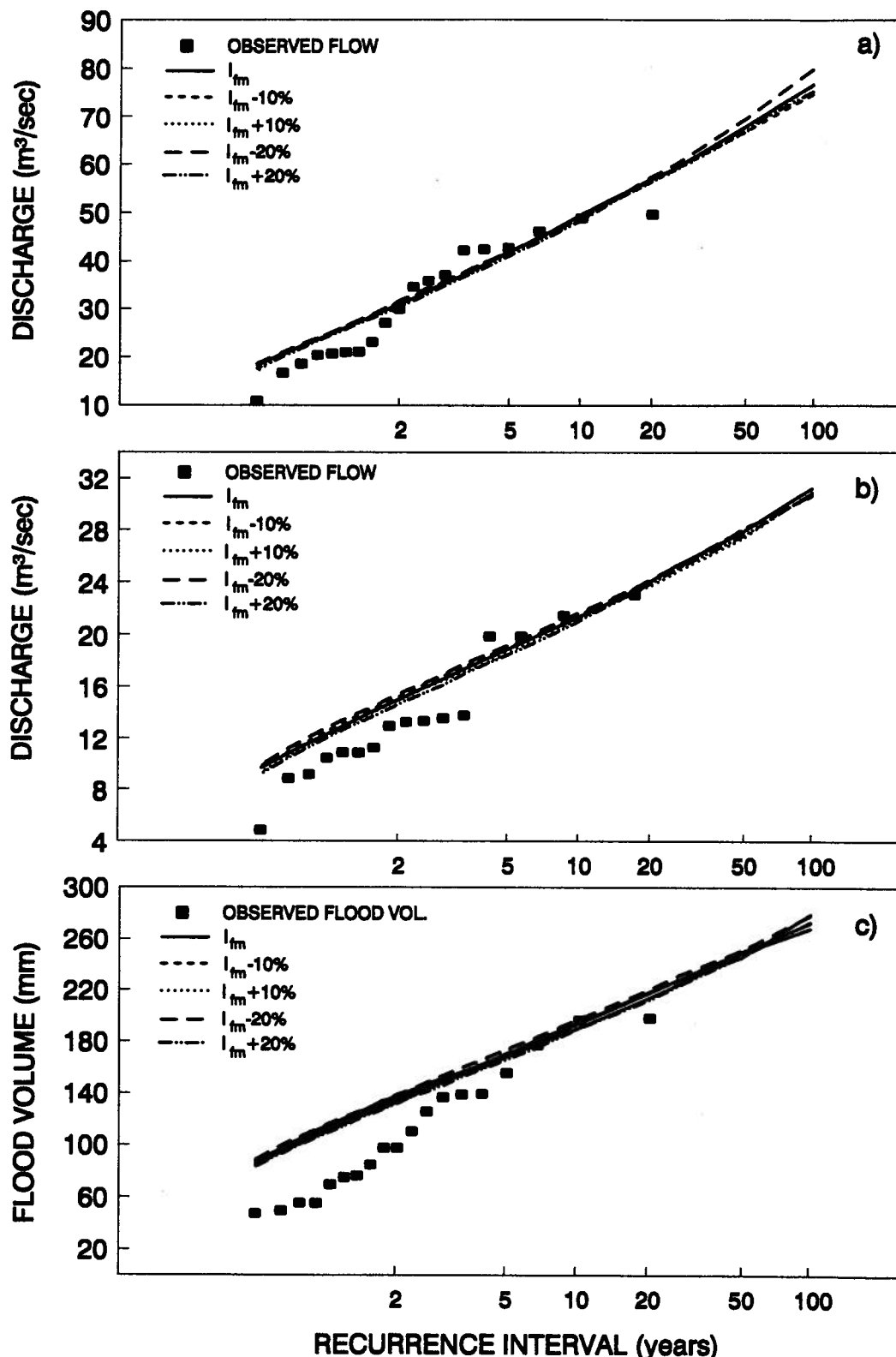


Fig. 8.20 Sensitivity of the procedure to the change of mean final infiltration abstractions (I_{fm}) for a) hourly flow, b) daily flow and c) flood volume for Carnation Creek watershed.

Chapter 8. A PHYSICALLY BASED STOCHASTIC-DETERMINISTIC PROCEDURE FOR THE ESTIMATION OF FLOOD RUNOFF

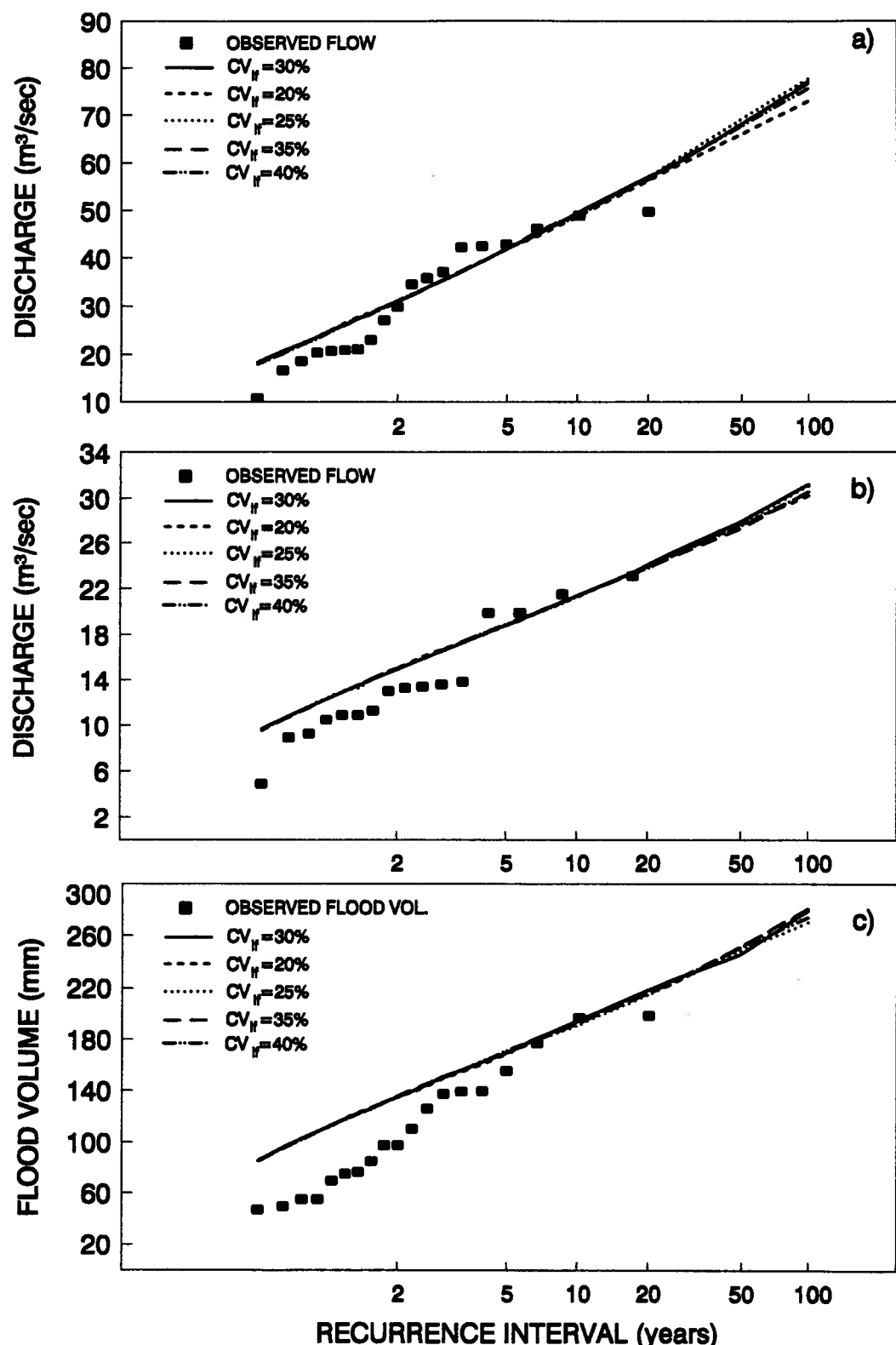


Fig. 8.21 Sensitivity of the procedure to the change of coefficient of variation of infl. abstr. (CV_H) for a)hourly flow, b)daily flow and c) flood volume for Carnation Creek watershed.

Chapter 8. A PHYSICALLY BASED STOCHASTIC-DETERMINISTIC PROCEDURE FOR THE ESTIMATION OF FLOOD RUNOFF

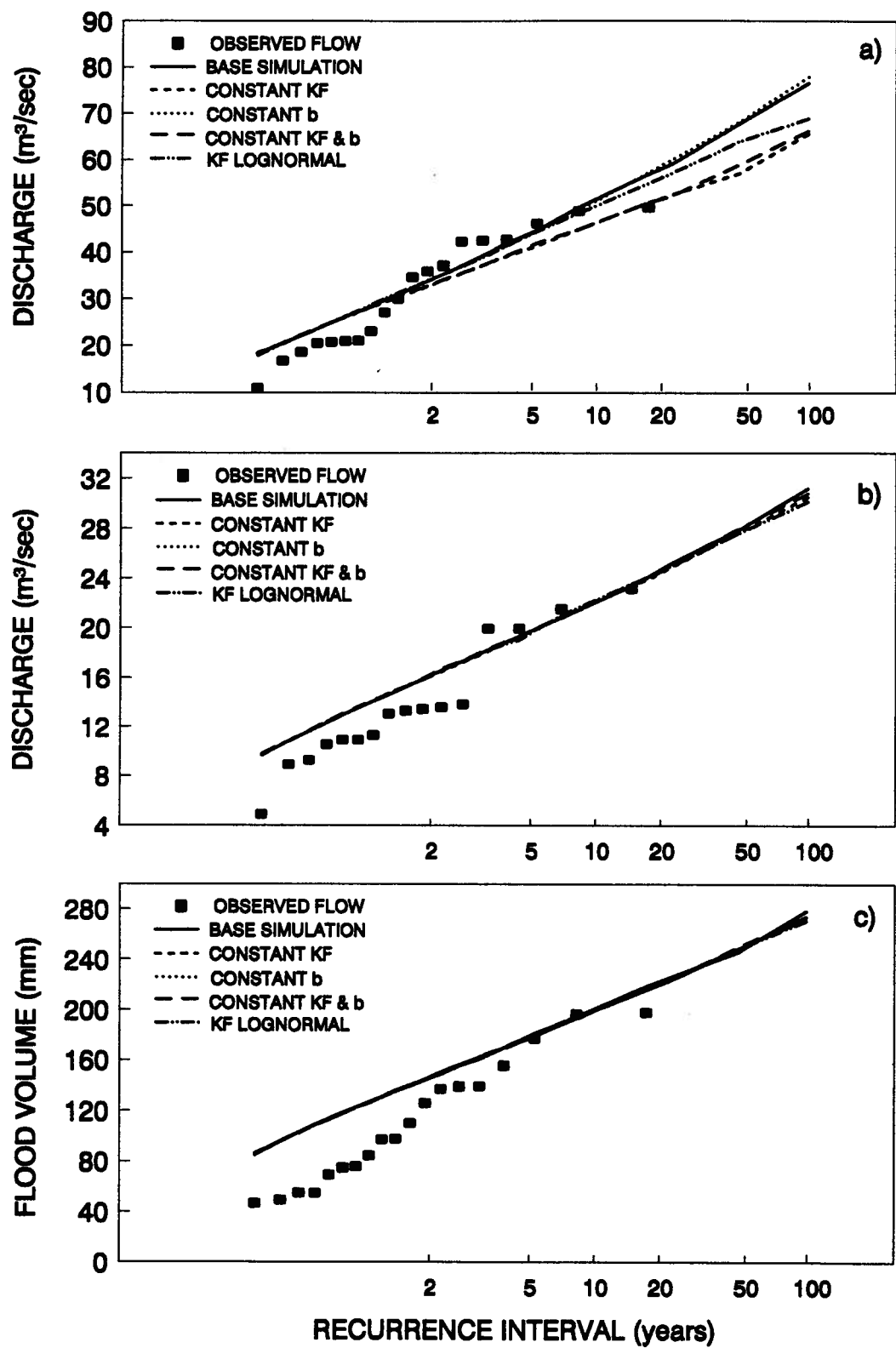


Fig. 8.22 Sensitivity of the procedure to the form of procedure parameters for
a) hourly flow, b) daily flow and c) flood volume for Carnation Creek watershed.

Chapter 8. A PHYSICALLY BASED STOCHASTIC-DETERMINISTIC PROCEDURE FOR THE ESTIMATION OF FLOOD RUNOFF

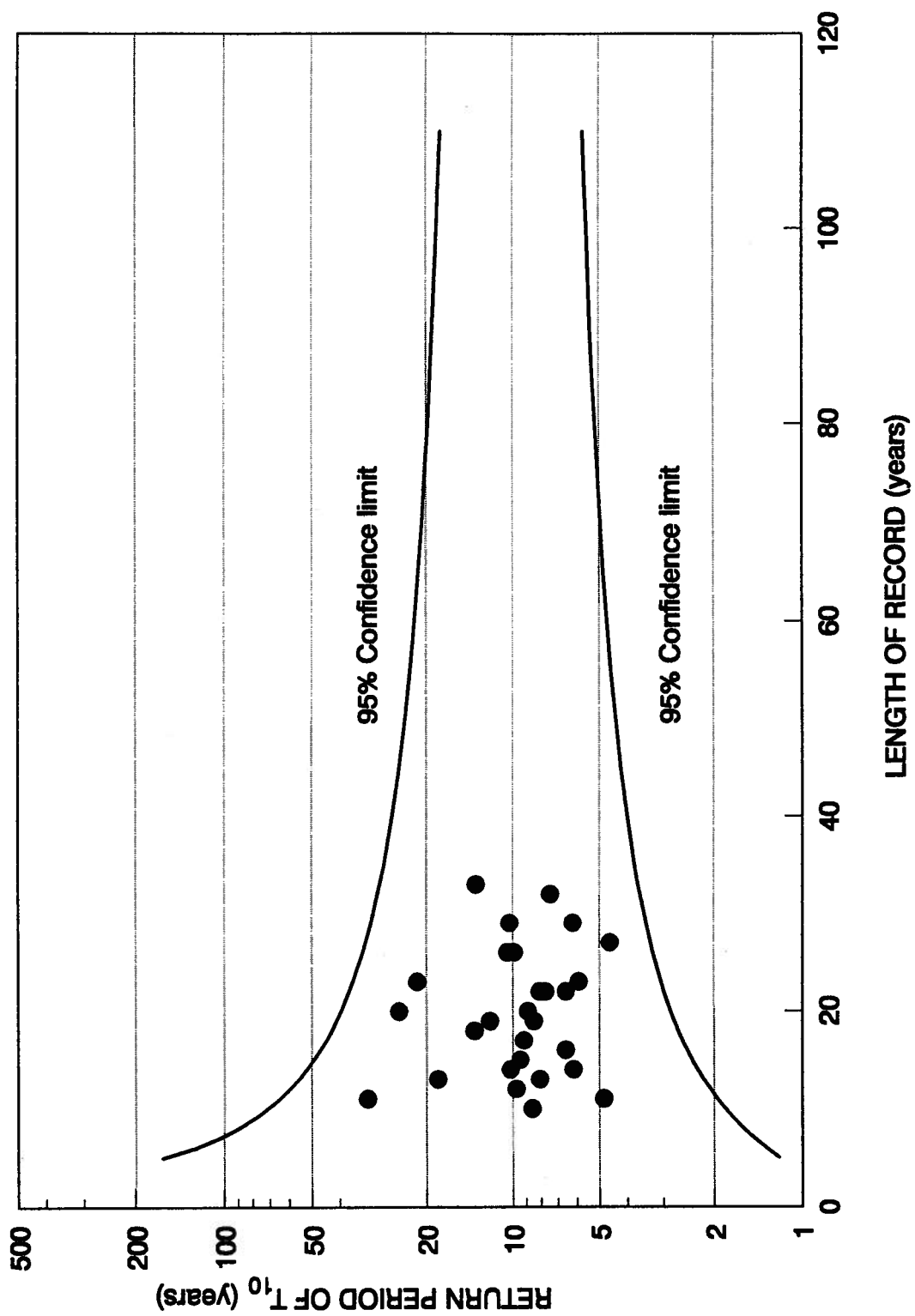


Fig. 8.23. Homogeneity test for peak instantaneous flow for the coastal British Columbia stations.

Chapter 8. A PHYSICALLY BASED STOCHASTIC-DETERMINISTIC PROCEDURE FOR THE ESTIMATION OF FLOOD RUNOFF

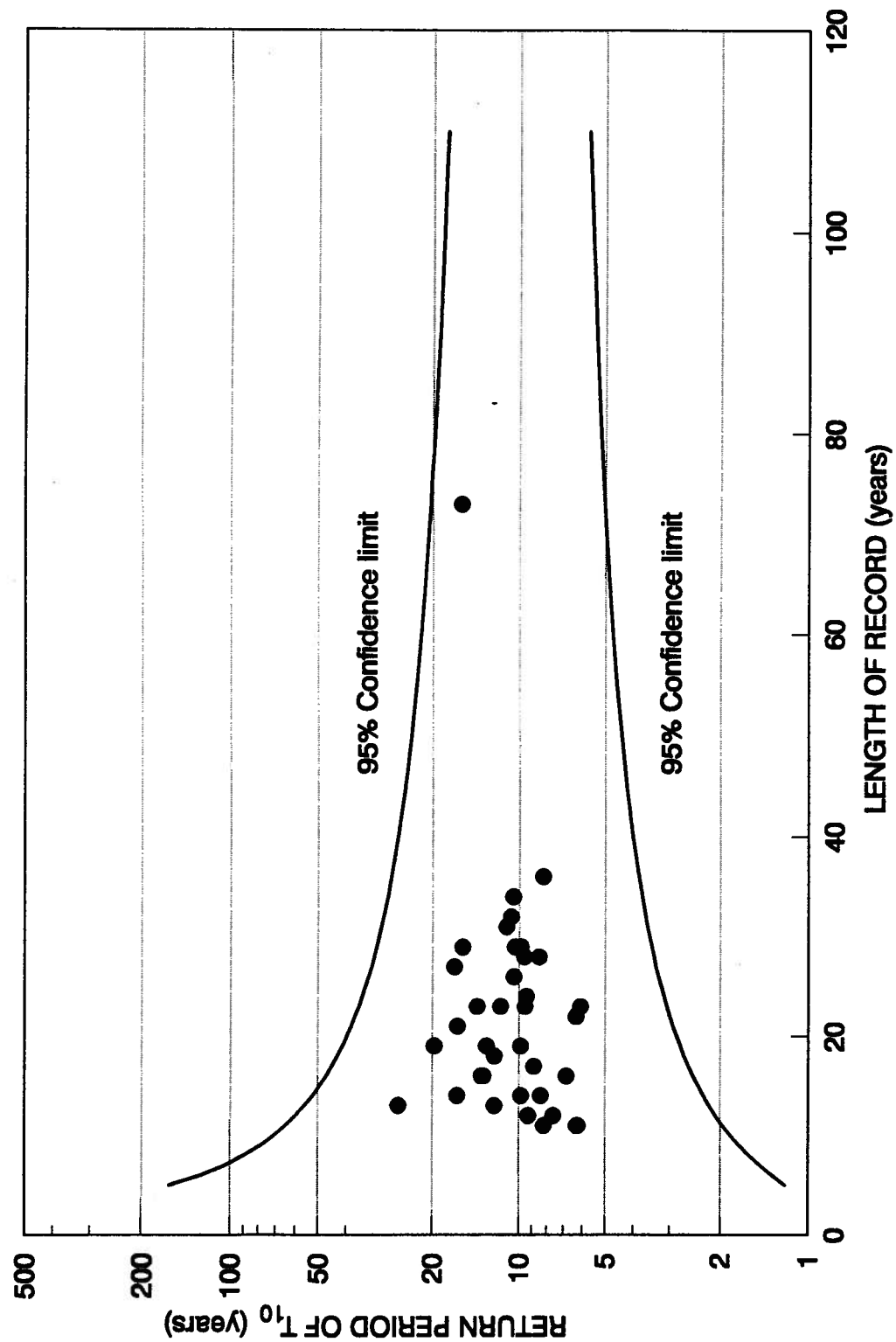
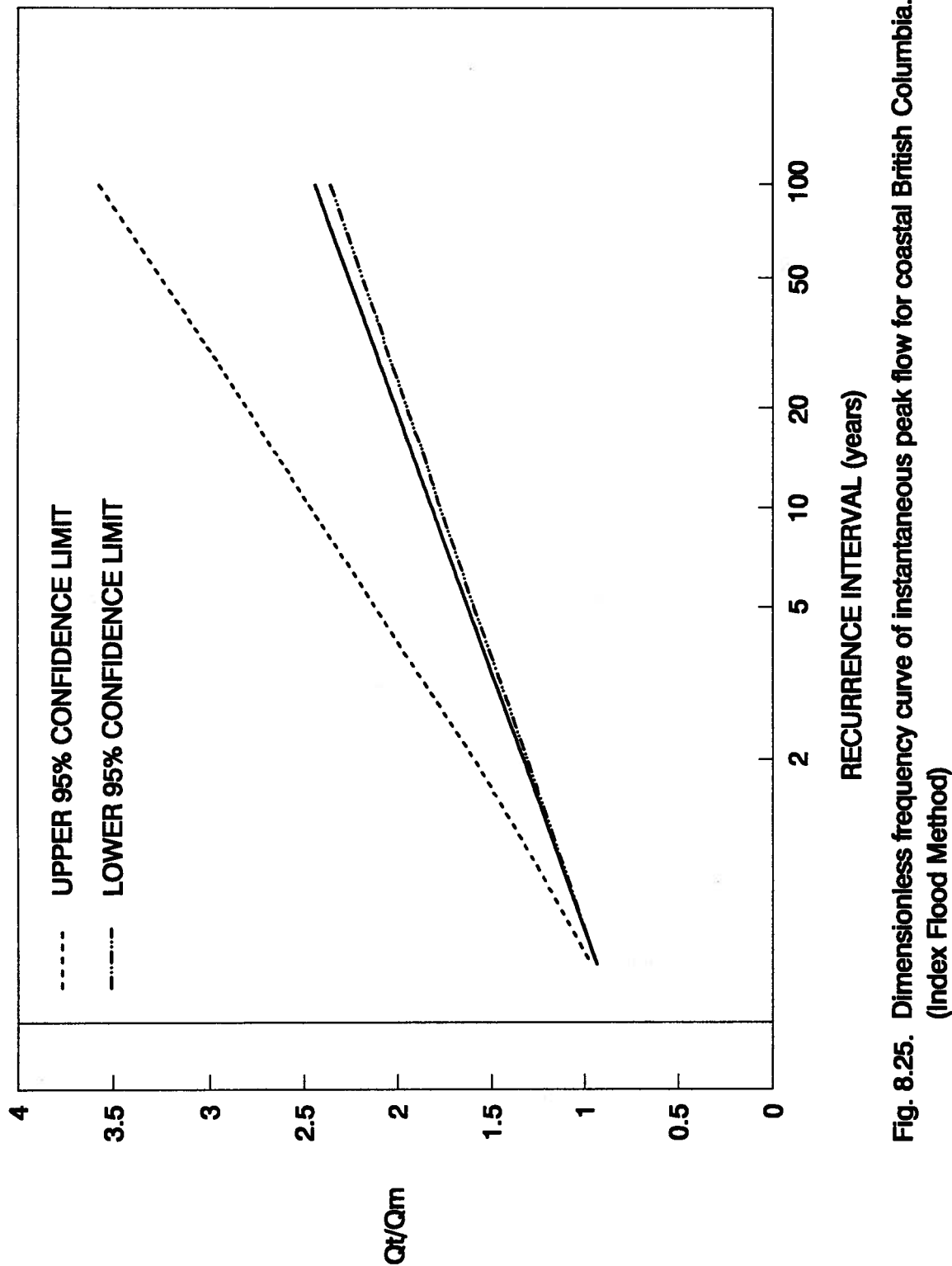


Fig. 8.24. Homogeneity test for peak daily flow for coastal British Columbia stations.



**Fig. 8.25. Dimensionless frequency curve of instantaneous peak flow for coastal British Columbia.
(Index Flood Method)**

Chapter 8. A PHYSICALLY BASED STOCHASTIC-DETERMINISTIC PROCEDURE FOR THE ESTIMATION OF FLOOD RUNOFF

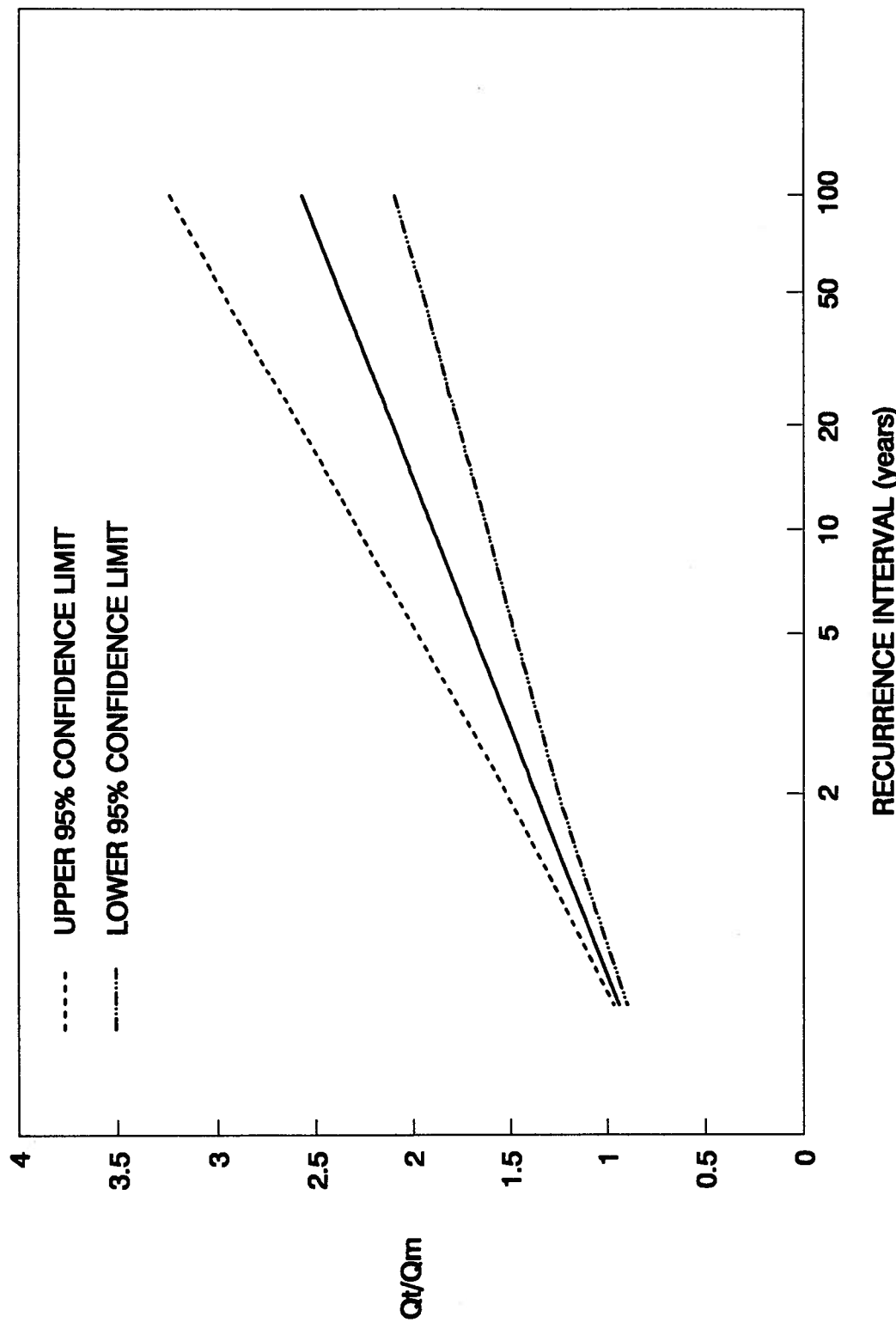


Fig. 8.26. Dimensionless frequency curve of daily peak flow for coastal British Columbia.
(Index Flood Method)

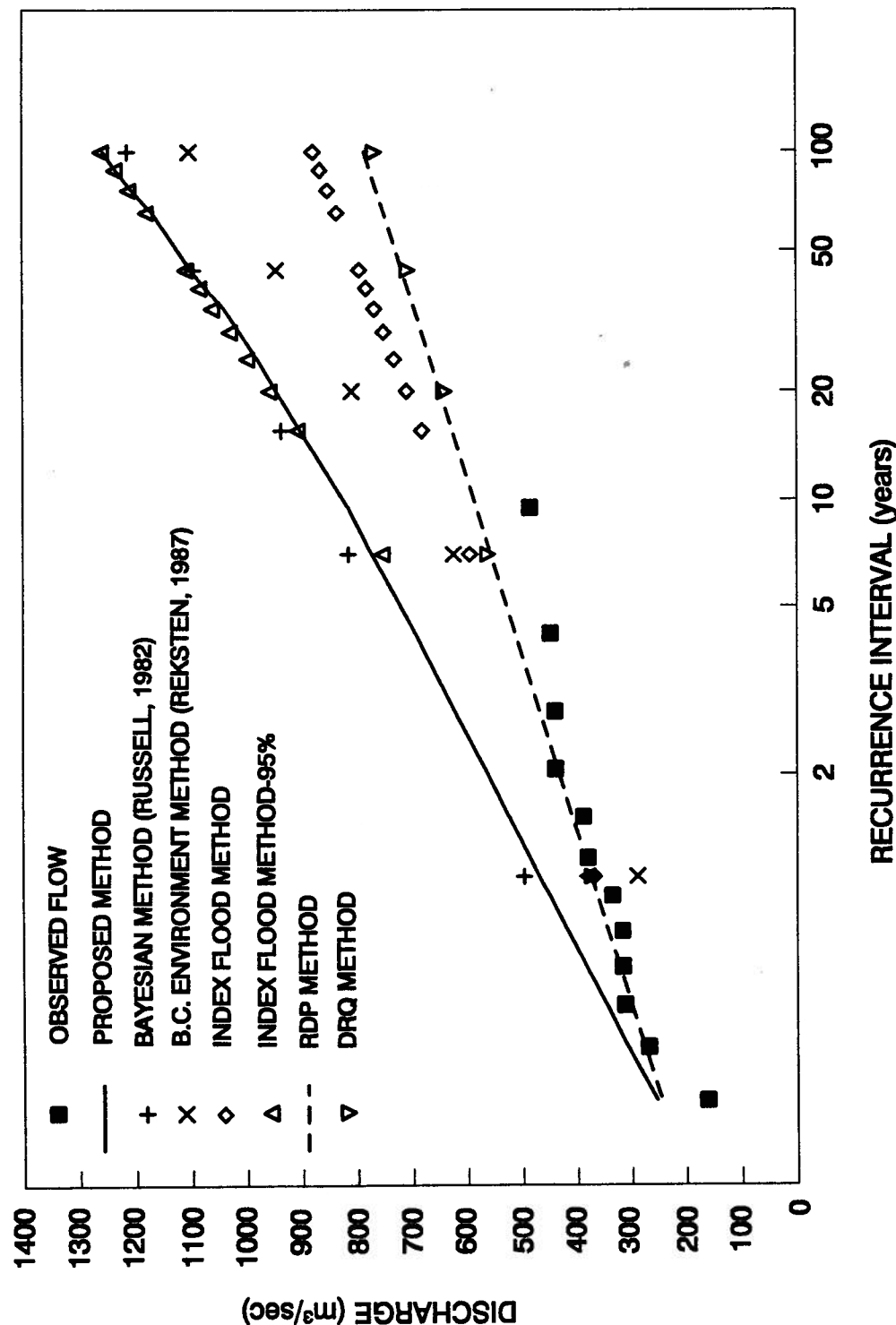


Fig. 8.27. Comparison of the frequency of the observed instantaneous peak flow with the frequency of the simulated instantaneous peak flow using various methods for Sarita River.

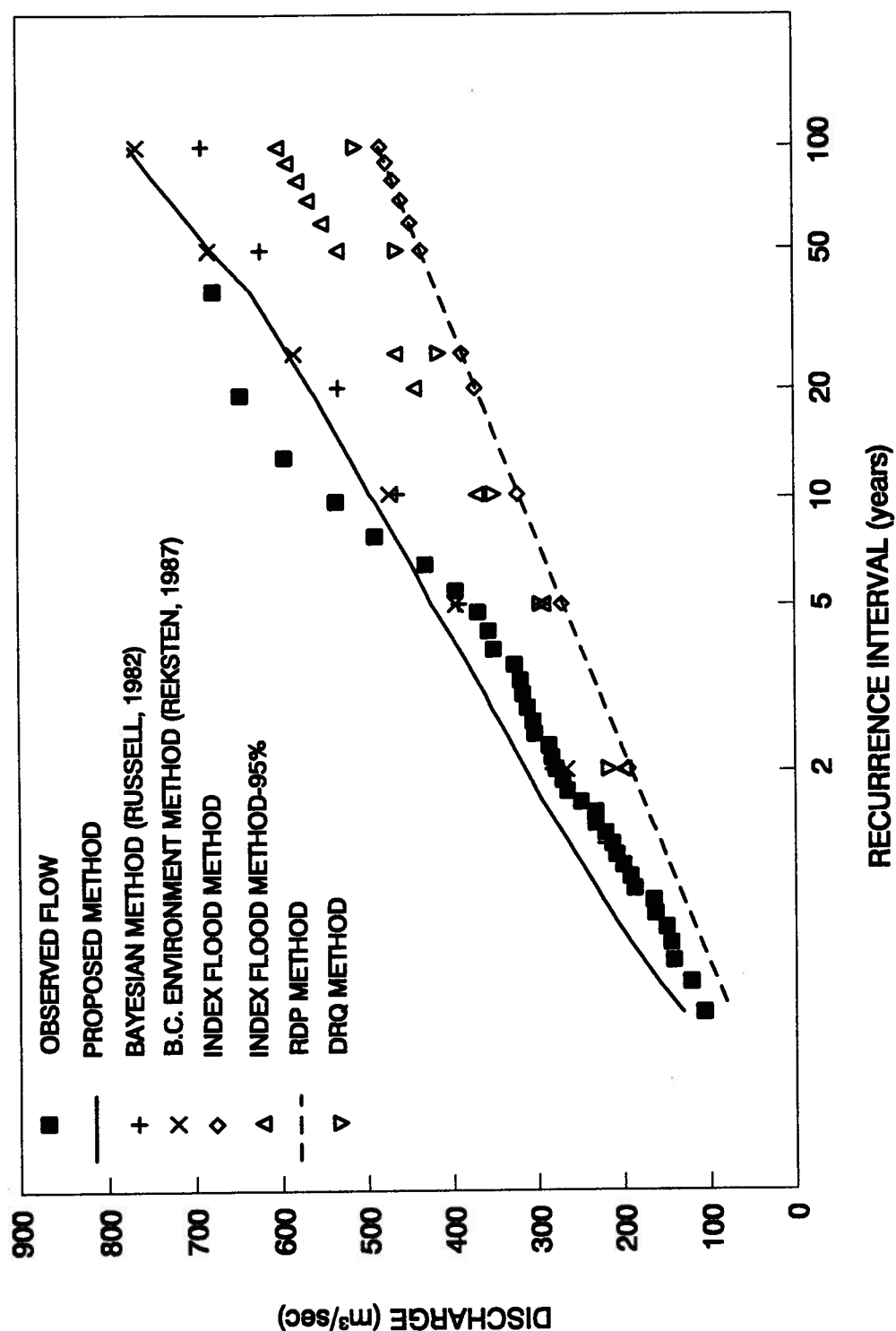


Fig. 8.28. Comparison of the frequency of the observed daily peak flow with the frequency of simulated daily peak flow using various methods for Sarita River.

CHAPTER 9

CONCLUSIONS AND RECOMMENDATIONS

9.1 Conclusions

The primary goal of this Thesis is to study the precipitation distribution in the mountainous coastal British Columbia and to use the results for the development of techniques for the reliable estimation of flood frequency for ungauged watersheds. This goal is achieved by combining results from each of the Chapters presented in this Thesis. Study components include the analysis of the long-term and short-term precipitation in two study watersheds, the Seymour River and Capilano River watersheds; generalization of the findings of the analysis to coastal British Columbia; study of extreme historical storms; application of a meteorological model for the estimation of short-term precipitation; and development of a physically-based stochastic-deterministic procedure which incorporates the findings of the previous research on precipitation and runoff generation for the estimation of the flood frequency from ungauged watersheds of the region. To illustrate the continuity between the study components, an overview of the results is included below.

The background information about the climate of coastal British Columbia and the topography of the study area have been presented in Chapter 2. It has been shown that most of the precipitation in the region is generated during winter and fall months from frontal systems that are developed over the North Pacific Ocean and travel eastward towards the coast of British Columbia.

The study begins with the analysis of the distribution of the long-term precipitation, namely annual, seasonal, and monthly and its distribution with elevation. The analysis shows

Chapter 9. CONCLUSIONS AND RECOMMENDATIONS

that the annual and the wet period October to March precipitation increases with elevation up to about 400 m in the Capilano River watershed whereas the topography of the Seymour River watershed reduces the elevation to about 260 m. The position of the maximum precipitation is the middle of the watersheds. After that point the precipitation either decreases as in the Seymour River watershed or levels off as in the Capilano River watershed. On the other hand, the dry period April to September precipitation is more uniformly distributed over the study watersheds and it is not affected by the elevation.

The Bergeron two-cloud mechanism has been identified as the mechanism which generates most of the precipitation in the region, and can explain the distinctive precipitation distribution observed in this study.

Another important finding of the study is that the valley and the adjacent mountain slope precipitation is similar at the same distance from the beginning of the mountain region. This result is very significant because most of the precipitation stations are located in the easily accessible river valleys. However, this distribution pattern has been observed in the two study watersheds only for the initial topographic rise because of the absence of high elevation data in the back range. It is therefore important that high elevation stations should be installed on the mountain slopes beyond the front range in order to confirm or deny the observations for the front mountains.

Regional precipitation and runoff data were used to examine the generality of the findings of the study of the precipitation distribution in the two study watersheds. This analysis showed that the initial results of the study are more general and regional in scale, and that long-term precipitation follows a similar pattern to that in the two study watersheds, increasing up to about 400-800 m elevation and then either leveling off or even decreasing at higher elevations. This finding is very important because it is usually assumed (Barry, 1992) that the precipitation in the mid-latitude mountainous areas increases almost linearly with

Chapter 9. CONCLUSIONS AND RECOMMENDATIONS

elevation up to the top elevation. This result has a very strong impact on the design and planning procedures of water resources of the region.

The next step was to study the short-term or storm precipitation in the Seymour River watershed. This short-term precipitation is one of the necessary components of the flood estimation procedures. The analysis of 175 storms for seven stations showed that the average precipitation follows a distribution pattern similar to the pattern found in the analysis of the long-term precipitation. This finding is very important since in coastal British Columbia only about one third of the existing precipitation stations are recording gauges capable of measuring the short-term precipitation. This preliminary result suggests that the long-term precipitation may be used as an indicator of the shorter-term precipitation, but further study of this issue is necessary. Moreover, the distribution pattern of the storm is not affected by the type of precipitation, whether rain, rain and snow or snow.

A part of the storm precipitation study was the analysis of the time distribution of the storms. This analysis showed that the storm time distribution is reasonably constant and does not vary significantly with the type of precipitation, elevation, storm duration, and storm depth. Also, examination of regional data from sparsely located coastal British Columbia stations showed that the storm time distribution does not change significantly over the region. This result indicates that the storm time distribution found in this study can be transposed over the whole region.

The final goal of the research program is to find techniques to accurately estimate the flood runoff from ungauged watersheds of the region, even when the data are limited. To assist in the estimation of flood runoff, the 24-hour design storm has been developed. The choice of the 24-hour storm duration was based on climatic, hydrological, and pragmatic reasons. The design storm has been developed with data from the Seymour River watershed and then it has been compared with other regional studies and data. This comparison showed

Chapter 9. CONCLUSIONS AND RECOMMENDATIONS

that the results for the Seymour River watershed do not differ significantly from the regional data, so that they can be transposed over the region. An event-based rainfall-runoff simulation was undertaken for a real watershed, the Sarita River watershed on Vancouver Island, and showed that only the 10% time probability distribution curve and the synthetic Soil Conservation Services type IA hydrograph are capable of accurately reproducing the flood hydrograph.

Another important finding of this analysis was that the 24-hour annual rainfall of a given return period is a constant percentage of the mean annual precipitation. This result is very important because it expands the results of this study both in space and in time since daily data is available from the storage precipitation gauges in coastal British Columbia. Also there are more storage gauges and they have longer records than the recording gauges. This result also suggests that the extreme 24-hour annual rainfall probably follows a similar pattern to that of the annual precipitation which is important for the estimation of the spatial distribution of the design storm.

The above findings for the short-term precipitation were examined for five extreme flood producing historic storms that occurred over the two study watersheds. This analysis showed that the results of the storm precipitation analysis are valid for the extreme storms, which adds confidence in their use in coastal British Columbia.

A theoretically-based meteorological model, the BOUND_P model, was tested to check whether it could predict the precipitation distribution and to confirm the results of the statistical analysis. The model was applied for the mountainous area of the two study watersheds, Seymour River and Capilano River. From the comparison of the model results with the observed precipitation, it was evident that the model is incapable, in its present form, of simulating the large precipitation amounts observed in the mountain areas and of reproducing the distinct precipitation distribution pattern found in this study. As a result, no

Chapter 9. CONCLUSIONS AND RECOMMENDATIONS

attempt was made to use the model for hydrologic modeling of the runoff from these mountainous watersheds, as was initially intended.

The final step of the research program was to develop a technique to estimate the flood frequency for ungauged watersheds with limited data. This was achieved using the method of derived distributions and the integration of the previous results of the precipitation analysis and the study of the watershed response. The proposed method is a physically-based method because all its parameters can be estimated by using physical variables, and it is stochastic-deterministic because it uses a deterministic watershed response model which has stochastic parameters, along with a stochastic rainfall generation model.

The proposed procedure was applied to eight coastal British Columbia watersheds and compared with other regional techniques. The results showed that the method is easy to apply, requires very limited data, and is efficient and reliable for determining the hourly and daily peak flows.

In summary, this Thesis examines the distribution pattern of precipitation with elevation; provides regional characteristics of long-term and storm precipitation for estimating input precipitation data to a hydrologic model; and proposes a physically-based stochastic-deterministic method for the estimation of flood frequency from ungauged watersheds in the coastal region of British Columbia.

9.2 Recommendations

One of the most important findings of this study is that precipitation does not continue to increase linearly with elevation, as has often been assumed (Melone, 1986; Barry, 1992). Consequently, water supply and design floods may both be overestimated if the leveling off

Chapter 9. CONCLUSIONS AND RECOMMENDATIONS

and even reduction of precipitation above even modest elevations of about 400 to 800 m is not taken into account.

Clearly, this decrease or levelling off of precipitation at higher elevations is a matter of such high economic importance that considerable effort and expenditure should be made to confirm or deny this result by gathering additional higher elevation data in the region. These data can be used also in the development and testing of more reliable meteorological models of mountainous precipitation.

Furthermore, these additional high elevation data can also be used to test another finding of this study, namely that the mountain slope and valley precipitation are similar at the same position. This finding is very important, and needs to be confirmed by expanding the data base to assist in the reliable evaluation of the areal precipitation, especially as most precipitation stations are located in the river valleys.

Another topic for further research is the application of the proposed procedure for the estimation of flood runoff to other areas of the coastal Pacific Northwest. Furthermore, the procedure could be applied to other areas of different climate from that of the coastal British Columbia. This application requires appropriate adjustments in the values of the model parameters. Also, another potential future application of the procedure is in evaluating the impact of watershed changes on flood magnitudes and frequencies. This evaluation would be produced for a given watershed with parameter values representing the modified or future conditions.

A last point which is considered significant for further research is the adaptation of the proposed procedure for the estimation of floods generated by rain on snow events. The focus in this research program was on the rain storm produced floods. Melone (1986) has shown that rain on snow is the second most important mechanism for the generation of peak flow in coastal British Columbia after the rain storms. Also, Melone proved that the increased

Chapter 9. CONCLUSIONS AND RECOMMENDATIONS

response of the coastal watersheds to these events is not due to a fundamental change of the watershed behaviour but it is the result of increased water input from the snowmelt.

To incorporate these processes in the proposed procedure, a research program should be set up to study the distribution and variation of the snowpack and temperature with elevation. A fundamental part of this type of study would be the identification of rain on snow events, which can be done if a good coverage of meteorological and hydrological stations exists.

In conclusion, this Thesis examines the precipitation distribution in space and time at various spatial and temporal scales; develops the 24-hour design storm rainfall for coastal British Columbia; tests a meteorological mathematically based model in the study area and finally incorporates the above findings of precipitation analysis and previous results of watershed response analysis and modeling into a physically-based stochastic-deterministic procedure for the estimation of flood frequency from ungauged watersheds of the region. The results of this research study are readily applicable for water resources design in coastal British Columbia, although they can be expanded and refined more, when additional data are available.

REFERENCES

- Amoroch, J. and B. Wu, 1977. "Mathematical Models for the Simulation of Cyclonic Storm Sequences and Precipitation Fields." *Journal of Hydrology*, 32, 329-345.
- Barry, R.G., 1992. "Mountain Weather and Climate." Routledge, London, England.
- Barry, R.G. and R.J. Chorley, 1987. "Atmosphere, Weather and Climate." Methuen, London, England.
- Beaudry, P.G. and D.L. Golding, 1985. "Snowmelt and Runoff During Rain on Snow in Forest and Adjacent Clearcut." In: *Snow Property Measurements Workshop*, Lake Louise, Alberta, 285-311.
- Berndtsson, R. and J. Niemczynowicz, 1988. "Spatial and Temporal Scales in Rainfall Analysis-Some Aspects and Future Perspectives." *Journal of Hydrology*, 100, 293-313.
- Berndtsson, R. and J. Niemcynowitz, 1986. "Spatial and Temporal Characteristics of High-Intensive Rainfall in Northern Tunisia." *Journal of Hydrology*, 87, 285-298.
- Bergeron, T., 1960. "Physics of precipitation." Washington, *American Geophysical Union*.
- Beven, K.J. and G.M. Hornberger, 1982. "Assesing the Effect of Spatial Pattern of Precipitation in Modeling Stream Flow Hydrographs." *Water Resources Bulletin*, 18(5), 823-829.

REFERENCES

- Blazkova, S., 1992. "Empirical Study of Nonlinearity in Direct Runoff on 100 km² Basin." *Hydrological Sciences Journal*, 37(4), 347-358.
- Bonta, J.V. and A.R. Rao, 1992. "Estimating Peak Flows from Small Agricultural Watersheds." *Journal of Irrigation and Drainage Engineering*, 118(1), 122-137.
- Bonta, J.V. and A.R. Rao, 1989. "Regionalization of Storm Hyetographs." *Water Resources Bulletin*, 25(1), 211-217.
- Bonta, J.V. and A.R. Rao, 1987. "Factors Affecting Development of Huff Curves." *Transactions of the ASAE*, 31(3), 756-760.
- Bras, R. and I. Rodriguez-Iturbe, 1985. "Random Functions in Hydrology." Addison-Wesley Publishing Company, Menlo Park, California.
- Bras, R.L., D.R. Gaboury, D.S. Grossman, and G.J. Vicens, 1985. "Spatially Varying Rainfall and Floodrisk Analysis." *Journal of Hydraulic Engineering*, 111(5), 754-773.
- B.C. Environment (British Columbia Ministry of Environment, Lands and Parks), 1992. "Snow Survey Bulletin." Water Investigations Branch, Victoria, British Columbia.
- Brown, R.A., 1981. "Modelling the Geostrophic Drag Coefficient for AIDJEX." *Journal of Geophysical Research*, 86, 1989-1994.

REFERENCES

- Browning, K.A., C.W. Pardoe and F.F. Hill, 1975. "The Nature of Orographic Rain at Winter Cold Fronts." *Quarterly Journal of the Royal Meteorological Society*, 101: 333-352.
- Browning, K.A., M.E. Hardman, T.W. Harrold and C.W. Pardoe, 1973. "The Structure of Rainbands within a Mid-latitude Depression." *Quarterly Journal of the Royal Meteorological Society*, 99, 215-231.
- Cadavid, L., J.T.B. Obeysekera and H.W. Shen, 1991. "Flood-Frequency Derivation from Kinematic Wave." *Journal Hydraulic Engineering*, 117(4), 489-510.
- Chacon, R. E. and W. Fernandez, 1985. "Temporal and Spatial Rainfall Variability in the Mountainous Region of the Reventazon River Basin, Costa Rica." *Journal of Climatology*, 5: 175-188.
- Chapman, A., D. Reksten and R. Nuhof, 1992. "Guide to Peak Flow Estimation for Ungauged Watersheds in the Vancouver Island Region." British Columbia Ministry of Environment, Lands and Parks, Water Management Division, Hydrology Section, Victoria, British Columbia.
- Cheng, J. D., (1976). "A Study of the Stormflow Hydrology of Small Watersheds in the Coast Mountains of Southwestern British Columbia." *Unpublished Ph.D. Thesis. Interdisciplinary Studies. University of British Columbia, Vancouver.*
- Chow, V. T., D.R. Maidment and L.W. Mays, 1988. "Applied Hydrology." McGraw-Hill Book Company, New York, N.Y.

REFERENCES

- Chilton, R., 1980. "December 1979 Rainstorms on the Lower Mainland and its Consequences." *Technical Report*, British Columbia Ministry of Environment, Victoria, British Columbia.
- Chuptha, P., and J.C.I. Dooge, 1990. "The Shape Parameters of the Geomorphologic Unit Hydrograph." *Journal of Hydrology*, 117, 81-97.
- Consuegra, D., P. Meylan and A. Musy, 1993. "A Probabilistic Approach to Estimate Design Parameters for Flood Control Projects." In: *Engineering Hydrology*, Proceedings of the ASCE International Symposium, San Francisco, California, 455-460.
- Corradini, C. and F. Melone, 1989. "Spatial Structure of Rainfall in Mid-latitude Cold Front Systems." *Journal of Hydrology*, 105, 297-316.
- Cudworth, A.G., 1989. "Flood Hydrology Manual." U.S. Bureau of Reclamation, Denver, Colorado.
- Danard, M., 1971. "A Simple Method of Computing the Variation of Annual Precipitation over Mountainous Terrain. *Boundary-Layer Meteorology*, 2, 188-206.
- Danard, M., 1977. "A Simple Model for Mesoscale Effect of Topography on Surface Winds." *Monthly Weather Review*, 105, 572-581.

REFERENCES

- Danard, M., 1988. "A Diagnostic Method for Computing the Surface Wind from the Geostrophic Wind Including the Effects of Baroclinity." *Monthly Weather Review*, 116, 2712-2716.
- Danard, M., 1989. "A Prognostic Model for the Surface Temperature, Height of the Atmospheric Boundary Layer, and Surface Wind." *Monthly Weather Review*, 117, pp. 67-77.
- Danard, M. and J. Galbraith, 1989. "A Mesoscale Wind Model for the Great Lakes and Vicinity." Prepared by Atmospheric Dynamics Corp. for Ocean Applications Group, NOAA, Monterey, California.
- Danard, M. and J. Galbraith, 1991. "A Mesoscale Prognostic and Nowcast Meteorological Model for British Columbia." Prepared by Atmospheric Dynamics Corp. for Protection Branch, Ministry of Forests, Victoria, British Columbia.
- Danard, M. and G. Jorgensen, 1992. "A Boundary-Layer Model for Calculating Precipitation in Complex Terrain." Prepared by Atmospheric Dynamics Corp. for B.C. Hydro and Power Corp., Burnaby, British Columbia.
- Diaz-Granados, M.A., J.B. Valdes and R.L. Bras, 1984. "A Physically Based Flood Frequency Distribution." *Water Resources Research*, 20(7), 995-1002.
- Dickerson, M.H., 1978. "MASCON-A Mass Consistent Atmospheric Flow Model for Regions with Complex Terrain." *Journal of Applied Meteorology*, 17, 241-253.

REFERENCES

- Dickinson, W.T., P.N. Kelly and H.R. Whately, 1992. "Extremes for Rainfall and Streamflow, How Strong Are the Links?". *Canadian Water Resources Journal*, 17(3), 224-236.
- Dingman, L.S., 1981. Elevation: A Major Influence on the Hydrology of New Hampshire and Vermont, U.S.A. *Hydrological Sciences Bulletin*, 26(4): 399-413.
- Eagleson, P.S., 1972. "Dynamics of Flood Frequency." *Water Resources Research*, 8(4), 878-898.
- Elliot, R.D. and R.W. Shaffer, 1962. "The Development of Quantitative relationships between orographic precipitation and air-mass parameters for use in forecasting and cloud seeding evaluation." *Journal of Applied Meteorology*, 1, 218-228.
- Environment Canada, 1981. "Canadian Climate Normals, 1951-1980, Temperature and Precipitation, British Columbia." Atmospheric Environment Service, Downsview, Ontario.
- Environment Canada, 1982. "Magnitude of Floods, British Columbia and Yukon Territory." Water Survey Canada, Ottawa, Ontario.
- Environment Canada, 1989. "Historical Streamflow Summary, British Columbia." Water Survey of Canada, Ottawa, Ontario.
- Fitzharris, B.B., 1975. "Snow Accumulation and Deposition on a West Coast Midaltitude Mountain." *Unpublished Ph.D. Thesis*, Department of Geography, University of British Columbia, Vancouver, British Columbia, Canada.

REFERENCES

- Fountain, A.G. and W.V. Tangborn, 1985. "The Effect of Glaciers on Streamflow Variations." *Water Resources Research*, 21(4): 579-586.
- Georgakakos, K.P., 1986. "A Generalized Stochastic Hydrometeorological Model for Flood and Flash-Flood Forecasting. 1. Formulation." *Water Resources Research*, 22, 2083-2095.
- Garcia-Guzman, A. and E. Aranda-Oliver, 1993. "A Stochastic Model of Dimensionless Hyetograph." *Water Resources Research*, 29(7), 2363-2370.
- Giorgi, F., 1990. "Stimulation of Regional Climate Using a Limited Area Model Nested in a General Circulation." *Journal of Climate*, 3, 941-963.
- Giorgi, F. and G.T. Bates, 1989. "On the Climatological Skill of a Regional Model Over Complex Terrain." *Monthly Weather Review*, 117, 2325-2347.
- Gumbel, E.J., 1958. "Statistics of Extremes." Columbia University Press, New York, New York.
- Haan, C.T., 1978. "Statistical Methods in Hydrology." Iowa State University Press, Ames, Iowa.
- Haan, C.T. and D.R. Edwards, 1988. "Joint Probability Estimates of Return Period Flows." *Transactions of ASAE*, 31(4), 1115-1119.

REFERENCES

- Hanson, C.L., 1982. "Distribution and Stochastic Generation of Annual and Monthly Precipitation on a Mountainous Watershed in Southwest Idaho." *Water Resources Bulletin*, 18(5): 875-883.
- Harrold, T.W., 1973. "Mechanisms Influencing the Distribution of Precipitation within Baroclinic Disturbances." *Quarterly Journal of the Royal Meteorological Society*, 99, 232-251.
- Hebson, C. and E.F. Wood, 1982. "A Derived Flood Frequency Distribution Using Horton Order Ratios." *Water Resources Research*, 18(5), 1509-1518.
- Hershfield, D.M., 1961. "Rainfall Frequency Atlas of the United States for Durations From 30 Minutes to 24 Hours and Return Periods from 1 to 100 Years." *Technical Paper 40*, U.S. Department of Commerce, Weather Bureau, Washington, D.C.
- Hershfield, D.M., 1962. "Extreme Rainfall Relationships." *Journal Hydraulic Engineering*, 88(6), 73-92.
- Hill, F.F. and K.A. Browning, 1979. "Persistence and Orographic Modulation of Mesoscale Precipitation Area in a Potentially Unstable Warm Sector." *Quarterly Journal of the Royal Meteorological Society*, 105, 57-70.
- Hogg, W.D., 1980. "Time Distribution of Short Duration Storm Rainfall in Canada." In: *Proceedings of the Canadian Hydrology Symposium*, NRCC, Ottawa, Ontario, Canada, 53-63.

REFERENCES

- Hogg, W.D., 1982. "Distribution of Rainfall with Time: Design Considerations." In: *American Geophysical Union Chapman Conference on Rainfall Rates*, April 27-29, Urbana, IL.
- Hogg, W.D. and D.A. Carr, 1985. "Rainfall Frequency Atlas for Canada." Canadian Government Publishing Centre, Ottawa, Ontario.
- Horita, M., 1981. "Heavy Rainfall over Greater Vancouver October 30-November 1, 1981. Pacific Region Technical Notes 81-024. Pacific Weather Centre, Vancouver, British Columbia.
- Hoskins, B.J., 1983. "Dynamical Processes in the Atmosphere and the Use of Models." *Quarterly Journal of the Royal Meteorological Society*, 109, 1-22.
- Hoskings, J.R.M., J.R. Wallis and E.F. Wood, 1985. "An Appraisal of the Regional Flood Frequency Procedure in the U.K.-Flood Studies Report." *Hydrological Sciences Journal*, 30(1), 85-109.
- Huff, F. A., 1967. "Time Distribution of Rainfall in Heavy Storms." *Water Resources Research*, Vol.(3), No. 4, 1007-1019.
- Hughes, D.A. and A. Wright, 1988. "Spatial Variability of Short-term Rainfall Amounts in a Coastal Mountain Region of Southern Africa." *Water SA*, 14(3), 131-138.
- IMSL, 1989. "Mathematical Library Software." User's manual, IMSL, Houston, Texas.

REFERENCES

- Inna, N., R. Loof and B. Hussain, 1993. "Estimation of Flood Flows for Ungauged Catchments in Kashmir (Pakistan)." In: *Proceedings of the 1993 CSCE Annual Conference*, Fredericton, New Brunswick, Canada, 179-187.
- Jarrett, R.D., 1987. "Flood Hydrology of Foothill and Mountain Streams in Colorado." *Unpublished Ph.D. Thesis*. Department of Civil Engineering. Colorado State University, Fort Collins.
- Kendrew, W.G. and D. Kerr, 1955. "The Climate of British Columbia and the Yukon Territory." Queen's Printer, Ottawa, Canada.
- Kite, G.W., 1978. "Frequency and Risk Analyses in Hydrology." Water resources Publications, Fort Collins, Colorado.
- Larson, C.L. and B.M. Reich, 1972. "Relationship of Observed Rainfall and Runoff Recurrence Intervals." In: *1973, Floods and Droughts*. E.F. Schulz, V.A. Koelzer, and K. Mahmood, (eds.). Water Resources Publications, Fort Collins, Colorado, 34-43.
- Lavoie, R.L., 1974. "A Numerical Model of the Trade-Wind Weather on Oahu." *Monthly Weather Review*, 102, 630-637.
- Linsley, R.K., M.A. Kohler, and J.L.H. Paulhus, 1982. "Hydrology for Engineers." McGraw-Hill, New York, N.Y.

REFERENCES

- Longacre, L.L. and H.L. Blaney, 1962. "Evaporation at High Elevations in California." American Society of Civil Engineers, *Journal of the Irrigation and Drainage Division*, 88(IR2): 33-54.
- Lotus Development Co., 1989. "Lotus 123 Version 2.1 - User's Guide." Cambridge, M.A.
- Loukas, A., 1991. "Analysis of the Response and the Rainfall Distribution in a Mountainous Watershed." *Unpublished M.A.Sc. Thesis*, Department of Civil Engineering, University of British Columbia, Vancouver, British Columbia, Canada.
- Loukas, A. and M.C. Quick, 1993a. "Hydrologic Behaviour of a Mountainous Watershed." *Canadian Journal Civil Engineering*, 20(1), 1-8.
- Loukas, A. and M.C. Quick, 1993b. "Rain Distribution in a Mountainous Watershed". *Nordic Hydrology*, 24(4), 225-242.
- Marsalek, J. and W.E. Watt, 1984. "Design Storms for Urban Drainage System." *Canadian Journal Civil Engineering*, 11(4), 574-584.
- Marwitz, J.D., 1974. "An Airflow Case Study Over the San Juan Mountains of Colorado." *Journal of Applied Meteorology*, 13, 450-458.
- Mass, C.J. Jr. and D.P. Dempsey, 1985. "A One-Level, mesoscale model for diagnosing Surface Winds in Mountainous and Coastal Regions." *Monthly Weather Review*, 113, 1211-1227.

REFERENCES

- Melone, A.M., 1985. "Flood Producing Mechanisms in the Pacific Coastal Region." *Canadian Water Resources Journal*, 10(1), 46-64.
- Melone, A.M., 1986. "Extreme Floods in the Pacific Coastal Region." *Unpublished Ph.D. Thesis*, Department of Civil Engineering, University of British Columbia, Vancouver, British Columbia.
- Miller, J.F., R.H. Frederick and R.J. Tracey, 1973. "Precipitation-Frequency Atlas of the Conterminous Western United States." *NOAA Atlas 2*, 11 vols. National Weather Service, Silver Spring, MR.
- Moore, R.D., 1992. "The Influence of Glacial Cover on the Variability of Annual Runoff, Coast Mountains, British Columbia, Canada." *Canadian Water Resources Journal*, 17(2): 101-109.
- Moughamian, M.S., D.B. McLaughlin and R.L. Bras, 1987. "Estimation of Flood Frequency: An Evaluation of Two Derived Distribution Procedures." *Water Resources Research*, 23(7), 1309-1319.
- Muzik, I., 1993. "The Method of Derived Distributions Applied to Peak Flows." In: *Engineering Hydrology*, Proceedings of the ASCE International Symposium, San Francisco, California, 437-442.
- Muzik, I. and C. Chang, 1993. "Hydrograph Prediction in Alberta Foothills." In: *Proceedings of the 1993 CSCE Annual Conference*, Fredericton, New Brunswick, Canada, 129-133.

REFERENCES

- Nickerson, E.C., D.R. Smith and C.F. Chappell, 1978. "Numerical Calculation of Airflow and Cloud During Winter Storm Conditions in the Colorado Rockies and Sierra Nevada Mountains." In: *Conference on Sierra Nevada Meteorology*, American Meteorological Society, Boston, Massachusetts, 126-132.
- O'Loughlin, C.L., 1972. "An Investigation of the Stability of the Steepland Forest Soils in the Coast Mountains, Southwest British Columbia." *Unpublished Ph.D. Thesis*, Faculty of Forestry, University of British Columbia, Vancouver, British Columbia.
- Overland, J.E., M.H. Hitchman and Y-J Han, 1979. "A Regional Surface Wind Model for Mountainous Coastal Areas." NOAA-TR-ERL 407, Pacific Marine Environmental Lab. 32, Seattle, Washington.
- Palisade Co., 1991. "Risk Analysis and Simulation Add-In for Lotus 123." Newfield, N.Y.
- Pelto, M.S., 1989. "Time-series Analysis of Mass Balance and Local Climatic Records from Four Northwestern North American Glaciers." In: *Snow Cover and Glacier Variations*, IAHS Publication No. 183, pp. 95-102.
- Phillip, J.R., 1960. "General Method of Exact Solution of the Concentration-Dependent Diffusion Equation." *Australian Journal of Physics*, 13(1), 1-12.
- Phillips, D., 1990. "Climates of Canada." Ministry of Supply and Services, Ottawa, Canada.

REFERENCES

- Quick, M.C., 1987. "Snowmelt Hydrology and Applications to Runoff Forecasting." National Lecture Tour 1986-1987 sponsored by the Associate Committee on Hydrology of NRC and the Hydrotechnical Committee of CSCE.
- Quick, M.C., 1993. "U.B.C. Watershed Model Manual." University of British Columbia, Department of Civil Engineering, Vancouver, British Columbia.
- Quick, M.C. and A. Pipes, 1989. "High Mountain Snowmelt and Applications to Runoff Forecasting." In: *Proceedings of the 1989 CSCE Annual Conference*, St. Johns, Newfoundland, 232-247.
- Rasmussen, L. A. and W. V. Tagborn, 1976. "Hydrology of the North Cascades Region, Washington 1. Runoff, Precipitation, and Storage Characteristics." *Water Resources Research*, 12(2): 187-202.
- Raines, T.H., and J.B. Valdes, 1993. "Estimation of Flood Frequencies for Ungauged Catchments." *Journal of Hydraulic Engineering*, 119(10), 1138-1154.
- Reksten, D.E. 1987. *A Procedure for Regionalization of Peak Flows in B.C.* British Columbia Ministry of Environment, Lands and Parks, Water Management Division, Hydrology Section, Victoria, British Columbia.
- Reich, B.M., 1970. "Flood Series Compared to Rainfall Extremes." *Water Resources Research*, 6(6), 1655-1667.

REFERENCES

- Rhea, J.O., 1978. "Orographic Precipitation Model for Hydrometeorological Use." Atmospheric Science Paper No. 287, Colorado State University, Fort Collins, Colorado.
- Rodriguez-Iturbe, I. and J.B. Valdes, 1979. "The Geomorphologic Structure of Hydrologic Response." *Water Resources Research*, 15(6), 1409-1420.
- Rodriguez-Iturbe, I. and P.S. Eagleson, 1987. "Mathematical Models of Rainstorm Events in Space and Time." *Water Resources Research*, 23, 181-190.
- Rodriguez-Iturbe, I., M. Gonzalez and R.L. Bras, 1982. "A Geomorphologic Climate Theory of Instantaneous Unit Hydrograph." *Water Resources Research*, 18(4), 877-886.
- Rohrer, M., 1989. "Determination of the Transition Air Temperature from Snow to Rain and Intensity of Precipitation. In: *Precipitation Measurement*, St. Moritz, Switzerland, 475-482.
- Ross, D.G., I.N. Smith, P.C. Marius and D.G. Fox, 1988. "Diagnostic Wind Field Modeling for Complex Terrain: Model Development and Testing." *Journal of Climatology and Applied Meteorology*, 27, 785-796.
- Rosso, R., 1984. "Nash Model Relation to Horton Order Ratios." *Water Resources Research*, 20(7), 914-920.
- Russell, S.O., 1982. "Flood Probability Estimation." *Journal of Hydraulic Engineering*, 108(1), 63-73.

REFERENCES

- Sabol, G.V., 1993. "Lag Relations for Semi-Arid Regions and Urban Areas." In: *Engineering Hydrology*, Proceedings of the ASCE International Symposium, San Francisco, California, 168-173.
- Sarino, and S.E. Serrano, 1990. "Development of the Instantaneous Unit Hydrograph Using Stochastic Differential Equations." *Stochastic Hydrology and Hydraulics*, 4, 151-160.
- Schermerhorn, V. P., 1967. "Relations Between Topography and Annual Precipitation in Western Oregon and Washington." *Water Resources Research*, 3(3): 707-711.
- Schaefer, D.G., 1973. "A Record-breaking Summer Storm over the Lower Fraser Valley." *Technical memorandum, TEC 787*, Atmospheric Environment Service, Environment Canada, Vancouver, British Columbia.
- Schaefer, D.G., 1978. "An Overview of the Climates of Western North America." In: *IUFRO-Joint Meeting of Working Parties*, Vancouver, British Columbia, Canada, pp. 1-23.
- Schaefer, D.G., 1979a. "Meteorological Developments Contributing to the Terrace Area Flood of Early November, 1978." *Technical Report*, Atmospheric Environment Service, Environment Canada, Vancouver, British Columbia.
- Schaefer, D.G., 1979b. "The Multi-Day Rainstorm of October-November, 1978, on the Queen Charlotte Islands." *Technical Report*, Atmospheric Environment Services, Environment Canada, Vancouver, British Columbia.

REFERENCES

- Schaefer, D.G., 1980. "The Rainstorm of December 13-18, 1979 over Southwestern British Columbia." *Technical Report*, Atmospheric Environment Service, Environment Canada, Vancouver, British Columbia.
- Schaefer, D.G., 1982. "Meteorological Conditions Associated with Slides and Floods in the Lower Mainland of British Columbia in late October, 1981." *Technical Report*, Atmospheric Environment Service, Vancouver, British Columbia.
- Schaefer, D. G. and S. N. Nikleva, 1973. "Mean Precipitation and Snowfall Maps for a Mountainous Area of Potential Urban Development." In: *Western Snow Conference*, 41, pp. 80-89.
- Sharon, D., 1980. "The Distribution of Hydrologically Effective Rainfall Incident on Sloping Ground." *Journal of Hydrology*, 46, 165-168.
- Sevruk, B., 1982. "Methods of Correction for Systematic Errors in Point Precipitation Measurement for Operational Use." *WMO- No. 589*, Geneva, Switzerland.
- Sevruk, B., 1989. "Reliability of Precipitation Measurement." In: *Precipitation Measurement*, B. Sevruk (ed.), St. Moritz, Switzerland, 13-19.
- Smith, R.B., 1989. "Mechanisms of Orographic Precipitation." *Meteorological Magazine*, 118: 85-88.

REFERENCES

- Storr, D. and H.L. Ferguson, 1972. "The Distribution of Precipitation in Some Mountainous Canadian Watersheds." In: *WMO Symposium for the Distribution of Precipitation in Mountainous Areas, II*, pp. 241-263.
- Terstriep, M.L. and J.B. Stall, 1974. "The Illinois Urban Drainage Area Simulator, ILLUDAS." *Illinois State Water Survey Bulletin 58*, Chicago, Illinois.
- U.S. Army Corps of Engineers 1990. "HEC-1 Flood Hydrograph Package." Hydrologic Engineering Center, Davis, California.
- U.S. Department of Agriculture-Soil Conservation Service, 1972. "Hydrology. Section 4, National Engineering Handbook." Soil Conservation Service. U.S. Department of Agriculture, Washington, DC.
- U.S. Department of Agriculture, 1980. "CREAMS - A Field-Scale Model for Chemicals, Runoff, and Erosion from Agricultural Management Systems." *Conservation research report No. 26*, Science and Education Administration, Washington, D.C.
- U.S. Department of Agriculture-Soil Conservation Service, 1986. "Urban Hydrology for Small Watersheds." *Technical Release No. 55*, Washington, D.C.
- Walker, E.R., 1961. "A Synoptic Climatology for Parts of the Western Cordillera." Arctic Meteorology Research Group, Publications in Meteorology No. 35, McGill University, Montreal, Quebec.

REFERENCES

- Watt, W.E. and K.C.A. Chow, 1985. "A General Expression for Basin Lag Time." *Canadian Journal of Civil Engineering*, 12, 294-300.
- Watt, W.E., K.C. Chow, W.D. Hogg and K.W. Lathem, 1986. "A 1-h Urban Design Storm for Canada." *Canadian Journal of Civil Engineering*, 13(2), 293-300.
- Watt, W.E., K.W. Lathem, C.R. Neill, T.L. Richards, and J. Rousselle, 1989. "Hydrology of Floods in Canada-A Guide to Planning and Design." National Research Council Canada-Associate Committee on Hydrology, Ottawa, Ontario.
- Watts, L.G. and A. Calver, 1991. "Effects of Spatially-Distributed Rainfall on Runoff for a Conceptual Catchment." *Nordic Hydrology*, 22(1), 1-14.
- Wheater, H.S., A.P. Butler, E.J. Stewart and G.S. Hamilton, 1991. "A Multivariate Spatial-Temporal Model of Rainfall in Southwestern Saudi Arabia. I. Spatial Rainfall Characteristics and Model Formulation." *Journal of Hydrology*, 125, 175-199.
- Wiesner, C.J., 1970. "Hydrometeorology." Chapman and Hall Ltd, Edinburgh, Great Britain.
- Williams, P., 1948. "The Variation of the Time of Maximum Precipitation along the West Coast of North America." *Bulletin of the American Meteorological Society*, 29(4), 143-145.
- Wilson, H.P., 1978. "On Orographic Precipitation ." In: *Climatic Networks: Proceedings of the Workshop and Annual Meeting of the Alberta Climatological Association*, Fisheries and Environment Canada, Edmonton, Alberta, 82-121.

REFERENCES

Yang, J.C., S.Y. Tarn, and Y.K. Tung, 1993. "Analyzing Uncertainty of IUH of Nash." In: *Hydraulic Engineering*, Proceedings of the ASCE National Symposium, San Francisco, California, 168-173.

Yung, K.C., 1974. "A Numerical Simulation of Wintertime, Orographic Precipitation." *Journal of Atmospheric Science*, 31, 1735-1767.

APPENDIX A

PRECIPITATION AND STREAMFLOW STATIONS USED IN THE STUDY OF LONG-TERM PRECIPITATION

APPENDIX A

Table A1. Precipitation Stations in coastal British Columbia.

Name	Station Number*	Elevation (m)	Period of Record
ABBOTSFORD	1100030	58	1944-1980
AGASSIZ CDA	1100120	15	1889-1966
AIYANISH	1070150	229	1924-1971
ALBERNI BC	1030180	91	1894-1959
ALBERNI LC	1030210	9	1948-1974
ALBERNI ML	1030220	43	1958-1973
ALBERNI RC	1030185	75	1962-1969
ALDERGROVE	1100240	76	1953-1980
ALERT BAY	1020270	52	1913-1980
ALICE ARM	1060330	314	1948-1964
ALOUETTE L	1100360	117	1924-1970
ALTA LAKE	1040390	668	1950-1976
ALTA LAKE2	1040420	640	1931-1969
AMPHITRITE P	1030425	11	1968-1980
BALLENAS LIGHT	1020590	11	1966-1980
BAMBERTON OC	1010595	85	1961-1980
BAMFIELD EAST	1030605	4	1959-1980
BEAR CR	1010720	351	1964-1971
BECHER BAY	1010780	12	1956-1966
BELLA BELLA	1060810	12	1964-1977
BELLA COOLA	1060840	18	1939-1980
BELLA COOLA BC H	1060842	14	1961-1980
BENSON LAKE	1030850	145	1959-1972
BLACK CREEK	1020880	46	1976-1980
BLIND CHANNEL	1020885	3	1956-1980
BONILLA ISL	1060902	16	1960-1980
BOWEN ISL AB	1040908	23	1959-1965
BOWEN ISL BB	104090R	8	1966-1978
BRITANNIA B	1041050	49	1913-1974
BUNTZEN LAKE	1101140	17	1969-1980
BURNABY BR	1101144	125	1959-1970
BURNABY CAPITOL	1101146	183	1960-1980
BURNABY MTN	1101155	137	1958-1980
BURNABY SFU	1101158	336	1965-1980
BURQUITLAM	1101200	61	1926-1975
CAMPBELL RIV	1021260	79	1936-1969
CAMERON LAKE	1021230	198	1924-1980
CAMPBELL RIV A	1021261	105	1965-1980
CAMPBELL RIV BCFS	1021262	128	1969-1980
CAPE LAZO	1021320	38	1935-1962

APPENDIX A

Table A1. Precipitation Stations in coastal British Columbia.(cont.)

Name	Station Number*	Elevation (m)	Period of Record
CAPE SCOTT	1031353	72	1965-1980
CAPE ST JAMES	1051350	89	1944-1980
CARMANAH POINT	1031402	38	1968-1980
CARNATION CREEK CDF	1031413	61	1971-1980
CENTRAL SAANICH ISL	10114F6	38	1970-1980
CENTRAL SAANICH V	1011467	53	1970-1980
CHATHAM POINT	1021480	20	1958-1970
CHEMAINUS	1011500	53	1934-1979
CHILLIWACK	1101530	6	1950-1980
CHILLIWACK GR	1101545	12	1961-1980
CHILLIWACK R FCR	1101565	457	1966-1980
CHILLIWACK R MT THURSTON	1101N65	198	1963-1980
CHILLIWACK RIV CT	1101564	488	1961-1976
CLOWHOM FALLS	1041710	23	1932-1980
COAL HARB	1031735	57	1970-1980
COBBLE HILL	1011745	61	1970-1980
COMOX A	1021830	24	1944-1980
COQUITLAM L	1101890	161	1924-1980
CORDOVA BAY	1011920	37	1951-1980
CORTES ISL	1021950	6	1947-1980
CORTES ISL TB	1021960	5	1960-1973
COURTENAY	1021990	24	1930-1980
COURTENAY GR	1021988	81	1972-1980
COWICHAN BAY	1012010	104	1953-1980
COWICHAN LAKE F	1012040	177	1949-1980
COWICHAN LAKE WEIR	1012055	163	1960-1980
CULTUS LAKE	1102220	46	1962-1980
CUMBERLAND	1022250	159	1922-1980
DAISY LAKE DAM	1042255	381	1968-1980
DELTA LADNER SOUTH	1102417	2	1971-1980
DELTA PEBBLE	1102420	12	1961-1980
DELTA TSAWWASSEN	1102424	53	1959-1969
DELTA TSAW. BEAC.	1102425	2	1971-1980
DENMAN ISL	1022430	35	1910-1965
DUNCAN BAY	1022560	7	1957-1980
DUNCAN FOR	1012570	6	1958-1980
EAST SOOKE	1012628	37	1966-1980
EGG ISL	1062646	12	1965-1980
ELK LAKE	1012655	114	1957-1978
ESQUIMALT M	1012700	12	1872-1950

APPENDIX A

Table A1. Precipitation Stations in coastal British Columbia.(cont.)

Name	Station Number*	Elevation (m)	Period of Record
ESTEVAN POINT	1032730	7	1908-1980
ETHELDA BAY	1062745	8	1957-1980
FALLS RIV	1062790	18	1931-1980
GABIOLA ISL	1023042	46	1967-1980
GALIANO ISL	1013045	15	1956-1977
GAMBIER HAR	1043048	61	1962-1980
GARIBALDI	1043060	381	1921-1980
GIBSONS	1043150	126	1949-1980
GIBSONS GP	1043152	34	1961-1980
GOLD RIV	1033232	117	1966-1980
GRAHAM INLET	1203255	660	1973-1980
HANEY CI	1103324	142	1960-1980
HANEY EAST	1103326	30	1959-1980
HANEY UBC RF SP17	1103334	373	1961-1972
HANEY UBC RFA	1103332	143	1961-1980
HANEY UBC RFLL	1103333	354	1962-1972
HANEY UBC RFM	110CCCC	114	1945-1972
HATZIC PR	1103342	9	1959-1976
HELLS GATE	1113420	122	1951-1980
HOLBERG	1033480	52	1956-1980
HOLBERG FD	1033483	46	1967-1980
HOLLYBURN RIDGE	1103510	951	1954-1980
HOPE A	1113540	39	1935-1980
HOPE KL	1113550	152	1955-1977
HOPKINS L	1043582	8	1969-1980
IOCO REF	1103660	53	1955-1980
JAMES ISL	1013720	54	1914-1978
KEMANO	1064020	70	1951-1980
KENSINGTON PR	1104080	27	1953-1978
KILDALA	1064138	30	1966-1980
KILDONAN	1034170	3	1972-1976
KINGCOME INLET	1064227	2	1974-1985
KITIMAT 2	1064321	17	1966-1980
KITIMAT MISSION	1064290	6	1939-1948
KITIMAT TOWN	1064320	128	1954-1980
KLEENA KL	1084350	899	1942-1968
KYUQUOT	1034440	3	1933-1959
LADNER	1104470	1	1952-1971
LADNER MSTN	1104477	0	1959-1971
LADNER PG	1104484	0	1960-1975

APPENDIX A

Table A1. Precipitation Stations in coastal British Columbia.(cont.)

Name	Station Number*	Elevation (m)	Period of Record
LAKELSE LK	1064497	85	1967-1980
LANGARA	1054500	41	1936-1980
LANGFORD LAKE	1014530	76	1953-1980
LANGLEY L	1104555	101	1957-1980
LANGLEY PR	1104560	87	1953-1980
LOIS RIV DAM	1044680	131	1954-1956
LUND	1044732	14	1960-1975
MALIBU JERVIS INLET	1044840	8	1974-1980
MASSET	1054920	3	1897-1968
MASSET CFS	10549BN	12	1971-1980
MAYNE ISLAND	1014931	30	1970-1980
MCINNES ISL	1064010	23	1954-1980
MERRY ISL	1045100	6	1942-1980
MESCHOSIN HV	1015107	76	1968-1980
MILL BAY	1015134	46	1972-1980
MILNER AIC	1105155	8	1967-1979
MILNES LANDING	1015160	38	1910-1956
MISSION	1105190	56	1957-1980
MISSION WA	1105192	221	1962-1980
MOUNT SEYMOUR	1105230	823	1958-1968
MUD BAY FRB	1025240	11	1971-1980
MUIR CR	1015242	30	1970-1980
MULE CR	1205248	884	1970-1980
NANAIMO	1025340	70	1892-1980
NANAIMO A	1025370	30	1947-1980
NANAIMO CHUB	10253P0	21	1969-1980
NANAIMO DEP BAY	1025C70	8	1970-1980
NEW WESTMINSTER	1105550	119	1894-1980
NEW WESTMINSTER BCPEN	1105553	18	1960-1980
NEW WESTMINSTER W	1105570	84	1960-1971
N.VANCOUVER 2ND NAR	1105666	4	1957-1980
N.VANCOUVER CAPILANO	1105655	67	1955-1980
N.VANCOUVER CLEVELAND	110EF56	157	1968-1980
N.VANCOUVER CLOVERL.	110EFEF	79	1968-1980
N.VANCOUVER HOLYROOD	1105659	183	1958-1968
N.VANCOUVER LYNN CR	1105660	191	1964-1980
N.VANCOUVER RDR	110N6F5	229	1973-1980
N.VANCOUVER SEYMOUR	110EFFF	9	1968-1980
N.VANCOUVER UP.LYNN	1105668	177	1960-1980
N.VANCOUVER WHARVES	1105669	6	1962-1980

APPENDIX A

Table A1. Precipitation Stations in coastal British Columbia.(cont.)

Name	Station Number*	Elevation (m)	Period of Record
N.VANCOUV. GROUSE	1105658	1128	1971-1980
OCEAN FALLS	1065670	5	1924-1980
OYSTER RIV UBC	1025915	11	1967-1980
PACHENA POINT	1035940	46	1924-1980
PARKSVILLE	1025970	82	1915-1960
PENDER ISL	1016120	15	1924-1965
PIERS ISL	1016169	0	1973-1980
PITT MEADOWS L	1106177	6	1960-1969
PITT POLDER	1106180	2	1951-1980
POINT ATKINSON	1106200	9	1968-1980
PORT ALBERNI	1036205	59	1917-1962
PORT ALBERNI A	1036206	2	1969-1980
PORT ALBERNI CCR	1036207	70	1960-1980
PORT ALBERNI RED	1036210	21	1947-1980
PORT ALICE	1036240	15	1924-1980
PORT CLEMENTS	1056250	8	1967-1980
PORT COQUITLAM	1106255	7	1958-1980
PORT HARDY A	1026270	22	1944-1980
PORT HARDY BHR	1026274	5	1959-1975
PORT KELLS	1106300	9	1953-1965
PORT MELLON	1046330	8	1942-1980
PORT MOODY GRFY	1106CL2	130	1970-1980
PORT RENFREW BCFP	1016335	6	1970-1980
POWELL RIVER	1046390	52	1924-1980
POWELL RIVER A	1046391	130	1953-1980
POWELL RIVER W	1046410	55	1960-1980
PRINCE RUPERT	1066480	52	1908-1963
PRINCE RUPERT A	1066481	34	1961-1980
PRINCE RUPERT MC	1066488	85	1959-1980
PRINCE RUPERT PARK	1066492	91	1959-1980
PRINCE RUPERT SH	1066193	11	1966-1980
QUALICUM RFR	1026563	8	1962-1980
QUATSINO	1036570	8	1895-1980
RIVER JORDAN	1016780	3	1908-1980
SAANICH DAO	10169DK	223	1916-1977
SAANICH DEN	1016942	38	1963-1974
SAANICTON CDA	1016940	61	1914-1980
SALT SPRING ISL	1016990	73	1945-1980
SALT SPRING IV	1017000	7	1955-1980
SANDSPIT A	1057050	5	1945-1980

APPENDIX A

Table A1. Precipitation Stations in coastal British Columbia.(cont.)

Name	Station Number*	Elevation (m)	Period of Record
SARDIS	1107080	107	1954-1980
SAYWARD BCFS	1027114	15	1973-1980
SECHELT	1047170	23	1927-1968
SEWALL MASSET IN	105PA91	3	1974-1980
SEWELL INLET	1057192	12	1973-1980
SEYMOUR FALLS	1107200	244	1927-1980
SHAWNIGAN L	1017230	137	1918-1980
SOOKE	1017556	27	1970-1980
SOOKE LAKE	1017560	173	1913-1966
SOOKE LAKE N	1017563	229	1966-1980
SOUTH PENDER ISLAND	1017610	61	1966-1980
SPRING ISL	1037650	11	1949-1979
SQUAMISH	1047660	2	1959-1980
SQUAMISH FMC CHEMICALS	1047662	3	1968-1980
STAVE FALLS	1107680	55	1959-1989
STEVENSON	1107710	1	1896-1980
STEWART	1067740	5	1926-1967
STEWART A	1067742	7	1974-1980
STEWART BCHPA	1067745	12	1967-1976
STILLWATER PH	1047770	24	1931-1980
STRATHCONA DAM	1027775	201	1967-1980
SUMAS CANAL	1107785	6	1957-1980
SURREY KP	1107873	93	1960-1980
SURREY MH	1107876	76	1962-1980
SURREY N	1107878	73	1960-1980
SURREY S	1107879	101	1960-1980
TAHSIS	1037890	5	1952-1980
TAHTSA LAKE WEST	1087950	863	1951-1980
TASU SOUND	1058003	15	1963-1980
TATLAYOKO LAKE	1088010	853	1928-1980
TERRACE A	1068130	217	1944-1980
TERRACE PCC	1068131	58	1968-1980
TEXADA ISL	1048140	24	1960-1980
TLELL	1058190	5	1950-1980
TOFINO A	1038205	20	1942-1980
TUNNEL CAMP	1048310	671	1924-1974
UCLUELET KENNEDY CAMP	1038330	12	1914-1948
VANCOUVER A	1108447	3	1936-1980
VANCOUVER CITY H	1108430	86	1924-1980
VANCOUVER DUNBAR	1108435	61	1955-1974

APPENDIX A

Table A1. Precipitation Stations in coastal British Columbia.(cont.)

Name	Station Number*	Elevation (m)	Period of Record
VANCOUVER HARBOUR	1108446	0	1925-1980
VANCOUVER KERRISDALE	1108449	88	1970-1980
VANCOUVER KITSILANO	1108453	34	1956-1980
VANCOUVER OAK 53	1108462	82	1970-1977
VANCOUVER PMO	1108465	59	1898-1979
VANCOUVER SF	1108475	64	1955-1972
VANCOUVER SOUTH	1108436	61	1966-1982
VANCOUVER UBC	1108487	87	1957-1980
VICTORIA A	1018620	19	1940-1980
VICTORIA GH	1018614	43	1959-1980
VICTORIA GHTS	1018610	69	1898-1980
VICTORIA HIGHLAND	1018616	152	1961-1980
VICTORIA L	1038640	29	1953-1962
VICTORIA MARINE	1018642	32	1967-1980
VICTORIA PS	101HFEE	8	1973-1980
VICTORIA SHELBOURNE	101QF57	38	1964-1974
VICTORIA SS	101QEFG	21	1961-1973
VICTORIA T	1018660	23	1958-1980
WANNOCK RIV	1068677	8	1974-1980
WHALLEY FN	1108890	84	1958-1980
WHITE ROCK	1108910	61	1929-1970
WHITE ROCK STP	1108914	15	1964-1980
WHONNOCK 269 ST	1108927	61	1960-1975
WHONNOCK HILL	1108925	213	1957-1969
WILLIAM HEAD	1018935	12	1959-1980
WOODFIBRE	1048974	6	1960-1980
W.VANCOUVER D	1108829	2	1971-1980
W.VANCOUVER M	1108840	38	1961-1980
W.VANCOUVER P	1108846	122	1961-1972
YOUBOU	1019010	174	1959-1967

*Official Environment Canada station number

APPENDIX A

Table A2. Streamflow gauging stations in the coastal British Columbia.

	Station Number*	Basin Mean Elevation (m)	Area (km2)	Years of Record
ANDERSON CREEK	08MH104	46	27	1965-1987
ATNARKO RIVER	08FB006	1024	2430	1965-1988
BELLA COOLA RIVER	08FB002	673	310	1948-1968
BELLA COOLA R.BBC	08FB007	920	3730	1965-1988
BINGS CREEK	08HA016	207	15.5	1961-1988
CAMPBELL RIVER	08HD001	589	1400	1910-1949
CARNATION CREEK	08HB048	765	10.1	1973-1988
CHAPMAN CREEK	08GA060	680	64.5	1971-1988
CHEAKAMUS RIVER	08GA024	1010	287	1925-1947
CHEMAINUS	08HA001	644	355	1915-1988
ENGLISMAN RIVER	08HB002	828	324	1915-1988
HIRSCH CREEK	08FF002	820	347	1966-1988
JACOBS CREEK	08MH108	483	12.2	1966-1978
KANAKA CREEK	08MH076	168	47.7	1960-1988
KEMANO RIVER	08FE002	912	583	1972-1988
KITIMAT RIVER	08FF001	960	1990	1967-1988
KOKISH RIVER	08HF001	799	290	1927-1941
KOKSILAH RIVER	08HA003	493	209	1960-1988
LITTLE WEDEENE R.	08FF003	855	188	1967-1988
MACKAY CREEK	08GA061	497	3.63	1974-1988
MAHOOD CREEK	08MH020	35	16	1927-1974
MAHOOD CREEK	08MH018	34	18.4	1927-1985
MAMQUAM RIVER	08GA054	911	334	1967-1986
MURRAY CREEK	08MH129	50	26.2	1970-1982
NICOMEKL RIVER	08MH105	29	64.5	1966-1984
NIMPkish RIVER	08HF002	802	1760	1928-1935
NOONS CREEK MD	08GA065	382	2.59	1977-1988
NOONS CREEK PM	08GA052	253	4.4	1965-1975
NORRISH CREEK	08MH058	598	117	1960-1988
NORTH ALLOUETTE R.	08MH006	478	37.3	1961-1988
NUSATSUM RIVERF	08FB005	897	269	1966-1988
OYSTER CREEK	08HD011	701	298	1974-1988
PALLANT CREEK	08DB002	519	76.7	1968-1987
RUBBLE CREEK	08GA023	673	74.1	1925-1934
SALLOOMT RIVER	08FB004	883	161	1965-1988
SAN JUAN RIVER	08HA010	414	580	1960-1988
SARITA RIVER	08HB014	442	162	1950-1988
SLESSE CREEK	08MH056	1104	162	1957-1988
STAWAMUS RIVER	08GA064	785	40.4	1972-1988

APPENDIX A

Table A2. Streamflow gauging stations in the coastal British Columbia.(cont.)

	Station Number	Basin Mean Elevation (m)	Area (km ²)	Years of Record
TSABLE RIVER	08HB024	681	113	1961-1988
TSITIKA RIVER	08HF004	792	360	1975-1988
UCONA RIVER	08HC002	589	185	1957-1988
YAKOUM RIVER	08DA002	351	477	1963-1987
YORKSON CREEK	08MH097	43	5.96	1965-1977
ZEBALLOS RIVER	08HE006	725	181	1960-1988
ZYMOETZ RIVER	08EF005	858	2980	1964-1988
ZYMOETZ RIVER TER.	08EF003	549	100	1953-1963

**Official Environment Canada station number*

APPENDIX B

RELATIONSHIP BETWEEN EXTREME 24-HOUR RAINFALL AND MEAN ANNUAL PRECIPITATION

APPENDIX B

Table B1. Characteristics of the sixty-one stations used in the analysis
of the 24-hour extreme rainfall.

Station	Mean annual Precipitation (mm)	Station Elevation (m)	24-hour Extreme Rainfall Return Period					
			(mm)					
			2	5	10	25	50	100
ABBOTSFORD A	1562.9	58	61.7	77.8	88.3	101.8	111.6	121.4
AGASSIZ A	1727.8	15	73	88.6	98.9	111.8	121.4	131
ALLOUETE LAKE	2775.3	117	97.7	117.6	130.8	147.6	159.8	172.1
ALTA LAKE	1415.4	668	43	56.2	64.8	75.8	84	92.2
BEAR CREEK	3513.9	351	141.8	205.2	247.2	300.2	339.4	378.5
BELLA COOLA H	2109.3	14	88.3	113.8	130.6	151.9	167.5	183.1
BUNTZEN LAKE	2909.5	17	111.4	151	177.4	210.5	235.2	259.7
BURNABY MTN BCHPA	1908.9	465	75.1	89.8	99.6	111.8	121	129.8
CAMPBELL R. BCFS	1655.9	128	54	65.3	73	82.6	89.8	96.7
CAMPBELL R.A.	1409.1	106	60	67.2	76.8	84	91.2	96
CAMPBELL RIVER BC.	1406	30	60	69.8	76.3	84.5	90.7	96.7
CARNATION CREEK	2770.3	61	91.9	119	137.3	159.8	176.9	193.7
CHILLIWACK MICR.	1850.5	229	55.2	66.5	73.9	83.5	90.5	97.4
CLOWHOM FALLS	2230	23	78	92.9	102.7	115.2	124.3	133.4
COMOX A	1187.6	24	58.1	69.4	77	86.4	93.6	100.6
COQUITLAM LAKE	3616	161	143.8	174.5	194.6	220.3	239.3	258.2
COURTENEY PUNTL.	1464.7	24	66.2	84.5	96.7	112.1	123.4	134.6
DAISY LAKE DAM	2054.2	381	66.2	78.7	87.1	97.7	105.4	113
ESTEVAN POINT	3180.6	7	131	168.2	193	223.9	247.2	270
HANEY MICR.	1763.9	320	78.7	97	109	124.3	135.6	146.9
HANEY UBC	2183.5	143	89.3	111.8	126.7	145.4	159.4	173.3
HOPE A	1915.7	39	86.4	120	144	165.6	187.2	208.8
KITIMAT	2740.1	17	88.8	109.7	123.6	141.1	154.3	167
LADNER BCHPA	981.7	2	43.2	56.2	64.6	75.6	83.5	91.4
ANGLEY LOCHIEL	1482.2	101	61.2	75.6	85.2	97.2	106.3	115.2
MISSION WEST A.	1841.5	221	72.5	85.4	94.1	105.1	113	121.2
NANAIMO DEP.BAY	955.6	8	41.3	50.4	56.4	64.1	69.8	75.4
N.VANC.LYNN CR.	2695.7	191	120.2	156.5	180.5	211	233.5	255.8
PITT MEADOWS STP	1804.7	5	67.7	85.7	97.4	112.6	123.8	134.9
PITT POLDER	2326.2	2	98.9	119	132.2	149	161.5	173.8
PORT ALBERNI A	1886	2	87.1	108.5	122.9	140.9	154.3	167.5
P. COQUITLAM CITY	1930.9	7	81.1	96.7	107	120	129.6	139.2
PORT HARDY	1870.6	22	89.5	116.6	134.6	157.4	174.2	190.8
PORT MELLON	3307.1	8	142.6	176.6	199.4	222.8	249.4	270.2
PORT MOODY G.	1889.3	130	84.5	105.4	119	136.3	149	161.8
PORT RENFREW BCFS	3943.2	3	168	197.3	217	241.4	259.7	277.9
PRINCE RUPERT A	2551.6	34	89.5	112.3	127.7	146.6	161	175

APPENDIX B

Table B1. Characteristics of the sixty-one stations used in the analysis
of the 24-hour extreme rainfall.(cont.)

Station	Mean annual Precipitation (mm)	Station Elevation (m)	24-hour Extreme Rainfall Return Period					
			(mm)					
			2	5	10	25	50	100
SAANICH DENSMORE	928.4	38	49.4	67	78.5	93.1	103.9	115
SANDSPIT A	1359.1	5	52.1	59.8	65	71.3	76.1	80.9
SEYMOUR 21A	3291.6	640	124.4	161.5	185.9	209.7	240.2	263.3
SEYMOUR 25B	3256.6	762	131.7	170.7	196.9	221.3	253.6	278
SEYMOUR ELBOW CR	3427.4	305	114	144.5	164	183.5	208.5	226.8
SPRING ISLAND	3155.1	11	121.7	156.7	179.8	209	230.9	252.5
STAVE FALLS	2296.8	55	83.8	106.3	121.4	140.4	154.3	168.2
STRATHCONA DAM	1381.2	201	61.7	88.1	105.4	127.4	143.8	160.1
SURREY KWANTLEN P.	1574.6	93	67.9	89.3	103.4	121.4	134.9	148.1
SURREY MUNICIPAL H.	1355.9	76	55.4	68.4	77	87.8	96	103.9
TERRACE A	1295.3	217	55.7	79.4	95.3	115.2	129.8	144.5
TERRACE PCC	1136.9	58	43.9	58.8	68.6	81.1	90.2	99.4
TOFINO A	3295.4	20	128.2	157	176.4	200.6	218.6	236.6
VANCOUVER A	1167.4	3	62.2	75.8	85	96.2	104.6	113.3
VANCOUVER HARBOUR	1540.3	0	52.8	66.5	75.4	86.6	95	103.4
VANCOUVER KITS.	1367.1	23	60.2	76.3	86.9	100.1	110.2	120
VANCOUVER PMO	1588.9	59	68.6	94.3	111.6	133	149	164.9
VANCOUVER UBC	1288.6	87	57.8	74.2	85.2	98.9	109	119
VICT. GONZALES H.	619.2	69	45.1	63.8	76.3	91.9	103.7	115.2
VICTORIA INT.A	857.9	19	49.4	63.1	72.2	83.8	92.4	101
VICTORIA MARINE R.	1226.9	32	64.8	84.5	97.4	114	126.2	138.5
VICTORIA SHELBOURNE	790	38	44.9	61.7	73	87.1	97.4	108
VICTORIA UVIC	708.2	46	49.9	67.7	79.7	94.6	105.6	116.6
WHITE ROCK STP	1098.2	15	50.4	64.8	74.4	86.6	95.5	104.6

APPENDIX B

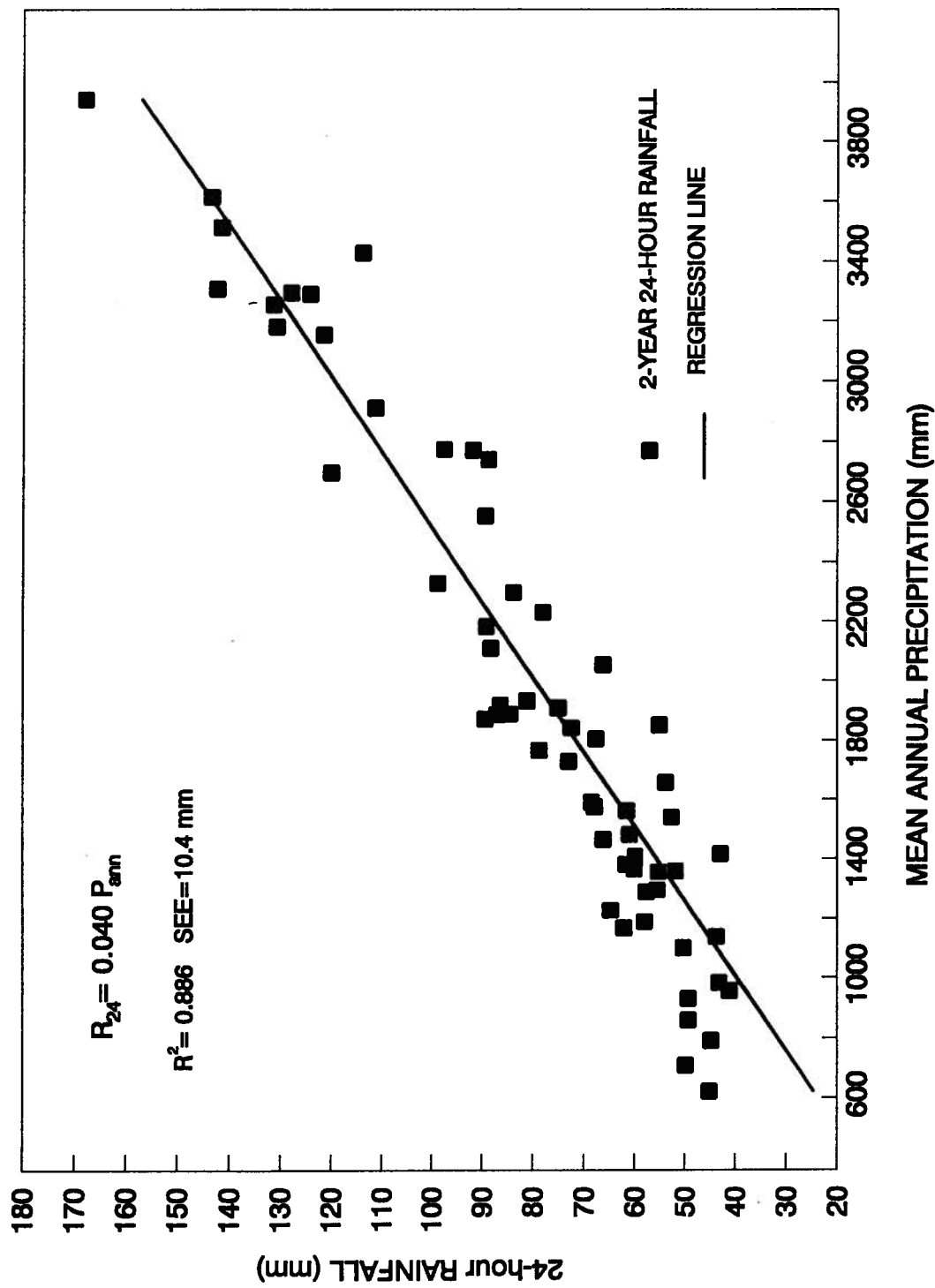


Fig. B1. Relationship of the 2-year 24-hour rainfall and mean annual precipitation for the sixty-one recording stations in coastal British Columbia.

APPENDIX B

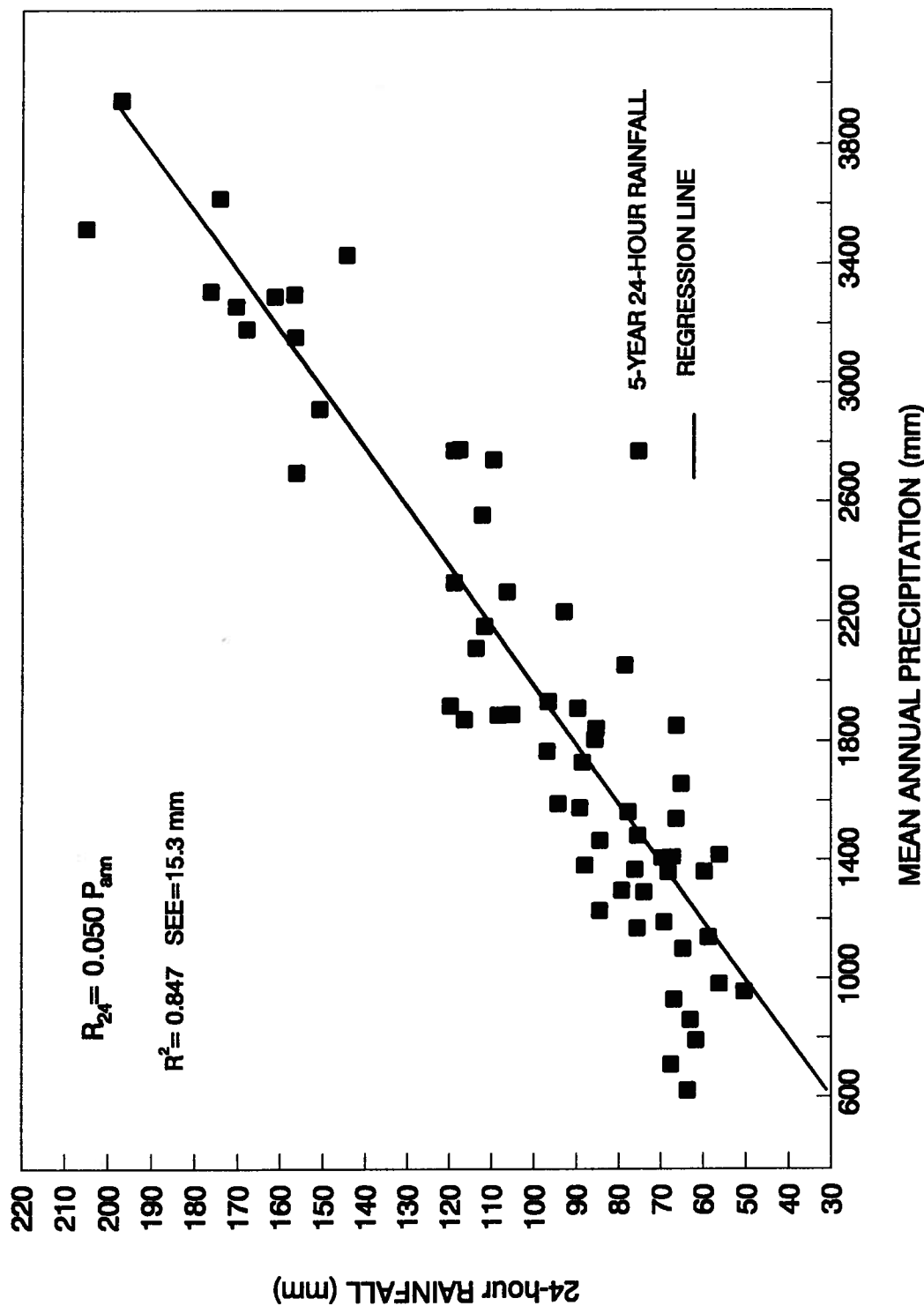


Fig. B2. Relationship of the 5-year 24-hour rainfall and mean annual precipitation for the sixty-one recording stations in coastal British Columbia.

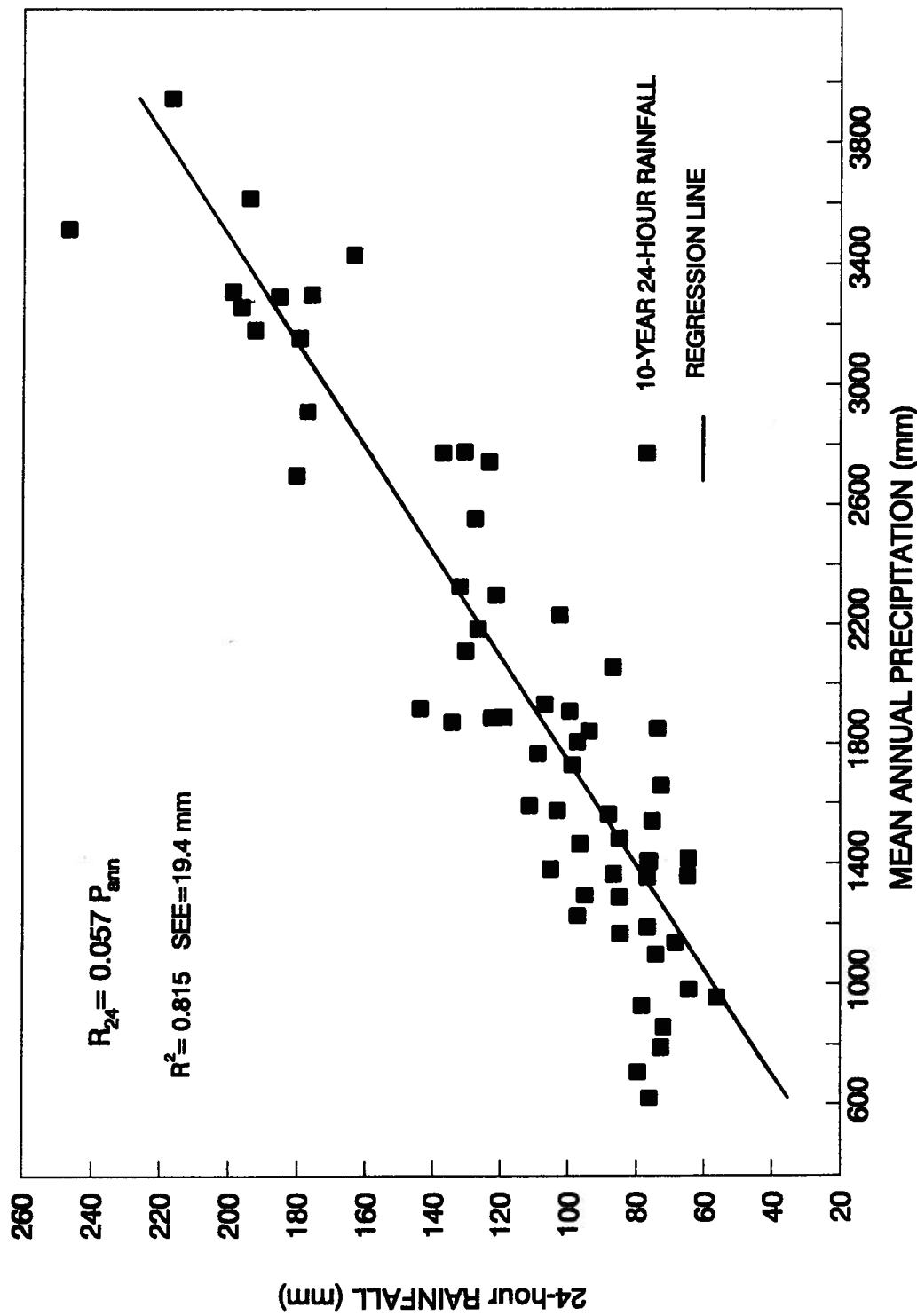


Fig. B3. Relationship of the 10-year 24-hour rainfall and mean annual precipitation for the sixty-one recording stations in coastal British Columbia.

APPENDIX B

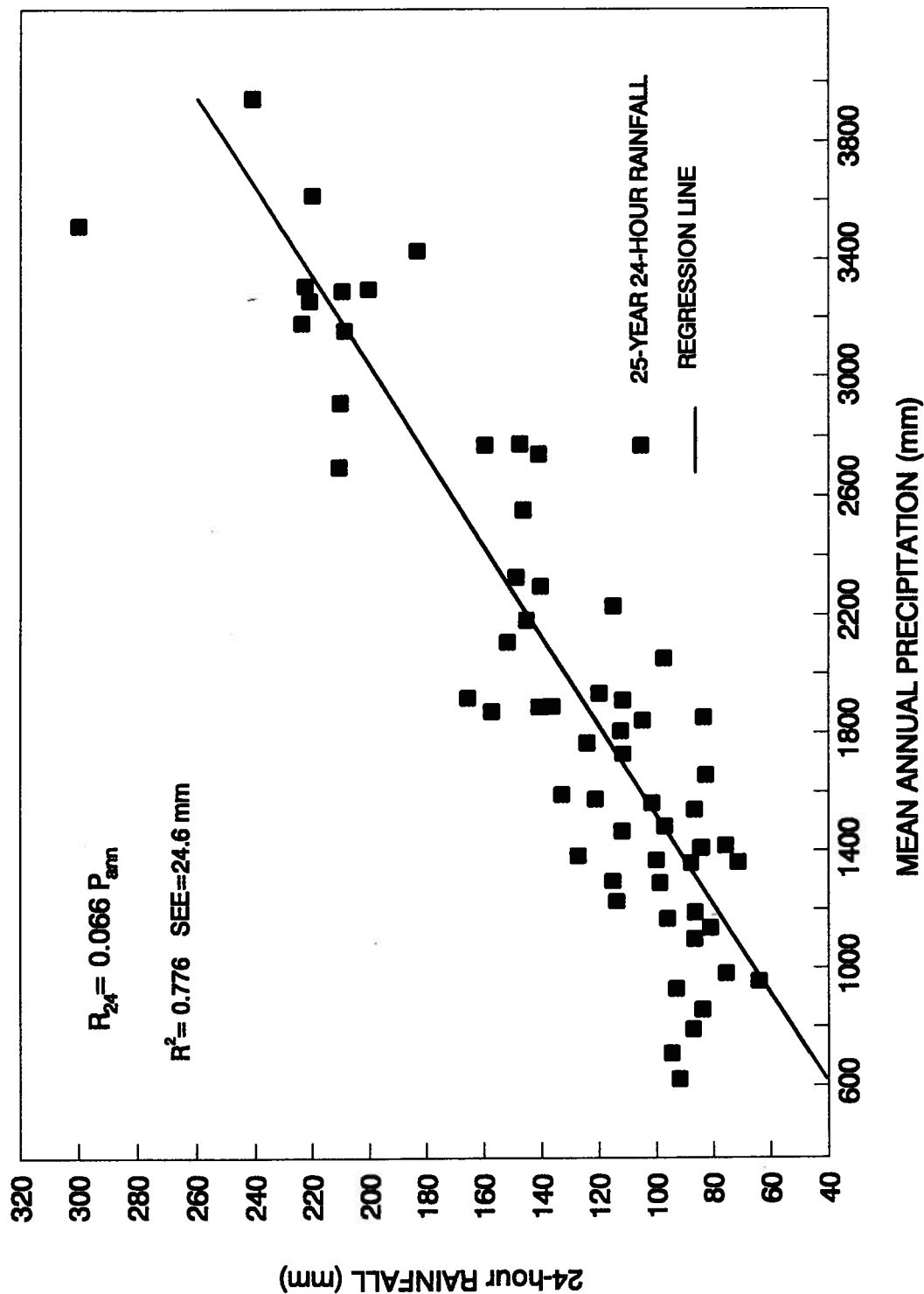


Fig. B4. Relationship of the 25-year 24-hour rainfall and mean annual precipitation for the sixty-one recording stations in coastal British Columbia.

APPENDIX B

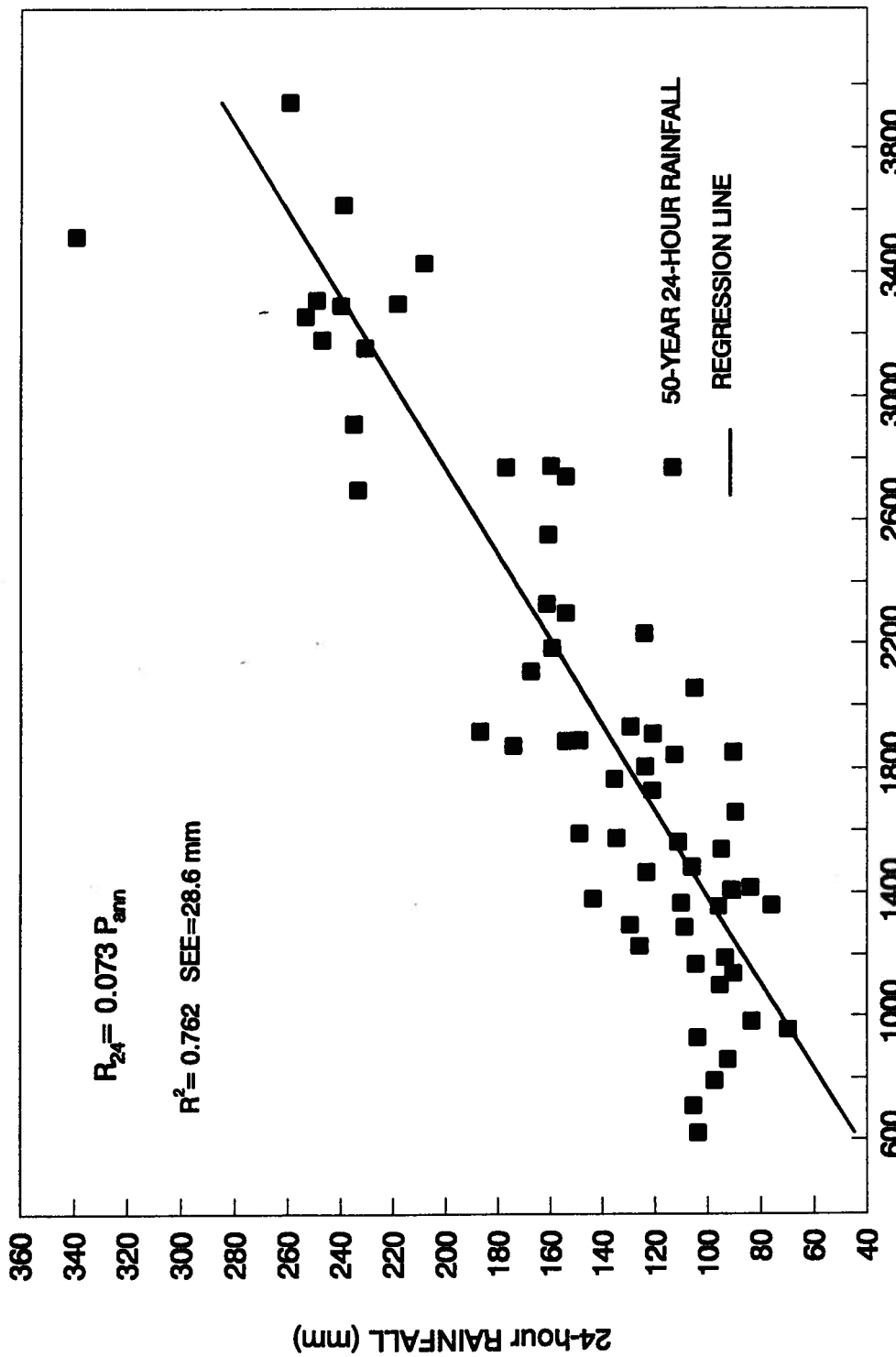


Fig. B.5 Relationship of the 50-year 24-hour rainfall and mean annual precipitation for the sixty-one recording stations in coastal British Columbia.

APPENDIX B

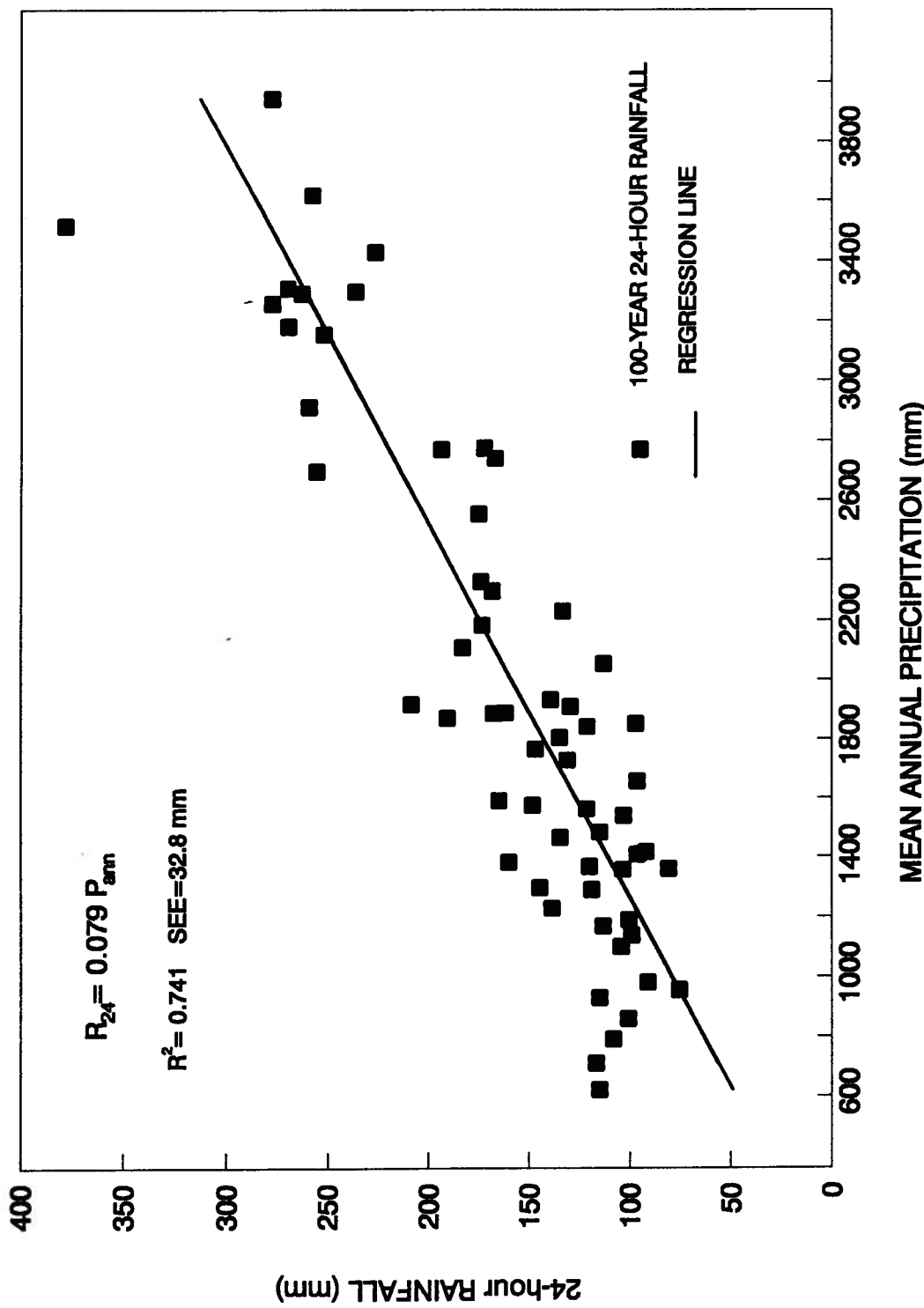


Fig. B6. Relationship of the 100-year 24-hour rainfall and mean annual precipitation for the sixty-one recording stations in coastal British Columbia.

APPENDIX C

CHARACTERISTICS OF THE 44 BASINS USED FOR THE TESTING OF THE MODIFIED SNYDER FORMULA

APPENDIX C

Table C1. Characteristics of the basins used in the independent test of the modified Snyder formula*.

Basin	Time Lag (h)	Area (km ²)	Length (km)	Str.Slope (m/m)
1	0.083	0.08	0.372	0.0489
2	0.167	0.21	0.656	0.0399
3	0.117	0.05	0.432	0.0544
4	0.283	0.44	1.2	0.0274
5	0.025	0.005	0.109	0.0978
6	0.05	0.01	0.205	0.0853
7	0.315	0.1	0.445	0.0151
8	0.443	1.17	1.76	0.0129
9	0.476	0.34	0.646	0.0066
10	0.436	0.18	0.838	0.0054
11	1.87	3.91	3.03	0.0051
12	1.81	4.01	2.7	0.0058
13	0.625	0.36	0.579	0.006
14	1.9	18.5	7.96	0.0053
15	0.24	0.31	0.969	0.0065
16	0.31	1.22	1.36	0.037
17	0.286	0.75	1.52	0.0115
18	0.117	0.03	0.206	0.0625
19	0.419	1.35	1.76	0.0203
20	0.116	0.1	0.305	0.0475
21	0.267	0.7	0.997	0.0217
22	0.417	1.4	2	0.0076
23	0.139	0.012	0.173	0.0141
24	0.165	0.011	0.178	0.0148
25	1.42	7.8	6.58	0.006
26	0.636	1.94	2.74	0.005
27	8.3	109	18.5	0.00302
28	6.4	58.8	8.21	0.00574
29	9	324	24.2	0.00217
30	9.3	89.1	19.5	0.00485
31	7.4	259	21.6	0.00671
32	9.5	165	30.3	0.00435
33	10.8	59.6	11.7	0.00268
34	6.9	85.5	16.4	0.00677
35	19.6	124	27.5	0.00153
36	13.5	132	19.8	0.00121
37	24	1210	97.4	0.0034

APPENDIX C

Table C1. Characteristics of the basins used in the independent test of the modified Snyder formula*. (cont.)

Basin	Time Lag (h)	Area (km ²)	Length (km)	Str.Slope (m/m)
38	22	1650	77.2	0.0046
39	22	824	24.1	0.0025
40	13	1130	85.3	0.0041
41	40	5850	196	0.0014
42	21.5	839	61.2	0.0045
43	13	642	48.3	0.0083
44	10	210	34.9	0.0058

* Data from Watt and Chow, 1985